

~~SECRET~~ D

B. F. Knalle

BIF-008-



052

-68

(Control Number)

This document consists of
310 classified pages.

BYE-SL-3263 '68

(y52)

Pgs

Bound

Engineering Analysis Report
Photographic Payload and Related
Support and Test Equipment
for MOL/DORIAN System

Volume II

Prepared by

EASTMAN KODAK COMPANY
Kodak Apparatus Division
Rochester, New York 14650


Contract No.

AF-18(600)2864

Approved by:

J. Maher

Date: 27 November 1968

In addition see Volume I, 

~~SECRET~~ D

Handle via BYEMAN
Control System Only

~~SECRET~~ D

BIF-008- [REDACTED] -68
(Control Number)

TABLE OF CONTENTS

VOLUME I

	<u>Page</u>
TABLE OF CONTENTS	i
LIST OF ILLUSTRATIONS	x
LIST OF TABLES	xix
LIST OF ABBREVIATIONS	xxi
INTRODUCTION	1
SECTION 1 FLIGHT CONFIGURATION AND MISSION DESCRIPTION	1-1
1.1 Manned Orbiting Laboratory (MOL)/Dorian Flight Vehicle Configuration	1-1
1.1.1 Titan III-M	1-1
1.1.2 Orbiting Vehicle	1-1
1.2 Objective and Mission Description	1-3
1.2.1 Objective	1-3
1.2.2 Sequence of Major Mission Events	1-4
1.2.3 Mission Requirements and Constraints	1-4
1.3 Description of the Photographic Payload	1-5
1.3.1 Mission Module Assembly (MMA)	1-7
1.3.2 Laboratory Module (LM) Assemblies	1-14
1.3.3 Support Module Assemblies	1-17
SECTION 2 SYSTEMS CONSIDERATIONS	2-1
2.1 Requirements of the Photographic Mission	2-1
2.1.1 General Requirements of the Dorian System	2-1
2.1.2 Requirements for Major Photographic Payload Functions	2-2

ⁱ
~~SECRET~~ D

Handle via **BYEMAN**
Control System Only

~~SECRET~~ D

BIF-008- [REDACTED] -68
(Control Number)

TABLE OF CONTENTS (Continued)

	<u>Page</u>
2.2 Modes of Operation	2-6
2.2.1 Manned/Automatic Mode	2-7
2.2.2 Automatic Mode	2-8
2.2.3 Operational Capabilities	2-8
2.3 Mission Operations (Manned/Automatic Mode)	2-9
2.3.1 Mission Operational Phases	2-11
2.3.2 Operational Sequences and Scheduling Considerations	2-13
2.3.3 Photographic Operations	2-18
2.4 Photographic Performance Considerations	2-22
2.4.1 Ground Test Object	2-22
2.4.2 Contrast	2-23
2.4.3 Lens Quality	2-24
2.4.4 Focus	2-40
2.4.5 Primary Optical System Alignment	2-47
2.4.6 Image Motion Compensation (IMC)	2-52
2.4.7 Time-Dependent Factors	2-57
2.4.8 Film Threshold Modulation	2-79
2.4.9 Dynamic Film-Resolution Prediction (Baseline)	2-81
2.5 Photographic Output	2-84
2.5.1 Film Format	2-84
2.5.2 Image Size and Scale of Photography	2-87
2.5.3 Data Block Format	2-99
2.5.4 Smear Slits	2-100
2.6 Data Return	2-103
2.6.1 Manned/Automatic (M/A) Mode	2-103

ii
~~SECRET~~ D

Handle via BYEMAN
Control System Only

~~SECRET~~ D

BIF-008- [REDACTED] -68
(Control Number)

TABLE OF CONTENTS (Continued)

	<u>Page</u>
SECTION 3 EASTMAN KODAK COMPANY (EKC) INTERFACES	3-1
3.1 General	3-1
3.2 Mission Module (MM) Interfaces	3-3
3.2.1 Mission Module Mechanical Interface	3-3
3.2.2 Mission Module Electrical Interfaces	3-5
3.2.3 Mission Module Thermal Interfaces	3-7
3.3 Laboratory Module Interfaces	3-8
3.3.1 Laboratory Module (LM) Mechanical Interfaces	3-8
3.3.2 Laboratory Module (LM) Electrical Interfaces	3-8
3.3.3 Laboratory Module Thermal Interface	3-13
3.4 Gemini-B Interface	3-13
3.4.1 Mechanical Interface	3-13
3.4.2 Electrical Interface	3-14
3.4.3 Thermal Interface	3-14
3.5 Interface Documentation	3-14
SECTION 4 DESIGN	4-1
4.1 Primary Optics, Mounts, Locks and Alignment	4-1
4.1.1 Optical Performance Parameters	4-2
4.1.2 Primary Optics Design	4-10
4.1.3 Mounts and Locks	4-23
4.1.4 Lens Alignment Description	4-40
4.2 Structural Assemblies and Mounts	4-54
4.2.1 Concept	4-55
4.2.2 Optical Support Structure, Ross Barrel, and Reference Rods	4-55

iii
~~SECRET~~ D

Handle via BYEMAN
Control System Only

~~SECRET~~ D

BIF-008- [REDACTED] -68
(Control Number)

TABLE OF CONTENTS (Continued)

	<u>Page</u>
4.2.3 Camera Optical Assembly Structure	4-63
4.2.4 Camera Optical Assembly (COA) Mounts	4-65
4.2.5 Access	4-66
4.2.6 Spacer Ring	4-66
4.2.7 Air Bag	4-67
4.3 Visual Optics	4-67
4.3.1 Requirements	4-67
4.3.2 Design Considerations	4-68
4.3.3 Hardware Description	4-79
4.3.4 Operation	4-91
4.3.5 Electrical Control	4-94
4.4 Camera Assembly	4-103
4.4.1 General Requirements	4-103
4.4.2 Constraints	4-104
4.4.3 General Design Selection	4-111
4.4.4 Shutter	4-112
4.4.5 Platen Assembly	4-119
4.4.6 Camera Film Handling	4-129
4.4.7 Filter	4-135
4.4.8 Focus Sensor	4-135
4.5 Film Handling	4-141
4.5.1 Requirements	4-141
4.5.2 Design	4-142

~~SECRET~~ D

~~SECRET~~ D

BIF-008- [REDACTED] -68
(Control Number)

TABLE OF CONTENTS (Continued)

	<u>Page</u>
4.6 Environmental Control	4-172
4.6.1 Prelaunch	4-173
4.6.2 Ascent	4-177
4.6.3 On-Orbit	4-179
4.7 On-Board Processor	4-195
4.7.1 General	4-195
4.7.2 Requirements	4-196
4.7.3 Configuration	4-197
4.7.4 Processor Mechanical and Thermal Design	4-200
4.7.5 Processor Electrical Design	4-202
4.8 On-Board Viewer	4-203
4.9 Electrical Design	4-205
4.9.1 Power	4-206
4.9.2 Commands	4-212
4.9.3 Instrumentation	4-212
4.9.4 Electromagnetic Compatibility (EMC)	4-221
4.9.5 Edge-Data Recording Control	4-222
4.10 Current Mass Properties Values	4-225

VOLUME II

SECTION 5 AUTOMATIC MODE	5-1
SECTION 6 PHOTOGRAPHIC PAYLOAD MODELS, TESTING, AND SUPPORT EQUIPMENT	6-1
6.1 Optical Tests	6-1

v
~~SECRET~~ D

Handle via BYEMAN
Control System Only

~~SECRET~~ D

BIF-008- [REDACTED] -68
(Control Number)

TABLE OF CONTENTS (Continued)

	<u>Page</u>
6.1.1 Test Requirements	6-1
6.1.2 Test Methods	6-3
6.1.3 Optical Component Tests	6-6
6.1.4 Master and Auxiliary Element Tests	6-8
6.1.5 Subsystems Tests	6-8
6.1.6 Special Environmental Considerations	6-11
6.2 Optical Test Equipment	6-11
6.2.1 Knife-Edge and Point Source Devices	6-12
6.2.2 Interferometers	6-14
6.2.3 Photographic Test Equipment	6-21
6.2.4 SDM-2 and Transmissibility Vibration Test Equipment	6-25
6.2.5 Data Recording and Processing	6-33
6.2.6 Pneumatic Mirror Support	6-38
6.2.7 Other Optical Devices and Fixtures	6-39
6.3 Developmental Models	6-40
6.3.1 Developmental Models	6-43
6.3.2 Qualification Model-Manned/Automatic Mode	6-48
6.4 Optical Assembly and Mission Payload System (MPS) Level Testing	6-50
6.4.1 Optical Assembly Testing	6-50
6.4.2 Mission Payload System Level Testing	6-62
6.5 Design and Analysis of Test Towers (Chambers)	6-77
6.5.1 Technical Description of Test Chambers	6-81

vi
~~SECRET~~ D

Handle via BYEMAN
Control System Only

~~SECRET~~ D

BIF-008--68
(Control Number)

TABLE OF CONTENTS (Continued)

	<u>Page</u>
6.5.2 Acoustic Test Facility	6-97
6.5.3 Test Chamber and Tower Accessories	6-103
6.6 Aerospace Support Equipment (ASE)	6-105
6.6.1 Photographic Payload	6-105
6.6.2 Mission Payload System-Level Aerospace Support Equipment	6-115
SECTION 7 RELIABILITY	7-1
7.1 Reliability Requirements and Goals	7-1
7.2 Reliability Apportionment	7-1
7.3 Reliability Estimates	7-3
7.3.1 Mission-Essential Operations	7-3
7.3.2 Reliability Mathematical Model	7-3
7.3.3 Launch and Nonoperation	7-6
7.3.4 Nonessential Components	7-7
SECTION 8 SYSTEM SAFETY ENGINEERING (SSE)	8-1
8.1 Introduction	8-1
8.2 Analysis	8-2
8.2.1 Hazard Analysis	8-2
8.2.2 Fault Tree Analysis	8-4
SECTION 9 NUMERICAL SUMMARY	9-1
9.1 General Data	9-1
9.1.1 Performance	9-1
9.1.2 Launch Parameters	9-1
9.1.3 Orbit	9-2
9.1.4 Orbital Coordinate Conventions	9-3

~~SECRET~~ D

~~SECRET~~ D

BIF-008-[REDACTED]-68
(Control Number)

TABLE OF CONTENTS (Continued)

	<u>Page</u>
9.1.5 Coverage	9-4
9.1.6 Weight Summary	9-4
9.1.7 Mass Properties	9-4
9.2 Requirements on Other Subsystems	9-5
9.2.1 Electrical Requirements	9-5
9.2.2 Film Retrieval	9-7
9.2.3 Image Smear	9-7
9.2.4 Stereo and Obliquity Ranges (Line-Of-Sight)	9-7
9.2.5 Laboratory Module (M/A Mode)	9-7
9.3 Photographic Payload Characteristics	9-8
9.3.1 Primary Lens Optical Parameters	9-8
9.3.2 Mission Module Environmental Requirements	9-9
9.3.3 Mirrors	9-10
9.3.4 Camera Parameters - Primary Film Strand	9-11
9.3.5 Camera Parameters - Secondary Film Strand	9-12
9.3.6 Film	9-12
9.3.7 Focus	9-14
9.3.8 Film Format	9-15
9.3.9 Visual Optics	9-15
9.3.10 Across-the-Format X-IMC Requirements	9-16
9.3.11 Optical Alignment	9-18
9.3.12 On-Board Processor	9-18
9.3.13 Film Handling (M/A Mode)	9-19
9.3.14 Data Return in Gemini B (M/A Mode)	9-20
9.3.15 Smear Slits	9-21
9.3.16 Image Smear Rate	9-21
9.3.17 Image Velocity Sensor	9-21

~~SECRET~~ D

~~SECRET~~ D

BIF-008-[REDACTED]-68
(Control Number)

TABLE OF CONTENTS (Continued)

	<u>Page</u>
APPENDIX A DERIVATION OF OFF-AXIS IMAGE RATE AND ACROSS-THE-FORMAT IMAGE MOTION COMPENSATION CAMERA SET-UP EQUATIONS	A-1
APPENDIX B TIME-DEPENDENT IMAGE STRUCTURE	B-1
APPENDIX C COMMAND AND INSTRUMENTATION LISTS	C-1
APPENDIX D RELIABILITY BLOCK DIAGRAMS AND BASIS FOR TIMES USED IN MATH MODEL	D-1
APPENDIX E ANALYSIS AND DESIGN OF TEST TOWERS	E-1

ix
~~SECRET~~ D

Handle via **BYEMAN**
Control System Only

~~SECRET~~ D

BIF-008- [REDACTED] -68
(Control Number)

LIST OF ILLUSTRATIONS

VOLUME 1

<u>Number</u>	<u>Title</u>	<u>Page</u>
1.1-1	MOL/Dorian Flight Vehicle Configuration - Manned/ Automatic Mode	1-2
1.2-1	Orbiting Vehicle M/A Mode	1-9
1.2-2	Orbiting Vehicle-Automatic Mode (Typical)	1-11
2.2-1	Dorian Objectives (Photographic Operations) (M/A Mode)	2-10
2.4-1	Surface Representation of a Normalized Modulation Transfer Function	2-27
2.4-2	Effect of Aperture Vignetting and Obstructions Upon Monochromatic MTF (Major Axis Azimuth)	2-29
2.4-3	Effect of Aperture Vignetting and Obstructions Upon Monochromatic MTF (Minor Axis Azimuth)	2-30
2.4-4	Effect of Residual Aberrations Upon Heterochromatic MTF (Major Axis Azimuth)	2-34
2.4-5	Effect of Residual Aberrations Upon Heterochromatic MTF (Minor Axis Azimuth)	2-35
2.4-6	Optical Quality Factor	2-38
2.4-7	Effect of Focus on Resolution	2-41
2.4-8	Focus Position vs Altitude and Look Angle	2-42
2.4-9	Meaning of Focus Control Terminology	2-45
2.4-10	Resolution vs Equivalent Primary Mirror Tilt	2-51
2.4-11	Relationship between Average-Minimum Apparent Scene Luminous Emittance and Solar Altitude	2-60
2.4-12	Spectral Transmittance of the Primary Optics for an Equal Energy Source and Independent of Film Sensitivity (Nadir Position)	2-62

X

~~SECRET~~ D

Handle via BYEMAN
Control System Only

~~SECRET~~ D

BIF-008- [REDACTED] -68
(Control Number)

LIST OF ILLUSTRATIONS (Continued)

<u>Number</u>	<u>Title</u>	<u>Page</u>
2.4-13	Relationship of Log Exposure to Resolution and Density	2-65
2.4-14	Procedure Used to Make Stereo-Pair Simulation	2-67
2.4-15	Simulation Showing Results of Exposure Bracketing	2-69
2.4-16	Simulation Showing Results of Exposure Bracketing	2-71
2.4-17	Stereo Pair Showing Dorian System Image Quality	2-75
2.4-18	Shutter Efficiency	2-78
2.4-19	Baseline Dynamic Film Resolution Prediction	2-82
2.5-1	Film Format (Simulated Image Scene)	2-85
2.5-2a	Primary Film Format Location of Data Blocks, Interframe Marks and Fiducial Marks as Viewed from Emulsion Side of Film	2-88
2.5-2b	Secondary Film Format Location of Data Blocks, Interframe Marks and Fiducial Marks as Viewed from Emulsion Side of Film	2-89
2.5-3	Dynamic Ground Resolution Related to Vehicle Altitude	2-91
2.5-4	Dynamic Ground Resolution Related to Image Plane Contrast	2-92
2.5-5	Dynamic Ground Resolution Related to Optical Quality Factor	2-93
2.5-6	Dynamic Ground Resolution Related to Focus Error	2-94
2.5-7	Dynamic Ground Resolution Related to Image Smear Rate	2-95
2.5-8	Dynamic Ground Resolution Related to Optical Misalignment	2-96
2.5-9	Dynamic Ground Resolution Related to Percent Veiling Glare	2-97
2.5-10	Dynamic Ground Resolution Related to Field Angle	2-98
2.5-11	Smear Slit Layout	2-102
2.6-1	Secondary Film Flow (processed film only)	2-104
2.6-2	Film Length vs Weight	2-107

xi
~~SECRET~~ D

Handle via BYEMAN
Control System Only

~~SECRET~~ D

BIF-008- [REDACTED] -68
(Control Number)

LIST OF ILLUSTRATIONS (Continued)

<u>Number</u>	<u>Title</u>	<u>Page</u>
3.2-1	Mission Module Thermal Interface Boundaries	3-4
3.2-2	MM Electrical Interfaces	3-6
3.3-1	LM Console Bays and Panels	3-10
3.3-2	LM Electrical Interfaces	3-11
4.1-1	Optical Configuration for MOL/Dorian System Showing Detail of Alignment Sensor Optics	4-3
4.1-2	Spherochromatism of Dorian Lens	4-5
4.1-3	Central Obstruction	4-7
4.1-4	Relative Illumination at Nadir vs Field Angle at Film Plane	4-8
4.1-5	Relative Illumination - Visual Optics and IVS Image Planes	4-9
4.1-6	Titanium Silicate Blank Deflection Test Configuration	4-13
4.1-7	Flexure Moment vs Lateral Deflection	4-26
4.1-8	Bending Stress vs Lateral Displacement	4-27
4.1-9	Primary Mirror Mounting Flexure Concept	4-28
4.1-10	Schematic Diagram - Diagonal Mirror Mount	4-30
4.1-11	Ross Diagonal Mirror Mount	4-32
4.1-12	Primary Mirror Launch Lock	4-35
4.1-13	Launch Lock Drive Module	4-36
4.1-14	Lock-Set Design for Cer-Vit Mirrors	4-39
4.1-15	Mirror Launch-Lock Electronics Block Diagram	4-41
4.1-16	Alignment Sensor and Servo Drive	4-43
4.1-17	Alignment Control System Block Diagram	4-47
4.1-18	Schematic of Alignment Sensor Configuration	4-48
4.1-19	Alignment Sensor Breadboard	4-49
4.1-20	Alignment Control System EM Components	4-50

~~SECRET~~ D

~~SECRET~~ D

BIF-008- [REDACTED] -68
(Control Number)

LIST OF ILLUSTRATIONS (Continued)

<u>Number</u>	<u>Title</u>	<u>Page</u>
4.1-21	ACS EM Mounted on Test Stand	4-51
4.1-22	Alignment Servos	4-52
4.2-1	Optical Assembly Structure and Mounts	4-56
4.2-2	Structural Development Model COA	4-57
4.2-3	Corrector and Diagonal Mirrors Support Structure	4-58
4.2-4	Ross Barrel Structure	4-61
4.2-5	Forward Support Structure	4-62
4.3-1	Schematic of Visual Optics Assembly	4-69
4.3-2	Target Viewed From 80mm at Magnification of 125	4-71
4.3-3	Target Viewed From 80mm at Magnification of [REDACTED]	4-73
4.3-4	Target Viewed From 80mm at Magnification of [REDACTED]	4-75
4.3-5	Target Viewed From 80mm at Magnification of [REDACTED]	4-77
4.3-6	Exit Pupil/Eye Pupil Relationships	4-80
4.3-7	VO Optical Element Configuration	4-81
4.3-8	Formula Sample - Visual Optics Relay and Eyepieces	4-82
4.3-9	Magnification Change Unit (Rotatable Galilean Telescope Pair) Mounted in Collimated Light Space of Variable Power Relays	4-84
4.3-10	Auxiliary Data Display	4-87
4.3-11	Retractable Interface Mount, VOA to Secondary Ross Barrel	4-90
4.3-12	Visual Optics Power Distribution Block Diagram	4-95
4.3-13	Visual Optics Control Signals Block Diagram	4-96
4.3-14	Reticule-Focus Control Block Diagram	4-98
4.3-15	Magnification and Flip Mirror Control Block Diagram	4-101

~~SECRET~~ D

~~SECRET~~ D

BIF-008- [REDACTED] -68
(Control Number)

LIST OF ILLUSTRATIONS (Continued)

<u>Number</u>	<u>Title</u>	<u>Page</u>
4.4-1	Camera Assembly	4-105
4.4-2	Camera Simulation Model	4-107
4.4-3	Camera Mock-Up	4-109
4.4-4	Shutter-Curtain Drive Tape System	4-113
4.4-5	Whiffletree Assembly	4-114
4.4-6	Curtain and Slit-Width Drive	4-115
4.4-7	Shutter Rotation Drive	4-116
4.4-8	Image Motion Compensation Schematic	
4.4-9	Schematic Diagram of Platen Interchange Mechanism Sequence	4-121
4.4-10	Focus Drive Schematic	4-127
4.4-11	Vacuum System Schematic	4-128
4.4-12	Primary Film Handling Assembly Schematic	4-131
4.4-13	Secondary Film Handling Assembly Schematic	4-133
4.4-13(a)	Focus Sensor Breadboard	4-137
4.4-14	Focus Sensor Schematic Block Diagram	4-138
4.4-15	Focus Sensor Image Planes	4-139
4.5-1	Film Handling Flow Chart	4-143
4.5-2	LM Film Handling Concept - M/A Mode	4-144
4.5-3	Block Diagram Primary Film Handling Control - Manned/	
4.5-4	Primary Supply Assembly	4-149
4.5-5	Primary Supply Assembly Engineering Model	4-150
4.5-6	Film Transport System Supply Spool and Take-Up Reel	4-151
4.5-7	Primary Take-Up Assembly Concept	4-153

~~SECRET~~ D

~~SECRET~~ D

BIF-008- [REDACTED] -68
(Control Number)

LIST OF ILLUSTRATIONS (Continued)

<u>Number</u>	<u>Title</u>	<u>Page</u>
4.5-8	Film Take-Up Assembly	4-154
4.5-9	Film Take-Up Assembly - Spool and DRC Mounting Flange	4-155
4.5-10	Film Neutral Axis	4-158
4.5-11	Neutral Axis Rotation Concept	4-159
4.5-12	Horizontal Chute Support	4-161
4.5-13	Roller Pivots and Guide Slots	4-162
4.5-14	LM Chute Assembly Concept	4-163
4.5-15	Film Transport System Engineering Model	4-165
4.5-16	Film Transport System Test Setup	4-167
4.5-17	Simulated Camera	4-169
4.6-1	Ground Conditioning System	4-176
4.6-2	MM Shell Thermal Requirements	4-180
4.6-3	Operating Temperature as a Function of Beta Angle and Coating Properties $\epsilon=0.84$	4-183
4.6-4	Orbital Temperature Profile	4-185
4.6-5	Hotdogging Curvatures	4-187
4.6-6	Damping Characteristics of the Thermal Annulus	4-188
4.6-7	Blanket Assembly Configuration	4-190
4.6-8	Heater Strips in Close Contact with the OA	4-191
4.7-1	Side View Schematic of On-Board Processor	4-199
4.8-1	Concept-Viewer Schematic	4-204
4.9-1	Electrical System Block Diagram	4-207

xv
~~SECRET~~ D

Handle via **BYEMAN**
Control System Only

~~SECRET~~ D

BIF-008- [REDACTED] -68
(Control Number)

LIST OF ILLUSTRATIONS (Continued)

VOLUME II

<u>Number</u>	<u>Title</u>	<u>Page</u>
6.1-1	Mirror Test Configurations	6-7
6.2-1	Knife-Edge Tester	6-13
6.2-2	MOD II Twyman-Green Interferometer Schematic	6-15
6.2-3	Twyman-Green Interferometer	6-17
6.2-4	Williams Interferometer Schematic	6-18
6.2-5	Williams Interferometer (Breadboard Model)	6-19
6.2-6	Photographic Test Equipment	6-22
6.2-7	Photographic Target Format	6-24
6.2-8	Optical Measurement of Image Smear	6-26
6.2-9	Time-Amplitude Traces - Optically Measured and Mechanically Measured (Accelerometer) Data	6-29
6.2-10	Typical Frequency Spectra	6-30
6.2-11	Sonagram of System Response	6-31
6.2-12	Sonagram of Ross Mirror	6-32
6.2-13a	Sonagram of File 4645, Noise at 1 Atmosphere Ch. 4 Folding Mirror	6-34
6.2-13b	Sonagram of File 4645, Noise at 1 Torr Ch. 4 Folding Mirror	6-35
6.2-14a	Sonagram of File 4645, Noise at 1 Atmosphere Ch. 4 Folding Mirror	6-36
6.2-14b	Sonagram of File 4645, Noise at 1 Torr Ch. 4 Folding Mirror	6-37
6.2-15	Profiling Spherometer on Pyroceram Master	6-41

xvi
~~SECRET~~ D

Handle via BYEMAN
Control System Only

~~SECRET~~ D

BIF-008-[REDACTED]-68
(Control Number)

LIST OF ILLUSTRATIONS (Continued)

<u>Number</u>	<u>Title</u>	<u>Page</u>
6.3-1	MMTHM Assembly Schematic	6-46
6.4-1	Mission Module Aft Section Isothermal Optical Quality Test Configuration in Chamber III	6-65
6.4-2	Tracking Mirror Thermo-Optical Tests	6-67
6.4-3	MMAS Thermal/Optical Test Configuration Chamber A	6-68
6.4-4	Sub-Aperture Optical Test Configuration	6-72
6.4-5	MM Thermal/Vacuum Test Configuration in Chamber A	6-75
6.5-1	Test Facility - High Bay Area	6-79
6.5-2	Chamber I _{em}	6-83
6.5-3	Chamber I	6-85
6.5-4a	Chamber I	6-86
6.5-4b	Chamber I _g	6-87
6.5-5	Chamber II _{em}	6-89
6.5-6	Chamber II _g	6-91
6.5-7	Chambers IIIA and B	6-92
6.5-8	Chamber A	6-94
6.5-9	Chamber A	6-95
6.5-10	MM Acoustic Vibration Test Configuration	6-98
6.5-11	Acoustic Test Chamber	6-99
6.5-12	Acoustic Test Facility	6-101
6.6-1	Positioner Dolly, Chamber II _{EM}	6-107
6.6-2	Upright Adjustable Mirror Support, Chamber I _{EM}	6-108
6.6-3	Instrumentation Processor Test Set, Front Panel View	6-109

~~SECRET~~ D

~~SECRET~~ D

BIF-008- [REDACTED] -68
(Control Number)

LIST OF ILLUSTRATIONS (Continued)

<u>Number</u>	<u>Title</u>	<u>Page</u>
6.6-4	Layout Drawing of Sensor Test System	6-111
6.6-5	Block Diagram of Sensor Test System	6-113
6.6-6	Horizontal Test Stand Setup	6-116
6.6-7	Checkout Cradle and Cantilever Catwalk (With SDM Aft Structure)	6-117
6.6-8	Thermal Data Management System Central Computer (IBM)	6-120
6.6-9	Thermal Data Acquisition Equipment Breadboard (Systems Engineering Laboratories), Shown being applied in Thermocouple Calibration	6-121
6.6-10	Mission Module Assembly Stand Scale Model	6-123
6.6-11	Test Body Transporter and Scaffolding Unit	6-125
8.2-1	Hazard Analysis	8-3
8.2-2	Fault Tree Analysis	8-5
8.2-3	Fault Tree Analysis Processor Subsystem	8-7
9.1-1	Orbital Coordinate Conventions	9-3

~~SECRET~~ _____

~~SECRET~~ D

BIF-008- [REDACTED] -68
(Control Number)

LIST OF TABLES

VOLUME I

<u>Number</u>	<u>Title</u>	<u>Page</u>
2.3-1	Typical Exposure Sequences for a MOL/Dorian Mission	2-21
2.4-1	TM Projection Relative to Optical Axis	2-31
2.4-2	Current Weighting Factors Used on Heterochromatic MTF Analyses	2-36
2.4-3	Dorian Focus Budget (On-Axis, Remote Record Mode)	2-48
2.4-4	X-IMC Camera Assembly Requirements for the Line-of-Sight Region	2-55
2.4-5	On-Axis Smear Budget	2-74
2.4-6	Smear Without/With X-IMC	2-77
2.5-1	Baseline Conditions Used for Performance Estimate	2-90
2.5-2	Smear Slit Tolerances	2-101
3.1-1	M/A Mode Major Interface Areas	3-2
3.3-1	EKC Laboratory Module Interface	3-9
3.5-1	Interface Documentation	3-15
4.1-1	Properties and Dimensions of Various 71-Inch-Diameter Mirror Blanks	4-11
4.1-2	Comparison of Cer-Vit and Titanium-Silicate Deflections for 10-Inch Thick Developmental Designs	4-14
4.1-3	Type of Material Used for Mirrors	4-15
4.1-4	Mirror Optical Quality Factor Contribution (Specification)	4-17
4.1-5	Lens Surface Optical Quality Factor Contribution	4-20
4.1-6	Inhomogeneity Optical Quality Factor Contributor	4-22

xix
~~SECRET~~ D

Handle via BYEMAN
Control System Only

~~SECRET~~ D

BIF-008- [REDACTED] -68
(Control Number)

LIST OF TABLES (Continued)

<u>Number</u>	<u>Title</u>	<u>Page</u>
4.3-1	Visual Optics Functions	4-97
4.6-1	Thermal Hotdogging	4-182
4.10-1	Contract Weight Budget Summary	4-226
4.10-2	Photographic Payload Weight Breakdown	4-227
4.10-3	Mass Properties Data, Manned/Automatic Mode	4-228

VOLUME II

<u>Number</u>	<u>Title</u>	<u>Page</u>
6.3-1	Definition of Manned/Automatic MPS-Level Prime Assemblies at EKC	6-42
6.3-2	Hardware Differences Between the Thermal Model and Flight Model	6-47
6.4-1	Reference Guide to Optical Assembly Tests at EKC	6-51
6.4-2	Reference Guide to MPS Testing at EKC	6-63
6.5-1	Summary Table of Test Chambers	6-82
7.2-1	Mission-Essential Component Reliability Apportioned Goals and Estimates	7-2
7.3-1	Reliability Estimates for Mission-Essential Operations	7-4
7.3-2	Reliability Estimates for Nonessential Components	7-7
8-1	Most Significant Class III Hazard Conditions in the Processor Subsystem	8-9

xx
~~SECRET~~ D

Handle via BYEMAN
Control System Only

~~SECRET~~ D

BIF-008- [REDACTED] -68
(Control Number)

LIST OF ABBREVIATIONS*

AAC	Automatic Alignment Control
ATS	Acquisition telescope
ATF	Acoustic test facility
ACO	Administrative contracting officer
AS	Aerospace Corporation
AFE	Aerospace flight equipment
AGE	Aerospace ground equipment
ASE	Aerospace support equipment
AIM	Aerial image modulation
ADC	Airborne digital computer
AF	Air Force
ACS	Alignment control system
AMS	Alignment monitoring system
AO	American Optical
BIMAT	Bimat film
CATS	Camera assembly test sets
COA	Camera optical assembly
cg	Center of gravity
CM	Compatibility model
CITE	Computer integrated test equipment
CDS	Command definition specification
CCN	Contract change notice
CDP	Contract definition phase
Hz	Cycles per second
DCU	Data conversion unit
DMS	Data management system

* The following listed abbreviations are not necessarily used in this report.

xxi
~~SECRET~~ D

Handle via BYEMAN
Control System Only

~~SECRET~~ D

BIF-008- [REDACTED] -68
(Control Number)

LIST OF ABBREVIATIONS (Continued)

DRV	Data re-entry vehicle
DRC	Data return container
DD	Department of Defense
DCCB	Design change control board
DCO	Design change order
EKC	Eastman Kodak Company
ETD	Edge thickness difference
EMC	Electro magnetic compatability
EMI	Electro magnetic interference
EMISM	Electro magnetic interferences safety margins
EDCTU	Electronic development compatability test unit
EAR	Engineering Analysis Report
EM	Engineering model
ECS	Environmental control system
FHE	Film handling electronics
FDR	Final design review
FVTL	Flight vehicle timeline
FCE	Focus control electronics
FCP	Focus control preamplifier
FS	Formula sample
FPDA	Fraction of planned data acquired
GE	General Electric Company
GFE	Government furnished equipment
H/SLS	Hardware/software limitations specification
IMC	Image motion compensation

~~SECRET~~ D

~~SECRET~~ D

BIF-008- [REDACTED] -68
(Control Number)

LIST OF ABBREVIATIONS (Continued)

IVS	Image velocity sensor
IFOT	In-flight on time
ICN	Interface change notice
IP	Instrumentation processor
ITCPS	Integrated testing computer programming specification
KAD	Kodak Apparatus Division
LM	Laboratory module
LMCU	Laboratory module control unit
LMPU	Laboratory module power unit
LMQTV	Laboratory module qualification test vehicle
LMQM	Laboratory module qualification model
LMTS	Laboratory module thermal simulator
LOCTP	Launch operations crew training plan
LV	Launch vehicle
M/A	Manned/Automatic
MOL	Manned Orbiting Laboratory
MDR	Major design review
MDAC-WD	McDonnell Douglas Astronautics Company-Western Division
MDAC-ED	McDonnell Douglas Astronautics Company-Eastern Division
MTTF	Mean-time-to-failure
MCC	Mission control center
MDAU	Mission data adapter unit
MM	Mission module
MMAS	Mission module aft section
MMA	Mission module assembly

~~SECRET~~ D

~~SECRET~~ D

BIF-008- [REDACTED] -68
(Control Number)

LIST OF ABBREVIATIONS (Continued)

MMCU	Mission module control unit
MMFS	Mission module forward section
MMIP	Mission module instrumentation processor
MMPU	Mission module power unit
MMQM	Mission module qualification model
MMSE	Mission module simulation equipment
MMTS	Mission module test set
MPS	Mission payload system
MPSS	Mission payload system segment
MES	Mobile environment shelter
MTF	Modulation transfer function
NASA	National Aeronautics and Space Administration
NPC	National Photocolor Corporation
n mi	Nautical miles
NAA	North American Aviation
OCTOPUS	Operational computer programming specif- ication
OA	Optical assembly
OAT	Optical assembly test
OQF	Optical quality factor
OV	Orbiting vehicle
PP	Photographic payload
PPS	Photographic payload system
PTE	Photographic test equipment
PM	Primary mirror
PDR	Preliminary design review
PLOT	Probable-launch-on-time

xxiv
~~SECRET~~ D

Handle via BYEMAN
Control System Only

~~SECRET~~ D

BIF-008- [REDACTED] -68
(Control Number)

LIST OF ABBREVIATIONS (Continued)

PRL	Project requirements list
PCM	Pulse code modulation
QM	Qualification model
QC	Quality control
RFD	Reference focal distance
RC	Reliability components
STC	Satellite Test Center
SAFSP	Secretary of the Air Force Special Projects
STS	Sensor test system
SW	Sensor worth
SRC	Slant range compensation
SSB	Source selection board
SGLS	Space ground-link subsystem
SIR	Special industrial requirements
STE	Special test equipment
ST	Special tooling
SLS	Static load structure
SDM	Structural development model
SM	Support module
SEL	Systems engineering laboratories
SSE	System safety engineer
TA	Technical advisor
TEM	Technical exchange meeting
TIM	Technical interface meeting
TC	Thermal components
TDMS	Thermal data management system

XXV
~~SECRET~~ D

Handle via **BYEMAN**
Control System Only

~~SECRET~~ D

BIF-008- [REDACTED] -68
(Control Number)

LIST OF ABBREVIATIONS (Continued)

THM	Thermal model
TCA	Time of closest approach
TBD	To-be-determined
TBR	To-be-resolved
TM	Tracking mirror
ULE	Ultra-low expansion
VAFB	Vandenberg Air Force Base
VO	Visual optics
VOA	Visual optics assembly
VOAC	Visual optics assembly control
XEPS	Xenon energy projection system
X-IMC	Across-the-format Image Motion Compensation
ZI	Zone of the interior

xxvi
~~SECRET~~ D

Handle via **BYEMAN**
Control System Only

~~SECRET~~ D

BIF-008- [REDACTED] -68
(Control Number)

SECTION 5
AUTOMATIC MODE

The unmanned configuration, designated automatic mode, is currently being studied by Eastman Kodak Company (EKC) in accordance with the provisions of CCN-28 to the basic EKC work specification. Initial EKC recommendations for the automatic mode configuration were given at the 5 December 1967 Air Force/Aerospace briefing, documented in F-022884-KH. The Final Study Report of this effort is due 3 February 1969. Configuration and design details therefore will not be discussed in this report, but will be presented in future editions.

5-1
~~SECRET~~ D

Handle via **BYEMAN**
Control System Only

~~SECRET~~ D

BIF-008- [REDACTED] -68
(Control Number)

SECTION 6
PHOTOGRAPHIC PAYLOAD MODELS, TESTING, AND SUPPORT EQUIPMENT

An orderly development and test program is required to meet photographic payload (PP) performance requirements. This section describes developmental models and tests, and the facilities and support equipment required for assembly and testing.

6.1 OPTICAL TESTS

Optical tests are performed for the purposes of:

- a. Calibrating and ascertaining quality of standard optical elements to be used for testing production optical elements.
- b. Proving PP optical element design.
- c. Determining acceptability and quality of production elements intended for flight hardware.
- d. Evaluating integrated system performance.

Paragraphs 6.1.1 through 6.1.6 discuss test requirements, test methods, optical component tests, master and auxiliary element tests, subsystem tests, and special environmental considerations, respectively.

6.1.1 Test Requirements

Test objects include reflecting spheres, aspheres, and flats; transmitting spheres; and various optical subsystems.

~~SECRET~~ D

~~SECRET~~ D

BIF-008- [REDACTED] -68
(Control Number)

Goals for optical test configurations (see paragraphs 6.2 and 6.1.3) include the following:

- a. Simplicity
- b. Minimum number of auxiliary optical elements
- c. Self-calibration and self-checking auxiliary elements.
- d. Optimum support of optical elements.
- e. Controlled and/or monitored test environment.
- f. Minimum number and magnitude of nondetectable optical errors.

The precision requirements for testing flight components and flight subsystems are determined by PP performance requirements. The precision requirements for reference and auxiliary optical element tests are determined by the precision requirements of the associated flight element, master element, or subsystem being tested. The optical assembly (OA) wavefront aberration tolerance at the exit pupil is 1/10 wavelength root-mean-square ($\lambda/10$ RMS). Uniform division of error between the five prime elements of the OA generates an approximate $\lambda/22.5$ -RMS tolerance on each element. The test system should be more precise by a factor of two to maintain a high degree of confidence in measurement results. Thus, an approximate level of required test precision is $\lambda/45$ RMS. Estimates of test precision in a vacuum environment meet or exceed this level of precision.

The precision required in auxiliary element calibration, or test-equipment calibration where the interferometer is included in the test equipment, is consistent with test precision requirements and varies with test geometry.

~~SECRET~~ D

~~SECRET~~ D

BIF-008- [REDACTED] -68
(Control Number)

6.1.2 Test Methods

Test methods can be grouped into optical and nonoptical categories. The nonoptical (that is, mechanical) test methods do not generally apply to test precision better than ~ 5 microinches. The limitation is a result of the instability of mechanical gages of the large sizes required. Optical test methods are most appropriate where test precision must be significantly better than 20μ inches.

Optical test methods which were considered for use on the current program include the Hartmann, caustic, knife edge (single and orthogonal cuts), point source, Ronchi (geometric and diffraction versions), and interferometric tests. Interferometric test devices considered include types of interferometers capable of producing two-beam, shearing, and multiple-beam interference patterns.

6.1.2.1 Noninterferometric Tests. The Hartmann test is a standard, critical, geometrical test. The test display, a spot pattern, is inadequate for determining the shape of the test wavefront with adequate precision. Caustic test methods, similar to Hartmann testing, also lack accuracy. Point-source tests are useful during alignment, but experience has shown a general inability of observers to detect changes in the diffraction pattern caused by wavefront aberrations much smaller than $\lambda/4$ peak-to-peak. It is also true that a point source test does not provide a localization of the wavefront error with respect to its origin on the exit pupil or component surface. See paragraph 6.2.1 for details of point source and knife-edge devices. Established knife-edge test techniques will be used to provide a sensitive measure of the smoothness of component

~~SECRET~~ D

~~SECRET~~ D

BIF-008- [REDACTED] -68
(Control Number)

surfaces. Small ripple-like errors which cannot be observed interferometrically can be seen with the knife edge. Knife-edge displays are qualitative rather than quantitative however, unless carefully calibrated with interferometric data.

6.1.2.2 Interferometric Tests. Interferometric displays can be generated by the following operations on a test wavefront:

- a. Superposition (standard two-beam interferometry) with known reference wavefront
- b. Shearing interferometers (lateral, radial, azimuthal)
- c. Multiple beam interferometry
- d. Holographic interferometry

Interferograms obtained with shearing interferometers are difficult to interpret and allow only relatively low spatial resolution of the object. Elaborate data reduction is required. Multiple beam interferometers do not have significant advantages at the scale and error levels involved in current optical testing. Superposition-type interferometers studied include the following:

- a. Michelson
- b. Twyman-Green
- c. Williams
- d. Kösters prism
- e. McLeod
- f. Scatter plate

6-4
~~SECRET~~ D

Handle via **BYEMAN**
Control System Only

~~SECRET~~ D

BIF-008- [REDACTED] -68
(Control Number)

- g. Birefringent lens
- h. Reconstructed reference

Each of these interferometers offers relative advantage in some area of operation. The topological displays of the Twyman-Green, Williams, McLeod, Kösters prism, and reconstructed reference interferometers are easily manipulated and directly interpretable. The unequal path Twyman-Green and Williams interferometers must be used with coherent sources such as He-Ne lasers. The McLeod, Köster prism, and reconstructed reference interferometers do not require high source coherence because of their equal path configurations.

6.1.2.3 Interference Displays and Display Utilization. Superposition type interference patterns are characterized by a 1λ difference in wavefront height between fringes. Displays which are to be analyzed by computer must contain a sufficient number of fringes to provide adequate spatial resolution of the surface or wavefront. Twenty or more fringes are generally required. Such fringe patterns can be obtained using a Twyman-Green, Williams, Kösters prism, McLeod, or reconstructed reference interferometer. Monotonic fringe displays are required for computer processing. Monotonicity is obtained by increasing the reference-to-sample beam tilt, and the number of fringes, until no fringe forms a closed loop in the display. All displays consist of a sinusoidal intensity distribution which appears localized on the subject. Considerations of imaging characteristics of interferometers are given in paragraph 6.2.2.

6-5
~~SECRET~~ D

Handle via BYEMAN
Control System Only

~~SECRET~~ D

BIF-008- [REDACTED] -68
(Control Number)

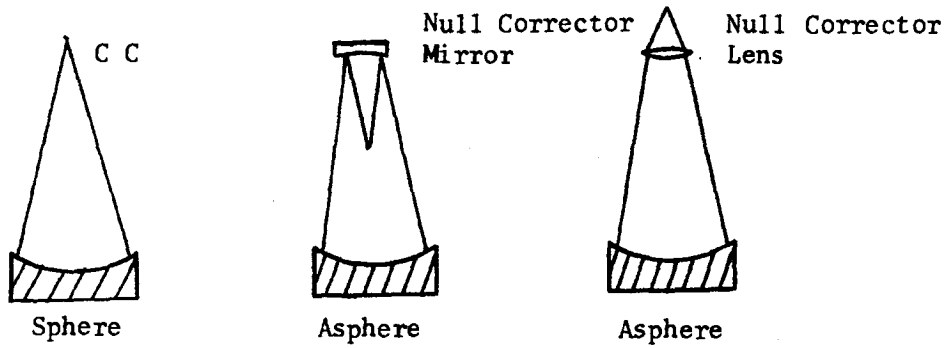
6.1.3 Optical Component Tests

6.1.3.1 Mirrors With Power. Reflective components with power (for example, master test spheres, primary mirrors, test aspheres) will be interferometrically measured at the center of curvature. Aspheric elements can be tested as if they are simple spheres provided that a residual aberration corrector (null corrector) is used. Test configurations are shown in Figure 6.1-1a. The interferometers to be used are discussed in paragraph 6.2.2. Parametric analysis by computer has shown that spherical mirrors can be used as null correctors. Limiting residual aberration levels are less than $\lambda/50$. Refractive null correctors in single positive lens form can be used, but with higher residuals (on the order of $\lambda/10$) for practical null-correcting lenses.

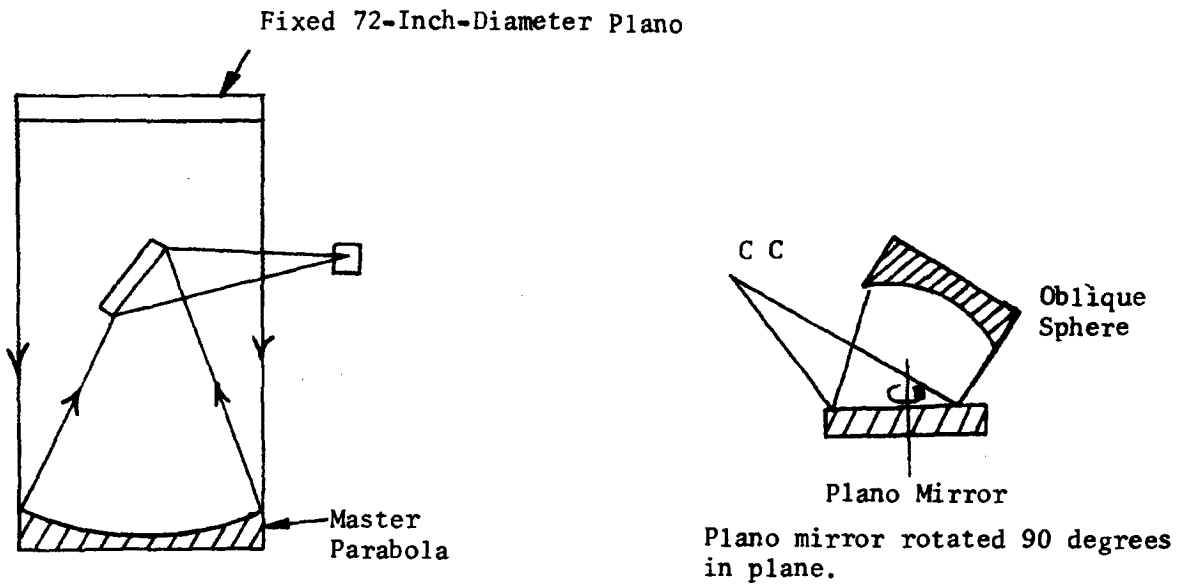
6.1.3.2 Plano Mirrors. Plano mirror tests are difficult to accomplish because any single test configuration has an associated surface error which cannot be detected with the degrees-of-freedom allowed in interferometric tests. If a plano mirror has a slight residual power, such a defect cannot be accurately measured unless a full-aperture collimator with a calibrated infinity focal point is used. Where collimators cannot be used because of size, oblique spheres can be used as shown in Figure 6.1-1b. However, there is a family of special surfaces which appear as simple power changes in this test setup. By rotating the plano mirror 90 degrees, it is possible to detect these special surfaces. At least two such positions are required and provided for in data processing.

6.1.3.3 Transmitting Elements. Materials used for transmitting elements are measured for index homogeneity to an accuracy of 1×10^{-6} . In addition, measurements of both faces and of a transmitted wavefront are made with a

~~SECRET~~ D



(a) Optical Test Configurations for Mirrors with Power



(b) Plano-Mirror Test Configurations

Figure 6.1-1. Mirror Test Configurations

~~SECRET~~ D

BIF-008- [REDACTED] -68
(Control Number)

calibrated interferometer. Transmitting components, all of which have spherical surfaces, can be independently measured interferometrically for each surface. Concave surfaces are measured as spherical mirrors. Convex surfaces are currently measured using precision test-glass methods.

6.1.3.4 Noninterferometric Tests. Noninterferometric tests will also be performed on components. These include the familiar knife-edge and point-source autocollimation tests (see paragraph 6.2.1).

6.1.4 Master and Auxiliary Element Tests

Test geometries (for example, f /No., diameter) for master and auxiliary elements are identical to geometries for equivalent flight elements.

6.1.5 Subsystems Tests

6.1.5.1 Ross Correctors. Ross corrector assemblies require a complementary asphere for interferometric tests. If the asphere is previously known, the Ross error function $E_R(x,y)$ can be defined by subtracting the asphere contribution from the measured values; that is,

$$E_R(x,y) = E_M(x,y) - E_A(x,y),$$

where: $E_M(x,y)$ is an array of measured wavefront errors, and
 $E_A(x,y)$ is a corresponding array of known wavefront errors for the reference asphere. This operation can be performed automatically with currently developed computer programming.

~~SECRET~~ D

~~SECRET~~ D

BIF-008- [REDACTED] -68
(Control Number)

6.1.5.2 Optical Assembly (OA) Tests. Tests of the optical assembly are performed by autocollimation against a master-quality plano mirror. Interferometric data are collected by either a monochromatically illuminated interferometer such as the Williams, or a heterochromatic reconstructed reference interferometer. The resultant wavefront data can then be studied directly, or computer processed to obtain information on aberration levels and to obtain heterochromatic modulation transfer function (MTF) and heterochromatic resolution estimate data. Photographic data are also collected by autocollimation techniques. The method is more fully described in paragraph 6.2.3.

A. Optical Assembly Isothermal Optical Quality Test. The most important OA test, from the standpoint of performance prediction, is the OA isothermal optical quality test. This test is an isothermal, full-field full-aperture double-pass optical quality test which provides the data necessary to evaluate heterochromatic image quality and field tilt of the OA. The test results are used to (1) determine compliance with design specifications and (2) provide data to be used in performance prediction. The test configuration consists of the OA mounted in Chamber III together with a 72-inch-diameter reference mirror. The OA and autocollimating reference mirror are mounted in Chamber III as shown in Figure 6.4-1. After evacuating the chamber to a soft vacuum and thermally stabilizing the OA, a remotely controlled heterochromatic laser interferometer is used to produce interferograms of the system in four colors and at five field positions. A through-focus sweep is generated computationally to obtain a best focal plane. The heterochromatic laser interferometer module is used to make simultaneous measurements in each color for the correct determination of longitudinal and lateral color aberrations. The laser

~~SECRET~~ D

~~SECRET~~ D

BIF-008- [REDACTED] -68
(Control Number)

source provides the four wavelength source points in the system focal plane. The interference obtained within the reconstructed reference interferometer provides direct information on the system wavefront. The laser source, associated video monitor, positioning, and photographic functions are controlled remotely from outside the test chamber. Vibration isolation and optical vacuum are used to reduce image motion and subsequent smearing of the interferograms.

Interferogram data processing is used to provide the wavefront contour produced by the OA and the coordinate location of the heterochromatic on-axis best focal point. Off-axis (four positions) heterochromatic best focal points will be used to determine platen tilt of the flight camera with respect to the Ross barrel/camera mounting reference points.

B. Optical Assembly Photographic Test. This test provides a visually interpretable confirmation of the optical performance of the OA and is designed as a supplement to the interferometric test described above. The test configuration is essentially the same as that of the isothermal optical quality test with the exception of the replacement of interferometer module by the photographic test equipment. The test camera provides photographic images of the types of targets provided. These images can then be subjected to both visual and electro-optical examination. The photographic test equipment used is discussed in paragraph 6.2.3.

6.1.5.3 Performance Testing. At the mission module (MM) assembly level, the configuration of the tracking mirror (TM) and camera optical assembly (COA) combination is such as to preclude correct support for testing in a gravitational environment. One or more elements sags under its own weight if the mission module assembly (MMA) configuration is adhered to. Optical performance estimation of the total subsystem will therefore be

6-10
~~SECRET~~ D

Handle via BYEMAN
Control System Only

~~SECRET~~ D

BIF-008- [REDACTED] -68
(Control Number)

inferred from individual tests of the OA and the TM. In the separate tests gravitational effects can be minimized. Contributions to the total subsystem aberration will be combined analytically and the subsystem resolution estimates computed.

6.1.6 Special Environmental Considerations

A vacuum environment for high-precision tests is required to avoid turbulence and convection flow phenomena which would otherwise limit obtainable precision to values greater than $\lambda/10$.

Vibration-reducing structures and isolation systems are required to provide adequate conditions for data collection.

For zero-g simulation, all elements which sag more than their surface tolerance must be supported so that deflections are reduced to acceptable levels. The method for support depends on restrictions imposed by element design. Tests at component level will depend considerably on air-bag type mounts. The function of an air bag is to provide uniformly distributed support over the back surface of the mirror during ground tests. This procedure is intended to reduce sag which would otherwise occur if the mirror were simply supported at the rim in a one-g environment (see paragraph 6.2.6).

6.2 OPTICAL TEST EQUIPMENT

The optical test equipment for the Dorian Program is being designed and developed to provide the necessary precision and sensitivity for evaluation

~~SECRET~~ D

~~SECRET~~ D

BIF-008- [REDACTED] -68
(Control Number)

of large plano and aspheric mirrors, as well as refractive components and optical assemblies. Objective and quantitative techniques are planned for all acceptance tests with emphasis on interferometry and computerized data processing. Heterochromatic interferometers using newly developed multi-wave lasers are being designed and developed. In addition, considerable progress has been made in such areas as remote displays and real-time data recording by the use of image orthicon and video-tape devices.

6.2.1 Knife-Edge and Point Source Devices

6.2.1.1 Knife-Edge Tester. The Foucault knife-edge test is a classically rapid, sensitive method for determining surface smoothness and regularity. The test is preferably used in conjunction with an interferometer to provide quantitative information because the test is otherwise largely subjective and qualitative in nature.

The knife-edge method uses an illuminated slit rather than a pinhole for the brightest image, with one edge of the slit common to the source and the return slit image. The use of a common, straight knife edge, when aligned to the optical axis of the test sample, provides a highly desirable co-linear, equi-path configuration. The knife-edge tester shown in Figure 6.2-1 is mounted on a three-axis mount for full orthogonal positioning capability.

6.2.1.2 Point-Source Autocollimation Microscope. The point-source microscope provides a classic method for testing optics for quality and performance, as well as providing utility in collimating and aligning optics prior to tests. A microscope system is arranged to project a point or

~~SECRET~~ D

BI F-008 - [REDACTED] -68
(Control Number)

~~SECRET~~ D

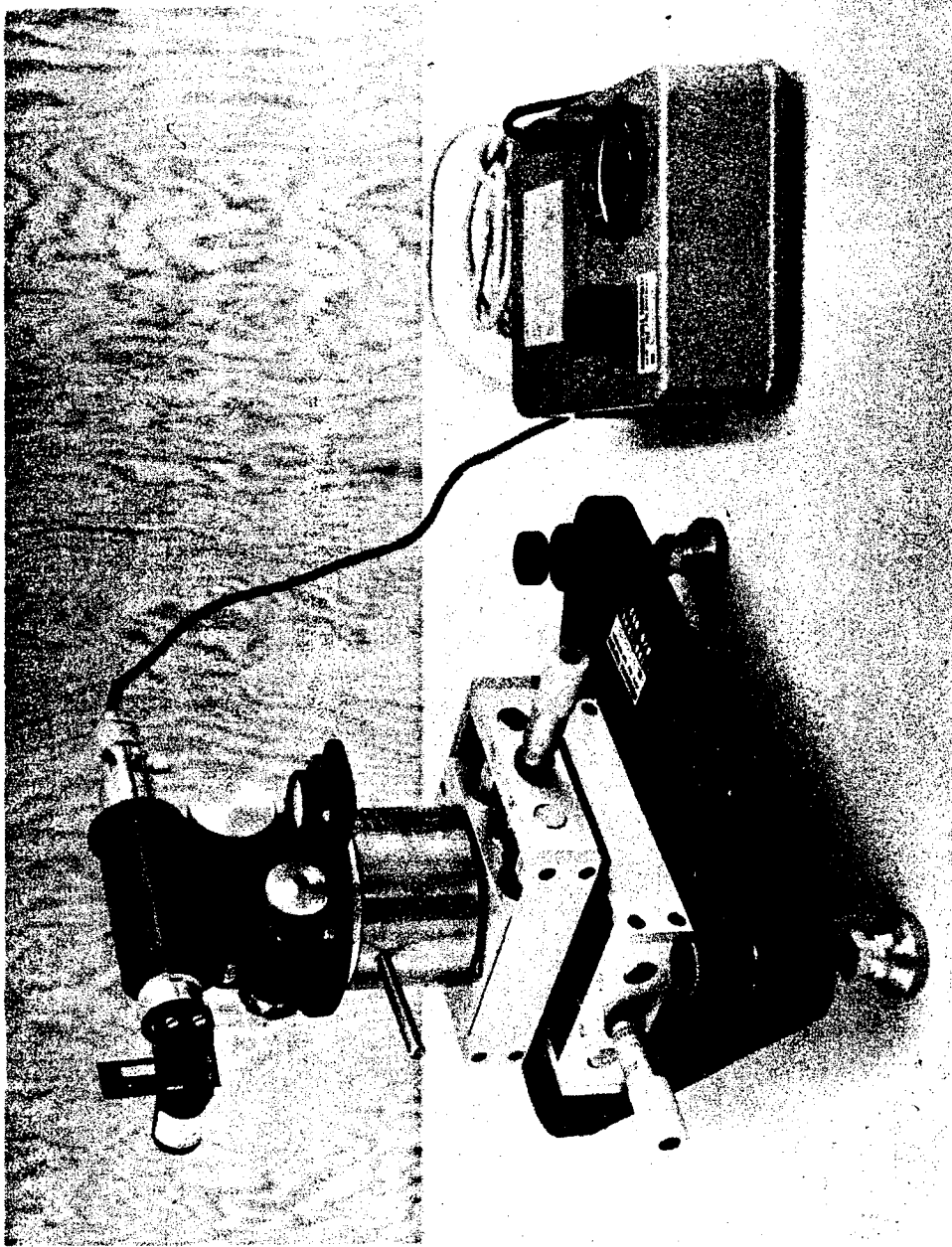


Figure 6.2-1. Knife-Edge Tester

Handle via BYEMAN
Control System Only

~~SECRET~~ D

~~SECRET~~ D

BIF-008- [REDACTED] -68
(Control Number)

star source to optics being tested as well as to view the return image. The point source is minified to form an object for the optic being tested, which is geometrically smaller than the required theoretical diffraction disc. The reflected and/or refracted return-star image provides a measure of the test-optic quality in terms of the point-spread function.

The point-source microscope uses a modified Leitz beam-dividing system with infinity corrected objectives for minimum residual spherical aberration (that is, less than $\lambda/10$ aberration at half-aperture, double pass). An efficient zirconium-arc source illuminates a 25-micron-diameter sealed-in-glass pinhole which is further reduced by the microscope objectives from 4 to 20 times. A 4X objective is used for testing focal ratios exceeding $f/10$ (Airy disc 5×10^{-4} inches), a 10X objective for focal ratios from $f/5$ to $f/10$, and a 20X from $f/2.5$ to $f/5$. The test optic is therefore always illuminated by a point source which is diffraction limited.

6.2.2 Interferometers

6.2.2.1 Twyman-Green Interferometer. The Twyman-Green interferometer, as diagrammed in Figure 6.2-2, is the instrument used for the majority of optical tests. The major feature of this instrument is the use of a continuous wave, He-Ne laser source to remove equal path restrictions and permit the long paths necessary for testing large-aperture optical surfaces and systems.

Contributions to residual errors in this instrument can be made by the objective lens, beam splitter, reference mirror, and viewing optics. A flat mirror of $\lambda/100$ quality is used as the reference surface. The beam splitter and objective must also be of comparable accuracy because the

~~SECRET~~ D

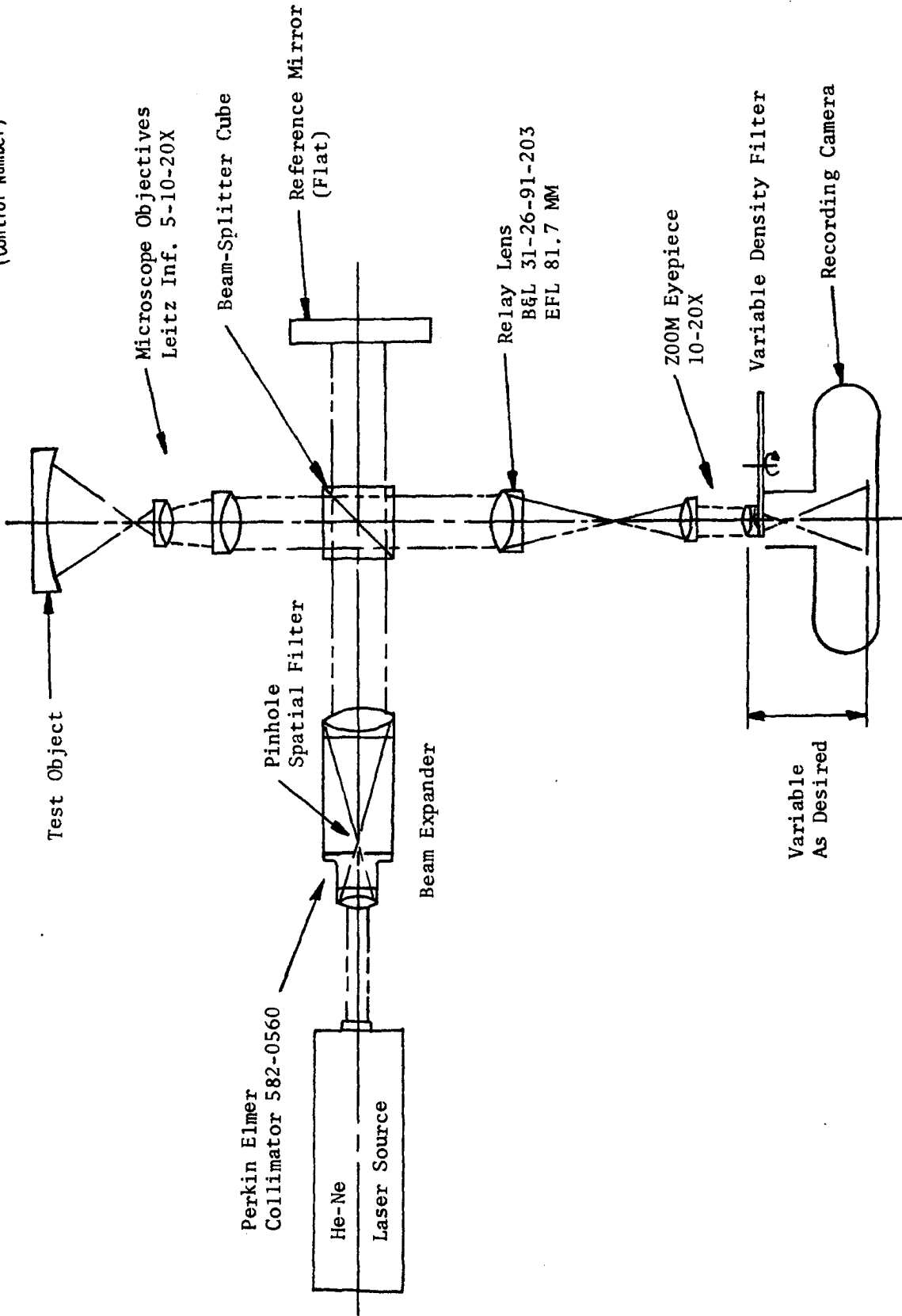


Figure 6.2-2. MOD II Twyman-Green Interferometer Schematic

~~SECRET~~ D

BIF-008- [REDACTED] -68
(Control Number)

beam travels through these elements twice. To ensure an accuracy of $\lambda/40$ in the instrument, the beam splitter and objective should have errors less than $\lambda/100$. Because these tolerances are not usually met, the instrument has to be calibrated against a known test mirror.

High signal-to-noise ratio interferograms can be obtained with a Twyman-Green interferometer. A pinhole-type spatial filter in the beam expander eliminates noise and diffraction patterns resulting from any foreign matter on the optics preceding the filter. The pinhole also eliminates interference between the lenses in the beam expander. Spurious interference patterns can also be obtained from any two orthogonal faces on the beam splitter cube. These patterns can be significantly reduced by high-efficiency multi-layer anti-reflection coatings, optimized for the wavelength in use. All air-glass surfaces have to be relatively free from dust and dirt which produce diffraction patterns.

The Twyman-Green interferometer shown in Figure 6.2-3 requires mechanical controls of high precision. Rack and pinion slides are used to accurately position the objective and the viewing optics, and a precision screw slide is used to laterally position the entire instrument. The reference mirror assembly requires fine pitch screws to independently control the tilt of the reference mirror in order to achieve the desired interference fringe display.

6.2.2.2 Williams Interferometer. The Williams interferometer is an unequal path instrument similar in some respects to the Twyman-Green. This interferometer uses a spherical reference mirror, objective lens, spatial filter (pinhole), beam splitter, and He-Ne gas laser. A diagram of the Williams interferometer is shown in Figure 6.2-4 and a breadboard model is pictured in Figure 6.2-5.

~~SECRET~~ D

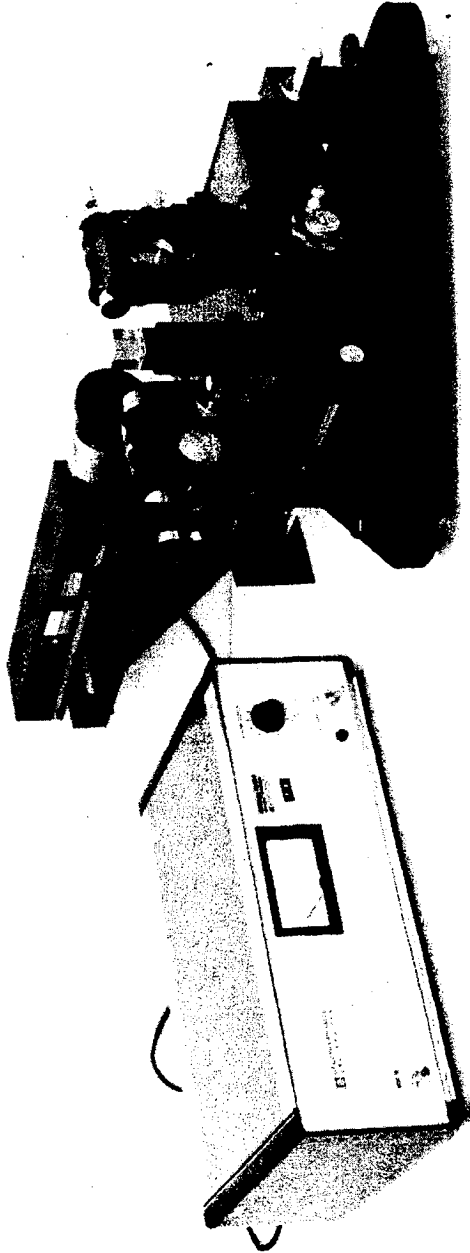


Figure 6.2-3. Twyman-Green Interferometer

Handle via BYEMAN
Control System Only

~~SECRET~~ D

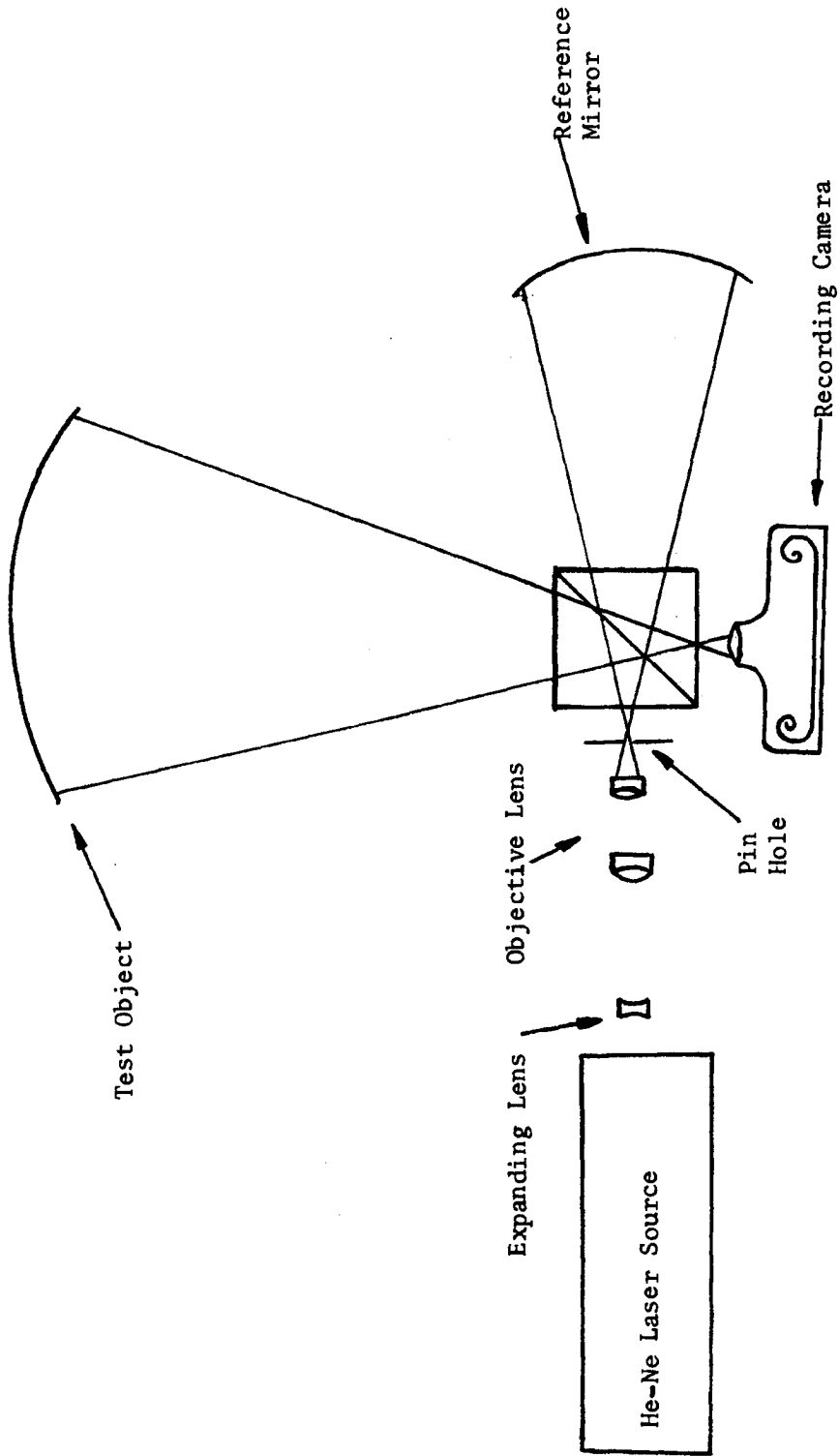


Figure 6.2-4. Williams Interferometer Schematic

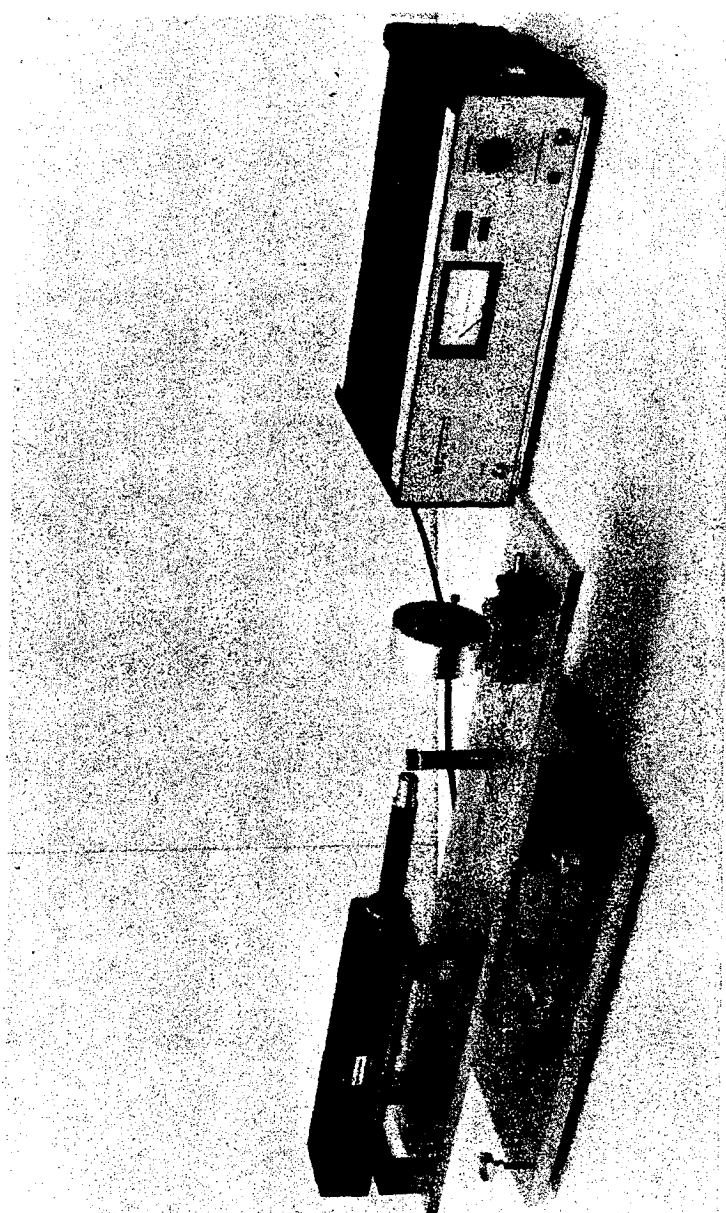


Figure 6.2-5. Williams Interferometer (Breadboard Model)

Handle via BYEMAN
Control System Only

~~SECRET~~ D

BIF-008-

(Control Number)

-68

Interference between the sample and reference beams occurs when the two spherical wavefronts recombine at the beam splitter. To obtain a fringe pattern of straight lines, the two beams have to be translated with respect to each other. This translation is small; that is, 0.001 inch for 20 fringes with an $f/4$ test object and 0.003 inch for 20 fringes with an $f/12$ test object.

Errors can be contributed by the reference sphere, objective, beam splitter, and camera lens distortion. The errors in the objective will be eliminated by the use of a diffraction-limited pinhole. The errors in the beam splitter are common to both beams, and will cancel if their magnitude is small. The two primary sources of error which are uncorrected by the design are the reference sphere, which is always of highest optical quality, and the recording camera lens distortion. These errors can be reduced to less than $\lambda/40$ by the selection of correct elements.

The Williams design eliminates major ghost interference patterns from the beam-splitter faces, because the beam splitter is working with diverging and converging light. Other sources of stray interference patterns in the objective are eliminated by the pinhole spatial filter. Interference patterns obtained with the Williams are generally of high contrast and noise free. Another feature is that it is possible to test aspheres at their center of curvature and see undistorted fringes to the edge of the test piece. This fact results because the depth of field is not limited by the objective but rather by the recording-camera lens.

The construction of a Williams interferometer is simplified by the reduced number of optical elements compared to the Twyman-Green. An accurate tri-axial cross slide assembly is needed for focus, lateral movement, and height adjustment.

6-20

~~SECRET~~ D

Handle via BYEMAN
Control System Only

~~SECRET~~ D

BIF-008- [REDACTED] -68
(Control Number)

6.2.3 Photographic Test Equipment

6.2.3.1 Test Requirements and Approach. The photographic test equipment is required to provide a means for the photographic tests of the OA. See Figure 6.2-6. The test requirements were analyzed with respect to the test geometry and availability of auxiliary optical elements. Photographic records will be on Type 3404 Film and processed to correspond to flight-recording material characteristics. The selected approach allows maximum subsystem utilization and requires a minimum number of auxiliary optical elements. An autocollimating geometry is used which allows field splitting of the target and recording medium in the image plane of the subsystem. Target (object) information placed in the target half of the subsystem image plane can be imaged in either of two ways. By keeping the autocollimating mirror parallel to the optical axis, the target areas are re-imaged in diametrically opposite positions in the other half of the image plane. This operational mode provides double sensitivity to longitudinal focal shifts in the image plane, and allows the contour of the image plane to be determined as a function of field position. By tilting the autocollimating mirror to half the desired field angle, at the correct field azimuth, the axial target can be imaged at any position in the other half of the image plane. This mode of operation is directly analogous to that used in heterochromatic interferometry. Placement of Type 3404 Film in the receiving half of the image plane allows either type of double passed image to be recorded and subsequently analyzed. By placing target information at selected points in the target half plane and recording the target image at the set of field points required, the quality of the double-passed images can be studied at those field points of the OA.

~~SECRET~~ D

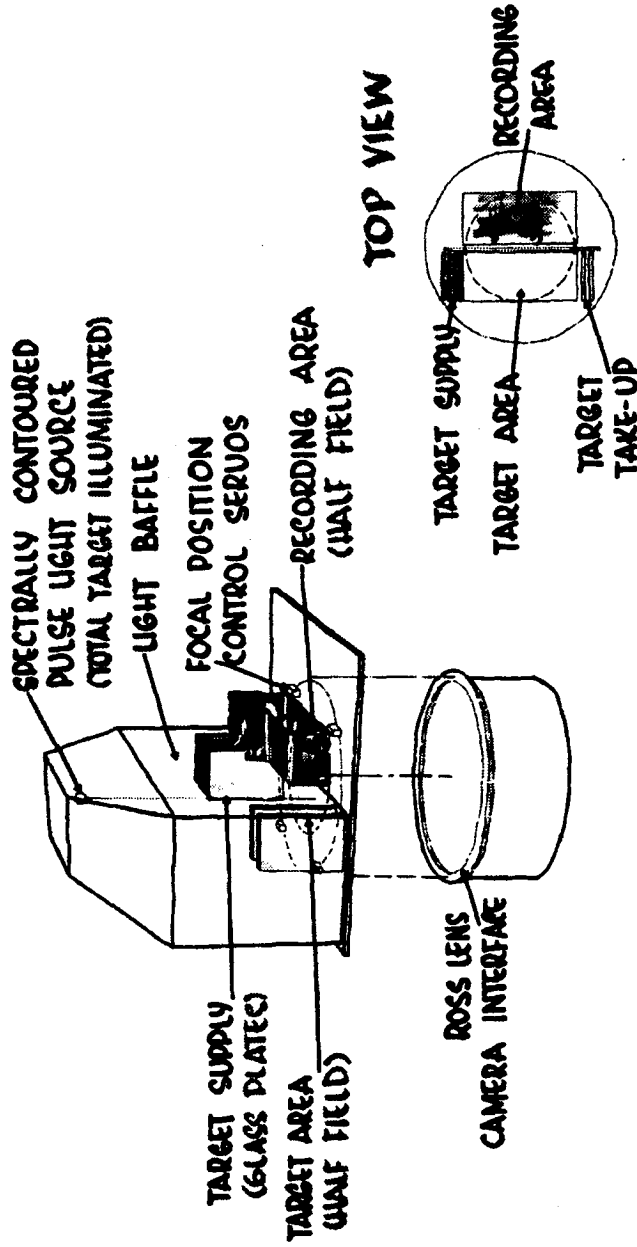


Figure 6.2-6. Photographic Test Equipment

Handle via BYEMAN
Control System Only

~~SECRET~~ D

~~SECRET~~ D

BIF-008- [REDACTED] -68
(Control Number)

6.2.3.2 Equipment Design Considerations. The photographic test equipment has coplanar target and recording medium planes placed in the image plane of the OA subsystem. The test environment exterior to the device is a thermally isotropic optical vacuum. The test environment maintained internal to the photographic test equipment is a thermally isotropic five-psi environment. Five psi is used for the internal pressure in order to duplicate the flight operational environment and to allow the photographic materials to be more easily utilized.

The photographic test equipment interfaces with the Ross barrel at the flight-camera mounting flange.

Engineering analysis indicates that a minimum set of targets to be used in testing and/or performance demonstration consists of:

- a. Tri-bar targets
- b. Seven-bar targets
- c. Scenic targets (actual or simulated)

Current target configuration is shown in Figure 6.2-7. A total of eleven target areas are shown for a typical target plane. Each target area contains a complete spatial frequency sweep for target types (a) and (b) or a single scene. The spatial frequency range to be included extends from approximately 18 lines/mm to approximately 340 lines/mm, except for scenic targets, whose upper frequency limit will correspond to approximately [REDACTED] ground resolution. The targets will be held in a magazine-like assembly. The magazine geometry and associated drives will allow fully automatic and remote interchange of target plates, each plate containing one type of target subject matter.

~~SECRET~~ D

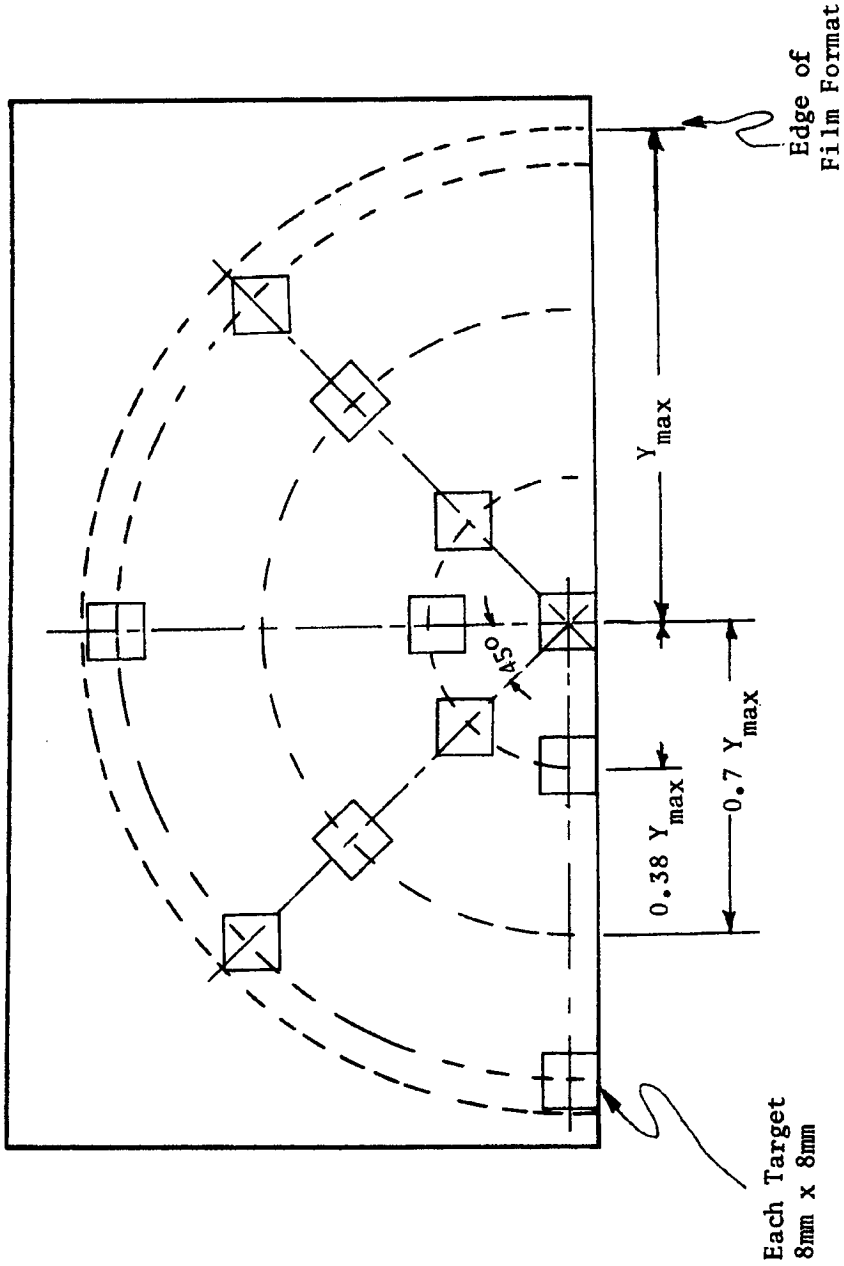


Figure 6.2-7. Photographic Target Format

Handle via BYEMAN
Control System Only

~~SECRET~~ D

~~SECRET~~ D

BIF-008- [REDACTED] -68
(Control Number)

Type 3404 Film will be supplied to a vacuum platen in the half-plane adjacent to the target half-plane.

Illumination of the targets is provided by a fiber optic/pulsed Xenon-lamp source unit. Illumination incident on the Type 3404 Film will have spectral, temporal, power, and angular characteristics equivalent to operational levels.

6.2.3.3 Data Utilization and Analysis. Data collected in the form of photographic records of the three types of targets can be subjected to visual and electro-optical examination. The transformation from double to single-pass results will utilize knowledge of the actual wavefront contour rather than assuming an equivalent focal shift.

6.2.4 SDM-2 and Transmissibility Vibration Test Equipment

Current requirements for performance prediction and analysis necessitate simultaneous measurement of image smear and smear-contributing vibrations. These tests are complicated by the number of significant contributors; the level of sensitivity required in detection, measurement, and recording; and the need for techniques permitting computer analysis. The foregoing demand unique, state-of-the-art components, configuration, and techniques.

The measurement of image smear has been accomplished by an autocollimating technique in which the optical system forms a superimposed grating image and test grating at the image plane (see Figure 6.2-8). The vibration of the optical system results in relative motion of the grating image with the test grating. The relative motion causes variation in the light rays relayed to a photo sensor. Two orthogonal sets of gratings give vibrations along orthogonal axes.

~~SECRET~~ D

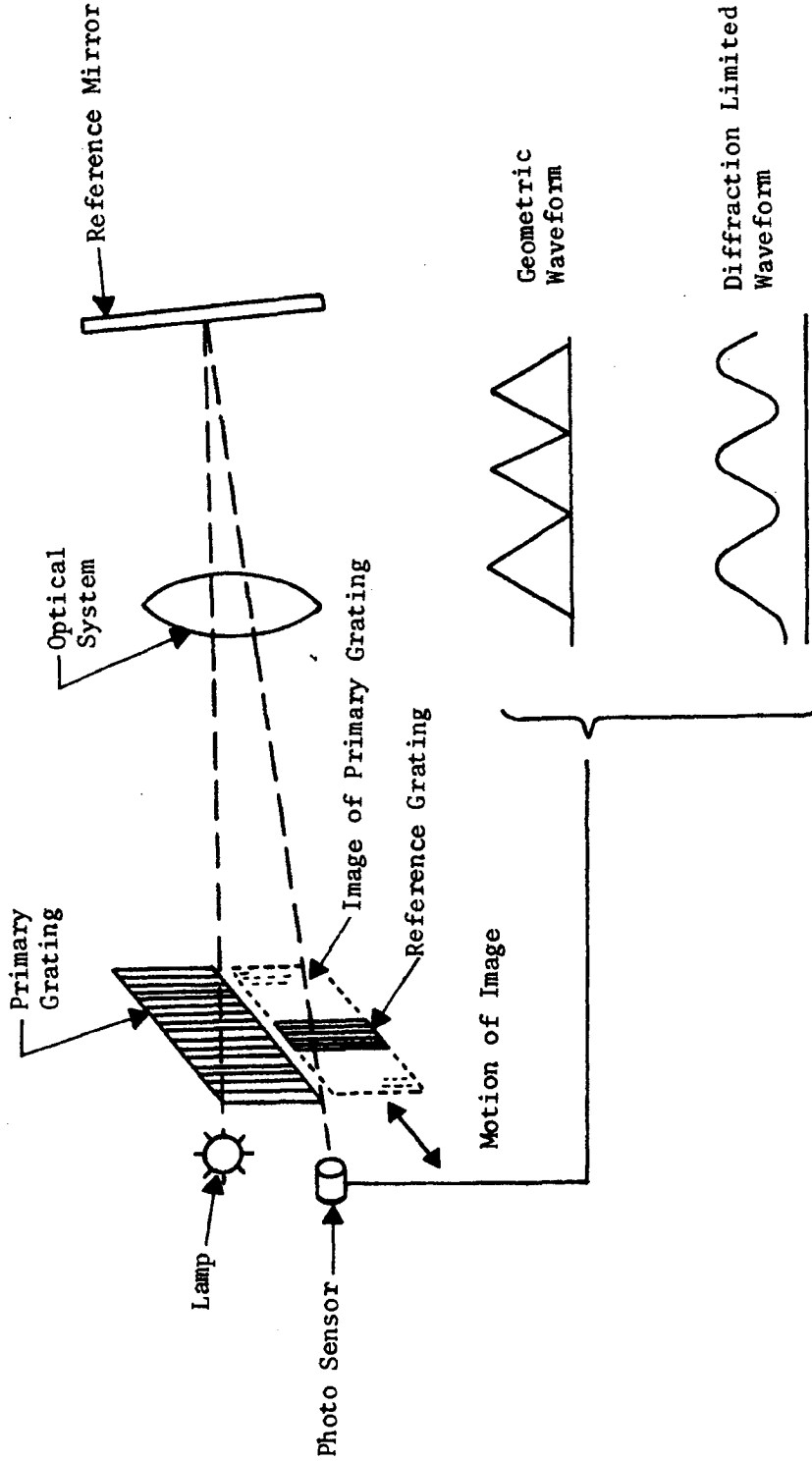


Figure 6.2-8. Optical Measurement of Image Smear.

Handle via BYEMAN
Control System Only

~~SECRET~~ D



~~SECRET~~ D

BIF-008- [REDACTED] -68
(Control Number)

When the grating spacings are large with respect to the wavelength of light, the output as a function of displacement is determined by geometrical considerations producing a triangular waveform. When the grating spacings approach the diffraction limit of the optics being tested, the gratings favor the fundamental spatial frequency producing a sinusoidal waveform.

The localization, identification, and measurement of significant smear contributing vibrations is accomplished by placing accelerometers on the significant structural elements. Acceleration measurements present unique requirements for sensitivity in displacement resolution of 0.1 micron or better. This may be as low as $10^{-6}g$ at 5 Hertz (Hz) at the primary mirror edge. Such low output signals require low noise amplifiers with low distortion at the sensor to raise the signal level in the 1 to 10 μ volt range to the order of millivolts for transmission to the data recording equipment.

Continuous electrical integration of the outputs of accelerometers attached to optical elements provides an immediate or real-time measure of the displacement of the element with time, and facilitates the correlation of element vibration with optical image motion. Integrators of this type have been designed, constructed, and tested with results which indicate their usefulness in visual data correlation as well as simplification of computer analysis.

The correlation of accelerometer-derived displacement measurements with optically measured displacement has been demonstrated with several breadboards of increasing complexity. The first, made with a simple optical system, clearly demonstrated the principle that the optical and inertial

~~SECRET~~ D

~~SECRET~~ D

BIF-008- [REDACTED] -68
(Control Number)

measuring techniques give comparable results. The second, with a more complex optical system, showed that contributions of individual elements are separable by data conversion techniques using the frequency domain. The third, with an autocollimated optical system in a vacuum chamber, showed that the mechanism of vibration transfer can be secured from the frequency-time amplitude plot (sonogram).

The correlation of accelerometer-derived displacement measurements with optically measured displacement has been demonstrated at the simple bread-board level. Representative time-amplitude traces as recorded are presented in Figure 6.2-9. The upper trace is the optically measured displacement, and the lower trace is the accelerometer-derived rotational displacement. The data were transformed from time to frequency domain by computer. The frequency spectra are presented in Figure 6.2-10 and show excellent correlation.

The contribution of one of several excited elements in a more complex system is shown in Figures 6.2-11 and 6.2-12. Figure 6.2-11 shows the system response and Figure 6.2-12 the equivalent Ross folding-mirror response. The upper left of each figure shows the time series as recorded; the upper right shows the amplitude of the various frequency components and the lower center shows the frequency distribution over the seven-second period which includes two sets of impulses exciting the optical system.

The region below 5 Hz shows the effects of ground noise and air turbulence. The response of the folding mirror is shown in the upper right by the coincidence of frequency response at 22 Hz, 52 Hz and 75 Hz. At the lower center of the sonagram, the folding mirror contribution is also discernible by the time lag of about a second in the first set of impulses.

~~SECRET~~ D

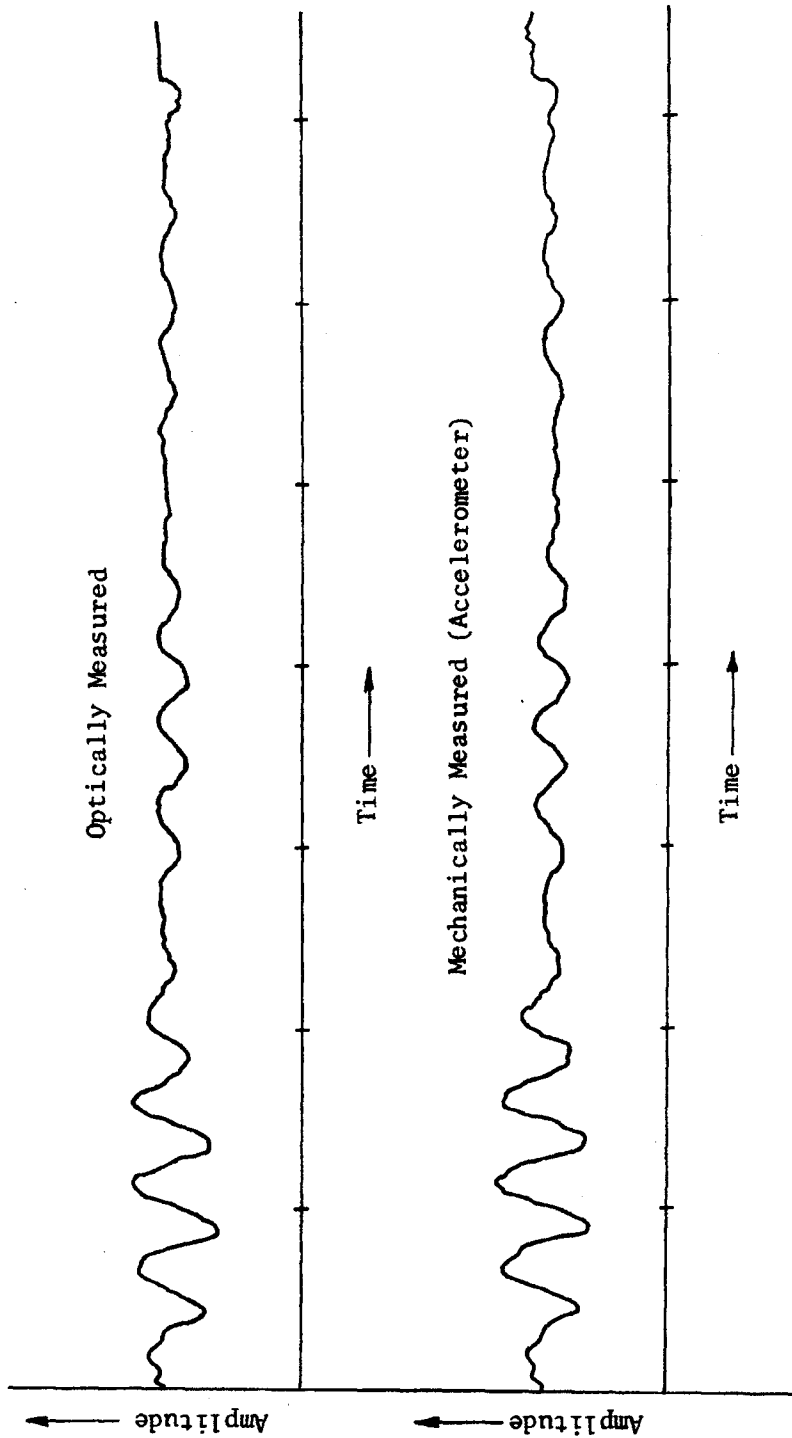


Figure 6.2-9. Time-Amplitude Traces - Optically Measured and Mechanically Measured (Accelerometer) Data

Handle via **BYEMAN**
Control System Only

~~SECRET~~ D

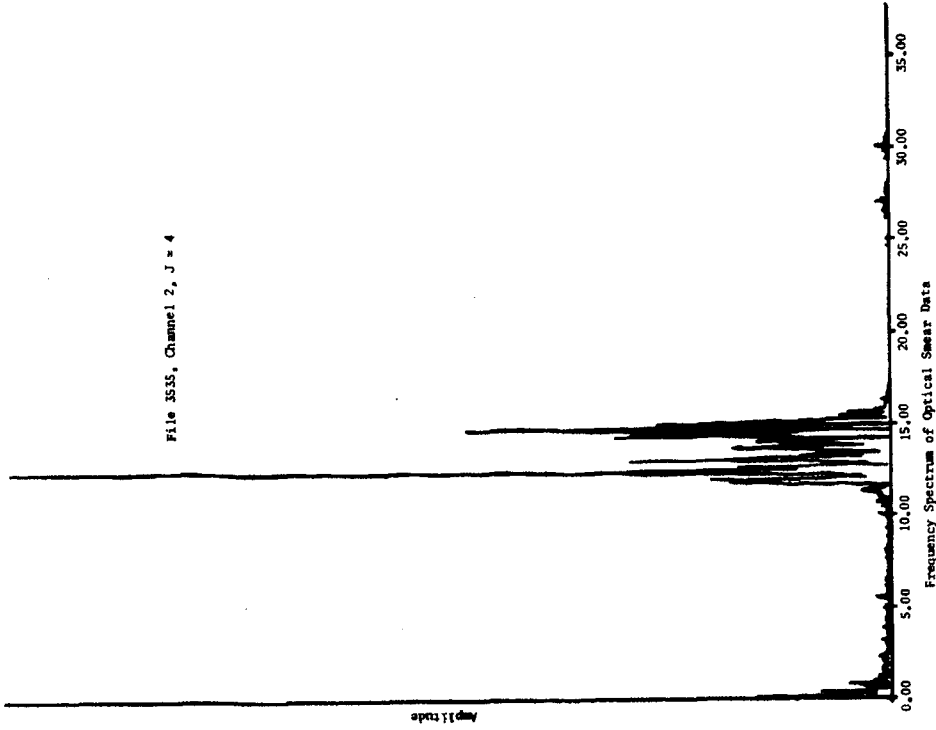
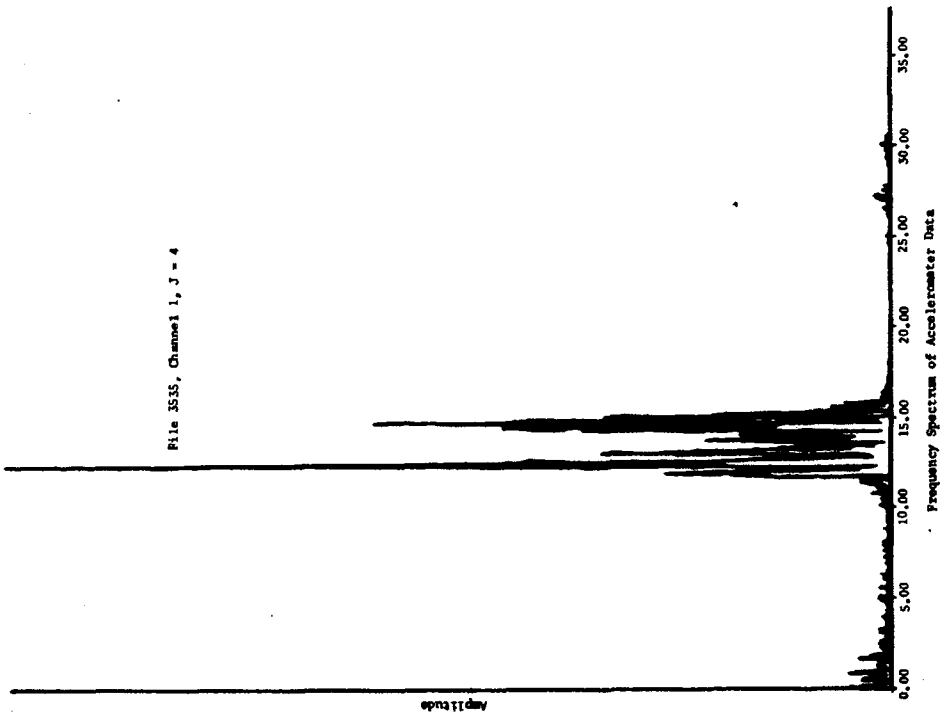


Figure 6.2-10a and 6.2-10b. Typical Frequency Spectra

Handle via BYEMAN
Control System Only

~~SECRET~~ D

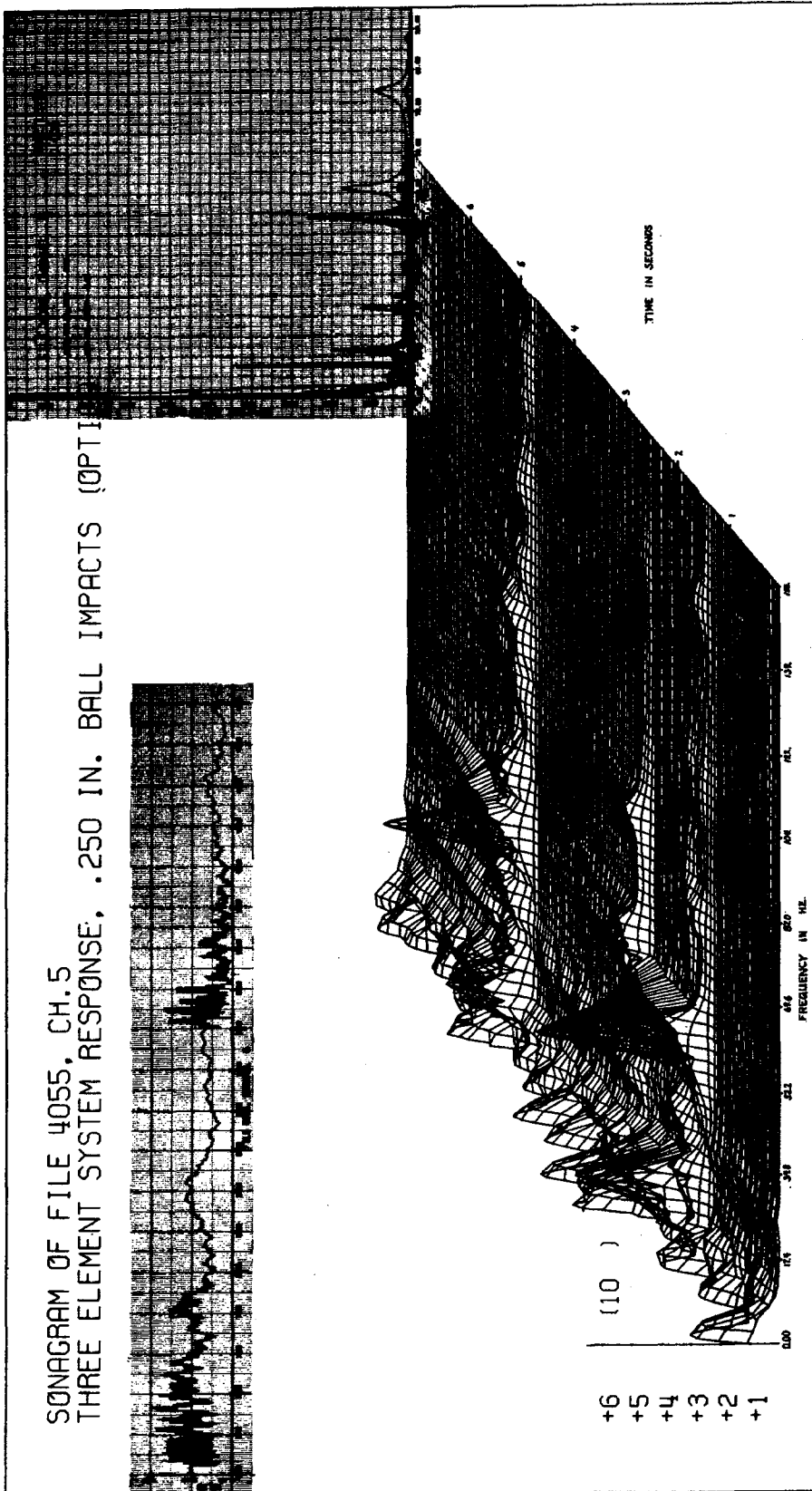


Figure 6.2-11. Sonagram of System Response

Handle via **BYEMAN**
Control System Only

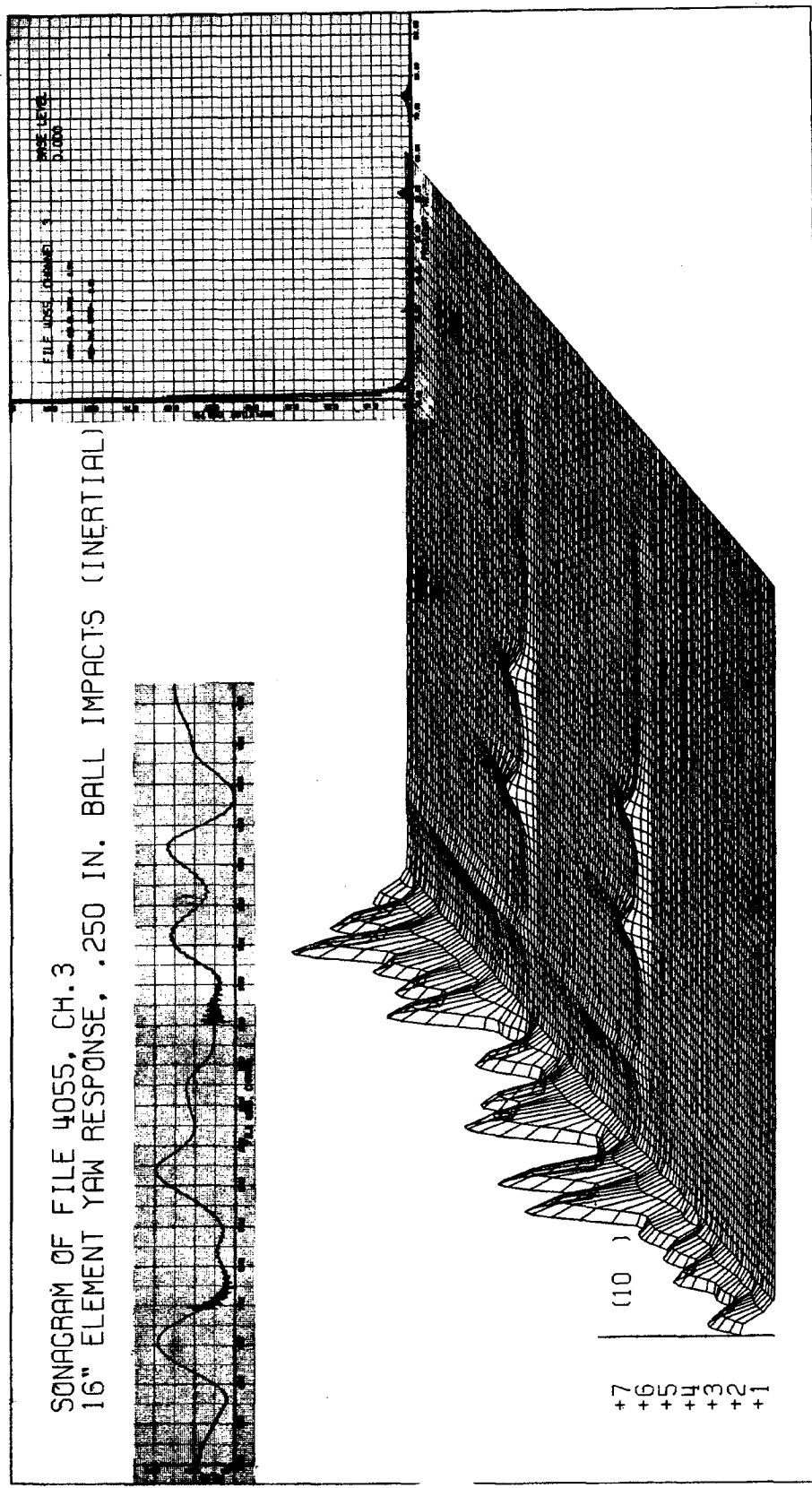


Figure 6.2-12. Sonogram of Ross Mirror

Handle via BYEMAN
Control System Only



~~SECRET~~ D

BIF-008-[REDACTED]-68
(Control Number)

The differing mechanisms of noise excitations of a mirror in a test chamber at one atmosphere (760 Torr) and one Torr are indicated by the sonagrams of Figures 6.2-13 and 6.2-14. The high-level ground noise and chamber sway were removed from Figure 6.2-13 by the computer discarding all data 5 Hz and lower, to give Figure 6.2-14. The one atmosphere data of Figure 6.2-14a shows a high amplitude response at 60 Hz and little in the 30-to 55-Hz region. The one Torr of Figure 6.2-14b shows low response at 60 Hz and significant undulations in the 30- to 55-Hz region. This indicates a strong airborne 60-Hz drive of the mirror and an air damping of the natural frequencies of 30 to 55 Hz of the mirror and support. The 120-Hz unknown results from relative motion of opposite edges of the 12-inch folding mirror on the order of 0.02 micro meter, an easily detected quantity.

6.2.5 Data Recording and Processing

6.2.5.1 Interferometric Data Recording. A 35mm reflex camera will be used to record interferometric data for component and some COA, optical tests, and a 70mm recorder will be used for heterochromatic interferogram data recording. Most of these tests will be performed in a vacuum environment so that recording cameras and interferometers will be remotely controlled.

An image-orthicon camera using the reflex viewer, will be used to relay the interferometric display from the test station to the central console and monitor display. For special test purposes, interferometric data can be obtained by recording the output of the image orthicon camera on magnetic tape and replaying the tape in slow motion, stopping at appropriate frames where stable interference patterns appear and recording these frames from the monitor with an auxiliary 35mm camera.

~~SECRET~~ D

~~SECRET~~ D

BIF-008- [REDACTED] -68
(Control Number)

SONOGRAM OF FILE 4645, NOISE AT 1 ATMOSPHERE
CH. 4. FOLDING MIRROR

SPL LEVEL
0.000

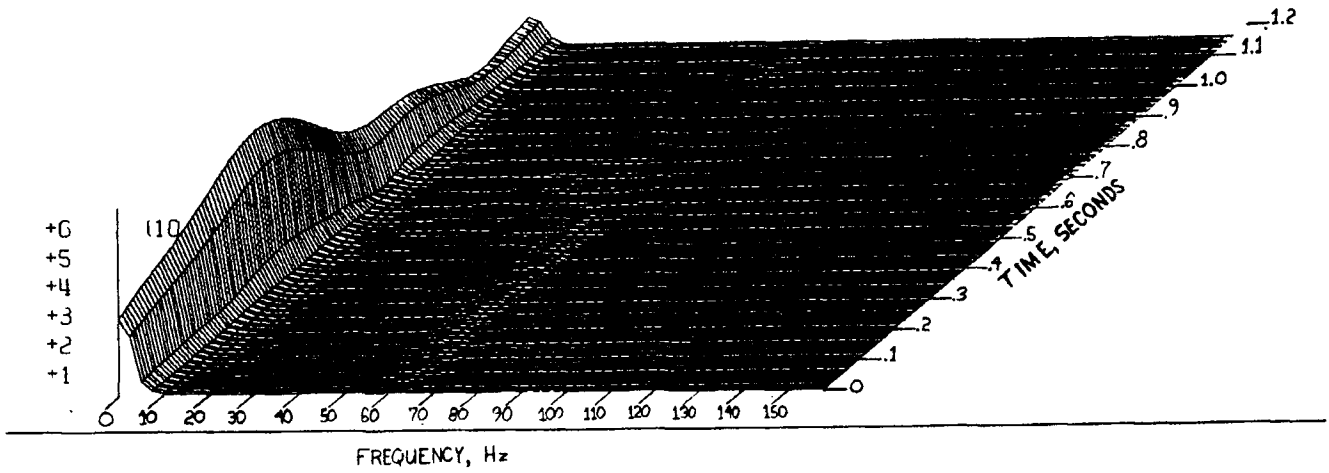


Figure 6.2-13a. Sonogram of File 4645, Noise at 1 Atmosphere
Ch. 4. Folding Mirror

~~SECRET~~ D

Handle via **BYEMAN**
Control System Only

~~SECRET~~ D

BIF-008- [REDACTED] -68
(Control Number)

SONAGRAM OF FILE 4654, NOISE AT 1 TORR
CH. 4, FOLDING MIRROR

NOISE LEVEL
0.000

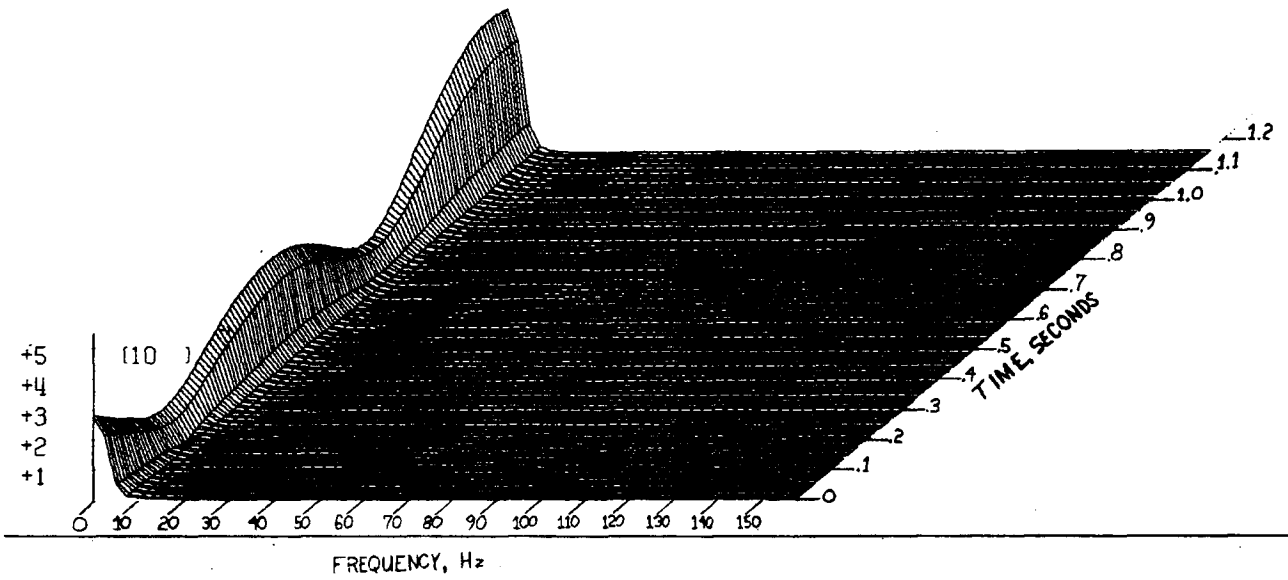


Figure 6.2-13b. Sonagram of File 4645, Noise at 1 Torr
Ch. 4. Folding Mirror

~~SECRET~~ D

Handle via BYEMAN
Control System Only

~~SECRET~~ D

BIF-008- [REDACTED] -68
(Control Number)

SONAGRAM OF FILE 4645, NOISE AT 1 ATMOSPHERE
CH. 4, FOLDING MIRROR

LINE STEP
0.000

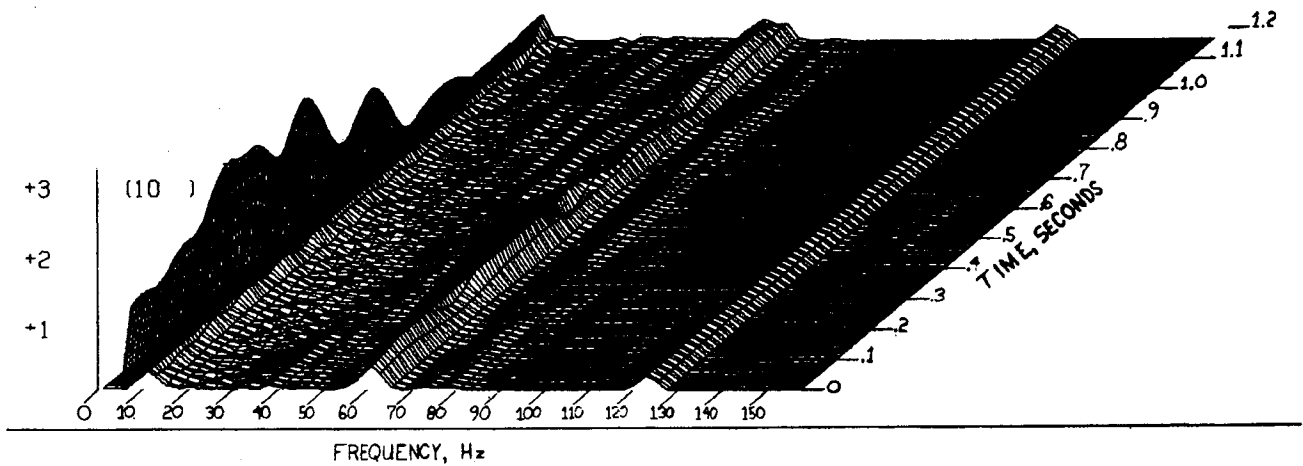


Figure 6.2-14a. Sonagram of File 4645, Noise at 1 Atmosphere
Ch. 4. Folding Mirror

6-36

~~SECRET~~ D

Handle via BYEMAN
Control System Only

~~SECRET~~ D

BIF-008- [REDACTED] -68
(Control Number)

SONAGRAM OF FILE 4654, NOISE AT 1 TORR
CH. 4, FOLDING MIRROR

TIME STEP
0.008

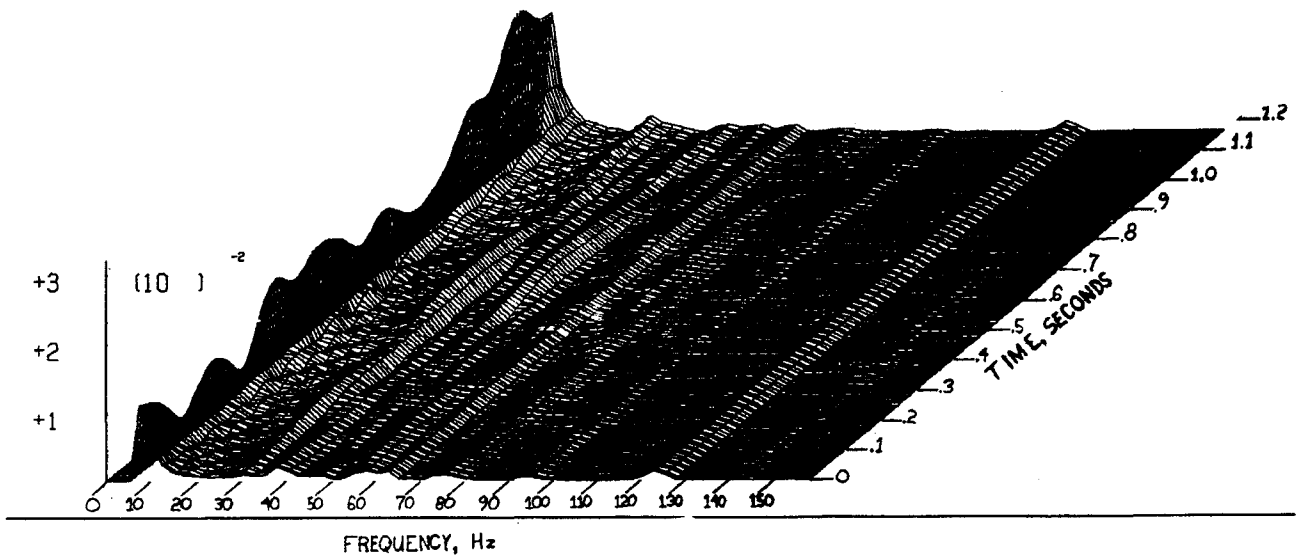


Figure 6.2-14b. Sonagram of File 4645, Noise at 1 Torr
Ch. 4. Folding Mirror

6-37
~~SECRET~~ D

Handle via BYEMAN
Control System Only

~~SECRET~~ D

BIF-008-

(Control Number)

-68

6.2.6 Pneumatic Mirror Support

Through analysis it is predicted that pneumatic support of major program optics will provide a test accuracy of better than $\lambda/20$ if correct air-bag operating pressure is established and maintained to within ± 1 percent. This sensitivity was experimentally verified with a test mirror of equivalent rigidity (4λ) to MOL-optics. Strictly speaking, this ± 1 percent criteria applies only to support of the plano TM; the deflection resulting from incorrect air-bag support is essentially parabolic, permitting relaxation of control requirements to approximately ± 5 percent for sphere and asphere testing.

An intuitive and experimentally indicated need for mirror-membrane friction reduction/elimination is to be satisfied by a mirror-hovering air jet. This method is advantageous in that once the membrane stress has been relieved, maximum friction is restored to retard any change in support condition.

The air bag is a thin flat membrane made from Butyl rubber with its perimeter sealed to a flat metal plate. The air bag is designed to be inflated to a pressure differential of approximately 0.25 psi (the area density of the mirror). Air-bag tests must satisfy two stringent requirements: (1) the free surface of the bag must be tangent to the edge of the mirror back, and (2) the bag must not cause any mechanical load to be transmitted to the Invar reference rods abutting the mirror being tested. Preliminary calculations show that pressure differential control on the order of a few parts in 1,000 over a 15-minute period is necessary. Commercially available pressure controllers were obtained to provide the required control. The correct pressure-differential control points for these units are determined for each optic by tangency of the free surface of the bag to the edge of the mirror back.

~~SECRET~~ D

~~SECRET~~ D

BIF-008- [REDACTED] -68
(Control Number)

The adequacy of air-bag support, in an absolute sense, can be established only to the accuracy to which the absolute figure of a test mirror is known. To provide this baseline, a thin flexible plano was alternately supported on and suspended from three points, thus producing equal and opposite deflections. The true zero-g figure of the test plano given by the simple average of these two (computer evaluated) deflected surfaces was compared with the figure of the same plano as determined via air-bag support. Results show a correlation to within $\pm\lambda/20$ over 80 percent of the area with the differences being random and indicative of data scatter rather than attributable to the air bag.

6.2.7 Other Optical Devices and Fixtures

6.2.7.1 Homogeneity Test Fixture. The use of relatively large diameter refractive elements of high precision in the leading lens of the Ross corrector assembly necessitates determinations of the variability of the refractive index of the lens blanks before optical processing. The tolerance in refractive index variability is $\pm 2.5 \times 10^{-6}$, approaching state-of-the-art limits in glass homogeneity.

A test fixture was designed and procured which has the capability of measuring variations in refractive index in glass blanks 5cm thickness or greater to a precision of $\pm 1 \times 10^{-6}$. The fixture uses a parabolic mirror of 26-inches free-aperture diameter arranged in an autocollimated Newtonian configuration. The beam is collimated by the parabola, folded and returned by an external plano mirror, and passes through the glass sample twice in transmission tests. The mirror has been made to highest optical standards ($< \lambda/20$ peak-to-peak surface errors per element) and has a measured double-pass system quality of $\lambda/8$.

~~SECRET~~ D

~~SECRET~~ D

BIF-008-[REDACTED]-68
(Control Number)

6.2.7.2 Test-Glass Radius Measuring Fixtures. Test glasses of long radii are required to test the surface radius and sphericity of the primary asphere, master parabola, reflective null correctors, and Ross lens elements. Several optical benches 190 and 400 inches in length were designed and assembled to provide test-glass radius measuring capability. Readout of the display is by laser interferometer.

6.2.7.3 Profiling Spherometer. The planarity or sphericity of the flight mirrors and large-diameter reference mirrors during grinding is determined by a fixture known as the profiling spherometer. This fixture has 15 Johansen "Mikrokater" comparators spaced along a bridge structure designed to measure surface deflections along a diameter of the primary asphere or plano TM. The gages have a reading sensitivity of 1×10^{-5} inch/division and the spherometer by test has a repeatability of $\pm 2 \times 10^{-5}$ inch in surface readout. The spherometer is illustrated in Figure 6.2-15 with a Pyroceram-master surface block.

6.3 DEVELOPMENTAL MODELS

In order to develop a flight model payload capable of meeting performance requirements, it is necessary to design, assemble, and test several developmental models. Two structural development models (SDM), a thermal model (THM), and an engineering model (EM) are assembled for developmental and design validation purposes. A qualification model (QM) is acceptance tested and qualified prior to flight model (FM) acceptance. Table 6.3-1 lists the assemblies and simulators which are required for these models.

~~SECRET~~ D

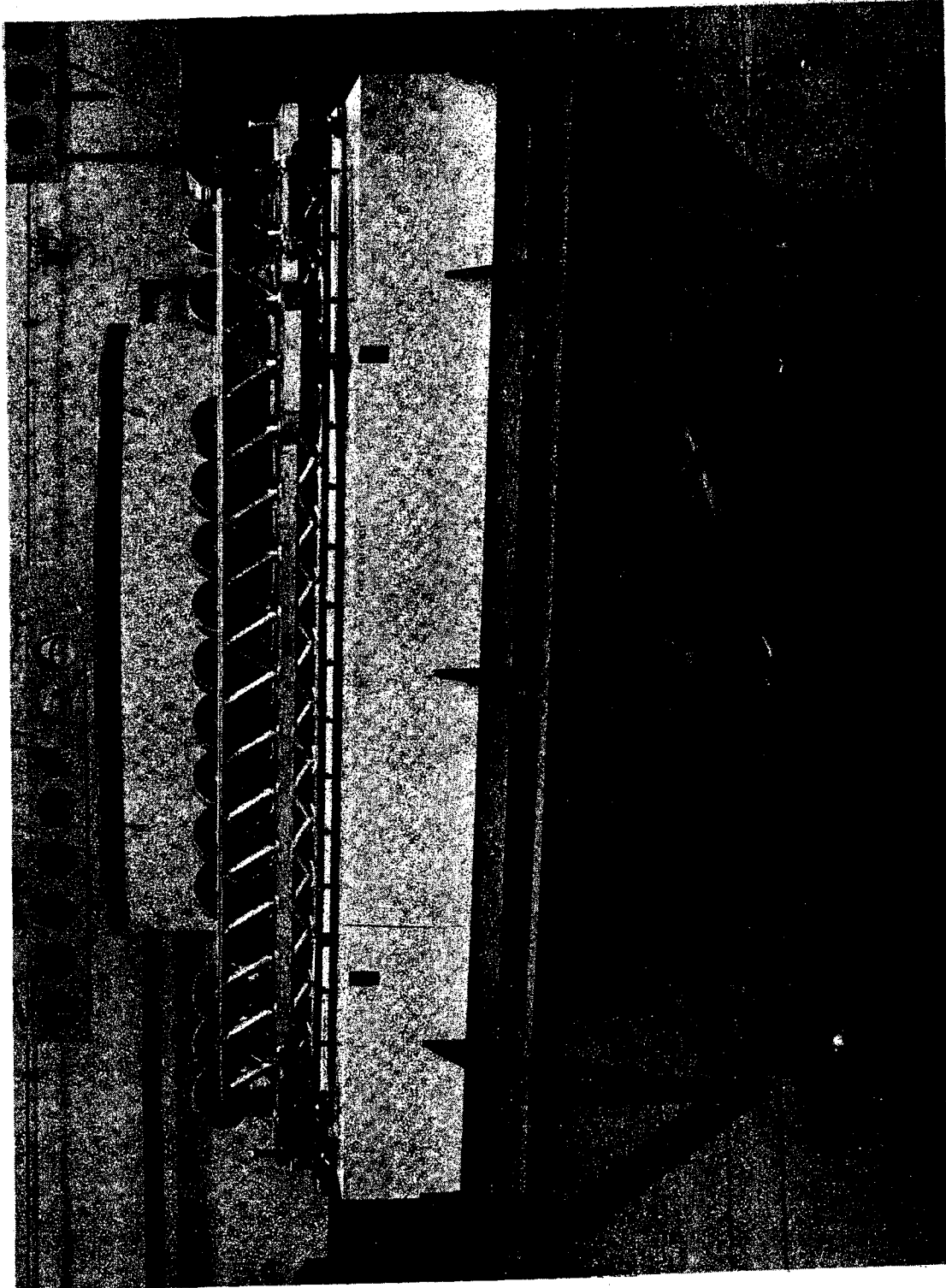


Figure 6.2-15. Profiling Spherometer on Pyroceram Master

Handle via **BYEMAN**
Control System Only

~~SECRET~~ D

~~SECRET~~ D

BIF-008- [REDACTED] -68
(Control Number)

TABLE 6.3-1
DEFINITION OF MANNED/AUTOMATIC MPS-LEVEL PRIME ASSEMBLIES AT EKC

<u>Mission Module</u>	<u>Model</u>					
	<u>SDM 1</u>	<u>SDM 2</u>	<u>THM</u>	<u>EM</u>	<u>QM</u>	<u>FM</u>
Optical Assembly	X	X	X	X	X	X
MMAS structure (GFE)	X	X	X	X	X	X
MMFS w/simulated TM (GFE)	X	X				
MMFS thermal simulator (GFE)			X			
MMFS simulator				X	X	X
MMFS w/TM drive (GFE)				X	X	X
TM and mount			X	X	X	X
Bellows assembly (GFE)	X		X	X	X	X
COA mount set	X		X	X	X	X
<u>LM Subsystem</u>						
Camera				X	X	X
Film handling				X	X	X
Console components				X	X	X
Processor/dryer				X	X	X
Visual optics				X	X	X
Electronics				X	X	X

~~SECRET~~ D

~~SECRET~~ D

BIF-008- [REDACTED] -68
(Control Number)

6.3.1 Developmental Models

6.3.1.1 Structural Development Models. The two SDM's consist of a camera optical assembly (COA) structure (see Figure 4.2-2) similar to that intended for the FM's; that is, similar in materials, mass distributions, stiffness and weight. The SDM's include mass simulations of mirrors, lenses, camera and other components which may have a significant affect on the dynamic characteristics of the PP. The purpose for the SDM's is to determine the dynamic characteristics of the COA through structural and component response to external vibratory inputs during physical testing.

Major tests to be performed on the SDM's include a COA-level modal survey, performed on SDM 1, to determine its dynamic characteristics, an SDM 2 MM-level acoustic vibration test, an SDM 2 operational dynamics test, performed in an MM simulator, and subsequent failure inspection on both models.

Two SDM's will be assembled, one for testing and one for back up should the first be damaged. SDM 1, the back-up model, will not be as prime-like in its configuration as SDM 2; that is, certain structural material and fastener substitutions were made as indicated in the following list.

The SDM's differ from the FM's in the following respects:

- a. Sliding Mask. Because the SDM masks are not operational, the forward bottom structure is not slabbed off.
- b. COA Barrel. Because of the FM design growth, the COA-barrel skin patterns and thicknesses are slightly different.

~~SECRET~~ D

~~SECRET~~ - D

BIF-008- [REDACTED] -68
(Control Number)

- c. Forward COA Structure. The SDM forward COA structure is not modified to permit full TM clearance as required for the FMs.
- d. Access Panels. FM updates in the pattern of removable access panels have not been included in the SDM's.
- e. Electronic Packages. The SDM 1 dummy-electronic boxes are not located in the prime positions as are boxes for SDM 2 and the FM.
- f. Air Bag. Because of the types of tests required for SDM 2 an air bag will be installed in the primary mirror assembly, whereas, SDM 1 will not require one.
- g. Invar Optical Support Structure. SDM 2 will have the FM Invar optical support structure because of the nature of the testing it will undergo. SDM 1 will have stainless-steel substitutions in some noncritical areas.
- h. Tracking Mirror. The SDM TM's will be inertial substitutes without separate mount rings on flexures.

6.3.1.2 Thermal Model (THM).

6.3.1.2.1 Requirements. During thermal development tests, the THM must simulate the thermal performance of the flight hardware. This simulation requires that the thermal properties of the THM such as sizes, power dissipations, solid conductances, radiant conductances, and thermal capacitances duplicate the corresponding properties of the flight hardware.

The THM will be used in two distinct phases, first, as an optical assembly thermal model, then as a mission module thermal model (MMTHM). This division permits early development and checkout tests at the optical assembly (OA) level, where modification can be more easily performed, and also permits MM-level tests later on. These tests will subject the THM to the simulated thermal environments of prelaunch, ascent, and orbital operations.

~~SECRET~~ - D

~~SECRET~~ D

BIF-008- [REDACTED] -68
(Control Number)

The THM optics will simulate the prime optics thermally. The structural capability of the THM need only be sufficient to withstand the induced loads of ground handling and testing.

6.3.1.2.2 Design Approach. THM design makes use of existing EM designs where available (see paragraph 6.3.1.3), simplifying where possible without compromising the thermal characteristics. Optical glass in the optical elements is replaced with plate glass buildups. Electronics not required for thermal performance are replaced with blocks equaling the thermal capacitance of the components, and resistors simulating the power dissipations.

The flight heater is modified to provide flexibility during tests. These modifications consist of providing manual OFF/ON switching for overriding each heater if desired, and providing for variable power output from each heater.

The MMTHM was designed to be hung from the forward end by a laboratory module thermal simulator (LMTS), eliminating nonrealistic support-related thermal boundary conditions.

6.3.1.2.3 Hardware Description. The OA configured THM is designed by EKC and is a thermal simulation of the flight OA. The MMTHM consists of the OA, assembled with the LMTS, the mission module forward section thermal simulator, the MM aft shell, the THM bellows and thermal model tracking mirror assembly. This assembly is shown schematically in Figure 6.3-1. Hardware differences between the THM and FM's are summarized in Table 6.3-2.

~~SECRET~~ D

~~SECRET~~ D

BIF-008- [REDACTED] -68
(Control Number)

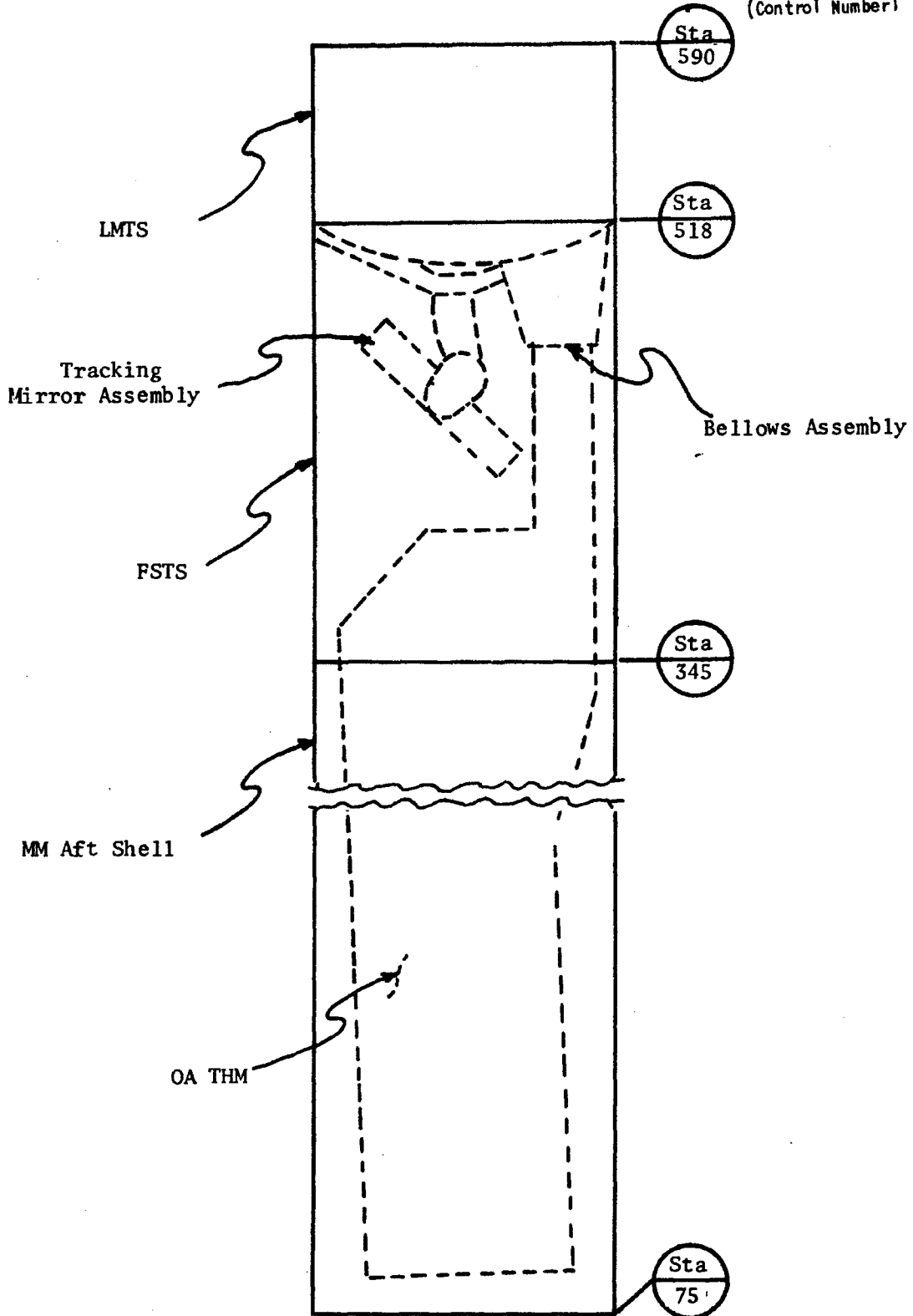


Figure 6.3-1. MMTHM Assembly Schematic

6-46
~~SECRET~~ D

Handle via BYEMAN
Control System Only

~~SECRET~~ D

BIF-008- [REDACTED] -68
(Control Number)

TABLE 6.3-2
HARDWARE DIFFERENCES BETWEEN THE THERMAL MODEL AND FLIGHT MODEL

<u>Component</u>	<u>THM Difference</u>
a. Heater system	None
b. Temperature sensors	None
c. Thermal blankets	No significant difference (thermocouples penetrate blanket)
d. Optical elements	Plate-glass buildups, prime coatings
e. Alignment servos	Mass/power simulations
f. Instrumentation processor	Temperature monitoring portion is prime, remainder mass/power simulation
g. Electronic boxes	Mass/power simulation
h. Launch locks	Manually operated, mass simulation
i. Structures	Dimensionally and thermally - no difference
j. FSTS	Thermal characteristics same as flight hardware
k. LMTS	Aft LM bulkhead is dimensionally correct, as is LM-MM attachment; ring-heaters simulate LM temperature
l. Thermal coatings	None

~~SECRET~~ D

~~SECRET~~ D

BIF-008- [REDACTED] -68
(Control Number)

6.3.1.3 Engineering Model (Manned/Automatic Mode). The EM consists of an MM and a grouping of M/A mode LM PP items. The EM is of prime design, and consists of essentially prime equipment in a flight configuration. The EM is not required to meet thermal and environmental requirements. To meet schedule requirements, deviations from systems requirements may be necessary with regard to optical operating characteristics.

The purpose for the EM is to provide experimental verification of conformance with electrical, mechanical, and optical functional performance specifications. Therefore, the tests listed in Tables 6.4-1 and 6.4-2 are designed to provide the following:

- a. An indication of any deviations from FM performance requirements.
- b. Data for performance prediction math-model evaluation.
- c. Verification of mechanical and electrical interfaces.
- d. Evaluation of test techniques and procedures.
- e. Evaluation of test equipment capabilities.
- f. Verification of assembly and alignment procedures.
- g. Development of tests for use on the QM and FM's.
- h. Providing background experience for testing the QM and FM's.

6.3.2 Qualification Model-Manned/Automatic Mode

The QM is prime hardware representative of the PP design for use in the qualification test program. The QM will be tested to demonstrate that the PP design can satisfactorily meet specified performance requirements during and after exposure to designated extremes of transportation, pre-launch, launch, and operational environments.

6-48

~~SECRET~~ D

Handle via BYEMAN
Control System Only

~~SECRET~~ D

BIF-008- [REDACTED] -68
(Control Number)

The QM includes a full complement of EKC prime M/A mode components and is fabricated from the same generation of drawings used for the first operational FM. The M/A QM is assembled in the following test configurations:

- a. Mission module qualification model (MMQM)
- b. Laboratory module subsystem qualification model (LM subsystem QM)

6.3.2.1 MMQM Assembly. The MMQM will be assembled to qualify the EKC MM design at the MPS level. The MMQM tests are performed in the following test configurations:

- a. Mission module (MM)
- b. Mission module aft section (MMAS) with a Mission module forward section (MMFS) simulator

The MMAS qualification tests are performed after the completion of the OA and MMAS acceptance tests.

The MM qualification tests are performed after the MM acceptance tests.

The MMQM is tested in accordance with paragraph 6.4.

6.3.2.2 LM QM Assembly. The LM subsystem QM will be assembled in Rochester to acceptance test all EKC LM components in the M/A mode at the MPS level. This LM configuration consists of the LM qualification test vehicle (LMQTV) components arranged within a support structure to simulate the prime LM PP spatially, mechanically, electrically, and functionally. Following the acceptance test at EKC (see paragraph 6.4), the LMQTV components are shipped to McDonnell Douglas Astronautics Corp. - Western

6-49
~~SECRET~~ D

Handle via **BYEMAN**
Control System Only

~~SECRET~~ D

BIF-008-[REDACTED]-68
(Control Number)

Division (DAC-WD) where they are mounted in a prime LM structure along with other associate contractor's LM components. This LM configuration is subjected to a series of acceptance and qualification tests.

6.4 OPTICAL ASSEMBLY AND MISSION PAYLOAD SYSTEM (MPS) LEVEL TESTING

The paragraphs which follow describe the optical, mechanical, thermal, photo-optical, environmental, and electrical tests performed on the optical assemblies, camera-optical assemblies, MM assemblies, and LM subsystems. Paragraph 6.4.1 discusses OA tests, and paragraph 6.4.2 discusses MPS-level tests.

6.4.1 Optical Assembly Testing

Tests are performed on the OA and COA to (1) evaluate conformance of the OA to design specifications, (2) evaluate operability of the OA, (3) determine optical, mechanical, thermal, and performance characteristics of the OA, and (4) provide data for further correlation and analyses. Table 6.4-1 contains a summary of OA and COA tests at EKC.

The test summary in Table 6.4-1 includes, for each OA test, (1) the test facility used, (2) the OA models tested, and (3) the type of test performed on each of the OA's (that is, developmental or acceptance test).

6.4.1.1 OA Safe-to-Power Test. The safe-to-power test will be performed to verify the physical integrity of the electrical subsystem. The test includes validation of cable-line continuity, verification that electrical connectors are correctly mated (continuity loop), and that the insulation resistance between each prime interface line and all other interface lines (tied to chassis) conform to design specifications.

~~SECRET~~ D

~~SECRET~~ D

BIF-008- [REDACTED] -68
(Control Number)

TABLE 6.4-1
REFERENCE GUIDE TO OPTICAL ASSEMBLY TESTS AT EKC

<u>Test</u>	<u>Test Facility</u>	<u>SDM-1</u>	<u>SDM-2</u>	<u>THM</u>	<u>EM</u>	<u>OATS</u>	<u>QM</u>	<u>FM</u>
OA safe-to-power	Assembly stand				D	D	A	A
OA AVE/AGE compatibility	Assembly stand				D	D	A	A
OA electrical functional	Assembly stand				D	D	A	A
OA electromagnetic compatibility	Assembly stand				D	D	A	A
OA alignment verification	Chamber III				D	D	A	A
OA calibration	Chamber III				D	D	A	A
OA optical conformance	Chamber III				D	D	A	A
OA isothermal optical quality	Chamber III				D	D	A	A
OA photo-optical	Chamber III					D	A	A
OA weight and cg	Load cells	D	D		D	D	A	A
COA modal survey	Horizontal mounts		D					
COA operational dynamics	Vertical fixture		D					
OA low temperature	Chamber B				D			
OA venting	Chamber B				D			
OA flow calibration	Chamber B				D			

Key: D - developmental test
A - acceptance test
SDM - structural developmental model
THM - thermal model
EM - engineering model
OATS - optical assembly test structure
QM - qualification model
FM - flight model

~~SECRET~~ D

~~SECRET~~ D

BIF-008- [REDACTED] -68
(Control Number)

Conformance of the bonding resistance measured between electrical boxes and supporting mounts and across the OA structure to design specifications will also be verified in this test.

Thus, the safe-to-power test ensures that the correct OA electrical interface is presented to test support equipment or to other prime hardware at higher levels of assembly.

6.4.1.2 OA AVE/AGE Compatability test. Data will be obtained with which to demonstrate the compatability of the OA and the sensor test system. The test will be performed to obtain data with which to verify compatability of individual electrical components, several components simultaneously, and finally, the complete electrical subsystem.

The instrumentation power buses, +5 v, +12 v and -6 v, are powered individually and all instrumentation points monitored to determine whether only those associated with a particular bus are operating.

The test is then performed with all buses powered and associated output instrumentation points checked for absence of cross-talk.

Using the sensor test set, commands will be sent through the MM control unit to the various electronics boxes. With prime operational power OFF, these commands will be verified by checking response at the command verification points in the sensor test set.

Operational power (+ 28-v d-c) will then be applied to the various busses; the appropriate command verification points will be checked. Bus current will also be monitored.

~~SECRET~~ D

~~SECRET~~ D

BIF-008- [REDACTED] -68
(Control Number)

With all (normal level) prime power ON, the isolation resistance between each operational power bus return and each instrumentation power bus return will be measured to obtain data with which to verify conformance to design specifications.

6.4.1.3 OA Electrical Functional Test - I. The OA electrical functional test-I will be performed to obtain data with which to demonstrate the correct operation of the electrical subsystems at the nominal power and then at high-and low-operational powers. The following subsystems are to be tested:

- a. Power subsystem
- b. Command subsystem
- c. Instrumentation subsystem
- d. Alignment subsystem
- e. Launch-lock subsystem
- f. Environmental control subsystem

The sensor test set will be used to provide power, commands, LM loads, and instrumentation readout.

6.4.1.3.1 OA Electrical Functional Tests II & III. These tests will be performed to obtain data with which to demonstrate correct functioning of the OA electrical subsystem at temperatures of 60 F (part II) and 80 F (part III). Prime power (operational and instrumentation) will be applied to the prime electrical interface.

Selected instrumentation commands will be initiated and command response checked at the command verification points.

6-53
~~SECRET~~ D

Handle via BYEMAN
Control System Only

~~SECRET~~ D

BIF-008-[REDACTED]-68
(Control Number)

6.4.1.4 OA Electromagnetic Compatability Test. This test will be performed to obtain data with which to demonstrate that the OA electrical subsystem meets the general specification for electromagnetic compatability requirements for manned spacecraft, SSD, Exhibit 64-4 (as ammended).

The test will be performed by investigating a number of critical lines, simultaneously, as a series of bus switchings and command sequences are commanded. Any electrical pulses beyond specific levels caused by bus switching or initiation of a command will be determined and reduced to an acceptable level as established in the specification. Confidence in the correction of a pulse and switching or command operation will be established by repeating the operation a number of times.

6.4.1.5 OA Alignment Verification. The objective of the alignment test is to obtain data to demonstrate conformance of the alignment control system (ACS) to performance specifications. The test consists of (1) aligning the optical assembly with the ACS, and (2) with an axicon. Because the axicon is estimated to be an order of magnitude more accurate than the ACS, it is possible to establish the accuracy of the ACS.

6.4.1.6 OA Calibration. The objective of the calibration test is to determine sensitivity of the optical assembly alignments to the weight and balance of test instrumentation. This determination is accomplished by measuring decentering, tilt, defocus of the primary mirror with respect to the Ross axis (resulting from perturbations in weight), and moment applied to the camera mounting plane over the expected range encountered in sub-segment optical tests. Weights will be placed at various positions on the X-Y translation table which mounts test instruments to the Ross barrel. With the weights in place, the changes in alignment and focus will be measured by axicon and Marechal focus sensor.

~~SECRET~~ D

~~SECRET~~ D

BIF-008- [REDACTED] -68
(Control Number)

6.4.1.7 Optical Conformance Test. The purpose of this test is to evaluate the lens characteristics including field, photometric, and magnification properties. Measurements will be made of back focus, field tilt, field curvature, relative illumination, effective focal length, and relative aperture. Point source imagery, precision focus sensing, and interferometry are used.

A point source microscope and/or Marechal focus sensor will be used to determine back focus and field configuration. These parameters, as well as the remaining ones, will also be measured with an interferometer.

6.4.1.8 Optical Assembly Isothermal Optical Quality Test. The isothermal optical quality test is performed on the OA EM to determine monochromatic image quality, location of the best focal point, and tilt of the image plane. The test results, when analyzed, are used to determine compliance with design specifications and establish a baseline for evaluating optical quality at subsequent levels of assembly.

The test is performed at the nominal orbital control temperature of 70 F and at the temperature extremes of 65 and 75 F to determine optical quality over the operational temperature range. The test is performed in a vibration-isolated soft-vacuum environment in Chamber III to reduce image motion resulting from ground noise and air turbulence. A monochromatic laser and interferogram recording camera are mounted to the forward end of the Ross corrector. A closed-circuit television device is used for remotely monitoring the interferometric patterns during the test. The laser is used to provide a coherent wavefront at the optical assembly focal plane. A horizontally mounted 72-inch-diameter master-plano mirror autocollimates the image through the optical system.

~~SECRET~~ D

~~SECRET~~ D

BIF-008- [REDACTED] -68
(Control Number)

The OA isothermal optical quality test begins with a preliminary alignment of the optics prior to chamber pumpdown to a soft vacuum. Following pumpdown, thermal stabilization, and optical realignment, interference patterns are photographed for several field positions and focus positions. The test is then repeated at the operational temperature extremes.

The interferometric test data are processed to provide the wavefront contour characteristics of the OA. Also determined from these data is the location of the best monochromatic on-axis focal plane. The camera's image-plane tilt, with respect to the Ross-corrector/camera interface is determined by performing the above test at four off-axis points. The plane containing all the test points is the image plane.

6.4.1.9 Optical Assembly Photographic Test. This test provides a visually interpretable confirmation of the optical performance of the OA and is a supplement to the interferometric optical quality test previously described. The test provides a photographic image of source targets such as tri-bar arrays and scene replicas. Trained operators view the images and determine the optical quality in terms of lines per millimeter. The test results serve as a reference for photographic tests performed at subsequent levels of assembly.

The OA photographic test is performed in Chamber III to effect a vibration-isolated, thermally stable (70 F), soft vacuum environment. The photographic test equipment (see paragraph 6.2.3) which is mounted at the forward end of the Ross corrector provides photographic test data.

6-56

~~SECRET~~ D

Handle via BYEMAN
Control System Only

~~SECRET~~ D

BIF-008- [REDACTED] -68
(Control Number)

The test sequence consists of suspension of the OA in the chamber, installation of the photographic test equipment, and checkout of the flight/test equipment. The chamber is then pumped down and after thermal stabilization at 70 F, the optics are aligned. Multiple targets are then selected and photographed using Type 3404 Film.

6.4.1.10 Optical Assembly Weight and Center of Gravity Test. The weight and center of gravity (cg) test is performed to measure the weight and to determine the location of the cg of the OA. A weight and cg test is performed separately on the camera assembly. The resultant data from the OA and camera tests are then combined to determine the weight and cg of the COA.

The OA weight and cg is determined by suspending the OA from three load cells with the OA X- and Y-axis in the horizontal plane. The OA is then rotated 90 degrees about the X-axis (X- and Z-axis in the horizontal plane) to determine the cg location in the third axis.

The test sequence begins with installation of special handling rings (with known weight and cg locations) to the optical assembly. The OA is then placed on the cradle assembly with the X-axis in the horizontal plane. The weight and cg kit is installed and load-cell readouts are taken in the two measurement positions described above.

The percent of load-cell capacity readouts recorded during the test are converted to pounds. OA weight is calculated by averaging the summed output of the load cells for each test configuration and subtracting the weight of mounting rings and test fixtures. The cg is calculated relative to the 0, 0, 0 point on the MM axis using the moment summation method.

~~SECRET~~ D

~~SECRET~~ D

BIF-008- [REDACTED] -68
(Control Number)

6.4.1.11 Camera Optical Assembly Modal Survey. This test is performed to experimentally measure the vibration characteristics of the SDM 1 COA structure and its fundamental components. Test data are correlated with analytical results obtained from the Government furnished equipment (GFE) math model.

Data are obtained to evaluate the COA natural frequencies in the range of 2 to 200 Hz and corresponding mode shapes, structural admittance, phase relationships, and modal damping.

The test is performed with the COA-SDM mounted horizontally at the three flight-mounting points. Shakers, load cells, and accelerometers are attached to the COA and are controlled and monitored by special vibration test equipment. The test is performed in two phases.

The first phase consists of a frequency sweep through the frequency range (2 to 200 Hz) in order to identify the basic natural frequencies of the COA. In addition, a measurement of the structural admittance, modal damping, and dynamic response of the simulated COA optical elements is performed.

The second test phase measures the dynamic response at each of the natural frequencies identified in phase one. The data from this test phase are used to plot and identify normalized mode shapes associated with predominant resonances.

6-58

~~SECRET~~ D

Handle via **BYEMAN**
Control System Only

~~SECRET~~ D

BIF-008- [REDACTED] -68
(Control Number)

The test is repeated for seven basic test setups representing seven different shaker configurations. The resultant test data are reduced to provide data for verification of math model predictions and for orthogonality checks.

6.4.1.12 Optical Assembly One-G/Zero-G Misalignment Test. The objective of this test is to measure changes in the OA internal alignment resulting from structural deflections occurring in the transition of the OA from a one-g to a zero-g environment.

Alignment changes measured are apparent motions of the primary mirror (tilt, decenter, and focus) with respect to the Ross-corrector assembly. The test method uses a light source placed at the center of the simulated primary mirror, and test optics placed along the OA optical path. The centerline of the Ross barrel is taken as reference and test data are read out at the image plane using a theodolite and a fringe-counting interferometer.

The test configuration consists of the OA-SDM 1 and SDM 2 mounted in a vertical support structure. This configuration represents the nominal FM optical test configuration except that the primary mirror is in a locked condition. Tilt, decenter, and defocus measurements are recorded for the OA in the vertical position. The OA is then inverted and optical measurements are again taken to determine changes in tilt, decenter, and defocus. The zero-g condition is then taken as the average of the two test conditions and the difference in alignment between the nominal one-g test configuration and zero-g is thereby obtained.

~~SECRET~~ D

~~SECRET~~ D

BIF-008- [REDACTED] -68
(Control Number)

The results of these tests are then used on FM's to set servos at the mid-range of predicted on-orbit alignment.

6.4.1.13 OA Operational Dynamics Test. The purpose of the operational dynamics test is to measure the response time history of SDM 2 COA to EM camera dynamic disturbances, determine whether the COA is compatible, and to determine the effect of air damping on the COA response.

The basic test method includes a modal check of the COA and measurement of the response of optical elements (simulations). Shakers are used for vibration inputs and accelerometers are used to measure response.

The various camera functions are then actuated and the force-time history of the COA response measured at the same points used for the modal check.

6.4.1.14 Optical Assembly Thermal Model Low Temperature Test. This test is performed on the OA THM to determine the thermal capabilities and to check out supporting control and instrumentation equipment prior to assembly and test of the MM THM.

The OA THM low temperature test is performed in Chamber B which provides a low-temperature hard-vacuum environment. The test configuration consists of the OA (including thermal blankets) horizontally mounted in a bird-cage structure which supports the OA at the flight-mounting points. Temperature, pressure, and power instrumentation are controlled and monitored by the THM control console and thermal data management system (TDMS).

~~SECRET~~ D

~~SECRET~~ D

BIF-008- [REDACTED] -68
(Control Number)

The temperature of the OA THM is reduced by bringing the walls of Chamber B to 40 F, with concurrent pumpdown of the chamber to hard vacuum. After the OA THM temperature is sufficiently below the orbital control level, the environmental control system (ECS) is powered and heater controller operation is determined. As the temperature of the OA reaches 70 F, the controller switchoff points are monitored and the level of capability of the ECS to control the OA THM at the design temperature level is determined.

6.4.1.15 Optical Assembly Venting Test. This test will be performed on the OA THM to obtain data with which to determine the venting capabilities of the OA THM and to check out the supporting control and instrumentation equipment prior to assembly and test of the MM THM.

The OA THM venting test will be performed in Chamber B which provides a rapid pumpdown capability. The test configuration is the same as that for OA low-level temperature test.

After completion of the low temperature test, the chamber is repressurized and an inspection of the OA is performed. The OA THM venting test is then performed by rapid pumpdown of the chamber in an ascent-type pressure profile. The venting test is performed to obtain preliminary data on the ability of the OA THM, and thus the prime OA, to survive the MM THM ascent venting test. Critical areas which are monitored include thermal blankets, simulated-optics venting, and pressure instrumentation operation. Following completion of the venting test, the OA THM is removed from Chamber B, inspected, and corrections are made as required.

~~SECRET~~ D

~~SECRET~~ D

BIF-008- [REDACTED] -68
(Control Number)

6.4.1.16 Optical Assembly Weight Air Flow Calibration. The purpose of the OA THM weight flow test is to calibrate the prime ground air-flow sensors such that they measure the weight rate of the ground-air flowing through the OA THM prior to assembly and test of the MM THM.

The test configuration is the OA THM, including thermal blankets, mounted vertically in the heater vertical assembly stands (HVAS). The HVAS supports the OA THM at the flight-mounting points. Conditioned air is ducted into the forward end of the OA THM. Temperature and flow rates of the air are controlled and monitored as the air enters and exits from the OA THM.

6.4.2 Mission Payload System Level Testing

The purpose for the MPS-level tests is to (1) provide developmental model data to evaluate the mathematical models used for on-orbit prediction, (2) provide flight model data for performance prediction, (3) provide calibration data for on-orbit operations, and (4) ensure compliance with applicable specifications and requirements. Table 6.4-2 contains a summary of MPS tests at EKC.

The test summary in Table 6.4-2 includes, for each MPS test, (1) the test facility used, (2) the models tested, and (3) the type of test performed on each of the models (that is, developmental, acceptance, and/or qualification).

6.4.2.1 Mission Module Aft Section Isothermal Optical Quality Test. The first test performed after the assembly of the OA in the MMAS shell is the MMAS isothermal optical quality test. This test is an isothermal, full-

~~SECRET~~ D

~~SECRET~~ D

BIF-008- [REDACTED] -68
(Control Number)

TABLE 6.4-2
REFERENCE GUIDE TO MPS TESTING AT EKC

<u>Test</u>	<u>Test Chamber</u>	<u>SDM</u>	<u>THM</u>	<u>EM</u>	<u>QM</u>	<u>FM</u>
MMAS isothermal optical quality	III				A Q	
MM/TM thermo/optical	B			D	A Q	A
MMAS thermo/optical	A			D	A Q	A
MMAS photographic	III				A Q	
MM compatibility test	MM					
MM electrical test	Assembly			D	A Q	A
MM functional test	Stand					
MM nonoperating temperature	B				Q	
MM ascent venting	B		D		Q	
MM subaperture optical	III			D	A Q	A
MM transmissibility test	III			D		
MM acoustic vibration	Acoustic	D			A Q	A
MM thermo-vacuum	A		D	D	A Q	A
MM ground thermal conditioning	F		D			
MM mission profile	A			D	A Q	A
LM subsystem compatibility test	LM Test Stand LM Test Stand					
LM subsystem electrical test				D	A *	A
LM subsystem functional test						
LM subsystem mission profile				D	A *	A

Key: D - Development test THM - Thermal model
 Q - Qualification test EM - Engineering model
 A - Acceptance test QM - Qualification model
 SDM - Structural development model FM - Flight model

* qualified after assembly at MDAC-WD - Not qualification tested at EKC.

~~SECRET~~ D

~~SECRET~~ D

BIF-008- [REDACTED] -68
(Control Number)

field full-aperture double-pass optical quality test which provides the data necessary to evaluate heterochromatic image quality and field tilt. Image quality and field tilt are then used to obtain a quantitative evaluation of the optical quality prior to thermal/optical tests. The test results are used to determine compliance level with design specifications. The test configuration consists of the MMAS mated with a simulated MMFS. The MMAS, MMFS simulator, and reference mirror are mounted in Chamber III as shown in Figure 6.4-1. After evacuating the chamber to a soft vacuum and stabilizing to 70 F, a remotely controlled heterochromatic, laser interferometer produces interferograms in four colors and five field positions. A through-focus sweep is generated computationally to obtain a best focal plane. A heterochromatic, laser-interferometer module (see paragraph 6.2.2.3) with an integral video-monitoring device is used to make simultaneous measurements in each color for the correct determination of longitudinal and lateral color aberrations. The laser source is used to provide the coherent source wavefront at the focal plane. The reference wavefront from the laser-source (that is, unaberrated wavefront) and the sample beam from the optical system are then combined to form the interference pattern. The laser source, video monitor, positioning, and photography of the interference pattern are controlled remotely from outside the test chamber. Vibration isolation and low atmospheric pressure are used to reduce image motion and subsequent smearing of the interferograms.

Interferogram data processing is used to provide the wavefront contour produced by the MMAS and the coordinate location of the best heterochromatic on-axis focal plane. Off-axis (four positions) heterochromatic best-focus points determine platen tilt of the flight camera with respect to the Ross-barrel/camera mounting reference points.

6-64

~~SECRET~~ D

Handle via BYEMAN
Control System Only

~~SECRET~~ D

BIF-008- [REDACTED] -68
(Control Number)

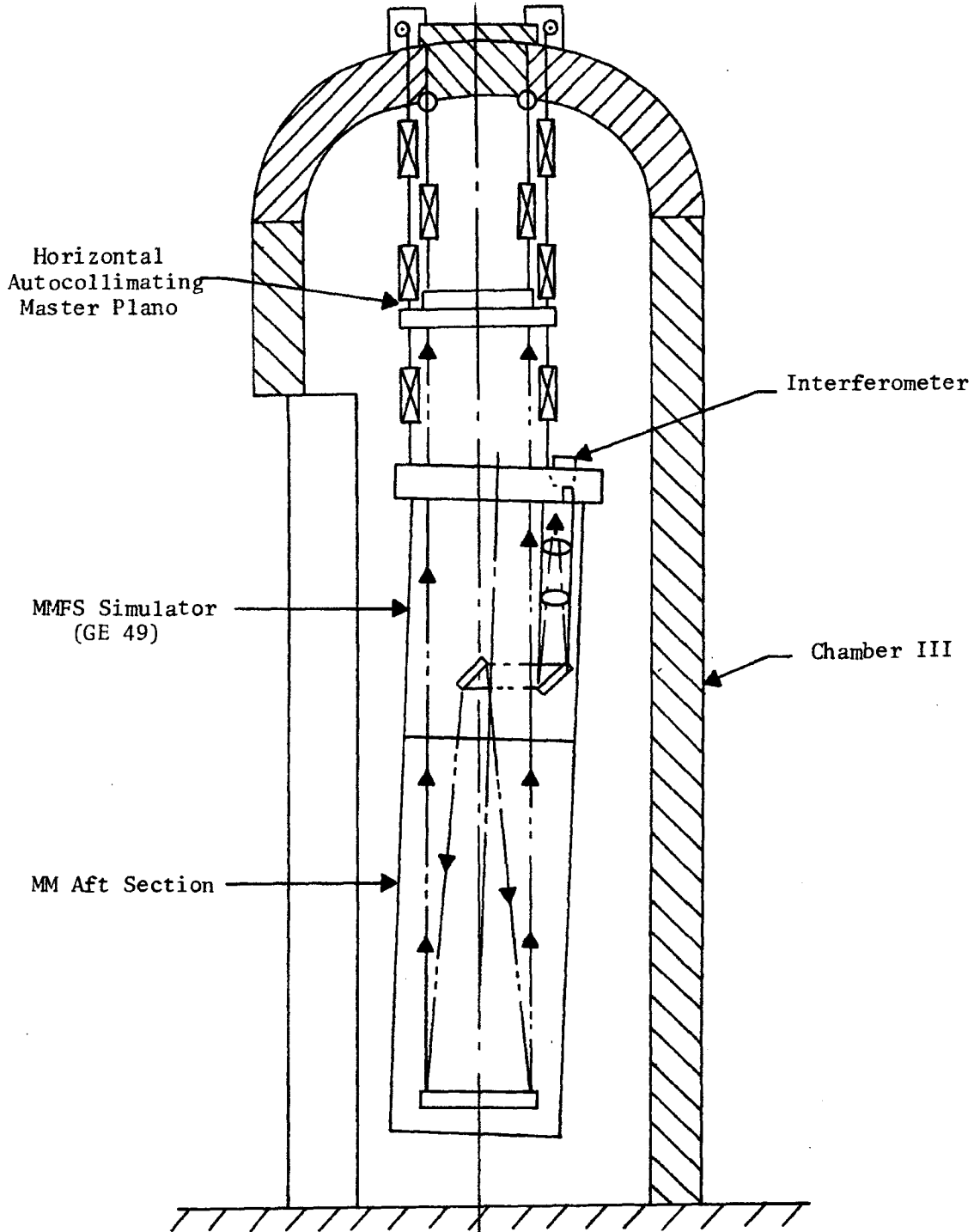


Figure 6.4-1. Mission Module Aft Section Isothermal Optical Quality Test Configuration in Chamber III

6-65
~~SECRET~~ D

Handle via BYEMAN
Control System Only

~~SECRET~~ D

BIF-008- [REDACTED] -68
(Control Number)

6.4.2.2 Mission Module/Tracking Mirror Thermo-Optical Test. Following the assembly of the TM into its mounting ring, optical tests are performed on the TM to determine correlation between measured and predicted optical quality degradation for known quantities of incident albedo-earth radiation. The TM thermo-optical test is a full-aperture double-pass optical test using the test configuration shown in Figure 6.4-2.

The test is performed in Chamber B in a hard vacuum environment. The optical quality of the TM is first measured (in Chamber II) under isothermal conditions to establish a baseline. The mirror is then subjected to measured flux pulses from the albedo-earth simulator and the transient optical responses are measured. The optical technique used for the thermo-optical test uses a laser interferometer located at the center of curvature of the concave mirror. The wavefront generated at the laser is reflected from the TM, refocused and reflected by the concave mirror, and returned to the interferometer after reflecting once again from the TM. In addition, temperature sensors mounted on the test mirror are monitored so that correlations can be made between temperature differentials and optical degradation.

6.4.2.3 Mission Module Aft Section Thermo-Optical Test. The MMAS thermo-optical test is performed to evaluate optical quality of the OA under simulated on-orbit conditions and to determine the adequacy of thermal control of the OA.

The test configuration includes the MMAS mated to a MMFS simulator and attached to the Chamber A LM-Thermal Interface Simulator (see Figure 6.4-3). Orbital pressure environment is simulated in Chamber A by evacuating the chamber to a hard vacuum.

6-66

~~SECRET~~ D

Handle via BYEMAN
Control System Only

~~SECRET~~ D

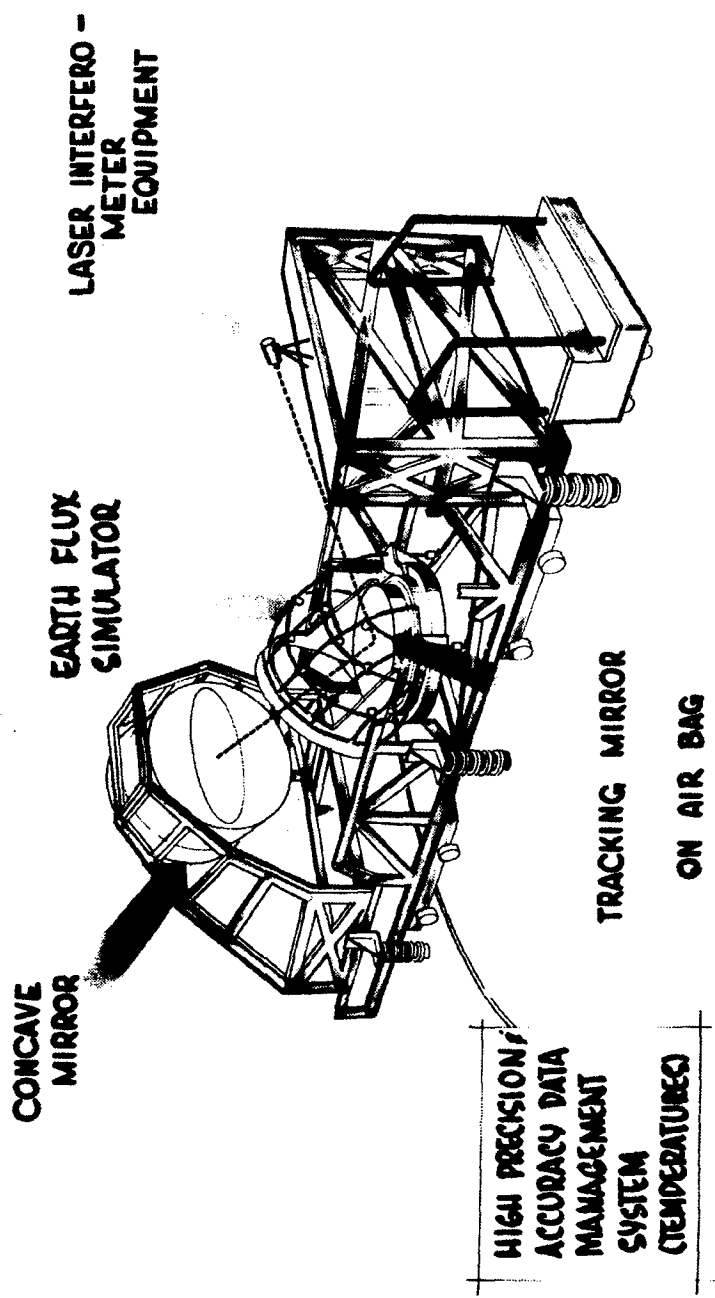


Figure 6.4-2. Tracking Mirror Thermo-Optical Tests

Handle via BYEMAN
Control System Only

~~SECRET~~ D

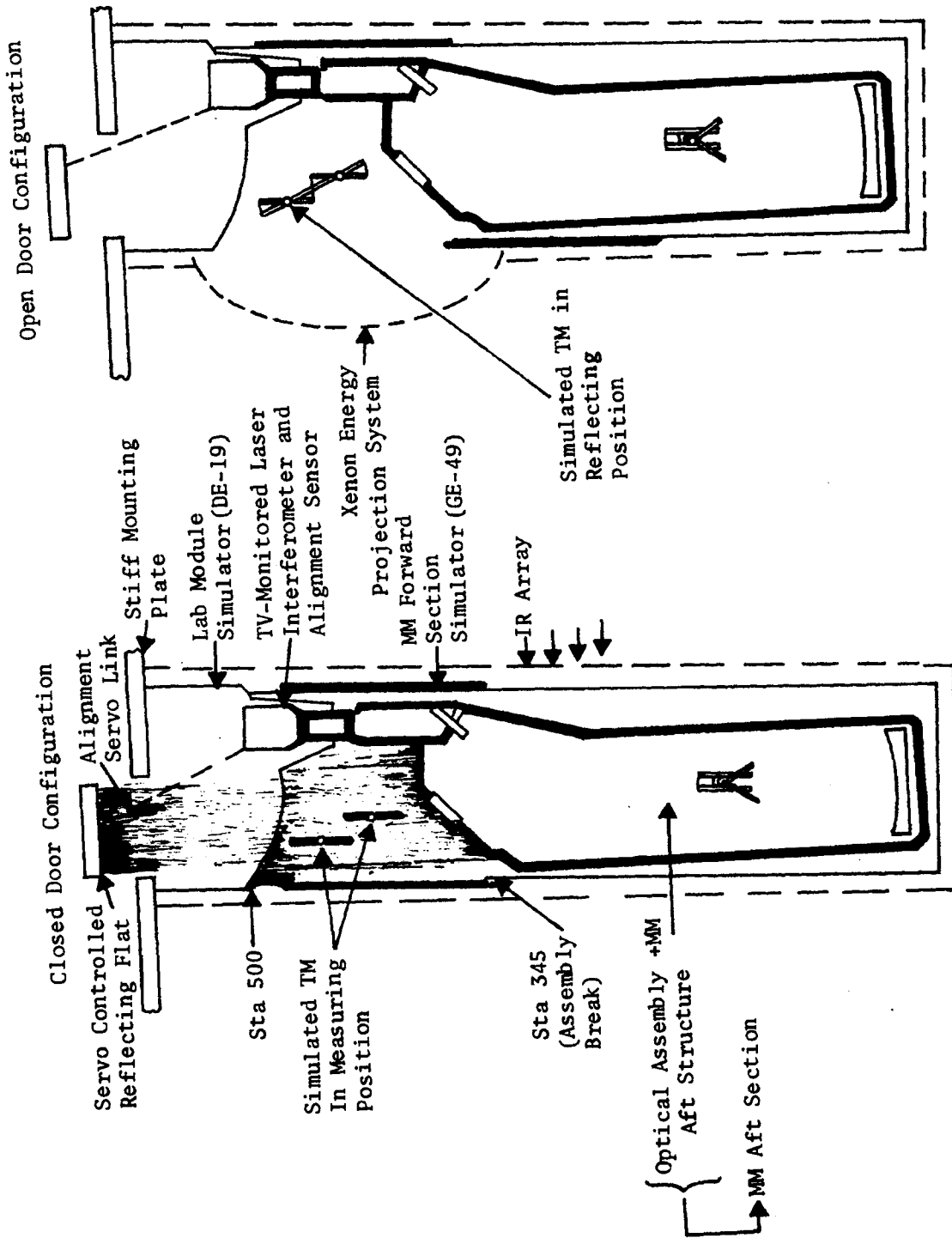


Figure 6.4-3. MMAS Thermal/Optical Test Configuration Chamber A

Handle via BYEMAN
Control System Only

~~SECRET~~ D

BIF-008- [REDACTED] -68
(Control Number)

The orbital thermal environment around the MM is simulated by a cryowall and a computer-programmed infrared source surrounding the test unit. In addition, a Xenon energy-projection system (XEPS) is used to simulate the energy of albedo radiation (total energy and partial spectral matching) incident upon the TM enclosure during on-orbit photography.

The MMFS simulator contains a simulated TM of lightweight sectioned sheets of aluminum capable of operating in a reflecting position (nadir look) and a measuring position (to obtain interferometric data). The aluminum sections have a hole through them so that the OA autocollimating mirror alignment can be maintained. The simulated TM is normally in its reflecting position with view-port doors closed. A horizontally mounted plano reference mirror is used to provide for this full-aperture double-pass optical test.

A closed-circuit television-monitored (monitoring does not provide the record for wavefront evaluation) monochromatic laser-interferometer assembly mounted in place of a prime camera is used to provide photographic data for determining wavefront contours. The test, which is performed with view-port doors first closed and then open, provides for evaluation of monochromatic optical quality both prior to door opening and resulting from open-door transient effects.

6.4.2.4 Mission Module Aft Section Photographic Test. The test camera provides a photographic image of source targets such as tri-bar arrays and scene replicas. Data collected from the photographs of the various types of targets will be subjected to visual and electro-optical examination. Transformation will be made from double to single-pass results using

~~SECRET~~ D

~~SECRET~~ D

BIF-008- [REDACTED] -68
(Control Number)

knowledge of the actual wavefront contours. The photographic test equipment used is discussed in paragraph 6.2.3.

6.4.2.5 Mission Module Functional Tests. Functional tests of the MM are performed to obtain data with which to determine the compatibility and interaction of EKC-MM equipment. MM tests for compatibility between units are restricted to those areas not checked at the OA level. Following compatibility checks, all MM equipment is sequenced to duplicate a flight profile and checks for interactions between subsystems are made.

6.4.2.6 Mission Module Ascent Venting Test. The ascent venting test is performed on the MM to evaluate the capability of the OA to vent. The test piece consists of an MMAS mated to a thermally prime MMFS and LM bulkhead. The test is performed on a test stand in Chamber B, using the rapid pump-down capability of the chamber. The test involves pumping down the chamber at a rate approximating changes during ascent. MM ascent venting data are acquired by monitoring pressure and pressure differential sensors.

6.4.2.7 Mission Module Sub-Aperture Optical Test. The MM subaperture optical test provides previbration and post-vibration optical baseline data. The requirements of this test are to observe and measure changes in the optical system caused by acoustic tests. No attempt is made to determine overall optical quality. The test permits detection and measurement of the effect of small surface defects in optical elements caused by cracked struts, potting failures, inelastic structural changes, and launch-lock mirror interaction. The subaperture test is designed to detect the presence of defects, not to identify them. The subaperture test does not require the disassembly of the MM other than the removal of the blow-off

~~SECRET~~ D

Handle via **BYEMAN**
Control System Only

~~SECRET~~ D

BIF-008- [REDACTED] -68
(Control Number)

door. The prime MM is mounted in Chamber III prior to acoustic tests. Following soft vacuum evacuation and thermal stabilization, the baseline subaperture optical figure test is performed. After acoustic tests in the acoustic test facility, the test piece is again mounted in Chamber III and re-examined.

A given area of the aperture is observed by autocollimation from a subaperture mirror positioned outside the open view-port doors before and after acoustic tests (see Figure 6.4-4). Observations are made over each area of the aperture independently. The before and after acoustic test measurements include photographic interferometric displays and knife-edge displays for the subaperture areas under observation. The displays are evaluated by standard methods and a point-to-point comparison is made between the pre- and post-vibration displays.

6.4.2.8 Mission Module Transmissibility test. A two-part transmissibility test is performed on the EM to provide data necessary to determine adequacy of OV math modeling procedures and to determine OV image motion resulting from selected PP operational disturbances.

The test configuration consists of a prime MM, an LM simulator which approximately simulates the structural characteristics of the LM, calibrated dynamic sources (shakers) in the LM and MM, and a flight-type camera and VO, with instrumentation which facilitates the measurement of image motion. The test is performed in Chamber III.

~~SECRET~~ D

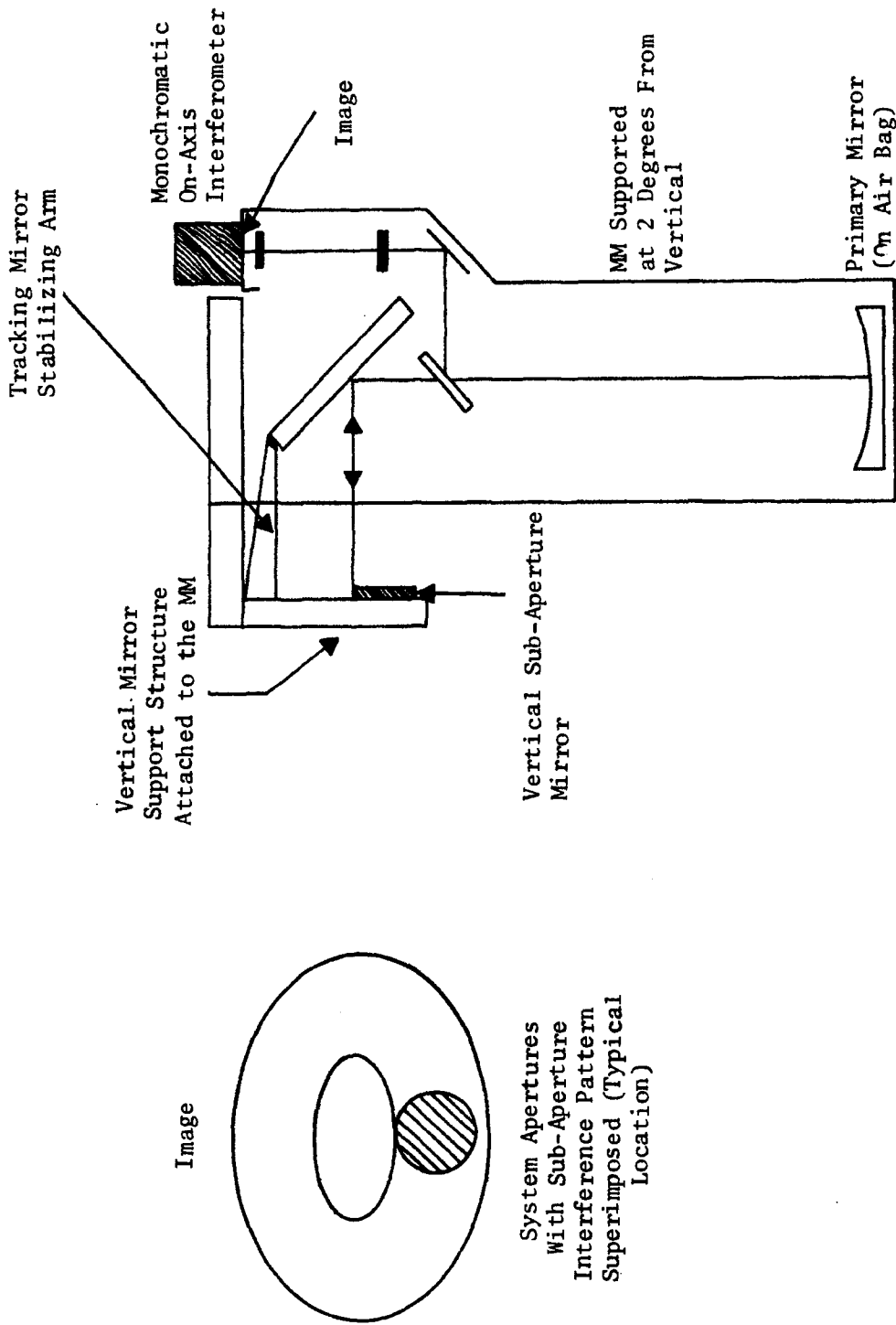


Figure 6.4-4. Sub-Aperture Optical Test Configuration

Handle via **BYEMAN**
Control System Only

~~SECRET~~ D

BIF-008- [REDACTED] -68
(Control Number)

Several low-level shakers mounted in the MM are actuated and instrumentation points located throughout the MM are monitored. Output data allows determination of natural frequencies and partial determination of mode shapes of the points instrumented. Shakers at selected critical points in the LM simulator and MM are then actuated. Comparison of measured motion at the points of excitation with measured motion at the optical elements will give the transmissibility of the structure. These transmissibilities can be compared with predicted values for the test configuration. Finally, selected payload dynamic sources will be actuated and the resulting line-of-sight motion at the image plane will be measured using techniques described in paragraph 6.2.4.

6.4.2.9 Mission Module Acoustic Vibration. An acoustic test is performed to increase confidence in the MM's ability to function correctly after experiencing ascent environment and to expose assembly or workmanship errors.

The test configuration (see Paragraph 6.5.2) consists of an MM mounted vertically in the acoustic test facility and mated to simulators representing the acoustic characteristics of the LM (forward) and Titan (aft) interfaces. The test configuration is subjected to the specified acoustic profile by the impingement and reverberation of a combination of low-frequency and middle-frequency horns. Following acoustic vibration tests, subaperture optical and electrical functional tests are repeated and the test results are compared to earlier established baselines.

6-73
~~SECRET~~ D

Handle via BYEMAN
Control System Only

~~SECRET~~ D

BIF-008- [REDACTED] -68
(Control Number)

6.4.2.10 Mission Module Thermal/Vacuum Test. The purpose for the MM thermal/vacuum test is to supply thermal data under simulated orbital environment with view-port doors closed or view-port doors operating as during a photographic mission. Unlike the MMAS thermal/optical test which supplies optical data, the MM thermal/vacuum test is used to determine whether (1) the TM enclosure provides the correct thermal control for the TM, (2) the aft section provides the correct thermal control for the OA, and (3) the thermal control subsystems of the entire MM are compatible and maintain design temperature levels.

This test includes an isothermal mission profile exercise to obtain thermal baselines, followed by exposure to simulated orbital environment with simulated door openings during which thermal variations are monitored.

The MM thermal/vacuum test configuration includes the prime MM and an LM thermal simulator within Chamber A (see Figure 6.4-5). Chamber A is equipped to simulate orbit and monitor conditions as discussed in paragraph 6.5.1.8. Monitoring of thermal instrumentation points during view-port door-open and door-closed periods provides TM, TM enclosure, and MMAS temperature control data. The temperature data are used with an MMFS thermal analog (a thermal/optical mathematical model) to predict the optical performance of the TM in its enclosure when exposed to the albedo energy pulse. The MMFS thermal analog is derived from MM THM tests and analysis is verified during FM and QM tests and analysis.

The preceding description does not apply to the MM THM thermo-vacuum test, which is more extensive in terms of data obtained and conditions simulated. The MM THM thermo-vacuum test will include investigation of both steady-state, and dynamic, and hot and cold orbits, with and without door-open periods. In addition, the response of the environmental control system to heater failures will be studied.

6-74

~~SECRET~~ D

Handle via BYEMAN
Control System Only

~~SECRET~~ D

BIF-008-
(Control Number) -68

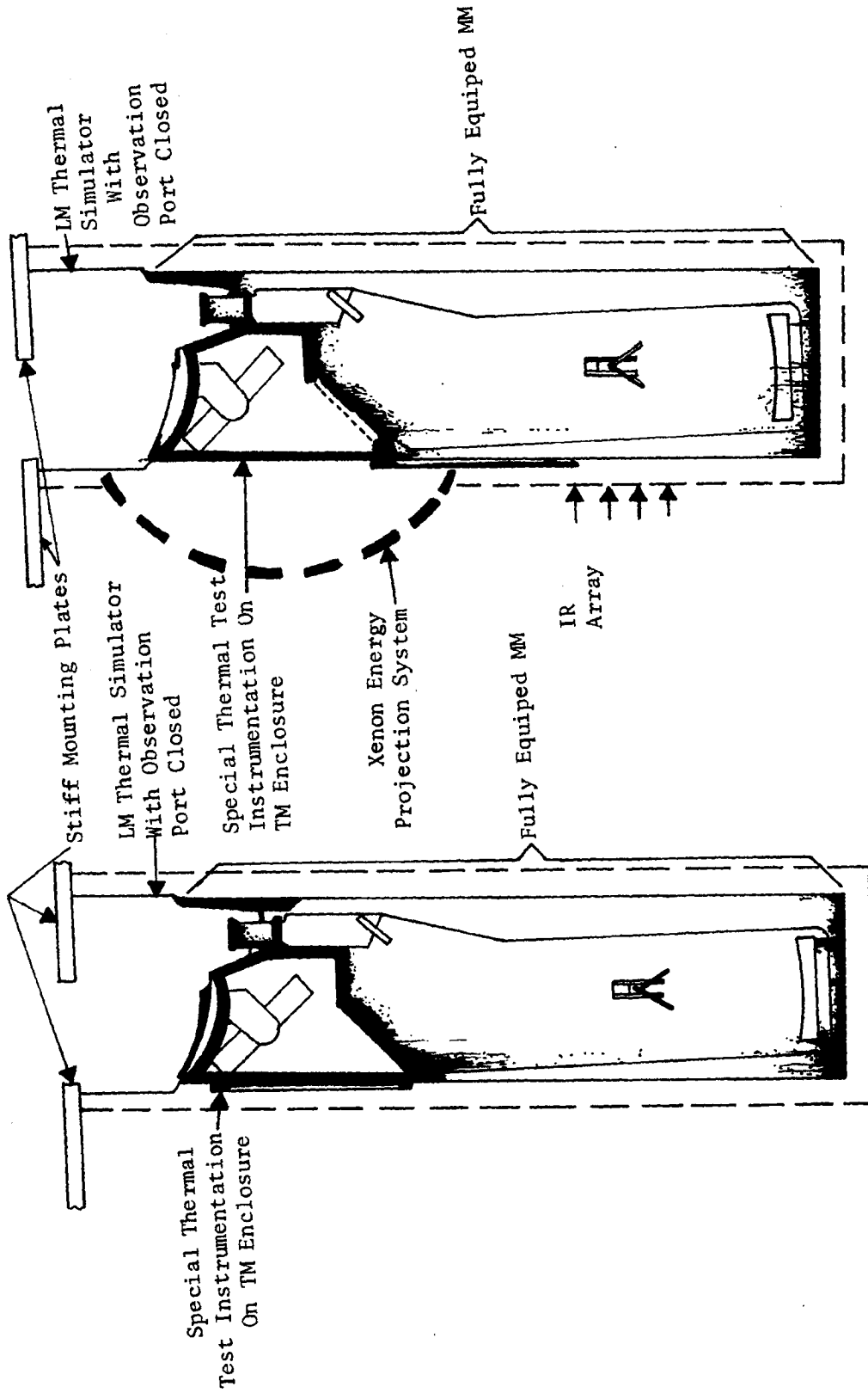


Figure 6.4-5. MM Thermal/Vacuum Test Configuration in Chamber A

~~SECRET~~ D

Handle via BYEMAN
Control System Only

~~SECRET~~ D

BIF-008- [REDACTED] -68
(Control Number)

6.4.2.11 Mission Module Ground Conditioning Test. A ground-conditioning test is performed on the MM to determine validation of ground-conditioning designs under simulated launch-pad conditions. The test configuration consists of a MMAS mated to MMFS and LM thermal simulators oriented vertically in Chamber F. Monitoring of pressure, air flow, temperature, and power measuring devices provides data to determine effects of temperature extremes, air-leakage passages, and recovery time of MM temperatures under various failure modes.

6.4.2.12 Mission Module and Laboratory Module Compatibility Tests. Compatibility tests are general in nature and are required to evaluate support and flight equipment MM and LM interfaces for mutual compatibility. The tests will be performed prior to any MM functional test. Compatibility tests apply to all components, assemblies, simulators, and test equipment and consist of checking mechanical interfaces, cabling and interconnections, and sequences of power application.

6.4.2.13 Mission Module and Laboratory Module Electrical Tests. These tests are performed subsequent to the buildup of a prime MM and LM components and subsystems to substantiate compliance with design requirements. A three-part test consists of: (1) monitoring power-command and instrumentation lines to derive power profiles, ensuring receipt of all commands and comparing instrumentation output against calibration curves, (2) checking operational performance of components at high- and low-voltage requirements, and (3) checking EMI safety margins for MM interface lines and interconnecting harnesses.

~~SECRET~~ D

~~SECRET~~ D

BIF-008- [REDACTED] -68
(Control Number)

6.4.2.14 Laboratory Module Functional Testing. With the LM components assembled in a simulated birdcage structure, a series of tests are performed to check nominal performances, systems compatibility, and interactions of all LM equipment. In addition, in-depth tests are performed on those components or systems which could not be tested at lower levels of assembly. Test film will be used to evaluate film-handling operations and camera data-block performance. The processor will be operated only for functional evaluation.

6.4.2.15 Mission Module and Laboratory Module Subsystem Mission Profile-Type Test. The mission-profile tests are performed to ensure that commanded functions of EKC components within the LM and MM take place in the correct time sequence and to provide final checkout for LM and MM components. The test configurations include a prime MM, and an LM subsystem.

The systems are individually sequenced through on-orbit operations, commands are actuated, and instrumentation outputs are monitored. Additional commands can be inserted where greater investigation of special interest areas is desired.

6.5. DESIGN AND ANALYSIS OF TEST TOWERS (CHAMBERS)

Designing a large test-tower facility to interferometrically test the quality of optics to a tolerance of $\lambda/40$ (5×10^{-7} inch) is a task comparable in magnitude to designing a flight camera and optical assembly structure. The rigidity and alignment problems are aggravated by (1) a more stringent tolerance, and (2) the presence of external disturbing vibrations. The one mitigating circumstance is that the test tower does

~~SECRET~~ D

~~SECRET~~ D

BIF-008- [REDACTED] -68
(Control Number)

not have a weight constraint. The design for the entire test complex involves nine towers. The new test facility at the Elmgrove Plant is shown in Figure 6.5-1.

Each test-tower study was broken down into several distinct tasks. A study was undertaken of the environment into which the test tower would be located, with special emphasis on vibrations and acoustic disturbances. The study showed anticipated vibration levels to be three orders of magnitude greater than permissible. Designing of isolation devices therefore became a necessity. As a result of differences in test scope, each test tower proved to be an unique problem.

Investigations indicated that a pneumatic isolation device was optimum for Chambers I_{EM}, I, I_G, II_{EM}, II, II_G, B, and C. For Chambers III and A, a combination pendulous and pneumatic isolation device was considered optimum. A detailed description of the selected isolation devices including theoretical derivation of performance and empirical validations are included in Appendix E.

The isolation device was designed considering the test tower as a rigid mass, with an objective of reducing the vibration amplitudes on this rigid mass to allowable levels. The method for determining allowable vibrations is given in Appendix E. The towers were then designed and analyzed to eliminate structural resonances which could raise the vibration amplitude above the allowable limit.

The concluding task was to analyze the test tower assembly, foundations, isolators, structure, instrument platforms, and refractive and reflective optics and mounts excited by a statistical model of the environment, and

6-78
~~SECRET~~ D

Handle via BYEMAN
Control System Only

~~SECRET~~ D

BIF-008- [REDACTED] -68
(Control Number)



Figure 6.5-1. Test Facility - High Bay Area

6-79

~~SECRET~~ D

Handle via BYEMAN
Control System Only

~~SECRET~~ D

BIF-008-[REDACTED]-68
(Control Number)

to predict performance. This task had to consider two test modes, evacuated and unevacuated. In the evacuated mode, ground vibrations predominate; in the unevacuated mode, acoustically induced vibrations cause serious problems.

The design for test facilities for the COA and MM levels (Chambers III and A) was complicated by the fact that these configurations are not nearly as rigid as the test towers. To achieve the required degree of isolation, a three-stage scheme was used: (1) a soft external (to the vacuum chamber) structure, (2) a pneumatic isolation device, and (3) a pendulous support device penetrating the vacuum shell and suspending the test object from a very rigid, massive ring.

6.5.1 Technical Description of Test Chambers

This paragraph presents a description of the test chambers to be used in testing the PP. Table 6.5-1 gives a summary of the test chambers.

6.5.1.1 Chamber I_{EM}. Chamber I_{EM}, shown in Figure 6.5-2, is an engineering model chamber for early testing of curved mirrors, in air. Two such towers were constructed at Building 601. The restricted height of the area where the chambers are located requires folded optical paths. The structures are housed in thermally insulated chambers to minimize air-thermal effects in the optical path. The chambers will test the 82-inch-diameter master sphere, the 72-inch-diameter master parabola, the 72-inch-diameter formula-sample solid asphere, and the 72-inch-diameter flight aspheres. Provisions are made for aspheres and parabolas to be tested with refractive and reflective null correctors, as required. These chambers are considered full-scale

~~SECRET~~ D

TABLE 6.5-1
SUMMARY TABLE OF TEST CHAMBERS

Chamber	Purpose	Inside Dimensions	Pressure	Thermal	Location	Quantity
A	Thermal/optical assembly tests	38' dia x 68' H	5 x 10 ⁻⁸	Torr-300F	Bldg 101	1
B	Thermal/optical component tests, and thermal assembly tests	15' x 15' x 45' L	10 ⁻⁷		Bldg. 101	1
C	Thermal/optical 1/2-scale tests	8' x 8' x 22' L	10 ⁻⁸		Bldg 601	1
D	LM simulator environmental tests	8' x 10' x 21' H	1		Bldg 101	1
X	Engineering breadboard tests	8' dia x 40' H (with extender)	1	Room temp.	Bldg 601	1
I _{EM}	Concave mirror tests, (aspheres and parabolas)	20'8" x 22'3" x 57'10" H	760	Room temp.	Bldg 601	2
I		23'6" dia x 86'3" H	1	"	Bldg 101	1
I _G		33' dia x 86'3" H	1	"	Bldg 101	1
II _{EM}	Plano-mirror tests	21' x 42'7" x 57'10" H	760	"	Bldg 601	1
II		20' x 38' x 52' H	1	"	Bldg 101	1
II _G	COA tests	30' x 38'6" x 52' H	1	"	Bldg 101	1
III		24' dia x 68' H	1	"	Bldg 101	2

Handle via BYEMAN
Control System Only

~~SECRET~~ D

~~SECRET~~ D

BIF-008- [REDACTED] -68
(Control Number)

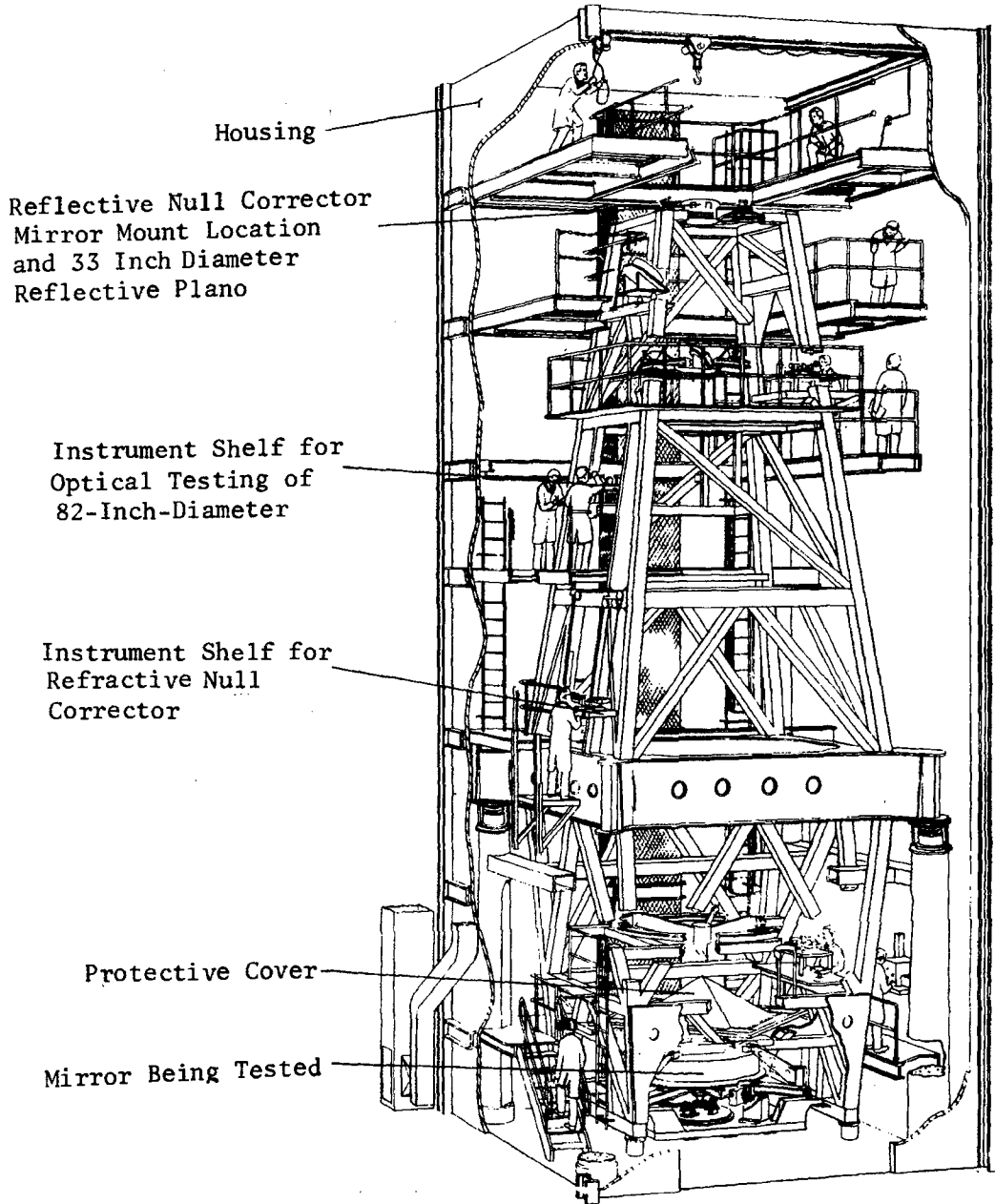


Figure 6.5-2. Chamber I_{em}

6-83

~~SECRET~~ D

Handle via BYEMAN
Control System Only

~~SECRET~~ D

BIF-008- [REDACTED] -68
(Control Number)

models, and as such, are fully instrumented, including closed-circuit television and remote-control operation of equipment. The chambers provide training for use of Chambers I and I_G. Limiting accuracy is less than $\lambda/10$ resulting primarily from air-turbulence effects.

6.5.1.2 Chamber I. Chamber I will be used for final tests of curved mirrors in a one-Torr vacuum and is located at the Elmgrove Plant in Building 101. Located in a pit to provide a direct 72-foot optical path, the chamber performs the same optical function as Chamber I_{EM} with a limiting accuracy which should be considerably better than $\lambda/10$, because of the vacuum environment. A sketch of Chamber I is shown in Figure 6.5-3. Figure 6.5-4a is a photograph of the chamber.

6.5.1.3 Chamber I_G. Chamber I_G will be used for final tests of curved mirrors in a one-Torr vacuum and is located in Building 101. The Chamber is the same as Chamber I, except that the vacuum chamber and structure provide for future growth, Figure 6.5-4b includes Chamber I_G.

6.5.1.4 Chamber II_{EM}. Chamber II_{EM} is an engineering model chamber for early plano mirror tests in air and is located at Building 601. Figure 6.5-5 is a drawing of Chamber II_{EM}. This chamber is in operation with a 52-inch-diameter reference sphere. The 82-inch-diameter reference sphere will be installed when available. The 72-inch-diameter reference planos and 72-inch-diameter TM will be tested in this chamber. As in Chamber I_{EM}, it is to be considered a full-scale model, and is fully instrumented to provide training for use of Chambers II and II_G. Limiting accuracy is about $\lambda/4$ with the use of the subaperture 52-inch-diameter sphere.

~~SECRET~~ D

~~SECRET~~ D

BIF-008- [REDACTED] -68
(Control Number)

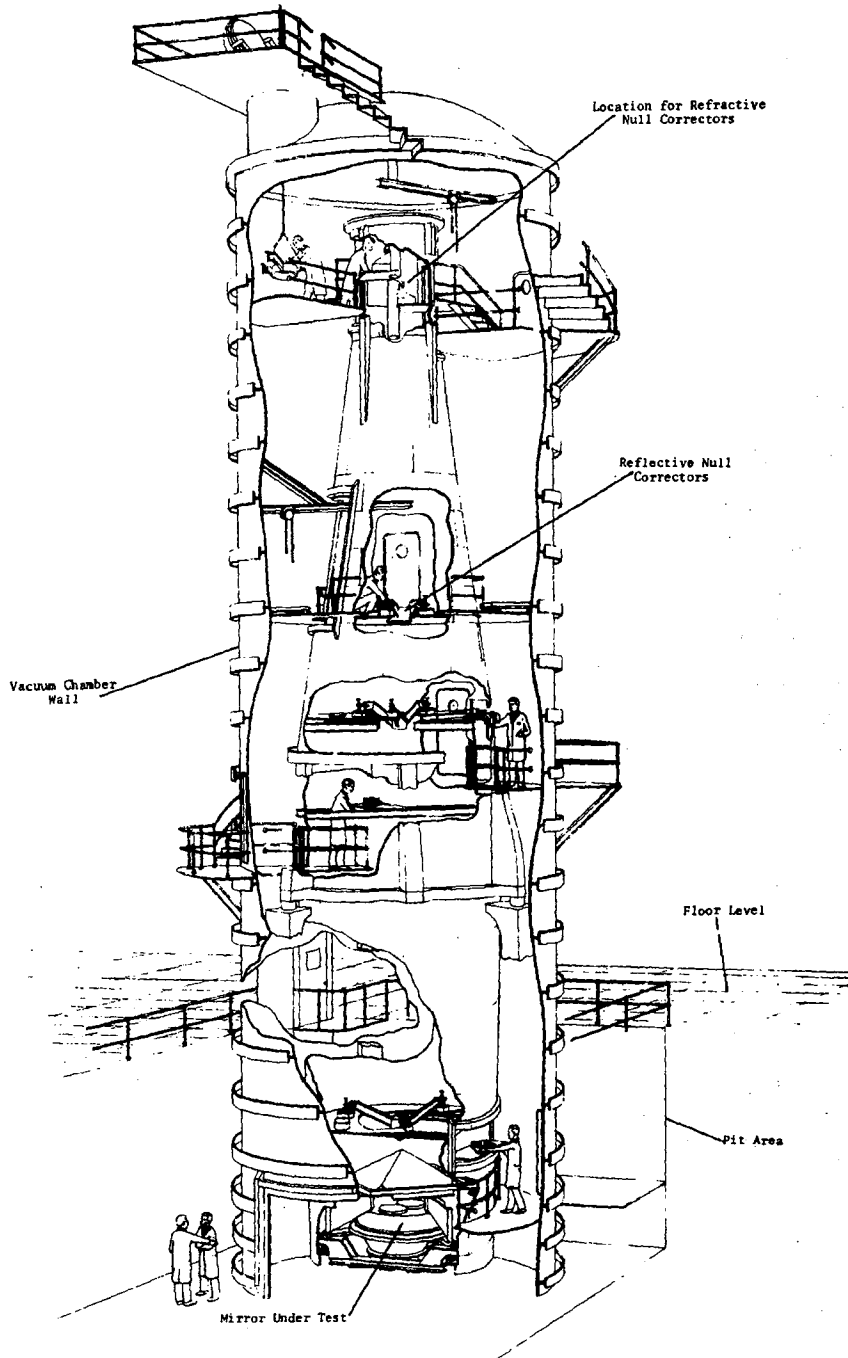


Figure 6.5-3. Chamber I

6-85

~~SECRET~~ D

Handle via **BYEMAN**
Control System Only

~~SECRET~~ D

BIF-008- [REDACTED] -68
(Control Number)

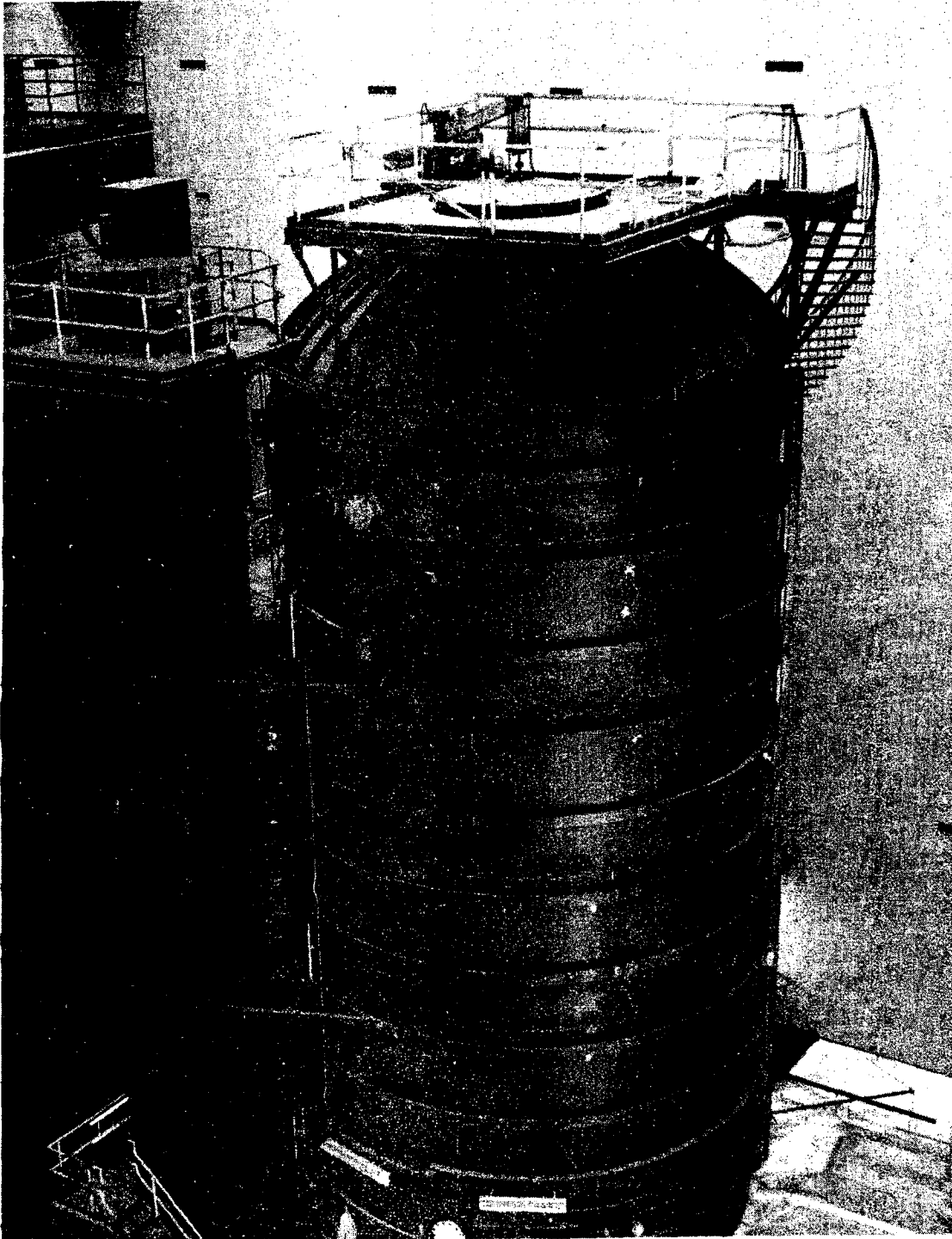


Figure 6.5-4a. Chamber I

6-86

~~SECRET~~ D

Handle via **BYEMAN**
Control System Only

~~SECRET~~ D

BIF-008- [REDACTED] -68
(Control Number)

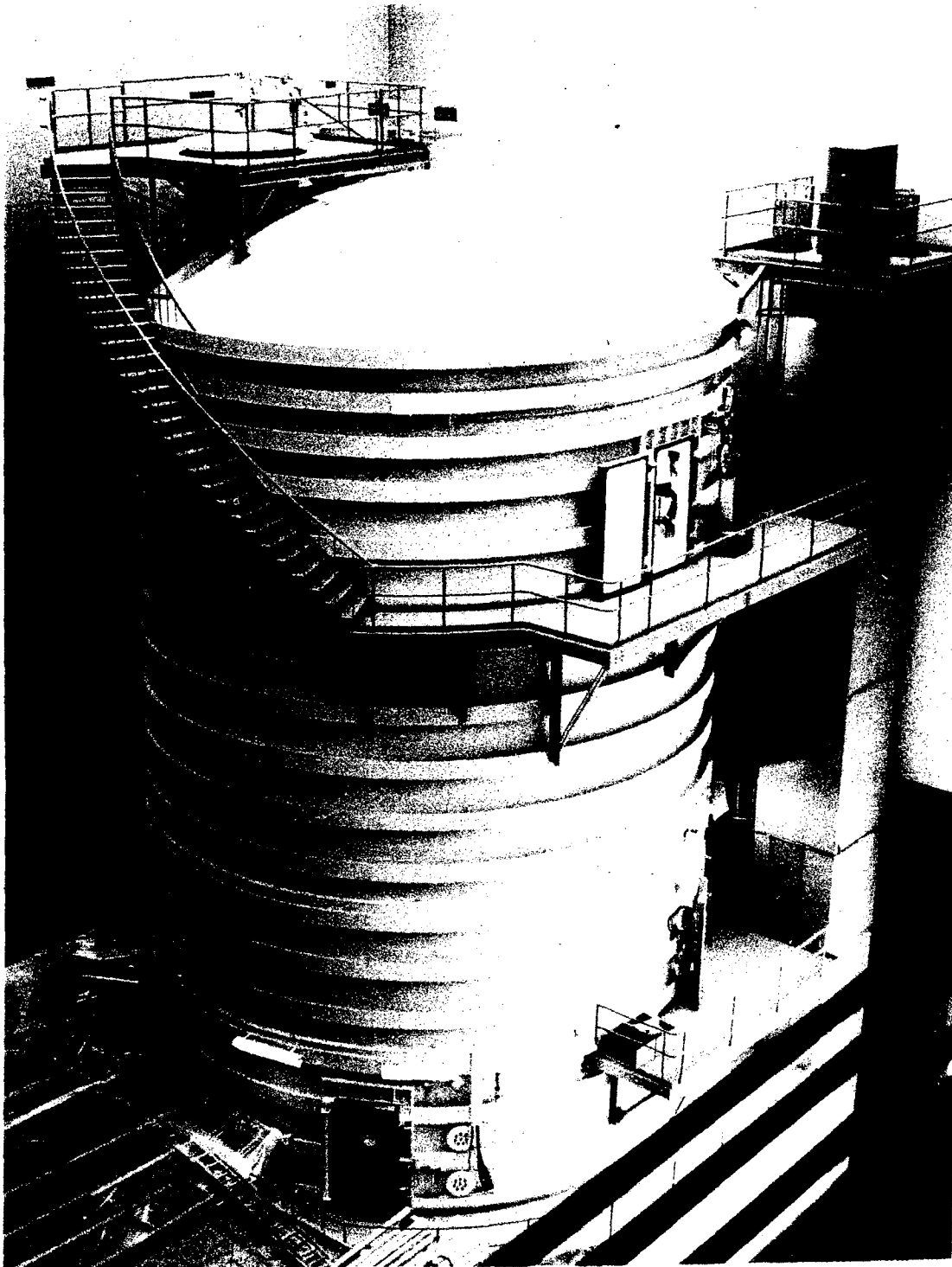


Figure 6.5-4b. Chamber Ig

6-87

~~SECRET~~ D

Handle via BYEMAN
Control System Only

~~SECRET~~ D

BIF-008- [REDACTED] -68
(Control Number)

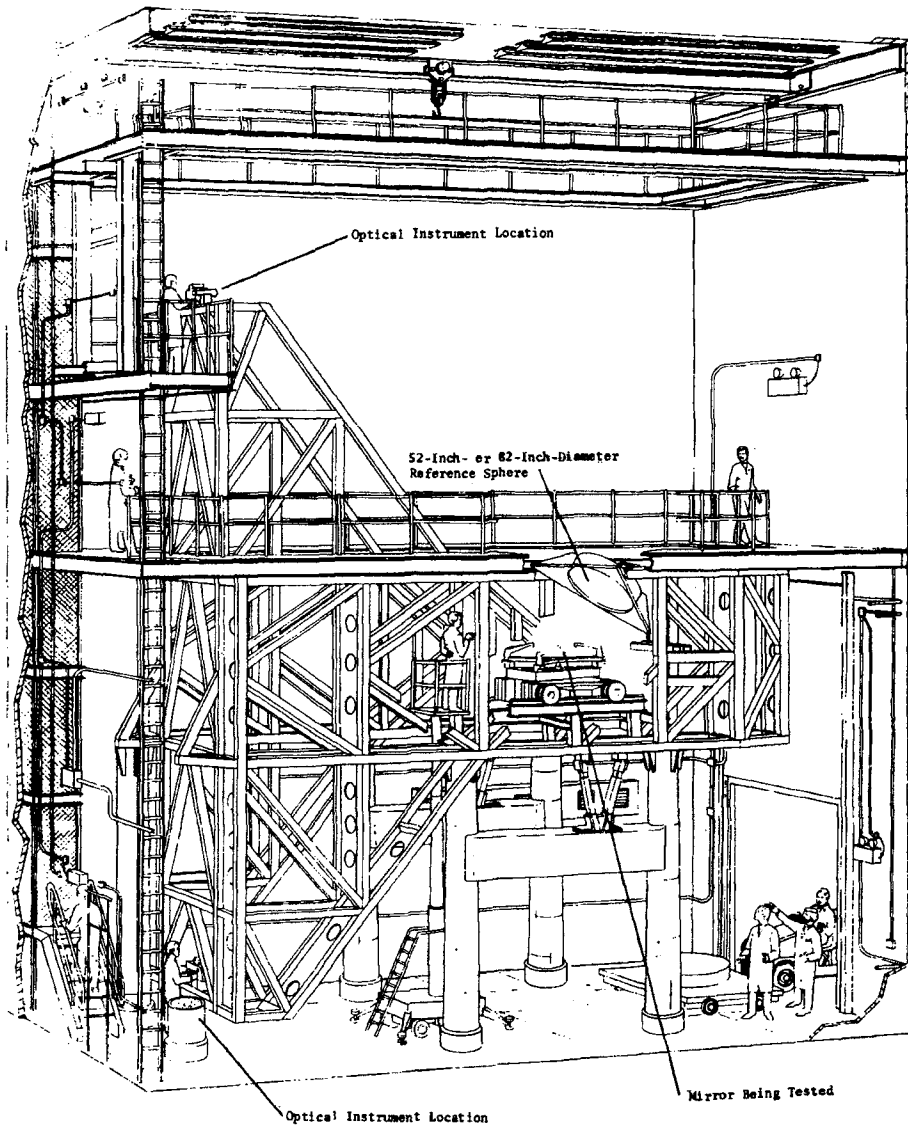


Figure 6.5-5. Chamber II_{em}

6-89

~~SECRET~~ D

Handle via BYEMAN
Control System Only

~~SECRET~~ D

BIF-008- [REDACTED] -68
(Control Number)

6.5.1.5 Chamber II. Chamber II will be used for final tests of plano mirrors in a one-Torr vacuum and is located in Building 101. The reference sphere is 82 inches in diameter. The chamber will perform the same functions as II_{EM}. Limiting accuracy should be better than $\lambda/10$ as a result of the vacuum environment, and the full-aperture reference sphere.

6.5.1.6 Chamber II_G. Chamber II_G will be used for final tests of plano mirrors in a one-Torr vacuum, and is located in Building 101. The chamber is the same as II except that the chamber and structure provide for future growth. Figure 6.5-6 is a photograph of Chamber II_G.

6.5.1.7 Chamber III. Chamber III will be used for testing complete optical assemblies in a one-Torr vacuum. Two chambers are located in Building 101. The formula sample and flight optics will be evaluated by autocollimation. The chambers are designed for the following tests:

- a. Formula sample
- b. COA
- c. MM
- d. Transmissibility
- e. Calibration of autocollimating flat by means of master parabola

The formula sample requires an auxiliary structure or barrel which also serves, in conjunction with the master parabola, to evaluate the suspension of the autocollimating flat. It is expected that such suspension evaluation will be made before each test of an assembly. The mount design for the autocollimating flat provides adjustment to improve the figure of the mirror. Figure 6.5-7 is a photograph of Chambers III-a and III-b.

~~SECRET~~ D

~~SECRET~~ D

BIF-008- [REDACTED] -68
(Control Number)

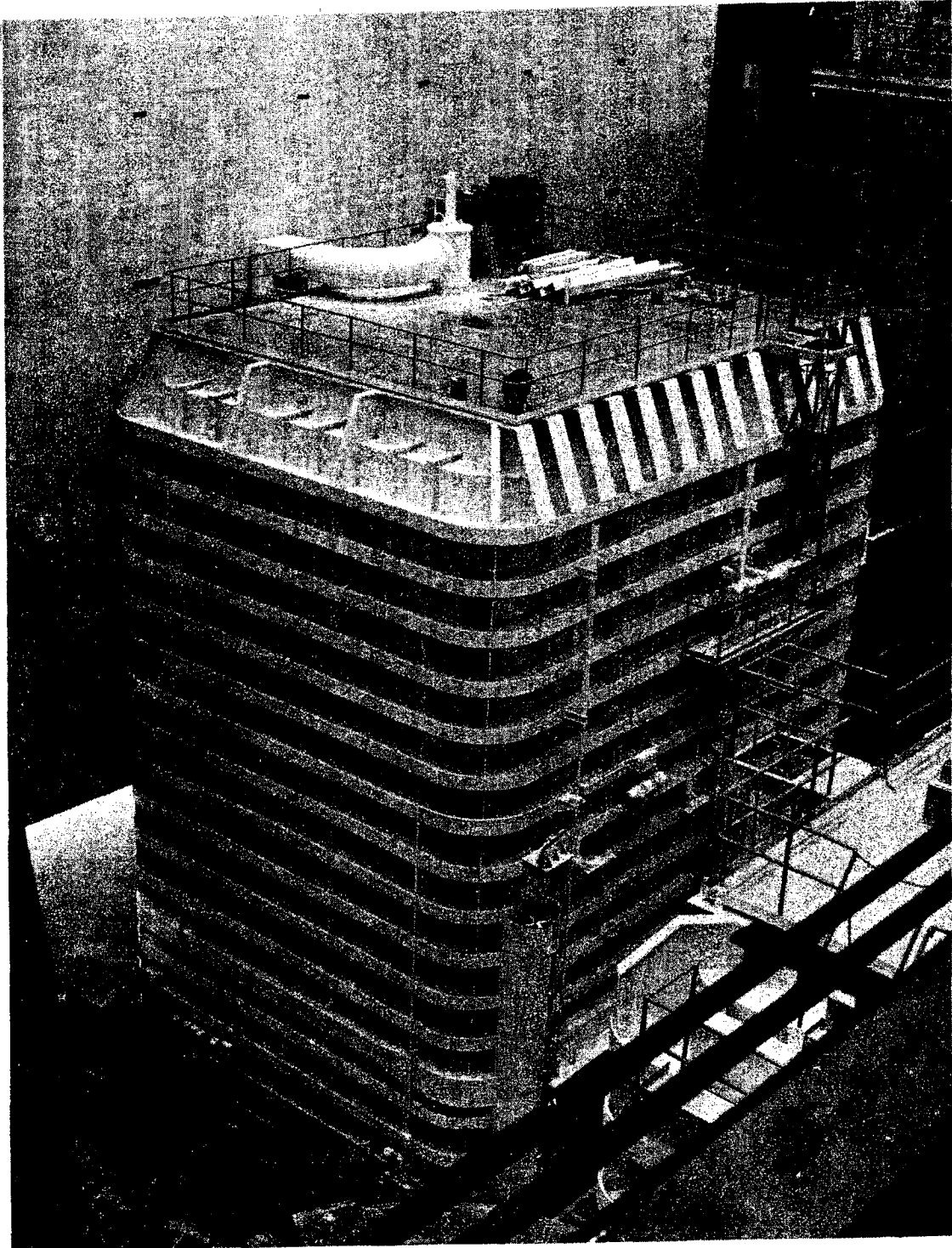


Figure 6.5-6. Chamber IIg

6-91

~~SECRET~~ D

Handle via BYEMAN
Control System Only

~~SECRET~~ D

BIF-008- [REDACTED] -68
(Control Number)

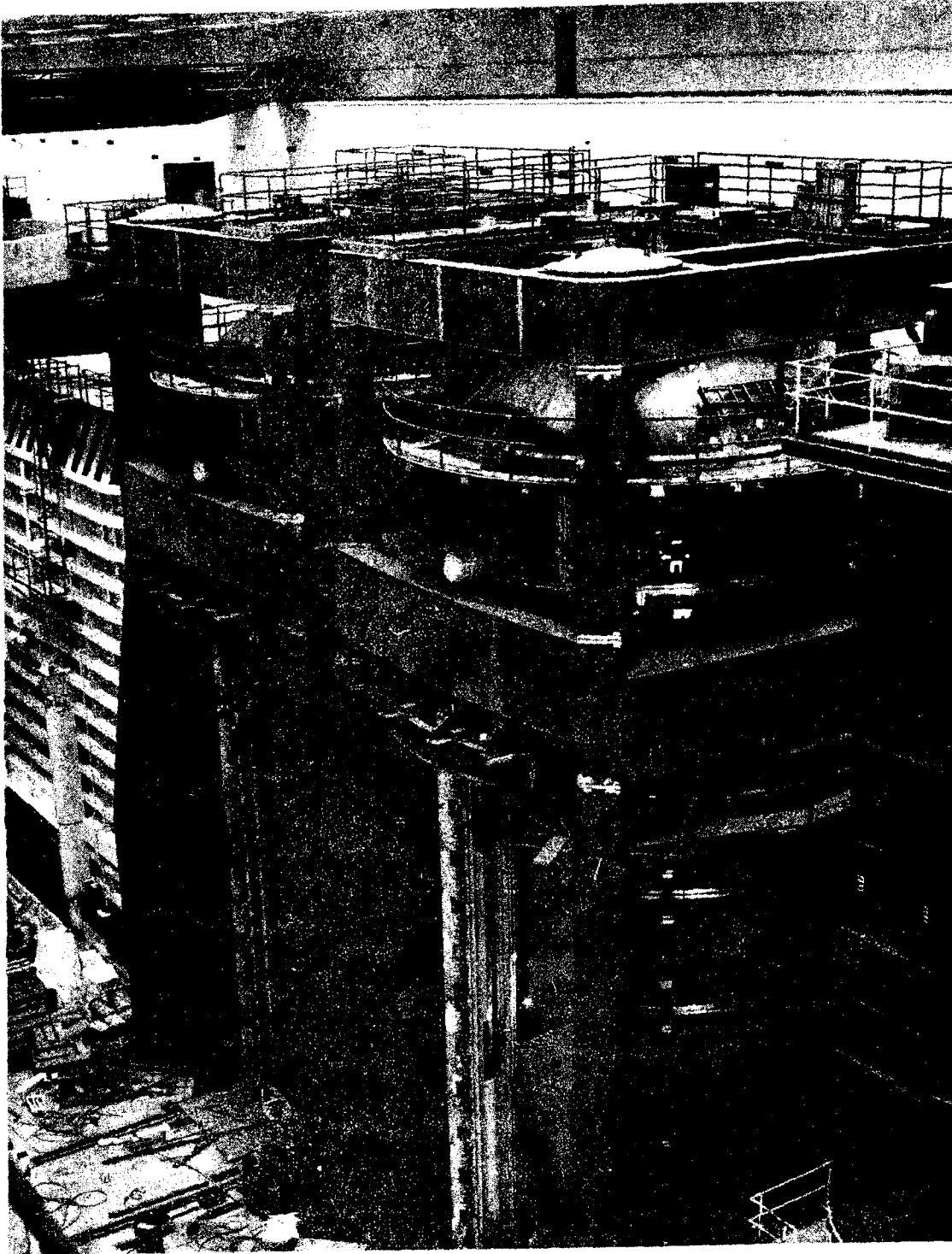


Figure 6.5-7. Chambers IIIa and b

6-92

~~SECRET~~ D

Handle via BYEMAN
Control System Only

~~SECRET~~ D

BIF-008- [REDACTED] -68
(Control Number)

6.5.1.8 Chamber A. Chamber A (see Figures 6.5-8 and 6.5-9) provides simulation of orbital environment for thermal and thermal/optical testing.

Chamber A is capable of simulating the following:

- a. Orbital pressure with a hard vacuum (to 5×10^{-8} Torr),
- b. Solar flux with an infrared (IR) array (180 watts/sq ft),
- c. Ultraviolet radiation into the TM bay as a result of albedo and earth radiation with a Xenon energy projection system (XEPS) (up to 75 watts/sq ft), and
- d. Cold space with 100 K, liquid nitrogen (LN₂) cooled, black-surface cryowalls.

Peripheral equipment for Chamber A includes:

- a. Thermal data management system (TDMS) (see paragraph 6.6.2.2.1),
- b. Optical measurement apparatus,
- c. Closed circuit television, readout system, and
- d. Miscellaneous measurement, control and connecting equipment.

6.5.1.9 Chamber B. Chamber B, located in Building 101, is a 15 by 15 by 45-foot-long high-vacuum (10^{-7} Torr) chamber having a rapid recycle capability. The chamber will be used for full-scale thermal engineering tests, THM tests, thermal optical tests, and ascent-venting tests.

A special portable structure was constructed for installation in Chamber B. The configuration follows the general design of structure II_{EM} and allows tests of TM's in a vacuum and in simulated albedo conditions.

~~SECRET~~ D

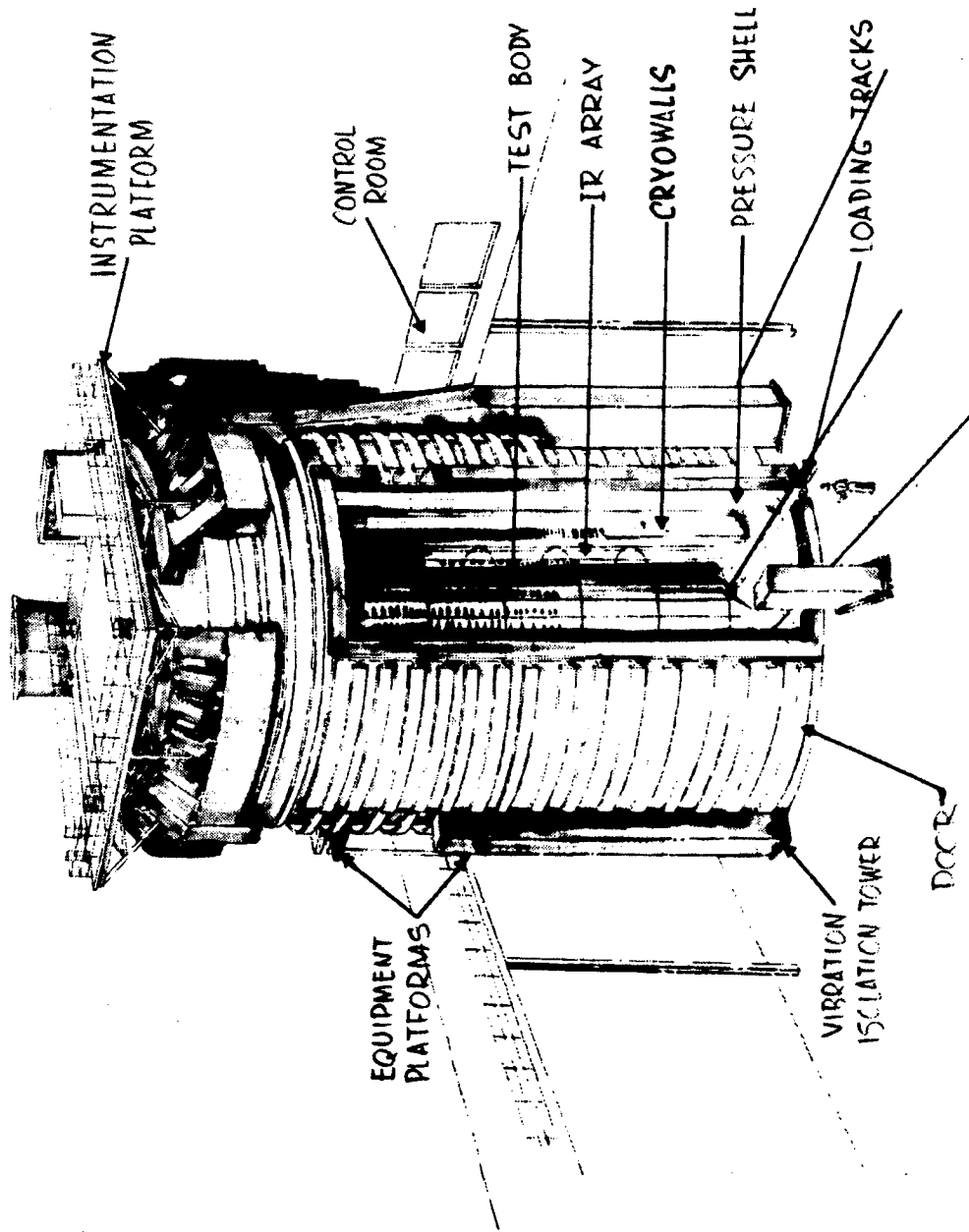


Figure 6.5-8. Chamber A

Handle via BYEMAN
Control System Only

~~SECRET~~ D

~~SECRET~~ D

BIF-008- [REDACTED] -68
(Control Number)

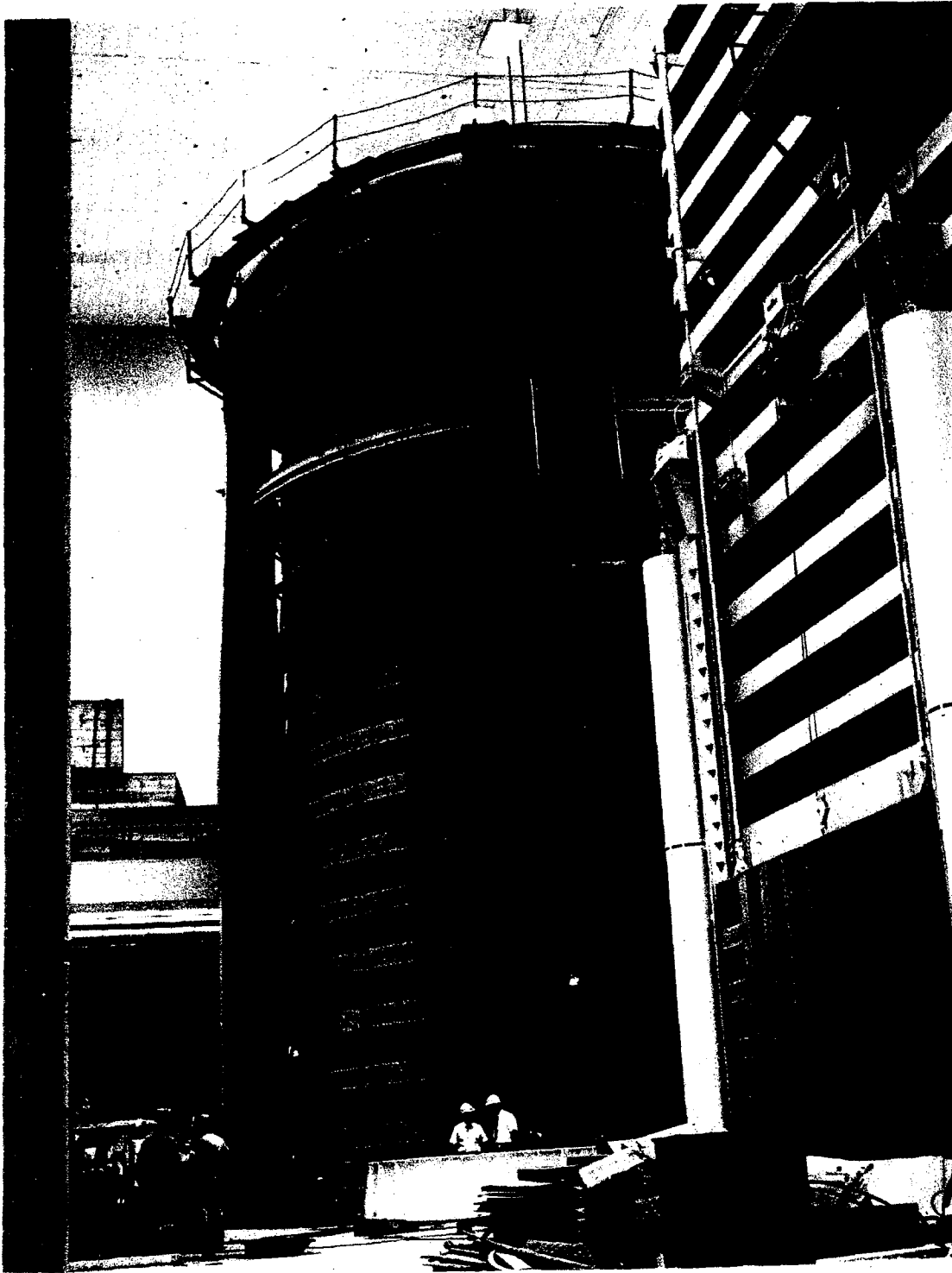


Figure 6.5-9. Chamber A

6-95

~~SECRET~~ D

Handle via BYEMAN
Control System Only

~~SECRET~~ D

BIF-008-[REDACTED]-68
(Control Number)

6.5.1.10 Chamber C. Chamber C is an 8 by 8 by 22-foot-long, high-vacuum chamber (10^{-8} Torr) now in use for early thermal studies, half-scale thermal tests, and thermal optical tests.

6.5.1.11 Chamber D. Chamber D is a 5-psi chamber capable of reproducing the oxygen-helium atmosphere of the LM for extended periods of time. The chamber will be used during engineering tests for EKC LM-mounted equipment and for acceptance and qualification tests of these components.

6.5.1.12 Chamber F. Chamber F is a weather box for a THM ground-conditioning test of the MM. Ground temperature extremes peculiar to the launch facility are provided. The chamber is fabricated of insulated plywood, and has air conditioners to simulate thermal conditions. There is no provision for rain, wind, or snow simulation.

6.5.1.13 Chamber X. Chamber X is located at Building 601 for the purpose of testing vacuum test equipment, such as interferometers, air bags, etc. The chamber will be capable of a soft vacuum and will be vibration isolated.

6.5.2 Acoustic Test Facility

The acoustic test facility being installed at the Elmgrove Plant was designed to provide an acoustic environment representative of the launch and ascent portions of flight. This facility will impart an equivalent internal vibrational environment to the MM assembly.

The facility is being designed to provide a two-level test environment (see Figures 6.5-10 and 6.5-11). The spectrum shape will be controlled in 1/3 octave bands from 37 to 1600 Hz. Significant energy will exist above 1600

6-97
~~SECRET~~ D

Handle via **BYEMAN**
Control System Only

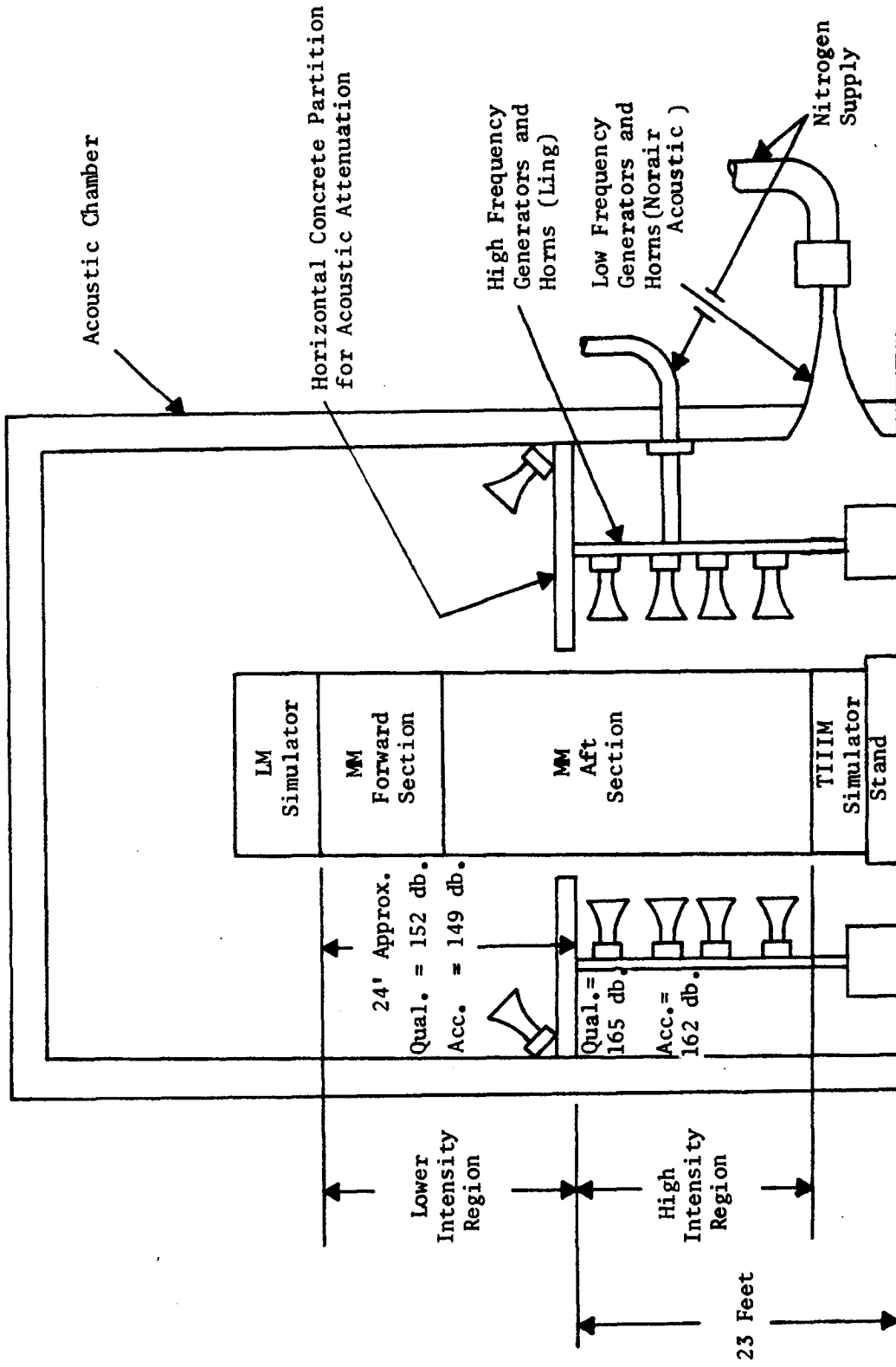


Figure 6.5-10. MM Acoustic Vibration Test Configuration

Handle via BYEMAN
Control System Only

~~SECRET~~ D

BIF-008- [REDACTED] -68
(Control Number)

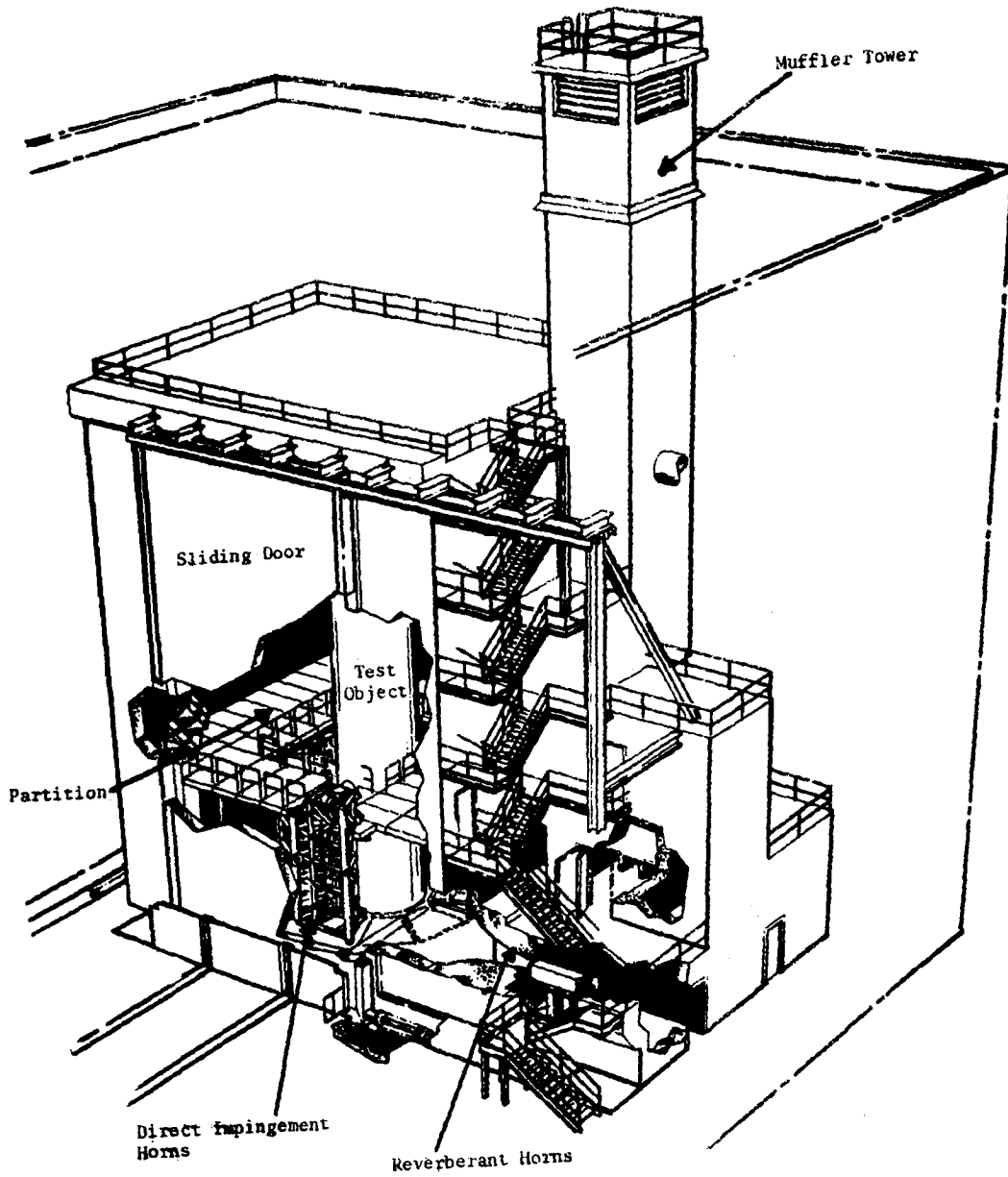


Figure 6.5-11. Acoustic Test Chamber

6-99

~~SECRET~~ D

Handle via BYEMAN
Control System Only

~~SECRET~~ D

BIF-008- [REDACTED] -68
(Control Number)

Hz, but will not be controlled. The spectrum shape is a composite of the launch and ascent portions of powered flight and, as such, is not fully representative of either.

The two-level test environment described above is achieved by dividing the test cell into two chambers by a 6-inch removable concrete partition as shown in Figure 6.5-11. The test chamber inside dimensions are 34-feet wide by 44-feet deep by 62-feet high. The partition, located 23 feet above the floor, provides a controlled gap of 1 to 8 inches around the MM.

Two large, low-frequency (37 to 400 Hz) horns driven by Norair electro-hydraulically modulated transducers, which provide the reverberant vibrations, are located in the lower chamber. The lower chamber also contains 40 direct-impingement horns driven by electro-pneumatic transducers with an effective frequency range of 200 to 4800 Hz. Eight additional electro-pneumatic transducers and horns are located in the upper chamber and operate in a reverberant mode to generate medium-and high-frequency noise. Figure 6.5-12 is a photograph of the acoustical test facility.

The facility also includes comprehensive data acquisition and processing equipment, which shares a small general purpose computer with facility control and monitoring equipment. Microphones, acceleration sensors, and strain gages provide inputs into a maximum of 236 data channels.

The acoustic test facility is designed for flexibility and growth capability. Design and construction was subcontracted. Included are major elements of support and handling equipment incidental to the use of the facility.

~~SECRET~~ D

BIF-008- [REDACTED] -68
(Control Number)

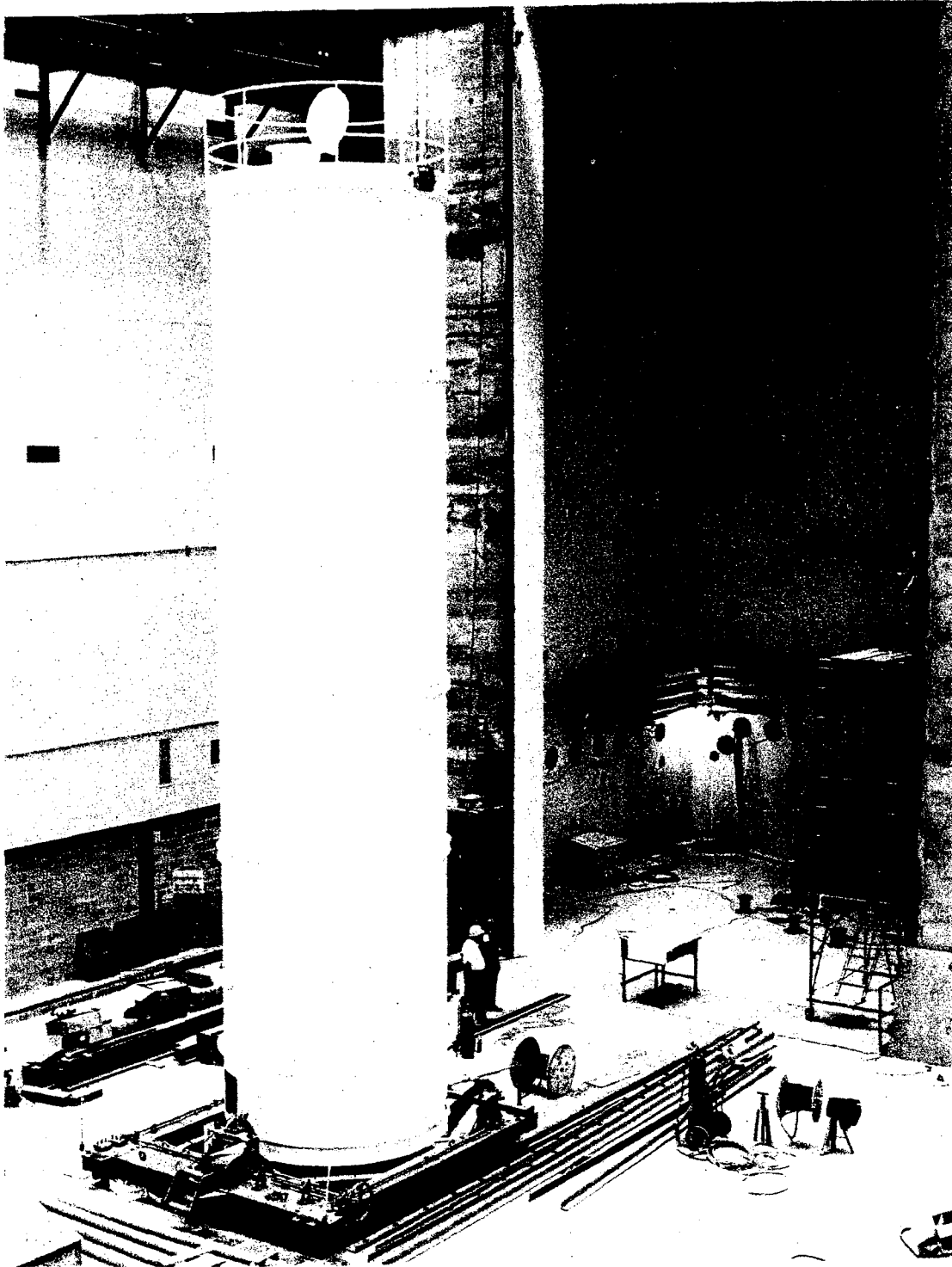


Figure 6.5-12. Acoustic Test Facility

6-101

~~SECRET~~ D

Handle via BYEMAN
Control System Only

~~SECRET~~ D

BIF-008- [REDACTED] -68
(Control Number)

6.5.3 Test Chamber and Tower Accessories

A basic test chamber consists of a vacuum or thermal chamber, structure and vibration isolation, precision mounting surfaces, instrumentation, remote-control devices, closed-circuit television, and a control console. In addition, there are work positioning tables and mirror mounts, many of which are for special purposes and are removable. The following accessories are described in more detail.

6.5.3.1 Precision Mounting Surfaces. All test chambers, whether for optical elements or complete optical assemblies, serve multiple functions and therefore require shifting of test apparatus and instrumentation. To provide accuracy and repeatability, and to eliminate time consuming setup and alignment, a system of 3 radial V-grooves is used, into which the ball ends of instrument leveling screws rest. This is used extensively for interferometers, knife edges, point sources, diagonal mirrors, folding mirrors, null correctors, and work positioning tables.

6.5.3.2 Data Recording Camera. Giannini Model 207 multi-data cameras are in use for all interferometer recording. These units provide:

- a. Double 35mm frame capability
- b. Frame numbering
- c. Data recording (including time)
- d. Complete remote-control operation in a vacuum
- e. Reflex finder
- f. 200-foot film capacity

~~SECRET~~ D

~~SECRET~~ D

BIF-008- [REDACTED] -68
(Control Number)

6.5.3.3 Closed-Circuit Television. To monitor the camera as it records an interferometer image on film, closed-circuit television is in use. The image orthicon readily transmits the camera viewfinder image to the monitor screen at the control console. Some of the advantages of TV are that it:

- a. Eliminates the need for optical relays,
- b. eliminates the need for observing and photographing through an optical window, and
- c. eliminates the safety hazard of an implosion with a window.

6.5.3.4 Remote Control. To operate the interferometer and to adjust various mirrors in a vacuum or at a distance of many feet, special stepper-type motors will be used which can be accurately and repeatedly controlled from a console or station. The output shaft of these motors rotates in increments as small as 0.45 degree (that is, 800 steps/rev) so that, generally, gear trains will not be required.

6.5.3.5 Control Console. Each test chamber has its own console for instrumentation control, where the interferometer can be monitored by TV, the camera can be actuated, and readings such as temperature and vibration are recorded and displayed.

6.5.3.6 Mirrors and Mounting. Horizontally suspended autocollimating mirrors will be uniformly supported at the edge of a specially designed mounting. The calculated one-g sag yields a radius of curvature approximately equal to 80 n mi. Multiple-point push-pull devices attached to the back of mirrors provide the ability to control optical figure.

~~SECRET~~ D

~~SECRET~~ D

BIF-008- [REDACTED] -68
(Control Number)

Vertically suspended autocollimating mirrors will be sling and edge mounted, with multi-point push-pull devices attached to the back to provide figure control.

Angularly supported mirrors will be sling and edge supported with provisions to pull up on the back with spring scales.

6.5.3.7 Work Positioning Tables. A typical work positioning table will hold work to be tested and provide tilt, rotation, and vertical translation. Horizontal translation is not required as work will be initially positioned accurately and small adjustments provided at the test instrument.

6.6 AEROSPACE SUPPORT EQUIPMENT (ASE)

EKC ASE is broadly defined as the equipment required to assemble, handle, procure, align, test, ship, and otherwise support EKC's role in the Dorian Program.

6.6.1 Photographic Payload

Photographic payload ASE is used for developmental and flight models to supplement assembly and testing of the COA, TM assembly, and LM components. It includes shipping containers for LM components, hardware shipped to associate contractors or to Vandenberg Air Force Base (VAFB) for EKC use, software, and related activation of support equipment.

ASE is subdivided into the following three functional groups:

~~SECRET~~ D

~~SECRET~~ D

BIF-008- [REDACTED] -68
(Control Number)

6.6.1.1 Aerospace Ground Equipment. AGE is the EKC support equipment which is delivered to associate contractors or to VAFB. Two major AGE items are the EKC LM and MM electrical equipment simulator consoles. This equipment will provide an electrical simulation (as seen at the EKC interface) of the EKC components which are located within the LM and MM, respectively. The simulators will accept command inputs, generate verification outputs, terminate power inputs, and provide typical outputs for instrumentation points common to EKC equipment.

6.6.1.2 Special Test Equipment (STE). STE is support equipment used by EKC to determine conformance of the photographic payload AFE with specifications and drawings during manufacture. This group includes the equipment required to test the electrical, optical, mechanical, and environmental performance of the photographic payload. Examples of STE are the positioner dolly (shown in Figure 6.6-1) to be used to support mirrors during test in Chamber II_{EM}; the upright adjustable platform for Chamber I_{EM} mirror supports (see Figure 6.6-2); the weight and center of gravity kit for the COA; the instrumentation processor test set (shown in Figure 6.6-3); the VO test set; the focus control preamplifier test set; and the sensor test system (described in paragraph 6.6.1.2.1) which is used to check out a completed COA or an EKC/LM subsystem.

6.6.1.2.1 Sensor Test System (STS). The STS is a major ASE item which provides a means for testing the EKC-provided LM components and the COA. A proposed layout drawing and a block diagram of the STS are shown in Figures 6.6-4 and 6.6-5.

~~SECRET~~ D

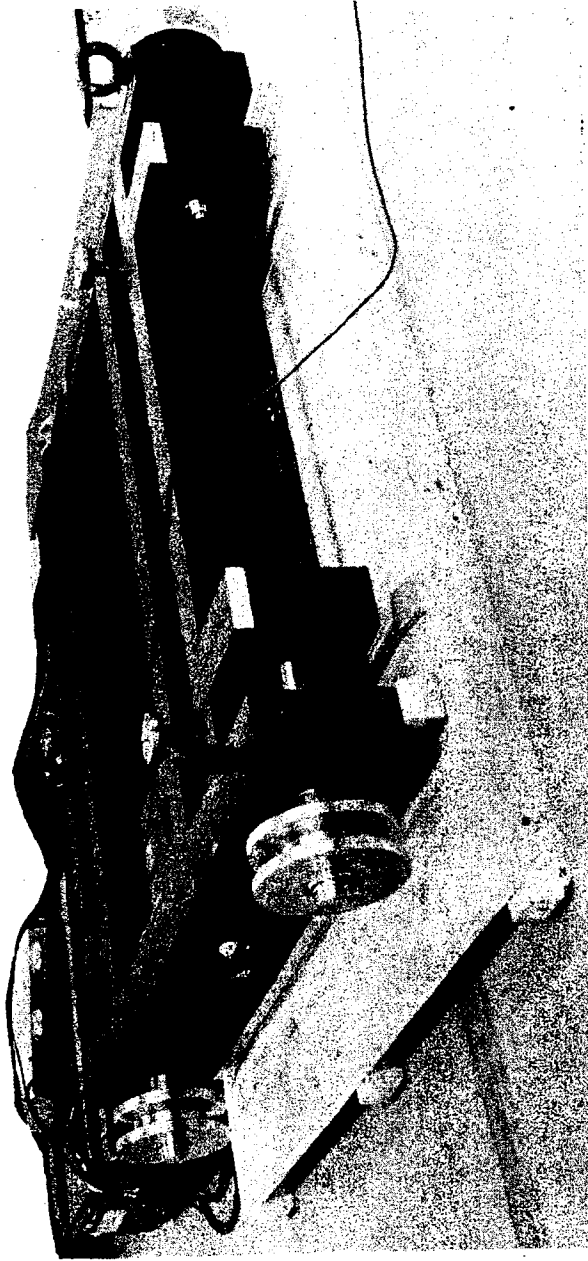


Figure 6.6-1. Positioner Dolly, Chamber II^{EM}

Handle via BYEMAN
Control System Only

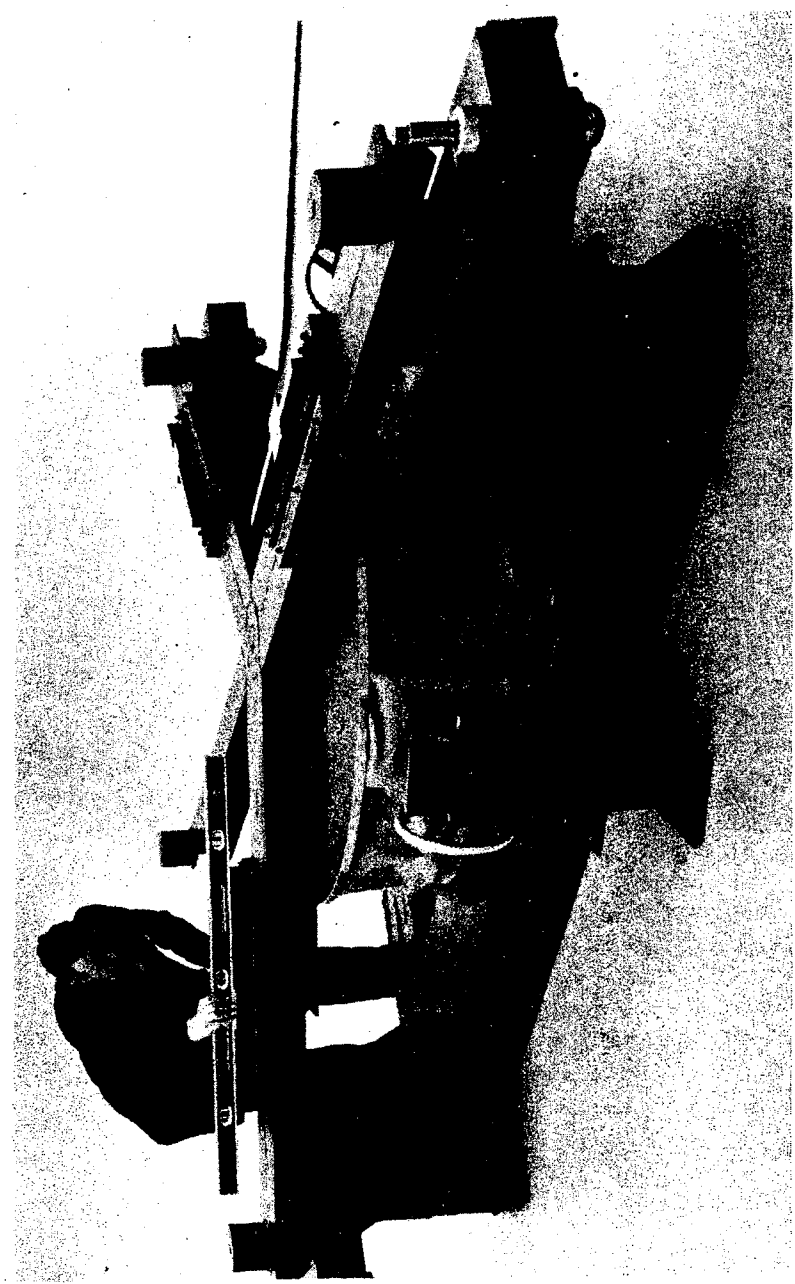


Figure 6.6-2. Upright Adjustable Mirror Support, Chamber I_{EM}

Handle via BYEMAN
Control System Only

~~SECRET~~ D

BIF-008- [REDACTED] -68
(Control Number)

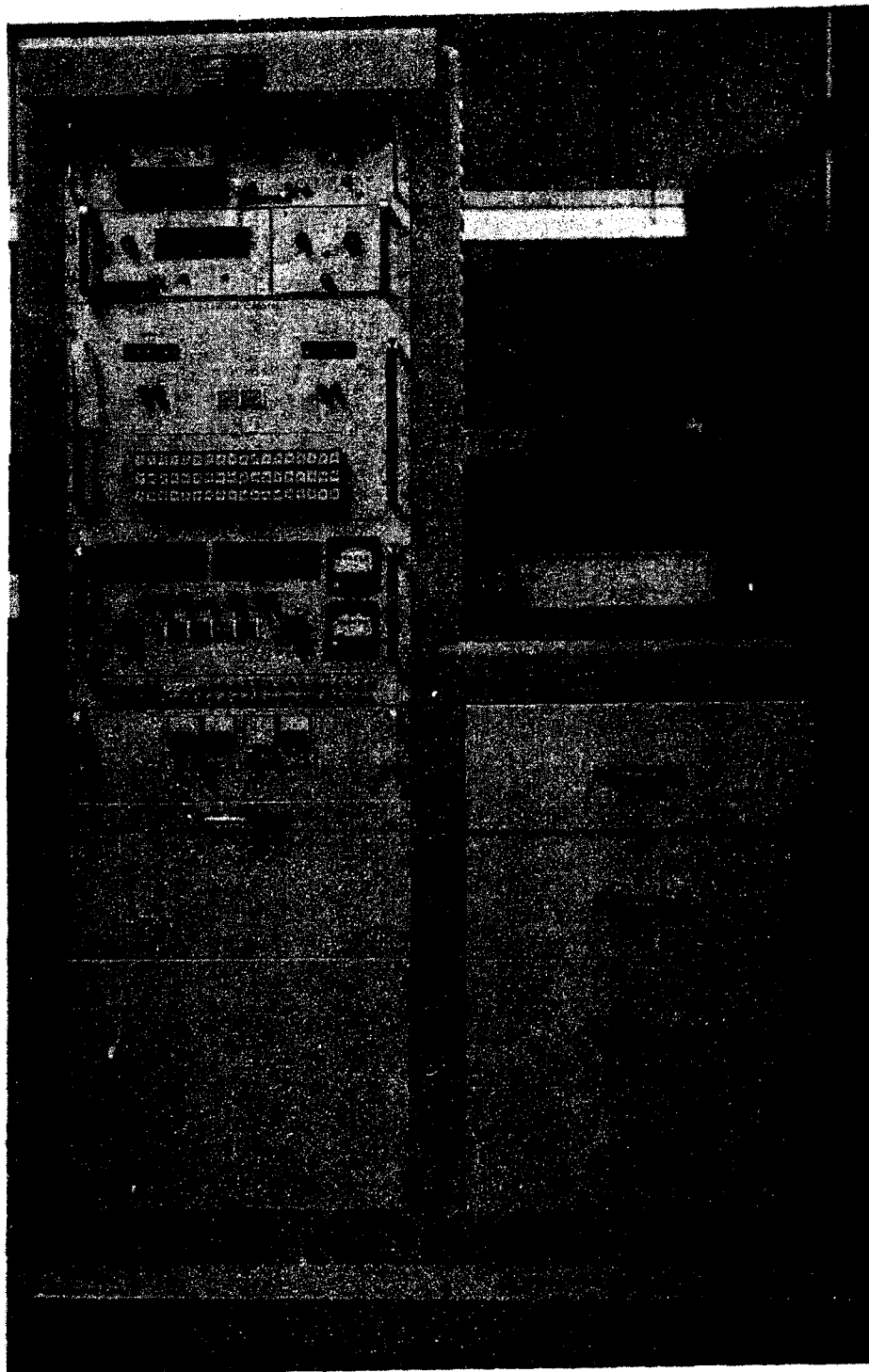
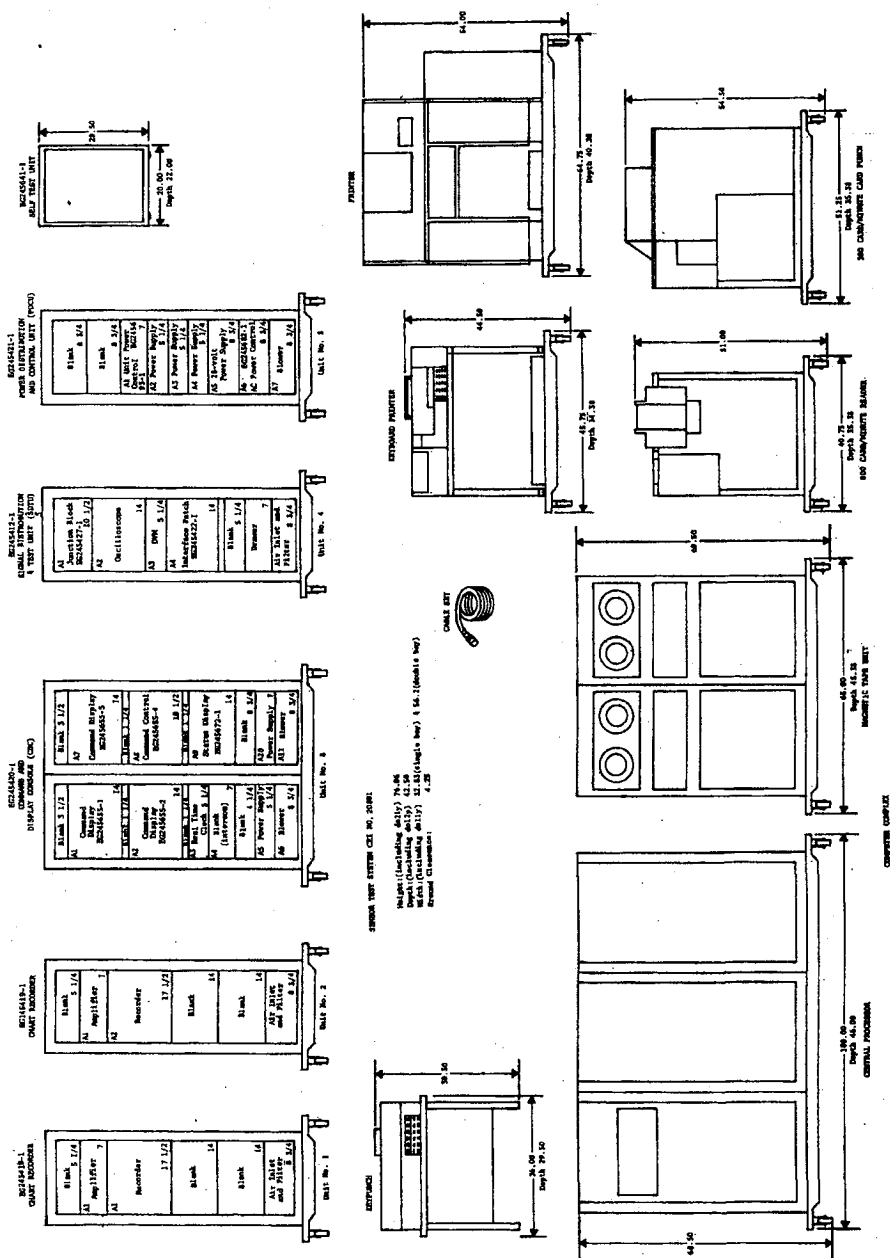


Figure 6.6-3. Instrumentation Processor Test Set
Front Panel View

6-109

~~SECRET~~ D

Handle via **BYEMAN**
Control System Only

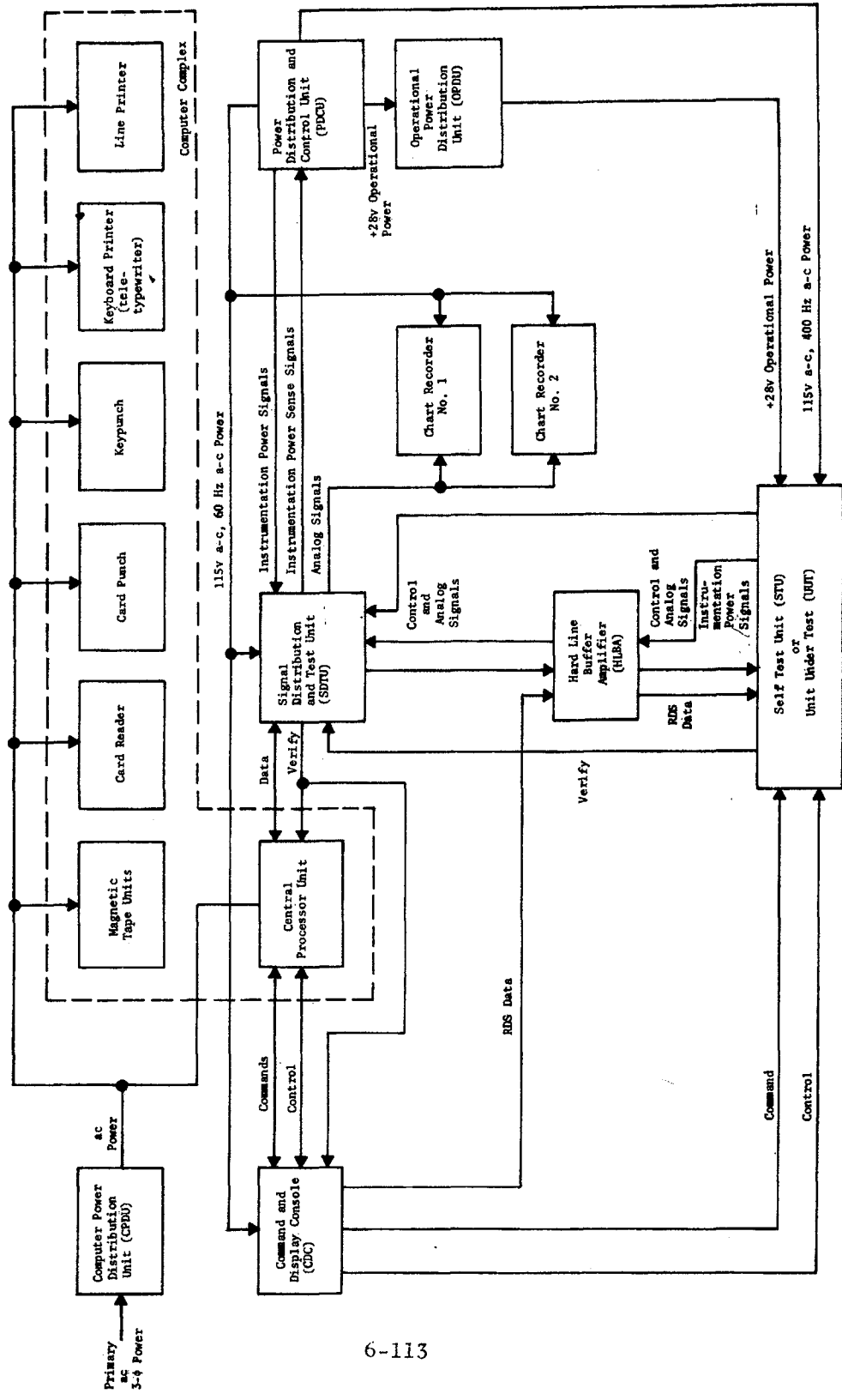


6-111

~~SECRET~~ D

Figure 6.6-4. Layout Drawing of Sensor Test System

Handle via BYEMAN
 Control System Only



6-113

Figure 6.6-5. Block Diagram of Sensor Test System

Handle via BYEMAN
Control System Only

~~SECRET~~ D

BIF-008- [REDACTED] -68
(Control Number)

The STS is a computer-controlled checkout system, with provisions for manual operation, which provides stimulus and response measurement capabilities with go-no-go test results in real time. The system is capable of recording all test results on a printer, magnetic tape, or analog recorder. The response monitor for automatic testing is an analog-to-digital converter which digitizes the correct instrumentation point and compares it to high-low limits stored in the computer. The magnetic tape unit records the test number, test time, command word, instrumentation points, limits, and test results for each test and provides a permanent record. Analog recorders are provided for continuous monitoring of critical instrumentation points. It has a self test capability to verify proper test system operation.

The modular design of the STS gives it versatility. Patchboards can be changed and modifications made to the software, for command generation, test programs, magnetic tape format, and data recorded on magnetic tape.

6.6.1.2.2 Recorder Drum Assembly Deflection Test Fixture. The Recorder Drum Assembly Deflection Test Fixture provides a means for supporting the OA in various positions with respect to the force of gravity so that deflections of the OA can be measured.

6.6.1.3 Special Tooling. Special tooling (ST) is support equipment used by EKC to handle, support, transport, and/or align the PP assemblies during manufacture. Examples of ST are the 72- and 82-inch-diameter master handling rings for gripping the large glass blanks; the universal handling ring lift yoke for handling three sizes of handling rings; the dollies for storing and transporting rings; the corrector assembly cradle

~~SECRET~~ D

~~SECRET~~ D

BIF-008- [REDACTED] -68
(Control Number)

and stand for holding, rotating, positioning and leveling the Ross-corrector barrel; the corrector assembly dolly and erector for transporting and erecting the Ross-corrector assembly; the corrector and diagonal mirrors support structure handler; the cantilever catwalk for providing workmen access to the inside of the OA while the OA is maintained in a horizontal position on a cradle; the assembly and checkout cradle assembly; the primary mirror assembly mobile assembly fixture; the primary mirror assembly fixture; and the lens assembly vertical assembly stand. Two ST items are shown in Figures 6.6-6 and 6.6-7.

6.6.2 Mission Payload System-Level Aerospace Support Equipment

MPS-level ASE is defined as that equipment used for developmental and flight models to implement assembly and testing of the MM and group testing of the LM components; it includes items of MPS exchange hardware provided by EKC for associate contractors or provided as GFE for EKC use. It further includes ASE which is peculiar to the acoustic test facility (ATF).

6.6.2.1 Mission Payload System Aerospace Ground Equipment. MPS AGE is the EKC support equipment which is delivered to associate contractors or to VAFB to support MPS-level activities. It includes items such as the TM mounting ring lifting yoke and the TM assembly guidance equipment required to install the TM into the MM forward section at GE; and the various LM component lifting yokes required to install the camera, processor, and other EKC LM components into the LM at MDD.

~~SECRET~~ D

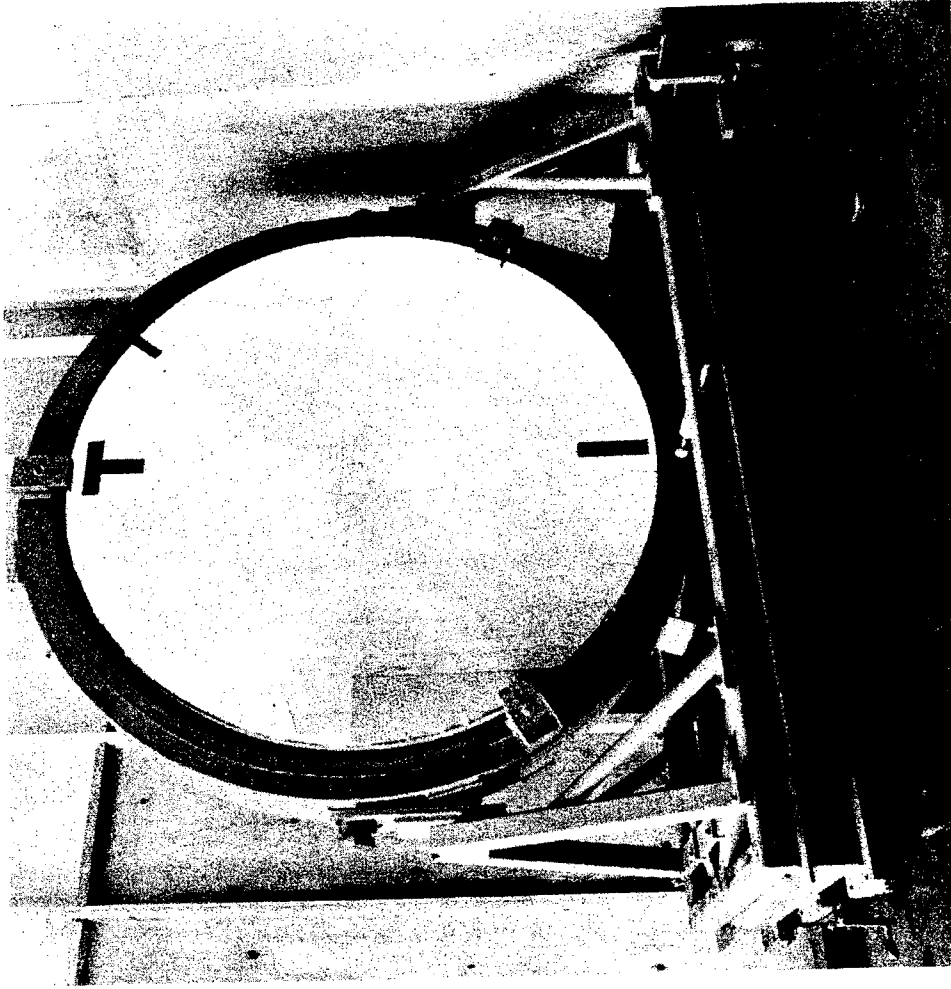


Figure 6.6-6. Horizontal Test Stand Setup

Handle via **BYEMAN**
Control System Only

~~SECRET~~ D

~~SECRET~~ D

BIF-008- [REDACTED] -68
(Control Number)

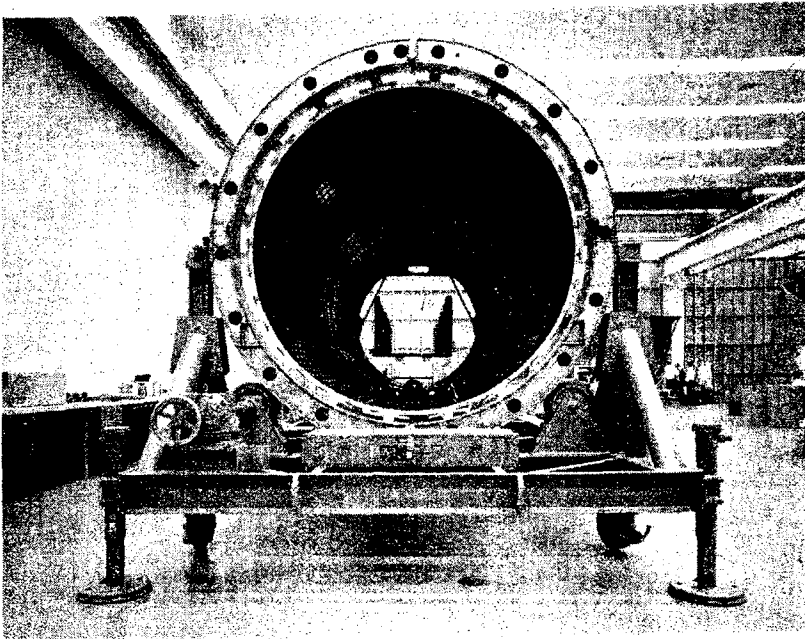
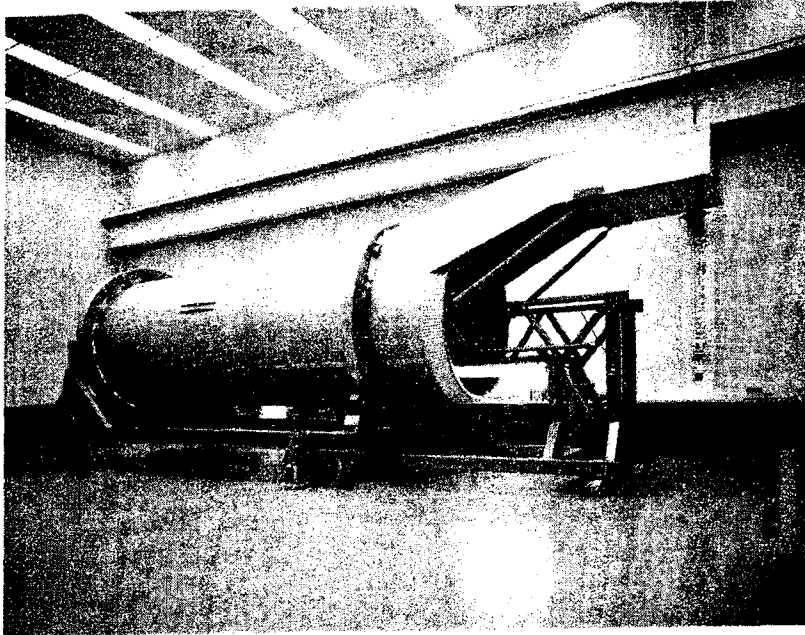


Figure 6.6-7. Checkout Cradle and Cantilever Catwalk
(With SDM Aft Structure)

6-117

~~SECRET~~ D

Handle via **BYEMAN**
Control System Only

~~SECRET~~ D

BIF-008- [REDACTED] -68
(Control Number)

6.6.2.2 Mission Payload System Special Test Equipment. MPS STE is support equipment used by EKC to determine conformance of the MM and the LM subsystem with specifications and drawings during manufacture and/or integration at EKC. This group includes the equipment required to test the electrical, optical, mechanical, and environmental performance of the MM and the LM subsystem. Examples of MPS STE are the horizontal test stand for the MM test in Chamber B; the ground conditioning equipment set used in simulating pad conditions for MM thermal model testing; the MM test set, provided by GE as exchange hardware, which integrates both EKC and GE requirements for testing of a complete MM in all test configurations at EKC; and the TDMS (discussed in paragraph 6.6.2.2.1).

6.6.2.2.1 Thermal Data Management System (TDMS). EKC is responsible for the orderly and timely performance and analysis of several large-scale thermal and thermo-optical tests. Each test will produce large volumes of data with complex interrelations. The TDMS is capable of acquiring all significant test data, of immediately processing and displaying sufficient data for the correct execution of the test, and of providing a time-correlated master-data file for post-test analysis. Temperature differences within optical elements of 0.2 F or greater can induce measurable distortions in fused-silica structure. The TDMS must therefore be capable of recording absolute temperature data to within ± 0.1 F inter-channel accuracy and stability for 95 percent of all samples for the duration of the test.

The TDMS combines a digital computer with programmable analog data acquisition equipment. The computer and its peripherals will provide all logical, computational and display functions. The analog equipment will provide all multiplexing, analog-to-digital conversion and raw data transmission functions.

~~SECRET~~ D

~~SECRET~~ D

BIF-008- [REDACTED] -68
(Control Number)

The TDMS computer is an IBM 1800 process control computer with printing, plotting, and magnetic tape output devices. The data acquisition equipment will be provided by Systems Engineering Laboratories (SEL) to EKC specifications. After study, copper-constantan thermocouples were selected as the temperature sensing elements, placing a requirement of ± 0.2 -microvolt, 30-day inter-channel stability on the analog signal processing equipment.

SEL has demonstrated this stability using a patented reed-relay multiplexer and analog-to-digital converter design and a carefully selected, high-gain differential amplifier. The TDMS will provide over 4000 analog input channels and a limited number of digital input registers. Over-all system stability and accuracy will be enhanced by the use of specially developed reference voltage sources and automatic self-recalibration.

A TDMS breadboard has been in service at EKC for over one year on a 24-hr/day schedule. The breadboard consists of (1) a 512-channel, prototype, analog multiplexer produced under subcontract by SEL, and (2) an IBM 1800 computer. Thirty-day stability tests on the breadboard confirmed the ± 0.2 -microvolt stability requirement was achieved by the analog signal processing equipment when used with secondary standard reference voltage sources. Also, experiments in the measurement of temperature distributions on 30-inch-diameter glass eggcrate structures, under vacuum environment in Chamber C, indicate that sensor, cabling, and reference junction assembly techniques are sufficiently reliable and stable to permit the overall system inter-channel error to be held within the required ± 0.1 F. Figure 6.6-8 is a photograph of the IBM 1800 data processing equipment. Figure 6.6-9 is a photograph of the SEL breadboard data acquisition equipment being used to calibrate thermocouples immersed in two reference temperature baths.

6-119

~~SECRET~~ D

Handle via BYEMAN
Control System Only

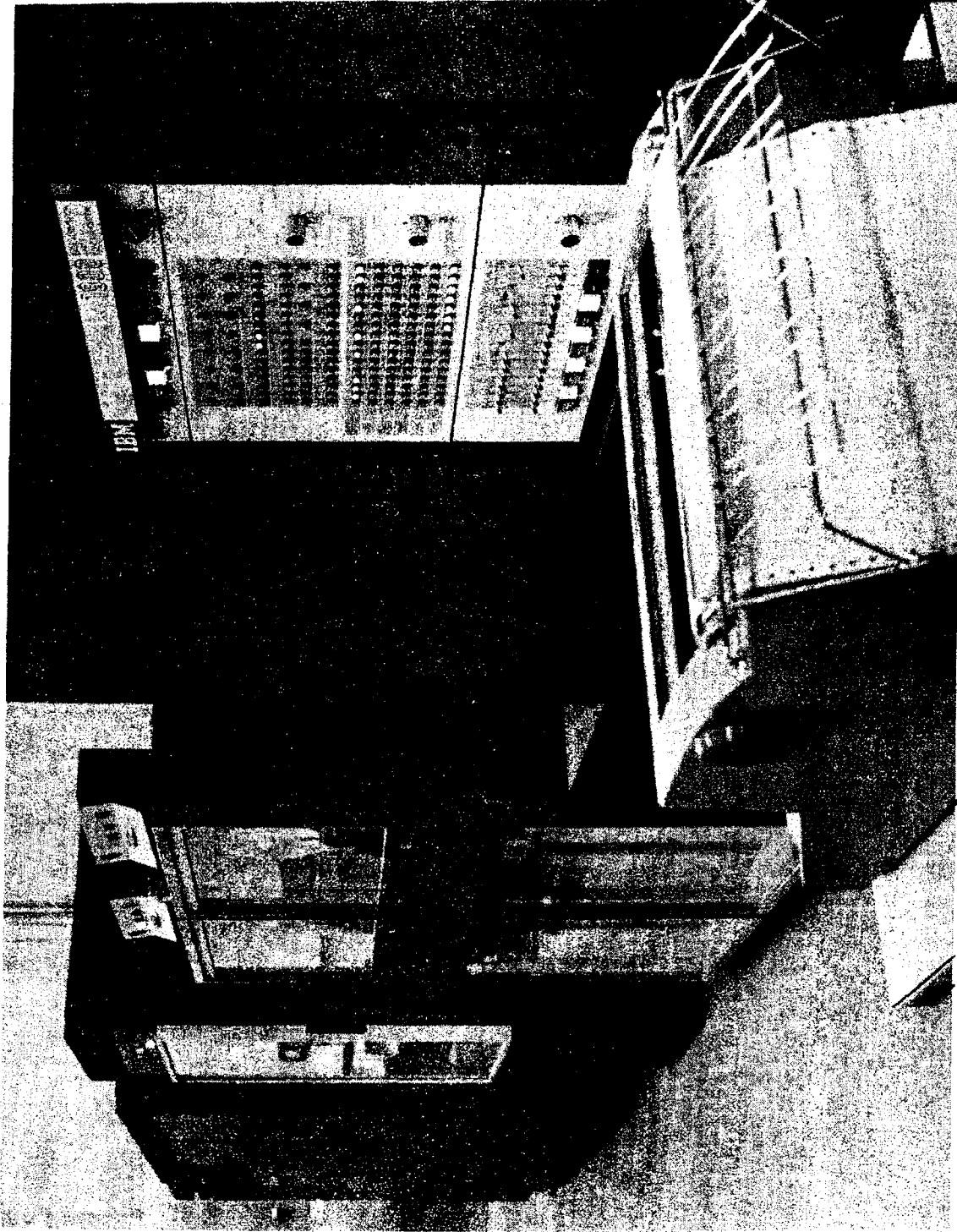


Figure 6.6-8. Thermal Data Management System
Central Computer (IBM)

Handle via BYEMAN
Control System Only

~~SECRET~~ D

BIF-008- [REDACTED] -68
(Control Number)

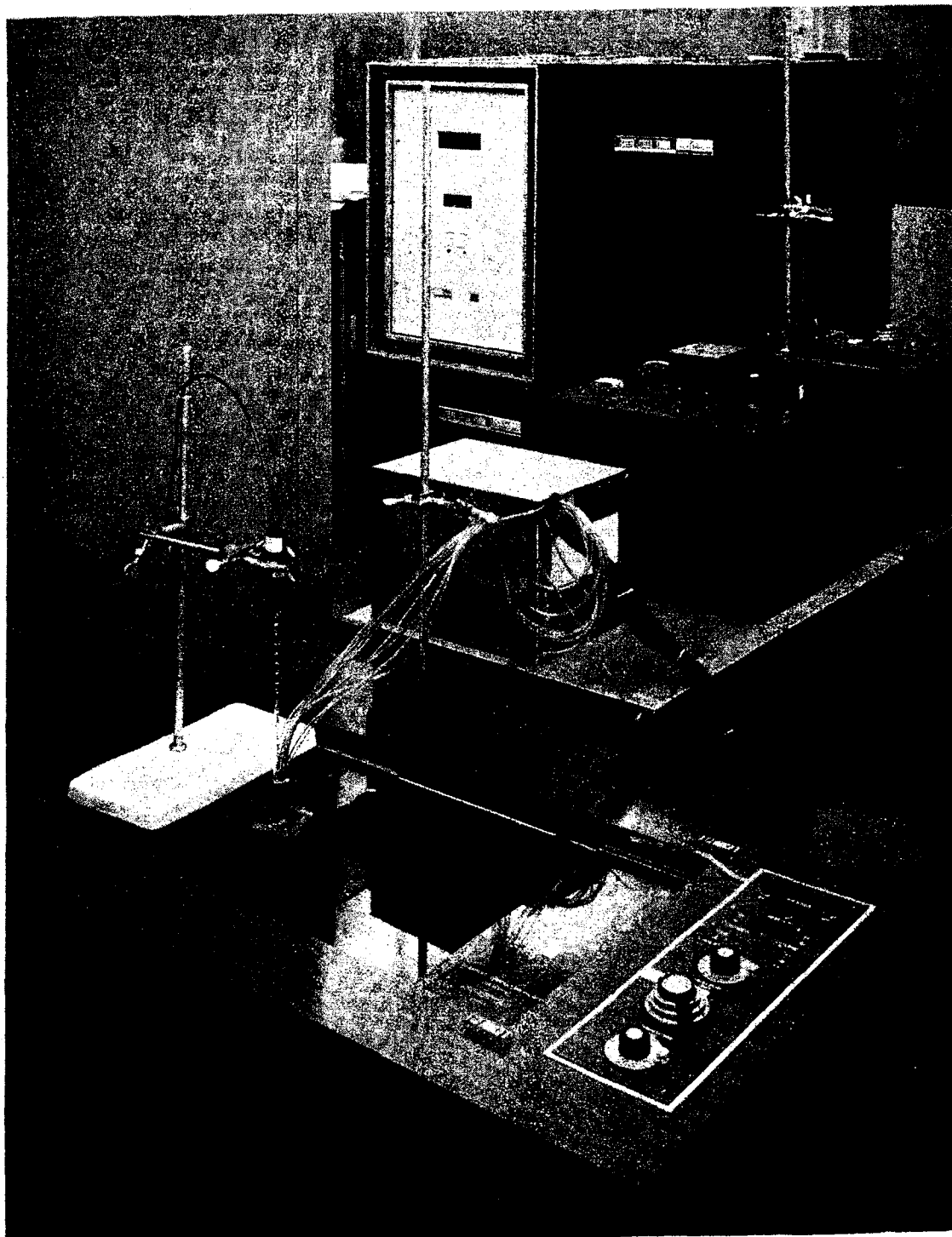


Figure 6.6-9. Thermal Data Acquisition Equipment Breadboard (Systems Engineering Laboratories), Shown Being applied in Thermocouple Calibration.

6-121

~~SECRET~~ D

Handle via BYEMAN
Control System Only

~~SECRET~~ D

BIF-008- [REDACTED] -68
(Control Number)

6.6.2.3 Mission Payload System Special Tooling (MPS ST). MPS ST is support equipment used by EKC to handle, transport, support, and/or align the MM and the LM subsystem during manufacture. Examples of ST are the MM assembly stand (shown in Figure 6.6-10); the LM subsystem test stand; shipping containers for primary film, secondary film and BIMAT film; and the vertical mating fixture used for guidance and insertion of the optical assembly into the MMAS.

6.6.2.4 Acoustic Test Facility Aerospace Support Equipment. ATF ASE is defined as the EKC support equipment used in conjunction with the basic test facility to support acoustic testing of the MM. The major items in this group are a data acquisition and recording device (described in paragraph 6.6.2.4.1); the test body transporter and scaffolding unit (described in paragraph 6.6.2.4.2); and the calibration test body which provides an acoustic substitute for the MM during calibration and checkout of the test chamber.

6.6.2.4.1 Data Acquisition and Recording Device. This configuration will provide the capability for data signal processing, multiplexing, demodulation recording, and computerized data analysis of approximately 200 electro-mechanical transducers mounted on the MM. Auxiliary features such as auto-calibration, programming, voice annotation, telecommunication, and display of analog instrumentation are also provided. Recording is accomplished via 14-track analog tape recorders. Playback of the recording is then digitized and fed to a general purpose digital computer for digital processing and formatting. The output is a digital magnetic tape suitable for direct input to an IBM 360 off-site computer for analysis.

6-122

~~SECRET~~ D

Handle via **BYEMAN**
Control System Only

~~SECRET~~ D

BIF-008- [REDACTED] -68
(Control Number)

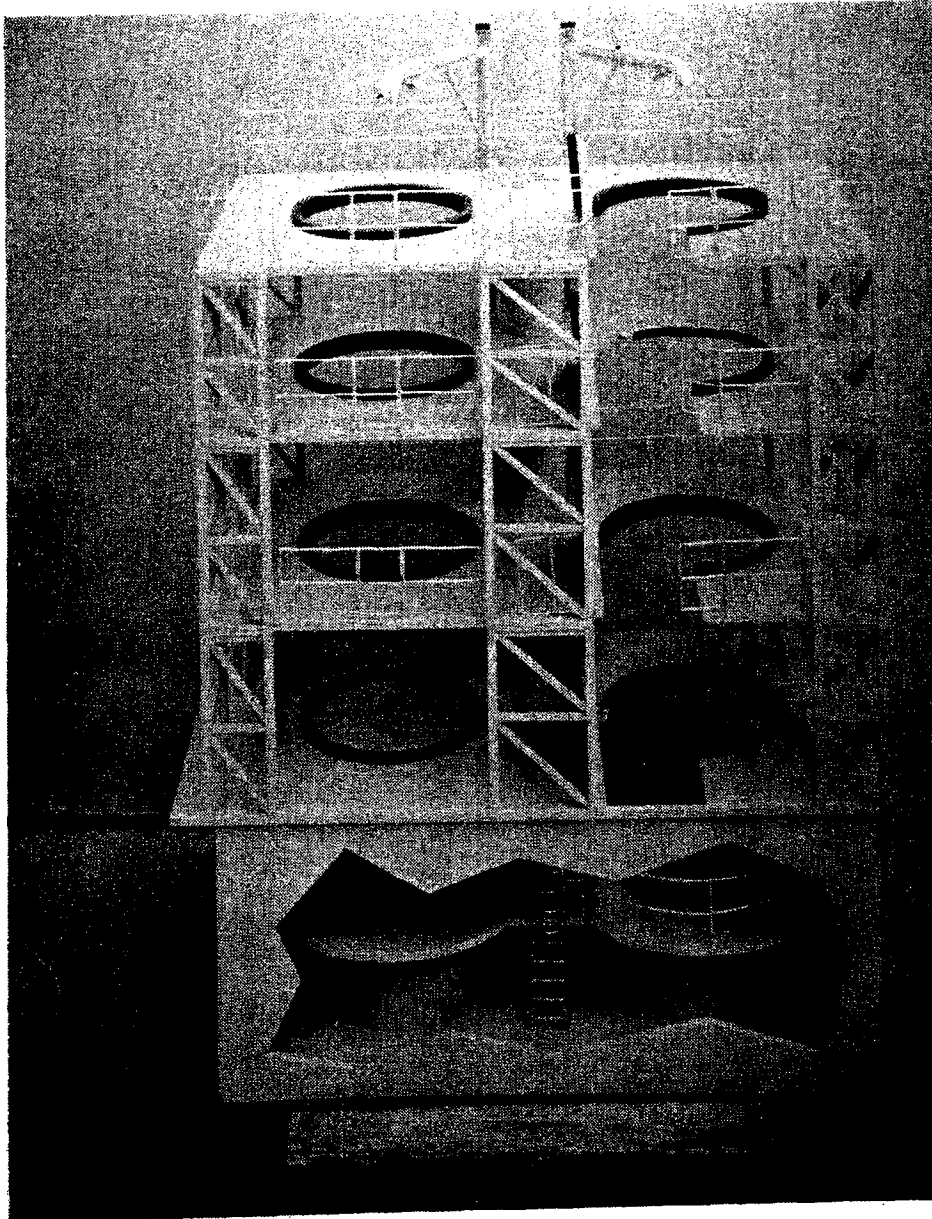


Figure 6.6-10. Mission Module Assembly Stand Scale Model

6-123

~~SECRET~~ D

Handle via **BYEMAN**
Control System Only

~~SECRET~~ D

BIF-008- [REDACTED] -68
(Control Number)

6.6.2.4.2 Test Body Transporter and Scaffolding Unit. This item is a large, motorized structure which: provides the capability for transporting itself and the MM in and out of the ATF; positions and lowers the MM onto the test object support system; and provides access and work platforms at various MM levels. A preliminary concept of the transporter is shown in Figure 6.6-11.

~~SECRET~~ D

Handle via **BYEMAN**
Control System Only

~~SECRET~~ D

BIF-008- [REDACTED] -68
(Control Number)

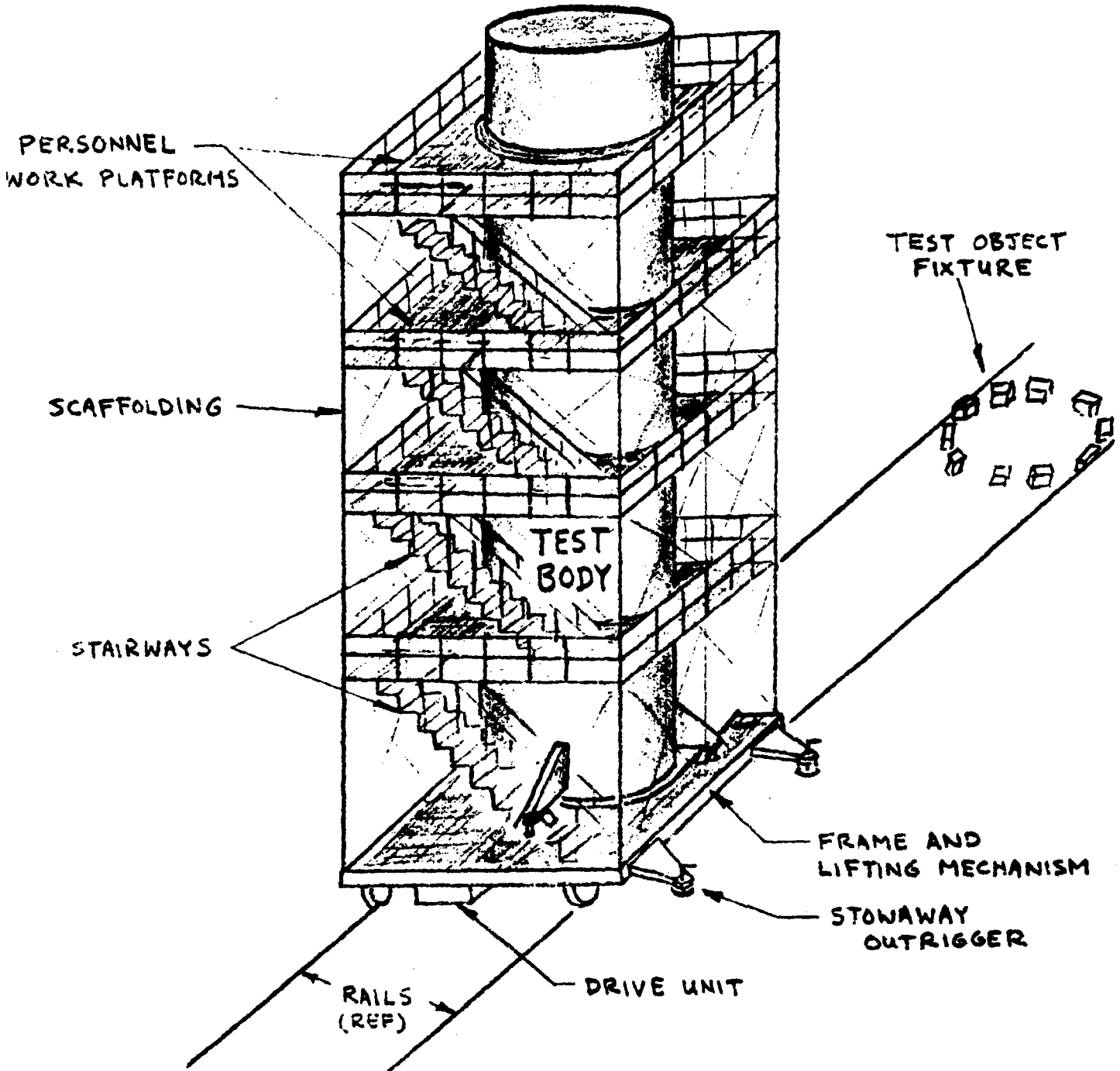


Figure 6.6-11. Test Body Transporter and Scaffolding Unit

6-125

~~SECRET~~ D

Handle via BYEMAN
Control System Only

~~SECRET~~ D

BIF-008- [REDACTED] -68
(Control Number)

SECTION 7 RELIABILITY

7.1 RELIABILITY REQUIREMENTS AND GOALS

Reliability is one of the objectives of the Manned Orbiting Laboratory (MOL)/Dorian System. The goal for the manned/automatic (M/A) mode photographic payload (PP) is at least 91.4 percent probability of exposing 14,000 feet of primary film at an acceptable quality level. The reliability figure is based on the correct operation of mission-essential components of the PP.

The currently estimated reliability of the PP is 92.0 percent for the M/A mode of operation. This estimate is based on the failure rates associated with the equipment parts in the current design and duty cycles of the various components.

7.2 RELIABILITY APPORTIONMENT

The specified reliability goal of the PP was apportioned to the individual components of the PP based on an estimated parts count for each component. The greater the number of active parts in a component (assuming a series configuration), the lower the probability of achieving a given reliability goal. Therefore, components with a large degree of complexity received a relatively high portion of the allowed failure probability (see Table 7.2-1).

~~SECRET~~ D

~~SECRET~~ - D

BIF-008- [REDACTED] -68
(Control Number)

TABLE 7.2-1
MISSION-ESSENTIAL COMPONENT RELIABILITY APPORTIONED GOALS AND ESTIMATES

<u>Components</u>	<u>Apportioned Reliability</u>	<u>Estimated Reliability</u>
Alignment optics sensor electronics	.99819	.99852
Camera assembly	.99413	.99927
Camera auxiliary electronics	.99808	.97808
Film handling electronics	.99782	.99654
Focus control electronics	.99960	.99733
Focus control preamplifier	.99964	.99986
Heater controller set	.98573	.98448
Heater set	.99995	.99388
Instrumentation processor	.99863	.92939
LM cable set	.99846	.99251
LM chute set	.99757	.99692
LM control unit	.99749	.99960
LM power unit	.99749	.99684
MM cable set	.99872	.99376
MM control unit	.99616	.99988
MM power unit	.99361	.99551
Primary mirror alignment servo	.99911	.99736
Primary mirror mount and lock set	.99596	.99988
Primary supply assembly	.99385	.98423
Primary take-up assembly	.99821	.99829
Ross corrector alignment servo	.99915	.99736
Shutter assembly	.99358	.98952
Tracking mirror mount and lock set	.99412	.99988

~~SECRET~~ - D

~~SECRET~~ D

BIF-008- [REDACTED] -68
(Control Number)

7.3 RELIABILITY ESTIMATES

The math model which was used to calculate the reliability estimate for the PP considers the duty cycle and function of each component in the PP.

7.3.1 Mission-Essential Operations

The primary objective of the PP was divided into several mission-essential operations. Even though the loss of some of these operations may not be sufficient cause to consider the mission to be unsuccessful, a catastrophic failure which results in the loss of any one of these mission-essential operations, will, for the purposes of this model, result in an unsuccessful mission. Table 7.3-1 lists the ten operations of the PP which were identified as being mission-essential, a brief description for each of the operations, and a reliability estimate.

7.3.2 Reliability Mathematical Model

Any component which is not used directly in one of the mission-essential operations was considered to be nonessential and was not included in the reliability estimate.

The steps involved in the calculation of the reliability estimate are discussed in the following paragraphs.

~~SECRET~~ D

~~SECRET~~ D

BIF-008- [REDACTED] -68
(Control Number)

TABLE 7.3-1
RELIABILITY ESTIMATES FOR MISSION-ESSENTIAL OPERATIONS

<u>Operation</u>	<u>Function</u>	<u>Reliability</u>
1. Launch	Attain orbit (accounts for the failure rates of all essential components with an application factor of 100)	.991542
2. Unlock launch locks	Unlock launch locks on primary and tracking mirrors	.999995
3. Focus	Sense focus errors and make adjustments as commanded	.992745
4. Alignment	Sense alignment errors and make proper corrections	.996874
5. Photography	Expose specified quantity of primary film with correct settings and adjustments	.979764
6. Film handling	Supply, transport, and store primary film	.996897
7. Platen interchange	Exchange primary platen with secondary platen and vice versa	.998519
8. Environmental control	Maintain the correct thermal environment	.991888
9. Cables	Maintain correct electrical connection for all cables and connectors throughout mission	.986725
10. Nonoperation	Accounts for failures of essential components during an inactive state (component failure rates are modified with an application factor of 0.01)	.983583
11. Structures		.999
Overall reliability estimate for M/A PP.		.920

7-4
~~SECRET~~ D

Handle via BYEMAN
Control System Only

~~SECRET~~ D

BIF-008- [REDACTED] -68
(Control Number)

- a. The subcomponents in the PP which are used in the performance of each operation were identified (see Appendix D). In some instances, an entire component need not be functioning during a specific operation. Therefore, only those subcomponents which are functioning were considered in calculating the reliability for that operation. One operation may include several components or parts of components, and one component or part of a component may be used in several operations.
- b. The total operating time for each piece of equipment identified in "a" was estimated. (see Appendix D)
- c. A failure rate was assigned to each part used in a mission-essential operation. These failure rates were based on the following assumptions:
 1. All failure rates were constant and the numerical data acquired from MIL-HDBK-217A was representative of the parts used in the PP.
 2. Component failure rates were modified by use factors to account for; (1) excessive shock and vibration on all components during launch operation, and (2) the nonoperational phase of components in an orbital quiescent or standby phase.
- d. Reliability block diagrams which identify each sub-component used in each operation were constructed (see Appendix D). These diagrams generally depict redundancy only at a significant level; redundancy at lower levels, if not specifically shown, is accounted for in the failure rate.
- e. Based on the assumption that the probability density function for individual parts is exponential and on the model depicted by the block diagrams, an estimate of the reliability was calculated for each mission-essential operation.

~~SECRET~~ D

~~SECRET~~ D

BIF-008- [REDACTED] -68
(Control Number)

- f. Because the role of the structures, mirrors, and lenses is passive during a mission and the design for these passive elements will be fully qualified during the testing phase of the program, these components are assumed to have a reliability of .999.
- g. The product of the reliability estimates for the mission-essential operations is the overall reliability estimate for the PP.
- h. Successful operations of all necessary associate contractor equipment was assumed.

7.3.3 Launch and Nonoperation

With the exception of block diagramming, the procedures outlined in paragraph 7.3.2 were followed step by step for launch and nonoperation. The component failure rates were modified by an application factor of 100 to account for shock and vibration during launch.

The failure rate of each essential component which experiences alternate periods of actuation and de-actuation was modified by an application factor of 0.01 to account for inactivity.

If both factors were applicable, as in a nonoperative component during launch, both factors were used. All components which are essential for any operation are included in the estimate of the launch and nonoperational phase reliabilities.

~~SECRET~~ D

BIF-008- [REDACTED] -68
(Control Number)

7.3.4 Nonessential Components

The components of the PP which have no direct function in attaining the primary objective are considered nonessential and are not included in the reliability estimate.

Table 7.3-2 shows the reliability estimates for the nonessential components.

TABLE 7.3-2
RELIABILITY ESTIMATES FOR NONESSENTIAL COMPONENTS

<u>Components</u>	<u>Estimated Reliability</u>
Controls and displays	*
Data conversion unit	.927965
Processor	.983
Secondary supply and take-up assembly	.998198
Vibration amplifiers	*
Visual optics**	.988883

* Estimate not available

** Included as part of a back-up alignment mode.

7-7
~~SECRET~~ D

Handle via BYEMAN
Control System Only

~~SECRET~~ D

BIF-008- [REDACTED] -68
(Control Number)

SECTION 8
SYSTEM SAFETY ENGINEERING (SSE)

8.1 INTRODUCTION

The objectives of the SSE task are to identify those conditions within the photographic payload (PP) which may be hazardous to the flight crew and to review these potential problem areas with design engineers. In this review, possible design changes to reduce the hazardous conditions are discussed. Subsequently, changes are implemented if there is no adverse affect on cost or schedule. If cost or schedule is involved, the course of action will be determined through negotiations with the Air Force. Techniques used to identify hazardous conditions consists of fault-tree analysis, hazards analysis and procedural analysis. The review activities utilize these analyses and other applicable material, such as the System Safety Handbook (DH-1). The system safety engineering activities are initiated in the design phase and continue through development, test, and operations. The degree of hazards which exists during the mission is defined as the probability of a flight-crew casualty attributable to a condition arising in the PP.

Detailed safety analyses of the processor subsystem are complete and are discussed in the following paragraphs. These analyses are representative of analyses being conducted or planned for the remainder of the PP sub-systems.

~~SECRET~~ D

~~SECRET~~ D

BIF-008- [REDACTED] -68
(Control Number)

8.2 ANALYSIS

8.2.1 Hazard Analysis

The purpose of this analysis is to systematically examine ways in which a component can cause a condition to arise which is hazardous to personnel. In general, these conditions will be of the form of Class III and IV hazards as defined in MIL-S-38130A, repeated here for convenience.

Class III - CRITICAL - Condition(s) such that personnel error, deficiency/inadequacy of design, or subsystem/component malfunction will degrade system performance by personnel injury or substantial damage or will result in a hazard requiring immediate corrective action for personnel or system survival.

Class IV - CATASTROPHIC - condition(s) such that personnel error, deficiency/inadequacy of design, or subsystem/component malfunction will degrade system performance and cause subsequent system loss or death or multiple injuries to personnel.

The prime use of the hazard analysis (Figure 8.2-1) is to identify hazardous conditions of the subsystem to assist in the construction of a fault tree analysis (paragraph 8.2.2). When the hazard analysis is used as a basis for the fault tree, the probability of occurrence of a condition is not entered on the hazard analysis table.

In those cases where only the hazard analysis is performed on a subsystem, the probability of occurrence will be listed in the table and will reflect the failure rate for the applicable basic faults.

~~SECRET~~ D

~~SECRET~~ D

BIF-008 - [REDACTED] -68
(Control Number)

COMPONENT: Processor		SYSTEM APPLICATION: Processor		ANALYST: Birch, J.A.		DESIGN ENGR:							
TOP DWG/SPEC:		Subsystem											
ITEM	REF/DWG	DESCRIPTION		HAZARDOUS CONDITION	METHOD OF DETECTION	EFFECTS ON		PROB OCCUR	CLASS	CORRECTIVE ACTION		REMARKS	APPLIC
		NAME/USE				PERSONNEL	EQUIPMENT			1	2		
14	Blower			<p>A. Excessive noise when operated with door open or the pressure shell not intact.</p> <p>B. Motor operates at wrong speed because switch is in wrong position and causes:</p> <ol style="list-style-type: none"> 1. Overheating due to slow speed operation during prelaunch checkout. (See Remark 1) 2. Winding/bearing overheating due to overspeed during orbit (See Remark 1) 3. Blade disintegrates due to overspeed causing: <ol style="list-style-type: none"> a. Overloaded wiring (See Remark 2) b. Ruptured or leaky tubing (See Remark 3) <p>C. Motor overspeed during LM orbit decompression could cause blade to disintegrate causing:</p> <ol style="list-style-type: none"> 1. Overloaded wiring (See Remark 2) 2. Ruptured or leaky tubing (See Remark 3) 	<p>Flight Crew Senses</p> <p>Flight Crew Senses</p> <p>Flight Crew Senses</p>	<p>A. Painful, and intolerable in confined space.</p> <p>Indirect: For hazardous Conditions B and C refer to the remarks for the direct effect on personnel.</p>	None					<p>1. Conditions B1 and B2 lead to overloaded wiring as a result of failures within discrete components (See Item 24C)</p> <p>2. Conditions B3 and C1 lead to overloaded wiring as a result of damaged electrical insulation (See Item 24A)</p> <p>3. For ruptured leaky tubing (See Item 23)</p>	Orbit 1
										<p>A. 1. Turn processor off</p> <p>2. Close door</p> <p>B. Switch to correct speed.</p>			
										<p>C. Processor standby mode prior to decompression</p> <p>Provide an automatic pressure sensitive switch for the fan (or processor) in emergency LM decompression</p>			

FORM N-0. 12/67

Note: 1 Although this hazardous condition could exist during previous mission phases, the Flight Crew would not be in the LM.

Handle via BYEMAN
Control System Only

Figure 8.2-1. Hazard Analysis

~~SECRET~~ D

~~SECRET~~ D

BIF-008- [REDACTED] -68
(Control Number)

8.2.2 Fault Tree Analysis

The fault tree analysis is a method for determining the probability of a casualty-producing failure by developing logically the critical sequence of events from the end event to the basic failure resulting in the casualty. The tree is constructed from a single, undesired event which is related to probable causes of the undesired event.

Basic faults, failure rates associated with the basic faults, and the manner in which the fault tree is developed, are based on engineering data gathered from design, hazard analyses, and safety studies.

Several items associated with the fault tree analysis are as follows:

- a. Each event block on the fault tree diagram has an associated probability of occurrence.
- b. The probability of occurrence of the events leading to a flight-crew casualty were computed by using probability theory.
- c. The probabilities of failure occurrence for the basic event blocks are calculated by taking the product of the failure rate and the operating time of a component.
- d. The probability of occurrence of each succeeding event block on the tree is calculated by combining the event block probabilities according to the logic portrayed in the tree.

The processor fault tree analysis is shown in Figures 8.2-2 and 8.2-3.

~~SECRET~~ D

~~SECRET~~ D

BIF-008- [REDACTED] -68
(Control Number)

Figure 8.2-2
Fault Tree Analysis Processor Subsystem

~~SECRET~~ D

Handle via BYEMAN
Control System Only

~~SECRET~~ ^D

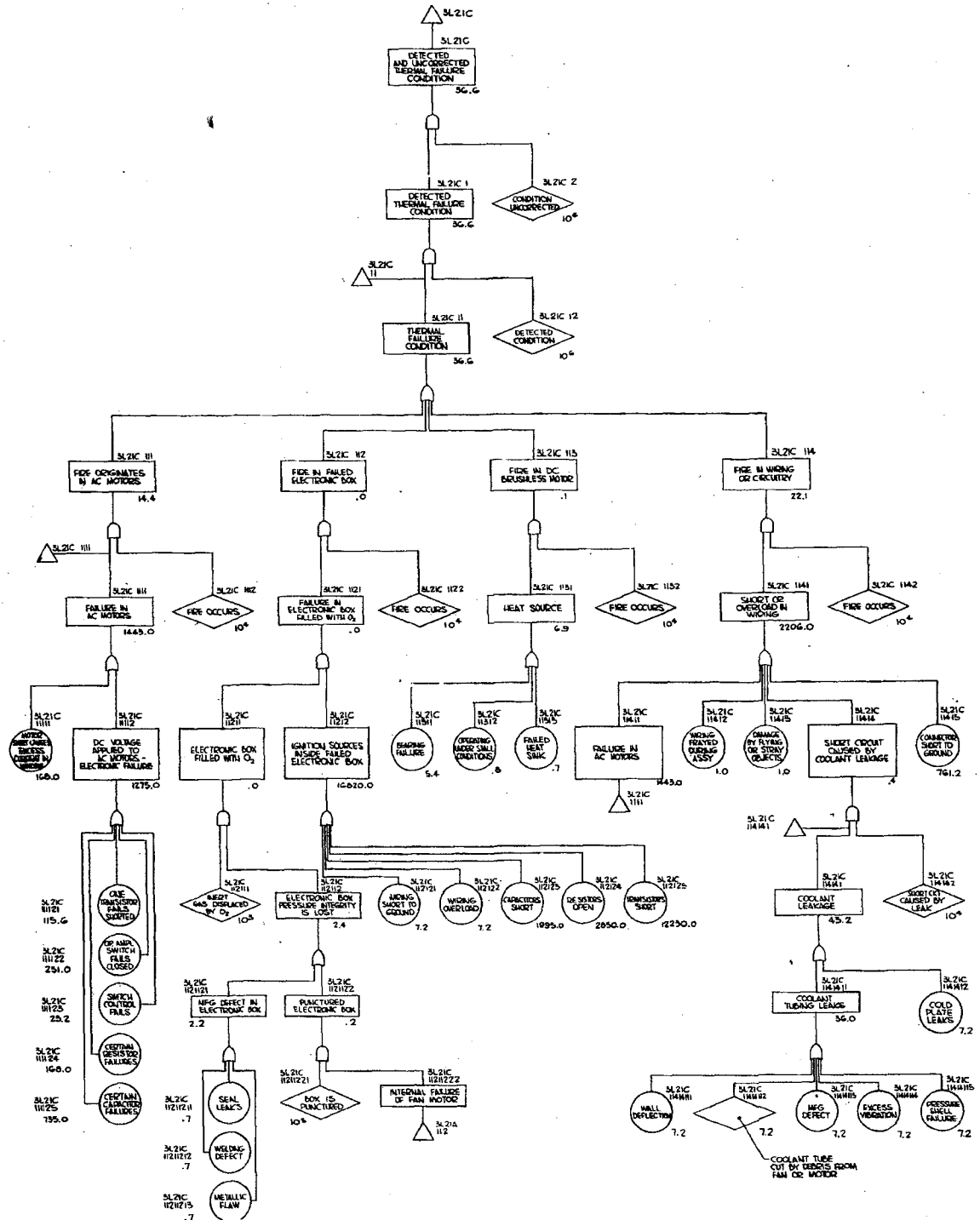
BIF-008- [REDACTED] -68
(Control Number)

Figure 8.2-3
Fault Tree Analysis Processor Subsystem

8-7

~~SECRET~~ ^D

Handle via **BYEMAN**
Control System Only



~~SECRET~~ D

BIF-008- [REDACTED] -68
(Control Number)

The five most significant Class III hazard conditions identified in the processor subsystem are listed in Table 8-1 together with their block reference number (BRN), and their associated probabilities of failure occurrence [P(f)].

TABLE 8-1
MOST SIGNIFICANT CLASS III HAZARD CONDITIONS IN THE PROCESSOR SUBSYSTEM

<u>Class III Hazard Condition</u>	<u>BRN</u>	<u>P(f)</u>
Failure in a-c motors	3L21C	1443 x 10 ⁻⁶
	1111	
Connector short to ground	3L21C	761 x 10 ⁻⁶
	11415	
Pressure-relief-valve failure	3L21A	7 x 10 ⁻⁶
	1111	
Pressure-shell-wall failure	3L21A	7 x 10 ⁻⁶
	1112	
Coolant leakage	3L21F	7 x 10 ⁻⁶
	111	

To summarize the results of the processor-subsystem fault-tree analysis, there are no Class IV hazard conditions identified, and the identified Class III hazard conditions have a relatively small probability of failure occurrence per flight (76.9 x 10⁻⁶).

~~SECRET~~ D

~~SECRET~~ D

BIF-008- [REDACTED] -68
(Control Number)

SECTION 9
NUMERICAL SUMMARY

9.1 GENERAL DATA

9.1.1 Performance

Nadir On-Axis Average Dynamic Ground Resolution Capability

System requirement:	[REDACTED]
Conditions:	
Altitude	80 nautical miles (n mi)
Film ¹	Type 3404 Film quality, with an aerial exposure index of 6
Process	One-step D-19 equivalent
Apparent contrast	2:1 at entrance pupil
Minimum scene luminous emittance	890 foot-lamberts
Transmittance (including vignetting)	29 percent
Focus error (2 σ)	± 0.002 inch
Angular smear rate (2 σ)	[REDACTED]
Exposure time	1/165 second
Obstructions	Newtonian mirror, mounting spider (17.2 percent)

9.1.2 Launch Parameters

Launch booster	Titan III-M
Launch site	WTR-Vandenberg
Direction	South

¹This film not currently available

~~SECRET~~ D

~~SECRET~~ D

BIF-008- [REDACTED] -68
(Control Number)

9.1.3 Orbit

9.1.3.1 Nominal Orbit¹

Perigee altitude	80 n mi
Apogee altitude	186 n mi
Eccentricity	0.015
Inclination	90 degrees
Average period	89 minutes
Closure	3 times in 30 days at 45° N latitude
Location of perigee	55 degree N Latitude
Mission duration	30 days (Manned/Automatic (M/A) Mode)
Satellite velocity at perigee	4.25 n mi/second

9.1.3.2 Orbit Envelope

Photographic altitude	70 to 230 n mi
Perigee altitude	70 to 85 n mi
Apogee altitude	Less than or equal to 230 n mi
Satellite travel during photography	Northbound or southbound
Eccentricity	Less than or equal to 0.0225
Inclination	80 to 100 degrees (required)
Minimum sun-elevation angle, at the target, for primary photography	5 degrees

¹The parameters of the nominal orbit are being reviewed by the Air Force and Aerospace Corporation (AF/AS).

9-2
~~SECRET~~ D

Handle via BYEMAN
Control System Only

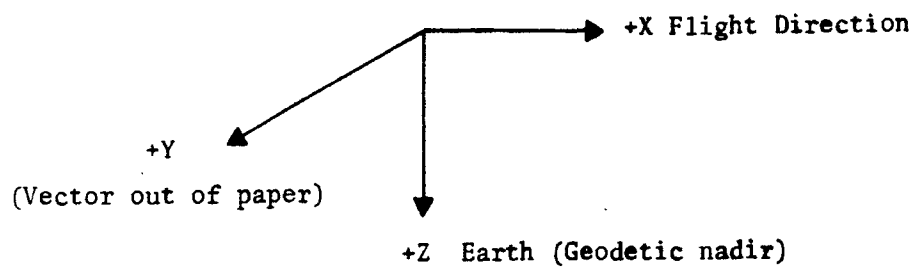
~~SECRET~~ D

BIF-008- [REDACTED] -68
(Control Number)

Beta-angle range (angle between the earth-sun line and the orbital plane)	±60 degrees
Photographic capability	90 degrees N to 90 degrees S Latitude
V/h range for envelope	0.0175 to 0.0615 radian/second

9.1.4 Orbital Coordinate Conventions

Orbital coordinate conventions are shown in Figure 9.1-1.



Right-hand rotations about these axes are positive.

Figure 9.1-1. Orbital Coordinate Conventions

~~SECRET~~ D

BIF-008- [REDACTED] -68
(Control Number)

9.1.5 Coverage

Ground format (from 80 n mi at nadir)	1.5 n-mi-diameter circle
Target size	3000-foot diameter (2 σ)

9.1.6 Weight Summary

	<u>M/A Mode (lbs.)</u>
COA components	3252
TM assembly	1278
Additional MM Equipment	36
LM components	1182
Gemini-B components	<u>24</u>
Total PP	5772
Weight Budget	5767

9.1.7 Mass Properties

	<u>Center of Gravity (cg)</u> (Sta inches)			<u>Moments of Inertia</u> (slug-ft-squared)		
	\bar{X}	\bar{Y}	\bar{Z}	I_{xx}	I_{yy}	I_{zz}
M/A Mode						
Total PP*	354.39	-1.96	-5.36	1,533	40,088	39,571

* Includes all PP components oriented in a flight configuration.

~~SECRET~~ D

BIF-008- [REDACTED] -68
(Control Number)

9.2 REQUIREMENTS ON OTHER SUBSYSTEMS

9.2.1 Electrical Requirements

9.2.1.1 Instrumentation (See Appendix C)

- a. Launch 4 continuous channels
(10 - 500 Hz)
- b. On-orbit M/A mode

<u>Quantity</u>	<u>Samples/Second</u>
157	1/4
188	1
60	2
120	8
11	16
5	32
<u>8</u>	64
549	

9.2.1.2 Commands (See Appendix C) 91 binary digits of parallel command information are reserved for the photographic payload.

9.2.1.3 Power and Energy

- a. Estimate (at interface voltage of 24v)
 - 1. Average power
 - Operational 80 watt-hours/hour
 - Environmental 195 watt-hours/hour

~~SECRET~~ D

~~SECRET~~ D

BIF-008- [REDACTED] -68
(Control Number)

2. Peak power per operational mode

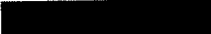
<u>Operational Mode</u>	<u>Peak Power in Watts</u>
Photographic	1126
TM slew	572
Focus	377
Alignment	607
Process	513
Telemetry	265
Unlock	349
Launch and boost	280
VO magnification change	852

b. Basis for estimates

1. Peak power duration 1 second (maximum)
2. Time over area of interest 100 minutes/day
 - Average frames/day 450
 - Frames/target 6
 - Targets/day 75
3. Processor operating time 2 hours/day
4. Optical alignment check Alignment operation Once per revolution
As necessary: 10 minutes/
operation
5. Visual optics magnification set 100 minutes/day (3 times/
target)
6. Instrumentation operative 7 hours/day
7. Film handling operative 100 minutes/day
8. Focus monitoring 1 hour/day
9. Environmental power Estimated for a cold case
(beta angle = 0 degrees)
orbit and a noon launch
from the WTR

~~SECRET~~ D

~~SECRET~~ D

BIF-008--68
(Control Number)

9.2.2 Film Retrieval

Manned/Automatic (M/A) Mode

Capability to return up to
230 pounds of photographic
film in the Gemini B

9.2.3 Image Smear

The smear rate induced by all associate contractors' (Other than EKC)
contributors (95 percentile circular probability).

Angular smear rate 

9.2.4 Stereo and Obliquity Ranges (Line-of-Sight)

Tracking Mirror Requirements

Stereo (Σ)

18 degrees forward

28 degrees aft (required)

40 degrees aft (design objective)

Obliquity (Ω)

\pm 43 degrees

Camera Design Requirements

Stereo (Σ)

\pm 30 degrees

Obliquity (Ω)

\pm 40 degrees

9.2.5 Laboratory Module (M/A Mode)

Pressure

5.0 \pm 0.2 psia

(O₂ - 3.5 psia

He - 1.5 psia)

Degraded Mode

5.0 \pm 0.2 psia (100% O₂)

~~SECRET~~ D

~~SECRET~~ D

BIF-008- [REDACTED] -68
(Control Number)

Relative Humidity	30 - 50 percent
Temperatures	
Dew point	60°F maximum
Film	T minimum (high enough to prevent condensation within film handling system)
	90°F (maximum) Special consultation necessary if 90°F must be exceeded (temperature up to 125°F may be allowed for Type 3404 Film for a limited time).
Atmosphere for film handling system, camera, processor, VO	60° to 90°F
Heat sinks for electronics	40° to 90°F
Coolant for BIMAT storage	34° to 42°F

9.3 PHOTOGRAPHIC PAYLOAD CHARACTERISTICS

9.3.1 Primary Lens Optical Parameters

a. Lens type	Ross-Telephoto
b. EKC Formula Number	R-359A
c. Lens aperture (major axis)	70 inches
d. Focal length	[REDACTED]
e. Relative aperture	[REDACTED]
f. Semi-field angle	± 0.54 degree
g. Telephoto ratio	89.9 percent
h. Effective tracking-mirror diameter	70 inches (circular)

~~SECRET~~ D

~~SECRET~~ D

BIF-008- [REDACTED] -68
(Control Number)

- i. Transmittance including tracking-mirror vignetting at nadir, reflectance and transmittance of optical elements, and Newtonian mirror obstruction 29 percent
- j. Obstruction 12.7 percent (Newtonian mirror)
4.5 percent (Mounting spider)
- k. Optical quality factor [REDACTED] percent (specification)
[REDACTED] percent(goal)
- l. Pellicle
 - 1. reflectance 8 to 10 percent (minimum)
 - 2. transmittance 86 percent (minimum)

9.3.2 Mission Module Environmental Requirements

- a. Pressure Unpressurized (approximately 10^{-6} to 10^{-8} Torr)
- b. Temperature
 - Photographic Payload
(before first door-open operation) Isothermal within 1°F (objective)
 - Optical Assembly Structure
Isothermal temperature level (any point in OA)
 - Optical quality limit (Isothermal compatibility with TM enclosure required) $70^{\circ} \pm 5^{\circ}\text{F}$
 - Maximum allowable temperature differentials
 - Axial 5°F
 - Transverse 2°F

9-9
~~SECRET~~ D

Handle via BYEMAN
Control System Only

~~SECRET~~ D

BIF-008- [REDACTED] -68
(Control Number)

Mirrors

Maximum allowable differential before first door opening (°F)

	<u>Fused Silica</u>	<u>ULE or CER-VIT*</u>
a. through Newtonian mirror	0.2	0.5
b. through Ross folding mirror	0.2	0.5
c. through primary mirror (front to back)	0.1	0.25
d. across primary mirror (radial)	0.25	0.6
e. through TM (front to back)	0.1	0.1
f. across TM (radial)	0.25	0.25

9.3.3 Mirrors

Allowable random deformation on mirrors

<u>Mirror</u>	<u>Resulting Optical Quality Factor of [REDACTED] Percent</u>		<u>Resulting Optical Quality Factor of [REDACTED] Percent</u>	
	<u>Manufacturing Tolerance</u>	<u>Test Uncertainty</u>	<u>Manufacturing Tolerance</u>	<u>Test Uncertainty</u>
Primary Newtonian Ross Tracking	[REDACTED]			

* with Coef. of exp $\leq .05 \times 10^{-6}/^{\circ}\text{C}$

~~SECRET~~ D

~~SECRET~~ D

BIF-008- [REDACTED] -68
(Control Number)

9.3.4 Camera Parameters - Primary Film Strand

- | | |
|--|--|
| a. Type | Frame |
| b. Film | 9- $\frac{1}{2}$ -inch wide, thin base (TB)
or ultra thin base* (UTB) |
| c. Allowable elapsed time
from exposure start of
primary to exposure start
of secondary frame | 2 seconds |
| d. Exposure | |
| 1. Range** | Capability of 4 photographic
stops |
| 2. Nominal settings** | 0.0025, 0.0036, 0.005, 0.007,
0.010, 0.014, 0.020, 0.040
second |
| 3. Maximum change of
exposure between
successive primary
frames within a
sequence | ± 1 stop |
| e. Shutter | |
| 1. Type | Focal plane |
| 2. Shutter travel time | 0.2 second (estimated) |
| 3. Frame rate | 1 frame/sec (maximum) |
| 4. Shutter efficiency
(at 1/160 second) | 85 percent minimum;
95 percent (goal) |
| 5. Shutter tolerances | |
| Frame-to-frame
repeatability of
exposure time
through mission | ± 10 percent of the commanded
exposure time |
| Within frame exposure
variability | ± 5 percent of the average
exposure time of the frame
for the nominal exposure command |

* Pre-mission selection

** Actual exposure times may be modified by selection
of circuit values

9-11
~~SECRET~~ D

Handle via **BYEMAN**
Control System Only

~~SECRET~~ D

BIF-008- [REDACTED] -68
(Control Number)

- f. Maximum frames of primary film per target sequence 10
- g. Film hold down at platen Vacuum

9.3.5 Camera Parameters - Secondary Film Strand

- a. Allowable elapsed time from exposure start of secondary to exposure start of primary frame 2 seconds
- b. Frame rate 1 frame/3 seconds (maximum)
- c. Maximum frames per target 2
- d. Camera film loss in changing secondary film types 4.5 feet (maximum)
- e. Camera film loss in removing batch for on-board processing 6.0 feet (maximum)

9.3.6 Film

9.3.6.1 Film Requirements

- a. Primary strand
 - Type Black-and-white
 - Length 11,000 feet (M/A)
 - Estimated number of useful photographic frames 12,425 (M/A)
 - Weight (planned loads) 190 ± 4 pounds (M/A)
- b. Secondary strand (manned/automatic mode)
 - Type Weight
 - Film for on-board processing 20 pounds

~~SECRET~~ D

~~SECRET~~ D

BIF-008- [REDACTED] -68
(Control Number)

Color	10 pounds
IR color	10 pounds
High speed black-and-white	10 pounds

9.3.6.2 Properties of Film

- a. Primary Film Support ESTAR thin base or ESTAR UTB*
9.460^{+0.010}_{-0.005} inches
- Black-and-white
(Primary strand)
- Film type A film having the resolution of Type 3404 Film but with an AEI of 6 (not currently available)
- Total thickness (A) 0.0030 ± 0.0002 inch (TB film)
(B) 0.0020 ± 0.0002 inch (UTB)
- Weight density (A) 0.022 ± 0.0012 lb/ft² (50 per-
cent RH) (TB film)
(B) 0.014 ± 0.0012 lb/ft² (50-per-
cent RH) (UTB)
- b. Secondary Film - (all will use TB support and will be
9.46 inches ^{+0.010}_{-0.005} inch width)
1. Black-and-white
- Film type A film having the resolution of Type 3404 Film (not currently available)
- Total thickness 0.0030 ± 0.0002 inch
- Weight density 0.022 ± 0.0012 lb/ft²
(50 percent RH)
- Aerial Exposure Index 4 using PS485/SO-111 process

* Pre-mission selection

~~SECRET~~ D

BIF-008- [REDACTED] -68
(Control Number)

2. Color

Film type	KODAK Aerial Color Film Type SO-121
Total thickness	0.0036 ± 0.0002 inch
Weight density	0.027 ± 0.0012 lb/ft ² (50 percent RH)
Aerial Exposure Index	13

3. Infrared color

Film type	KODAK Ektachrome Infrared Aerial Film, Type SO-180
Total thickness	0.0038 ± 0.0002 inch
Weight density	0.030 ± 0.0012 lb/ft ² (50-percent RH)
Aerial Exposure Index	18 using a KODAK Wratten 12 filter, or equivalent

4. High-speed black-and-white (Air Force choice of one)

a. Film type	KODAK Plus-X Aerial Film Type 3401
Total thickness	0.0031 ± 0.0002 inch
Weight density	0.023 ± 0.0012 lb/ft ² (50 percent RH)
Aerial Exposure Index	64
b. Film type	KODAK Panatomic-X Aerial Film Type 3400 (ESTAR TB)
Total thickness	0.0029 ± 0.0002 inch
Weight density	0.022 ± 0.0012 lb/ft ²
Aerial Exposure Index	20

9.3.7 Focus

a. Focus-sensor slant range	75 to 150 n mi
-----------------------------	----------------

~~SECRET~~ D

BIF-008- [REDACTED] -68
(Control Number)

- | | |
|---|---|
| b. Method of adjustment on orbit | Translation of platen along X-axis for operational adjustments and translation of primary mirror for large focus correction |
| c. Modes of operations | |
| 1. Slant-range corrections | Automatically controlled during photography |
| 2. Corrections for back-focus variations | Focus is sensed and corrections are manually (flight crew) or remotely (ground) commanded. |
| d. Focus tolerance | ± 0.002 inch (2σ) |
| e. Platen-positioning range | 0.1 inch |
| f. Stepping interval for platen translation | 0.0006 inch |
| g. Maximum focus change-rate capacity | 3 focus steps between frames at a 1 frame/second rate |

9.3.8 Film Format

- | | |
|---------------------------|---------------------------|
| a. Frame length | 10.4 \pm 0.125 inches |
| b. Image format | 9.4-inches circular image |
| c. Spacing between images | 1 inch |
| d. Edge-data capacity | 18 by 32 bit matrix |

9.3.9 Visual Optics

Number of eyepieces	2 (serial operations only)
---------------------	----------------------------

~~SECRET~~ D

~~SECRET~~ D

BIF-008- [REDACTED] -68
(Control Number)

9.3.9.1 Primary Eyepiece

- | | |
|-------------------------------------|--|
| a. Apparent full field | 40 degrees |
| b. Magnification | Four discrete values:
[REDACTED] |
| c. Full-field angle | |
| 1. Lowest magnification | 0.32 degree |
| 2. Highest magnification | 0.04 degree |
| d. Light input | 2.5 percent of total image
illumination |
| e. Light transmittance
(minimum) | 35 percent for relay optics
only |
| f. Eye relief (minimum) | 40 mm |

9.3.9.2 Secondary Eyepiece. The secondary system has the same characteristics as the primary as a goal. However, the performance may be degraded as far as the following in order to save weight:

Light transmittance (minimum)	30 percent
----------------------------------	------------

9.3.10 Across-the-Format X-IMC Requirements

9.3.10.1 General

- Provides partial off-axis X-IMC by correcting for line of maximum image motion.
- Required for primary strand only.
- Not used if:
 - $V_{\max} \leq 0.04$ inch/second
 - Manual override by crewman

~~SECRET~~ D

~~SECRET~~ D

BIF-008- [REDACTED] -68
(Control Number)

9.3.10.2 Ranges

- | | |
|--|--|
| a. Shutter orientation | ±111 degrees sector measured about X-axis with respect to Y-axis |
| b. Platen-velocity axis orientation | ±60 degrees sector measured about X-axis with respect to Z-axis |
| c. Platen-velocity amplitude range (magnitude) | 0 to 0.24 inch/second |
| d. Maximum slit rotation between consecutive frames at 1 frame/second rate | 55 degrees |
| e. Maximum platen velocity vector rotation between consecutive frames at 1 frame/second rate | 30 degrees |

9.3.10.3 Error Tolerances. (Includes both granularity error resulting from discrete positioning steps and accuracy of positioning)

- | | |
|---|-----------------------------------|
| a. Slit orientation | ±3 degrees |
| b. Platen-velocity-vector orientation | ±3 degrees |
| c. Platen-velocity amplitude | ±0.014 inch/second at field edges |
| d. Platen velocity will be zero within ±0.002 inch/second when the center of the slit crosses the optical axis. | |
| e. Platen velocity will be linear with a band defined by c and d above. | |

~~SECRET~~ D

~~SECRET~~ D

BIF-008- [REDACTED] -68
(Control Number)

9.3.11 Optical Alignment

- a. Primary optics alignment
 - Equivalent primary mirror tilt tolerance (includes total amount of decenter and tilt for the primary, Newtonian, and Ross mirrors)
 - a. [REDACTED] (Requirement)
 - b. [REDACTED] (goal)
- b. Modes Manual, automatic, or remote
- c. Alignment-sensor accuracy
 - Tilt 5 seconds of arc
 - Decentering 5 seconds of arc
- d. Alignment drive
 - 1. For Ross mirror
 - a. Range of motion of edge 0.10 inch
 - b. Positional accuracy 1.0×10^{-4} inch
 - 2. For primary mirror
 - a. Range of motion of edge 0.30 inch
 - b. Positional accuracy 3.0×10^{-4} inch

9.3.12 On-Board Processor

- a. Type BIMAT film
- b. Processing batch size capacity 50-frame batch plus 6 feet of leader
- c. Processing rate 5 inches of film per minute (goal)
5 min/frame (required)

~~SECRET~~ D

Handle via BYEMAN
Control System Only

~~SECRET~~ D

BIF-008- [REDACTED] -68
(Control Number)

- d. Storage environment for BIMAT supply 55 ⁺⁵/₋₁₀ F and 95 to 100 percent RH
- e. BIMAT material
 - 1. Type KODAK BIMAT Transfer Film (ESTAR Base) Type SO-111
 - 2. Imbibant type PS-485K
 - 3. BIMAT cassette capacity 1500 feet
 - 4. Nominal BIMAT load Sufficient to process 1270 feet in 43 batches
 - 5. Width 9.460 ^{+0.010}/_{-0.005} inches
 - 6. Weight (nominal)
 - a. Wet 0.047 lb/ft²
 - b. Dry 0.034 lb/ft²
- f. Resolution requirements Within 15 percent of the resolution obtainable with ground BIMAT processing of the same latent image

9.3.13 Film Handling (M/A Mode)

- a. Supply assembly for primary film
 - 1. Number of film reels 1
 - 2. Film capacity 240 lb*
 - 3. Nominal film load 190 lb (TB film)
121 lb (UTB film)
- b. Take-up assembly for primary film
 - 1. Number of film reels 3
 - 2. Nominal film load 60 lb each reel

* Film load is currently directed to be 190 lb.

~~SECRET~~ D

~~SECRET~~ D

BIF-008- [REDACTED] -68
(Control Number)

- c. Supply cassettes for secondary film
 - 1. Number 5
 - 2. Film capacity 10 lb each
- d. Take-up cassettes for secondary film

	<u>On-board Processed</u>	<u>Special Film Types</u>
1. Number	2 processor supply cassettes	3 secondary film cassettes
2. Film capacity	1 lb each	10 lb each

- e. Looper capacity for primary film Sufficient for 10 frames
- f. Time allowed to reload looper 5 seconds (for 10 frames)
- g. Transport of take-up cassette to Gemini B Manual

9.3.14 Data Return in Gemini B (M/A Mode)

- a. Data return containers (DRC's) for primary film
 - 1. Number 3 (thin-base film)
2 (ultra thin-base film)
 - 2. Nominal film load 60 lb each (TB film)
56 lb each (UTB film)
- b. DRC's for secondary film 2*

<u>Data</u>	<u>Number of reels</u>	<u>Nominal film load</u>
Processed film	3	20 lb total
Color film	1	10 lb
Infrared color film	1	10 lb
High-speed film	1	10 lb

* Three reels of processed film stored in the lower secondary DRC and remaining three reels of spliced film stored in upper secondary DRC.

~~SECRET~~ D

Handle via **BYEMAN**
Control System Only

~~SECRET~~ D

BIF-008- [REDACTED] -68
(Control Number)

9.3.15 Smear Slits

- a. Number 2
- b. Minimum measurable displacement between objects on film 0.0007 inch (estimated)
- c. Minimum detectable angular smear rate [REDACTED] (estimated)

9.3.16 Image Smear Rate

Allowable smear rate induced by PP component dynamic sources (95 percentile circular probability)

Angular smear rate [REDACTED]

9.3.17 Image Velocity Sensor

Light input

- a. 2.5 percent of the total image illumination with pellicle (minimum)
- b. 8 to 10 percent with mirror

~~SECRET~~ D

~~SECRET~~ D

BIF-008- [REDACTED] -68
(Control Number)

APPENDIX A

DERIVATION OF OFF-AXIS IMAGE RATE AND ACROSS-THE-FORMAT IMAGE MOTION COMPENSATION CAMERA SET-UP EQUATIONS

A.1 INTRODUCTION

Across-the-format image motion compensation (X-IMC) substantially compensates for off-axis image motion by matching the platen velocity to the line of maximum image motion. This requires the shutter slit to travel across-the-format at an angle corresponding to the angle of maximum image motion and the platen to simultaneously jog at an angle and magnitude corresponding to the image velocities along this line.

Paragraph A.2 contains the definitions of the various coordinate systems which are used in the derivations. Paragraphs A.3 and A.4 contain, respectively, the derivations of the off-axis-image rate equations and the X-IMC camera set-up equations.

A.2 DEFINITIONS

A.2.1 Orbit Coordinate System (OCS)

The OCS is defined in Figure A.2-1.

A-1

~~SECRET~~ D

Handle via **BYEMAN**
Control System Only

~~SECRET~~ D

BIF-008- [REDACTED] -68
(Control Number)

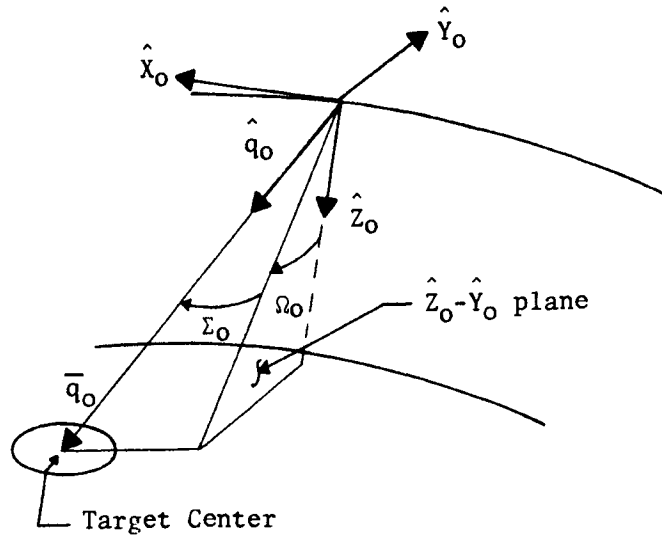


Figure A.2-1
Orbit Coordinate System

The center of the OCS is at the vehicle center-of-gravity (cg). The \hat{X}_0 - \hat{Z}_0 plane lies in the orbit plane with \hat{Z}_0 directed toward the earth center and \hat{X}_0 in the direction of flight. The \hat{Y}_0 -axis forms a right-hand triad with the \hat{X}_0 and \hat{Z}_0 axis.

The parameters defined in this system are given the following designation;

- Ω_0 - Orbit obliquity angle,
- Σ_0 - Orbit stereo angle,
- \bar{q}_0 - Line-of-sight (LOS) vector from satellite to center of target in OCS⁽¹⁾,

(1) Normally the line-of-sight vector is defined from the center of the tracking mirror. However, in the following analysis the centers of the various coordinate systems are assumed to coincide.

~~SECRET~~ D

~~SECRET~~ D

BIF-008- [REDACTED] -68
(Control Number)

α_0 - magnitude of \bar{q}_0 , and
 \hat{q}_0 - unit vector defining the direction of \bar{q}_0 .

The unit vector \hat{q}_0 is given by:

$$\hat{q}_0 = \begin{bmatrix} \sin \Sigma_0 \\ -\cos \Sigma_0 \sin \Omega_0 \\ \cos \Sigma_0 \cos \Omega_0 \end{bmatrix}. \quad \text{Equation A.2-1}$$

A.2.2 Vehicle Coordinate System (VCS)

The VCS is defined in Figure A.2-2.

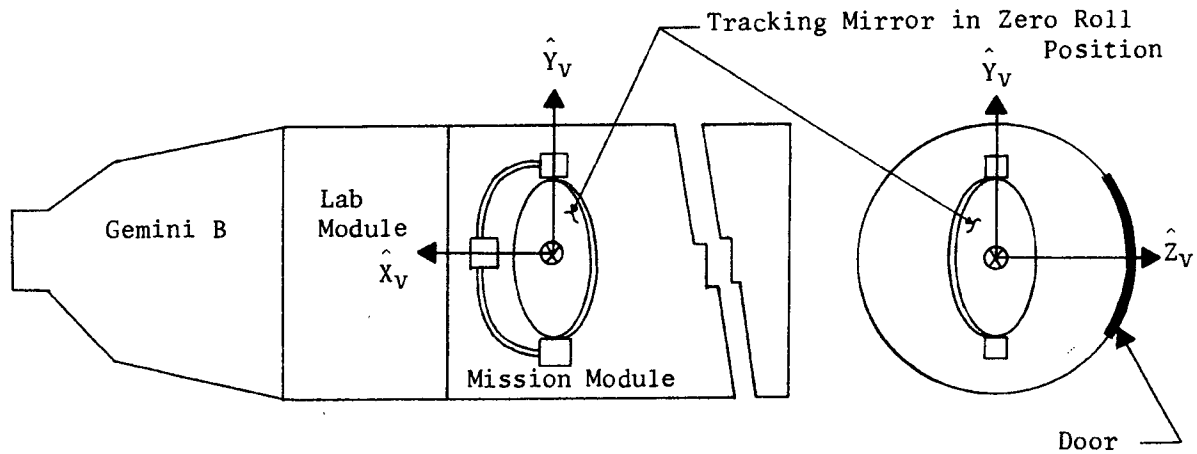


Figure A.2-2
Vehicle Coordinate System

~~SECRET~~ D

~~SECRET~~ D

BIF-008- [REDACTED] -68
(Control Number)

For the purposes of this analysis, the center of the VCS is assumed at the center of the tracking mirror. The \hat{X}_0 axis lies parallel to the vehicle center line and has a positive direction toward the Gemini B. The \hat{Z}_0 axis is perpendicular to the pitch axis of the tracking mirror when the tracking mirror is in a zero roll position and has a positive direction toward the view-port door. The \hat{Y}_0 axis forms a righthand triad with the \hat{X}_0 and \hat{Z}_0 axes.

A vector in the OCS can be expressed in the VCS by the following transformation;

$$\bar{P}_{vcs} = A \bar{P}_{ocs}, \quad \text{Equation A.2-2}$$

where: \bar{P}_{ocs} - vector in OCS,

\bar{P}_{vcs} - vector in VCS, and

A - vehicle attitude transformation matrix.

The vehicle attitude transformation matrix is given by;

$$A = \begin{bmatrix} 1 & 0 & 0 \\ 0 & \cos\phi & \sin\phi \\ 0 & -\sin\phi & \cos\phi \end{bmatrix} \begin{bmatrix} \cos\theta & 0 & -\sin\theta \\ 0 & 1 & 0 \\ \sin\theta & 0 & \cos\theta \end{bmatrix} \begin{bmatrix} \cos\psi & \sin\psi & 0 \\ -\sin\psi & \cos\psi & 0 \\ 0 & 0 & 1 \end{bmatrix}, \quad \text{Equation A.2-3}$$

where:

ψ, θ, ϕ - yaw, pitch, and roll angles respectively.

A.2.3 Optical Sensor Coordinate System (OSCS)

The OS CS is obtained by rotating the VCS by minus two degrees about the \hat{Y}_0 axis (Figure A.2-3).

~~SECRET~~ D

~~SECRET~~ D

BIF-008- [REDACTED] -68
(Control Number)

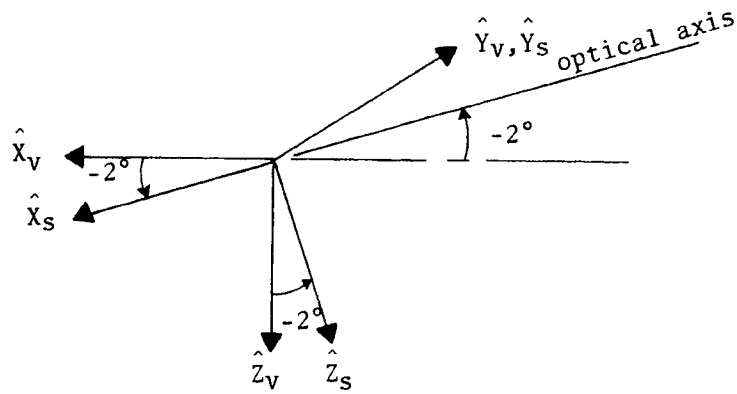


Figure A.2-3
Optical Sensor Coordinate System

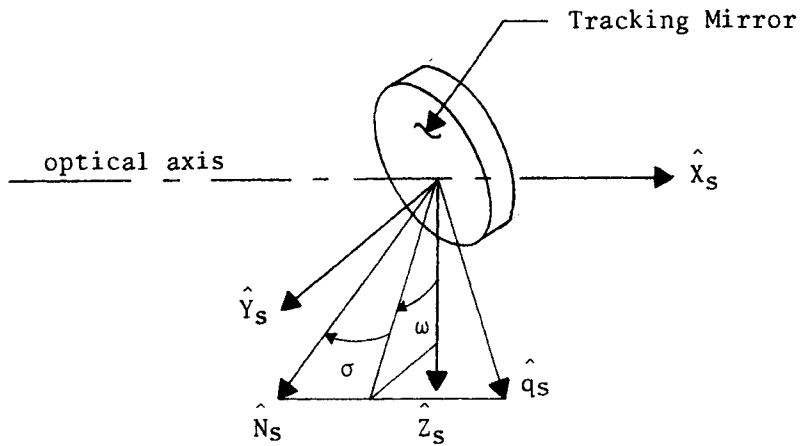


Figure A.2-4
Tracking Mirror Gimbal Angles

~~SECRET~~ D

~~SECRET~~ D

BIF-008- [REDACTED] -68
(Control Number)

The parameters defined in this system are given the following designation;

- ω - gimbal obliquity angle,
- σ - gimbal stereo angle, and
- \hat{N}_s - units normal to tracking mirror.

The tracking mirror normal is given by;

$$\hat{N}_s = \begin{bmatrix} -\sin\sigma \\ \cos\sigma \sin\omega \\ \cos\sigma \cos\omega \end{bmatrix}, \quad \text{Equation A.2-4}$$

\hat{q}_s - line-of-sight unit vector in OSCS.

The line-of-sight unit vector in OSCS is given by;

$$\hat{q}_s = \begin{bmatrix} \cos 2\sigma \\ \sin 2\sigma \sin \omega \\ \sin 2\sigma \cos \omega \end{bmatrix}. \quad \text{Equation A.2-5}$$

A vector in the VCS can be express in the OSCS by the following transform-
ation;

$$\bar{P}_{oscs} = R_y(-2^\circ) \bar{P}_{vcs}, \quad \text{Equation A.2-6}$$

where:

$$R_y(-2^\circ) = \begin{bmatrix} \cos 2^\circ & 0 & \sin 2^\circ \\ 0 & 1 & 0 \\ -\sin 2^\circ & 0 & \cos 2^\circ \end{bmatrix}.$$

~~SECRET~~ D

~~SECRET~~ D

BIF-008- [REDACTED] -68
(Control Number)

By combining equations A.2-1 and A.2-6, a vector in OCS can be expressed in the OSCS by the following transformation;

$$\bar{P}_{oscs} = R_y(-2^\circ)A\bar{P}_{ocs} \quad \text{Equation A.2-7}$$

A.2.4 Film Plane Coordinate System - FPCS

The FPCS is defined in Figure A.2-5

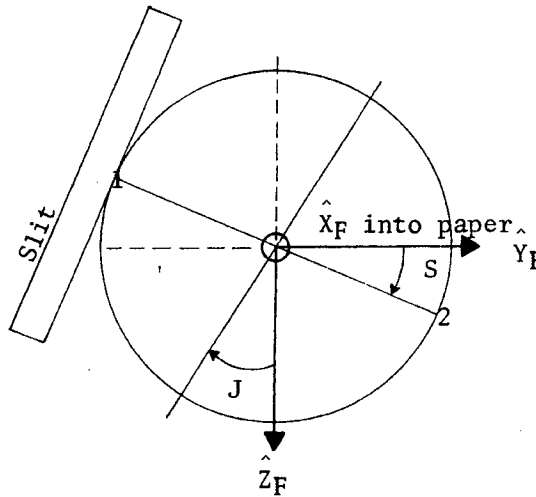


Figure A.2-5
Film Plane Coordinate System - FPCS

The origin of the FPCS lies at the center of the film format. The \hat{Z}_F - \hat{Y}_F plane is coincident with the film plane with the \hat{Z}_F and \hat{Y}_F axis pointing in the direction of \hat{Z}_v and \hat{Y}_v respectively.

The parameters defined in this system are given the following designations:

~~SECRET~~ D

~~SECRET~~ D

BIF-008- [REDACTED] -68
(Control Number)

- S - slit angle, angle of shutter travel across the film format, and
- J - platen angle, angle of platen jog during frame exposure.

When the slit angle is equal to zero degrees the slit is said to be at the neutral position. Positive direction of slit travel is defined as slit motion from point 1 to point 2.

When the platen angle is equal to zero degrees, the platen is said to be at the neutral position. The platen jog velocity is positive when its component in the \hat{Z}_F direction is positive.

A.3 OFF-AXIS IMAGE-RATE EQUATIONS

A.3.1 Assumptions

The off-axis image-rate equations are derived using the following assumed conditions:

- a. A flat earth model.
- b. The point at the center of the FPCS does not move during a frame exposure.
- c. The optical system has no aberrations .

A.3.2 Derivation

A.3.2.1 Procedure. Let \bar{q} be a general vector in the OCS. The intersection of \bar{q} with the earth defines a general point in the target plane. The center of the target is given by the intersection with the earth of \bar{q}_0 , where \bar{q}_0 is the line-of-sight vector in the OCS (see Figure A.3-1).

~~SECRET~~ D

~~SECRET~~ D

BIF-008- [REDACTED] -68
(Control Number)

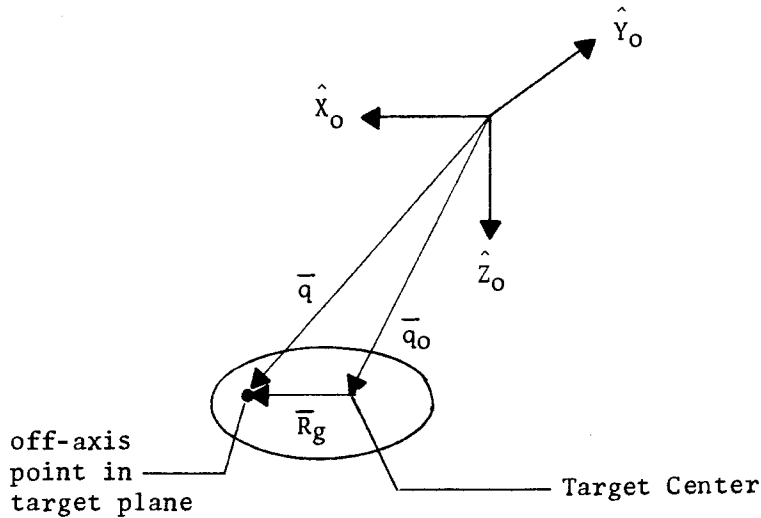


Figure A.3-1
Location of Points in Target

From Figure A.3-1 it can be seen that;

$$\bar{R}_g = \bar{q} - \bar{q}_0, \quad \text{Equation A.3-1}$$

where \bar{R}_g is a vector in the plane of the target that locates a general target point relative to the center of the target.

Let \bar{F} be a vector in the film plane coordinate system-FPCS. There exists a matrix B such that;

$$\bar{F}_g = B \bar{R}_g \quad \text{Equation A.3-2}$$

where \bar{F}_g is the projection of R_g .

A-9
~~SECRET~~ D

Handle via BYEMAN
Control System Only

~~SECRET~~ D

BIF-008- [REDACTED] -68
(Control Number)

The problem is to find the appropriate expression for B. The off-axis image rates are then obtained by simple differentiation.

A.3.2.2 OCS To OSCS Transformation. From equation A.2-7, the vector \bar{q} in the OCS can be expressed in the OSCS by;

$$\bar{U} = R_y(-2^\circ)A \bar{q} \quad \text{Equation A.3-3}$$

A.3.2.3 Tracking Mirror Reflection. The tracking mirror reflects the vector \bar{U} such that the reflected vector, denoted by \bar{Y} , is given by; (see Figure A.3-2)

$$\bar{Y} = M_T \bar{U} \quad \text{Equation A.3.4}$$

where M_T is the tracking mirror reflection matrix in the OSCS.

The matrix M_T is given by;

$$M_T = I - 2\hat{N}_S \hat{N}_S^t \quad \text{Equation A.3-5}$$

where

- I - identity matrix ,
- \hat{N}_S - tracking mirror normal in OSCS, and
- t - transpose operator.

~~SECRET~~ D

~~SECRET~~ D

BIF-008- [REDACTED] -68
(Control Number)

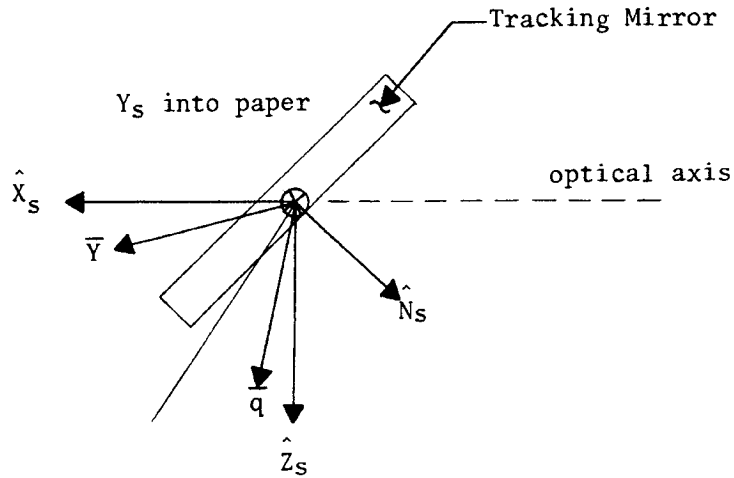


Figure A.3-2
Tracking Mirror Reflection

Using equation A.2-4 to expand equation A.3-5;

$$M_T = \begin{bmatrix} \cos 2\sigma & \sin 2\sigma \sin \omega & \sin 2\sigma \cos \omega \\ \sin 2\sigma \sin \omega & 1 - 2\cos^2 \sigma \sin^2 \omega & -\sin 2\omega \cos^2 \sigma \\ \sin 2\sigma \cos \omega & -\sin 2\omega \cos^2 \sigma & 1 - 2\cos^2 \sigma \cos^2 \omega \end{bmatrix}. \quad \text{Equation A.3-6}$$

Combining equations A.3-3 and A.3-4;

$$\bar{Y} = M_T R_y(-2^\circ) A \bar{q} \quad \text{Equation A.3-7}$$

A.3.2.4 Imaging By the Primary Mirror. If it is assumed that the primary mirror acts as a simple lens, then the image of \bar{Y} , denoted by \bar{S} is given by considering the primary mirror to be a plane surface (see Figure A.3-3).

A-11
~~SECRET~~ D

Handle via **BYEMAN**
Control System Only

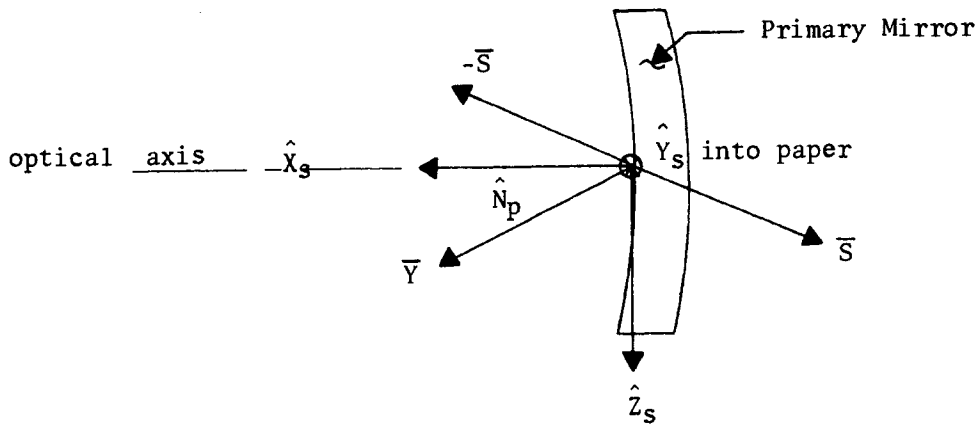


Figure A.3-3
Primary Mirror Imaging

The vector \bar{s} is given by; ⁽¹⁾

$$\bar{s} = M_p \bar{y}, \quad \text{Equation A.3-8}$$

where:

$$M_p = I - 2\hat{N}_p \hat{N}_p^t, \quad \text{Equation A.3-9}$$

and

$$\hat{N}_p = \begin{bmatrix} 1 \\ 0 \\ 0 \end{bmatrix} \quad \text{- Primary mirror normal at the center of the mirror.} \quad \text{Equation A.3-10}$$

Substituting equation A.3-10 into equation A.3-9, results in:

(1) For all practical purposes the center of the tracking mirror and the primary mirror are the same, because the distance between them is small compared to the distance between the tracking mirror and the ground.

~~SECRET~~ D

BIF-008- [REDACTED] -68
(Control Number)

$$M_P = \begin{bmatrix} -1 & 0 & 0 \\ 0 & 1 & 0 \\ 0 & 0 & 1 \end{bmatrix},$$

therefore;

$$\bar{S} = \begin{bmatrix} -1 & 0 & 0 \\ 0 & 1 & 0 \\ 0 & 0 & 1 \end{bmatrix} \bar{Y}$$

Equation A.3-11

A.3.2.5 Film Plane Coordinate System As Seen By The Primary Mirror. As shown in Figure A.3-4, the 1st and 2nd folding mirrors bend the optical axis in the $\hat{X}_S\text{-}\hat{Z}_S$ plane. The primary mirror "sees" the film plane as if it were located behind the 1st folding mirror at a distance equal to the lens focal length.

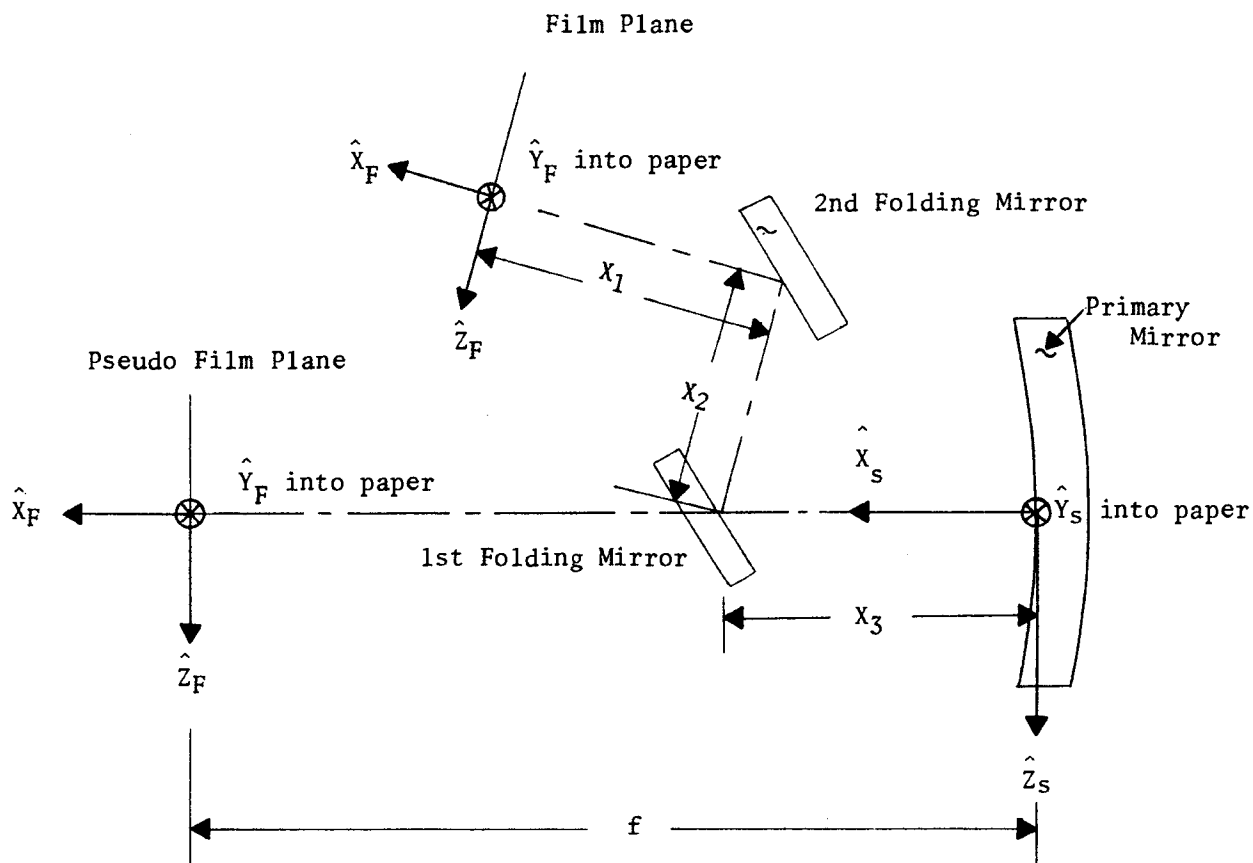
A.3.2.6 Projection on the Film Plane. The vector \bar{S} , obtained in paragraph A.3.2.4, can now be projected on to the film plane by the following procedure.

Because \bar{S} points away from the film plane, the negative of \bar{S} must be used, that is; (see Figure A.3-5)

$$\bar{U} = -\bar{S}, \quad \text{Equation A.3-12}$$

where \bar{U} is a vector at the center of the primary mirror that points toward the film plane.

~~SECRET~~ D



where $f = x_1 + x_2 + x_3 = \text{focal length}$

Figure A.3-4
Film Plane As Seen by the Primary Mirror

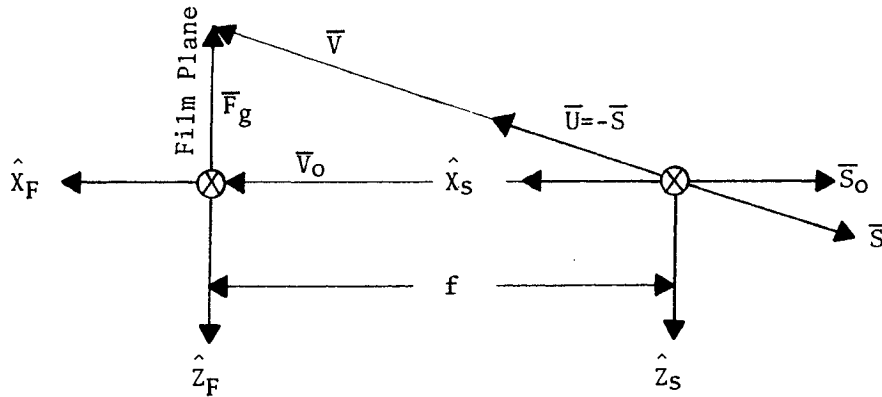


Figure A.3-5
Project on the Film Plane

The intersection of \bar{U} with the film plane defines the point in the film plane that corresponds to the ground point that is defined by \bar{q} .

Let \bar{F}_g be a vector in the film plane that coincides with the intersection of \bar{U} and the $\hat{Y}_F - \hat{Z}_p$ plane. The vector \bar{F}_g is given by;

$$\bar{F}_g = \bar{V} - \bar{V}_o \quad \text{Equation A.3-13}$$

where;

$$\bar{V} = K \bar{U} = -K \begin{bmatrix} -1 & 0 & 0 \\ 0 & 1 & 0 \\ 0 & 0 & 1 \end{bmatrix} M_T R_y(-2^\circ) A \bar{q} \quad , \quad \text{Equation A.3-14}$$

~~SECRET~~ D

BIF-008- [REDACTED] -68
(Control Number)

K - appropriate scale factor, and
 \bar{V}_o - projection of the line-of-sight on to the film plane.

The fact that \bar{V}_o is the projection of \bar{q}_o on the film plane follows from the assumption that the center of the target, as defined by \bar{q}_o , is assumed to be imaged at the center of the film plane. The vector \bar{V}_o is obtained by the same procedure as was used for \bar{V} . That is;

$$\bar{V}_o = -K_o \begin{bmatrix} -1 & 0 & 0 \\ 0 & 1 & 0 \\ 0 & 0 & 1 \end{bmatrix} M_{T^R} R_y(-2^\circ) A \bar{q}_o, \quad \text{Equation A.3-15}$$

where: \bar{q}_o - line-of-sight vector.

Determination of K and K_o ;

From Figure A.3-5 we see that the magnitude of \bar{V}_o equals the lens focal length f, that is;

$$\bar{V}_o \cdot \bar{V}_o = f^2. \quad \text{Equation A.3-16}$$

Substituting equation A.3-15 into A.3-16,

$$K_o^2 (\bar{q}_o \cdot \bar{q}_o) = f^2(1).$$

$$(\bar{M}\bar{A} \cdot \bar{M}\bar{A}) = \bar{A} \cdot \bar{A},$$

But;

$$\bar{q}_o \cdot \bar{q}_o = a_o^2 - \text{where } a_o \text{ is the slant range to the target center,}$$

(1) This equations make use of following the identity;

A-16
~~SECRET~~ D

Handle via BYEMAN
Control System Only

~~SECRET~~ D

BIF-008- [REDACTED] -68
(Control Number)

therefore;

$$K_o^2 = \frac{f^2}{a_o^2},$$

and

$$K_o = \frac{f}{a_o} . \quad \text{Equation A.3-17}$$

Because the \hat{x} s component of \bar{V} is equal to the lens focal length, we can write;

$$\bar{V} \cdot \bar{V}_o = f^2, \quad \text{Equation A.3-18}$$

or

$$K_o K_o (\bar{q} \cdot \hat{q}_o) = f^2.$$

However, $K_o = \frac{f}{a_o} .$

Therefore;

$$K_o f (\bar{q} \cdot \hat{q}_o) = f^2, \text{ where } \hat{q}_o = \frac{\bar{q}_o}{a_o}$$

dividing both sides by f ;

$$K_o = \frac{f}{\bar{q} \cdot \hat{q}_o} = \frac{f}{a_x} . \quad \text{Equation A.3-19}$$

The scalar expression $a_x = (\bar{q} \cdot \hat{q}_o)$ is just the projection of \bar{q} on \hat{q}_o as shown in Figure A.3-6.

~~SECRET~~ D

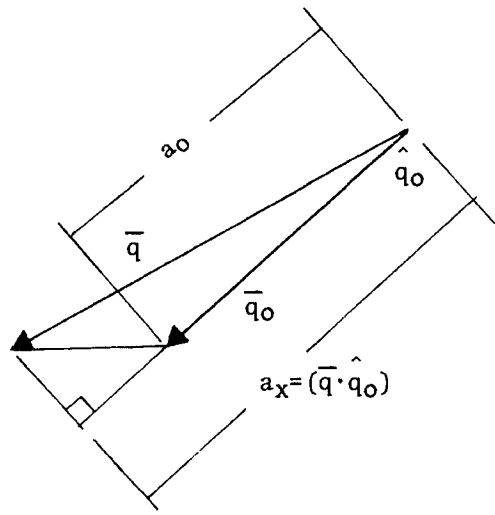


Figure A.3-6
 $a_x = (\bar{q} \cdot \hat{q}_0)$

Combining the various equations, the vector \bar{F}_g can be expressed as:

$$\bar{F}_g = \frac{f}{a_x} \begin{bmatrix} -1 & 0 & 0 \\ 0 & 1 & 0 \\ 0 & 0 & 1 \end{bmatrix} M_T R_y(-2^\circ) A \left[\bar{q} - \frac{a_x}{a_0} \bar{q}_0 \right] \quad \text{Equation A.3-20}$$

The above equation needs to be simplified, because the wish is to relate the ground vector \bar{R}_g , to the film plane vector \bar{F}_g . The vector in brackets of equation A.3-20 can be written as:

$$\bar{q} - \frac{a_x}{a_0} \bar{q}_0 = \bar{R}_g + \bar{q}_0 - \left[(\bar{R}_g + \bar{q}_0) \cdot \hat{q}_0 \right] \hat{q}_0, \quad \text{Equation A.3-21}$$

~~SECRET~~ D

BIF-008- [REDACTED] -68
(Control Number)

where: the following relationships have been used;

$$\hat{q}_0 = \frac{\bar{q}_0}{a_0},$$

$$\bar{q} = \bar{R}_g + \bar{q}_0, \text{ and}$$

$$a_x = \bar{q} \cdot \hat{q}_0 = (\bar{R}_g + \bar{q}_0) \cdot \hat{q}_0.$$

Expanding the dot product;

$$(\bar{R}_g + \bar{q}_0) \cdot \hat{q}_0 = \bar{R}_g \cdot \hat{q}_0 + \bar{q}_0 \cdot \hat{q}_0,$$

but;

$$\bar{q}_0 \cdot \hat{q}_0 = q_0,$$

therefore the last two terms on the right side of equation A.3-21 become:

$$\bar{q}_0 - [(\bar{R}_g + \bar{q}_0) \cdot \hat{q}_0] \hat{q}_0 = -(\bar{R}_g \cdot \hat{q}_0) \hat{q}_0,$$

substituting into equation A.3-21,

$$\bar{q} - \frac{a_x}{a_0} \bar{q}_0 = \bar{R}_g - (\bar{R}_g \cdot \hat{q}_0) \hat{q}_0,$$

but;

$$(\bar{R}_g \cdot \hat{q}_0) \hat{q}_0 \equiv (\hat{q}_0 \hat{q}_0^t) \bar{R}_g,$$

~~SECRET~~ D

~~SECRET~~ D

BIF-008- [REDACTED] -68
(Control Number)

therefore;

$$\bar{q}_o - \frac{a_x}{a_o} \bar{q}_o = (I - \hat{q}_o \hat{q}_o^t) \bar{R}_g. \quad \text{Equation A.3-22}$$

Substituting equation A.3-22 into equation A.3-20;

$$\bar{F} = - \frac{f}{a_x} \begin{bmatrix} -1 & 0 & 0 \\ 0 & 1 & 0 \\ 0 & 0 & 1 \end{bmatrix} M_T R_y(-2^\circ) A (I - \hat{q}_o \hat{q}_o^t) \bar{R}_g,$$

or

$$\bar{F} = B \bar{R}_g, \quad \text{Equation A.3-23}$$

where:

$$B = - \frac{f}{a_x} \begin{bmatrix} -1 & 0 & 0 \\ 0 & 1 & 0 \\ 0 & 0 & 1 \end{bmatrix} M_T R_y(-2^\circ) A (I - \hat{q}_o \hat{q}_o^t). \quad \text{Equation A.3-24}$$

The matrix B can be simplified by making use of the following relationship;

$$R_y(-2^\circ) A (I - \hat{q}_o \hat{q}_o^t) = (I - \hat{q}_s \hat{q}_s^t) R_y(-2^\circ) A,$$

where:

$$\hat{q}_s = R_y(-2^\circ) A \hat{q}_o \quad \text{line-of-sight unit vector in OSCS.}$$

Substituting the above relationship into equation A.3-24;

$$B = - \frac{f}{a_x} \begin{bmatrix} -1 & 0 & 0 \\ 0 & 1 & 0 \\ 0 & 0 & 1 \end{bmatrix} M_T (I - \hat{q}_s \hat{q}_s^t) R_y(-2^\circ) A. \quad \text{Equation A.3-25}$$

~~SECRET~~ D

~~SECRET~~ D

BIF-008- [REDACTED] -68
(Control Number)

As given in equation A.3-25, the matrix B is a 3x3 matrix. Because the vector \bar{F}_g lies in the \hat{Z}_F - \hat{Y}_F plane, one would suspect that B can be reduced to a 2x3 matrix. If the product $M_T(I - \hat{q}_s \hat{q}_s^t)$ is expanded by using equations A.3-2 and A.3-6, we get;

$$M_T(I - \hat{q}_s \hat{q}_s^t) = M_T',$$

where M_T' is identical to M_T except it contains zeros in the first row.

Therefore, the equation can be written:

$$\begin{bmatrix} 0 \\ Y_F \\ Z_F \end{bmatrix} = -\frac{f}{ax} M_T' R_y(-2^\circ) A \begin{bmatrix} R_{gx} \\ R_{gy} \\ R_{gz} \end{bmatrix}, \quad \text{Equation A.3-26}$$

where:

$$\begin{bmatrix} 0 \\ Y_F \\ Z_F \end{bmatrix} - \text{components of } \bar{F}_g, \text{ and}$$

$$\begin{bmatrix} R_{gx} \\ R_{gy} \\ R_{gz} \end{bmatrix} - \text{components of } \bar{R}_g.$$

If local altitude variations in the target plane are neglected and the flat earth model is assumed, then; $R_{gz} = 0$ and the equation can be written:

$$\bar{F}_g' = -\frac{f}{ax} T_p \bar{R}_g' \quad \text{Equation A.3-27}$$

~~SECRET~~ D

where:

$$\bar{F}_g' = \begin{bmatrix} Y_F \\ Z_F \end{bmatrix}$$

$$\bar{R}_g' = \begin{bmatrix} R_{gx} \\ R_{gy} \end{bmatrix},$$

and the elements of T_p are given by the expansion of $M_T R_y(-2^\circ)A$;

$$M_T R_y(-2^\circ)A = \begin{bmatrix} 0 & 0 & 0 \\ T_{21} & T_{22} & T_{23} \\ T_{31} & T_{32} & T_{33} \end{bmatrix} \quad \text{Equation A.3-28}$$

$$T_p = \begin{bmatrix} T_{21} & T_{22} \\ T_{31} & T_{32} \end{bmatrix} \quad (2 \times 2) \text{ matrix.} \quad \text{Equation A.3-29}$$

A.3.2.7 Off-Axis Image Rates. The off-axis image rates are obtained by differentiation of equation A.3-27.

$$\dot{\bar{F}}_g' = \begin{bmatrix} \dot{Y}_F \\ \dot{Z}_F \end{bmatrix} = \left(f \frac{\dot{ax}}{ax^2} T_p - \frac{f}{ax} \dot{T}_p \right) \bar{R}_g' \quad \text{Equation A.3-30}$$

but;

$$\bar{R}_g' = -\frac{ax}{f} T_p^{-1} \dot{\bar{F}}_g' \quad (\text{inversion of equation A.3-27})$$

where:

$$T_p^{-1} = \frac{1}{(T_{21}T_{32} - T_{31}T_{22})} \begin{bmatrix} T_{32} & -T_{22} \\ -T_{31} & T_{21} \end{bmatrix}$$

~~SECRET~~ D

BIF-008- [REDACTED] -68
(Control Number)

$$\dot{T}_p = \begin{bmatrix} \dot{T}_{21} & \dot{T}_{22} \\ \dot{T}_{31} & \dot{T}_{32} \end{bmatrix}$$

Therefore;

$$\dot{\bar{F}}_g' = (\dot{T}_p T_p^{-1} - \frac{\dot{a}_x}{a_x} I) \bar{F}_g' \quad \text{Equation A.3-31}$$

The term $\frac{\dot{a}_x}{a_x}$ is evaluated as follows; (see Figure A.3-7)

$$G^2 = a^2 + a_0^2 - 2a_0 a \cos(\mu)$$

but;

$$\cos(\mu) = \frac{a_x}{a},$$

therefore;

$$G^2 = a^2 + a_0^2 - 2a_0 a_x$$

Differentiating;

$$\dot{G}G = \dot{a}a + a_0 \dot{a}_0 - a_0 \dot{a}_x - a_x \dot{a}_0$$

Because the off-axis point in the ground plane does not move with respect to the target center, $G = 0$

therefore;

$$\dot{a}_x = \frac{a}{a_0} \dot{a} + \dot{a}_0 - \frac{a_0}{a_0} \dot{a}_x$$

~~SECRET~~ D

~~SECRET~~ D

BIF-008- [REDACTED] -68
(Control Number)

The nonlinear term results from the dependence of slant range on semi-field angle. Because the maximum semi-field angle is only 0.54 degree, the nonlinear term is small compared to the linear term. (See Figures A.3-8 and A.3-9) In addition, if the nonlinear term were included in the camera set-up equations, it would require the platen-jog profile to have a different nonlinear shape for each pointing situation.

A.4 X-IMC CAMERA SET-UP EQUATIONS

A.4.1 Polar Form

The linear term of equation A.3-32 can be written in component form as;

$$\dot{Y}_F = C_{11}Y_F + C_{12}Z_F, \quad \text{Equation A.4-1}$$

$$\dot{Z}_F = C_{21}Y_F + C_{22}Z_F, \quad \text{Equation A.4-2}$$

where: C_{ij} 's are elements of a C matrix given by;

$$C = \dot{T}_p T_p^{-1} - \frac{\dot{a}_0}{a_0} I.$$

Let

$$Y_F = R \cos\theta, \text{ and} \\ Z_F = R \sin\theta.$$

Equations A.4-1 and A.4-2 in polar form are given by;

$$\dot{Y}_F = R(C_{11}\cos\theta + C_{12}\sin\theta), \text{ and}$$

$$\dot{Z}_F = R(C_{21}\cos\theta + C_{22}\sin\theta),$$

~~SECRET~~ D

~~SECRET~~ D

BIF-008- [REDACTED] -68
(Control Number)

NOTE:

1. Image velocities are for the line of maximum image motion.

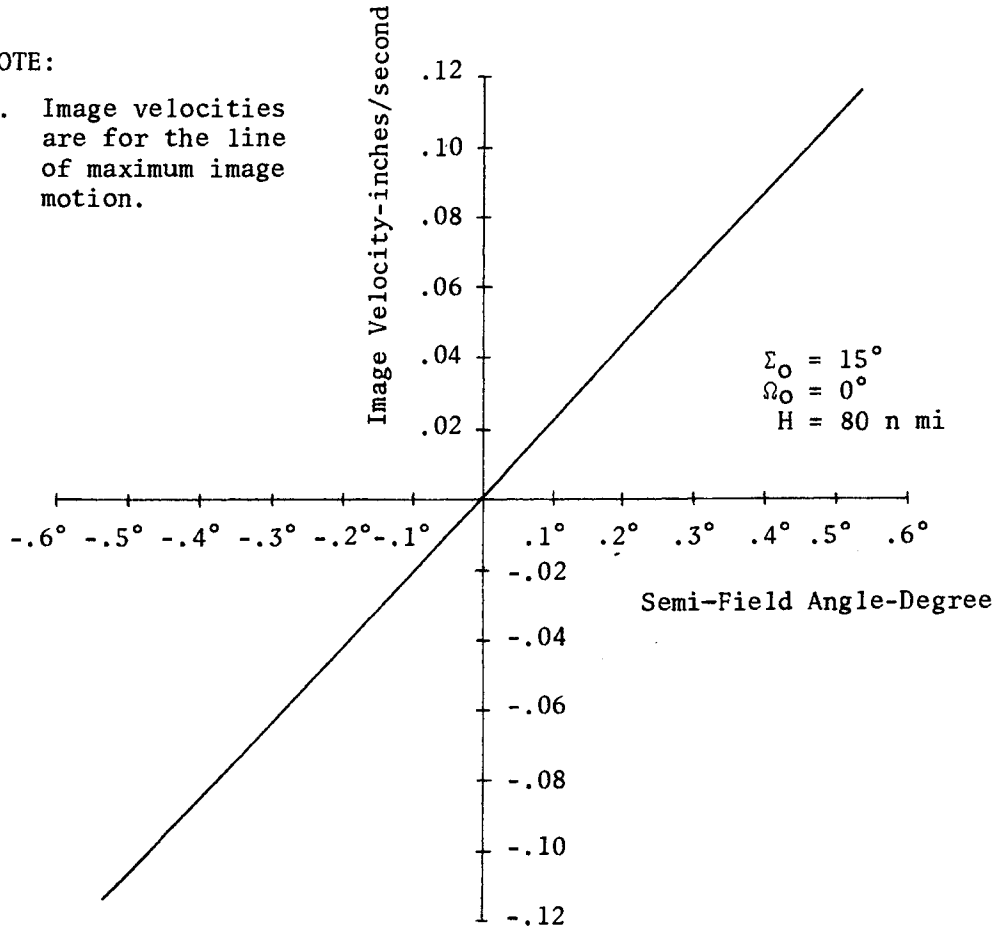


Figure A.3-8. Image Velocity vs Semi-Field Angle
Linear Term

A-26

~~SECRET~~ D

Handle via BYEMAN
Control System Only

~~SECRET~~ D

BIF-008- [REDACTED] -68
(Control Number)

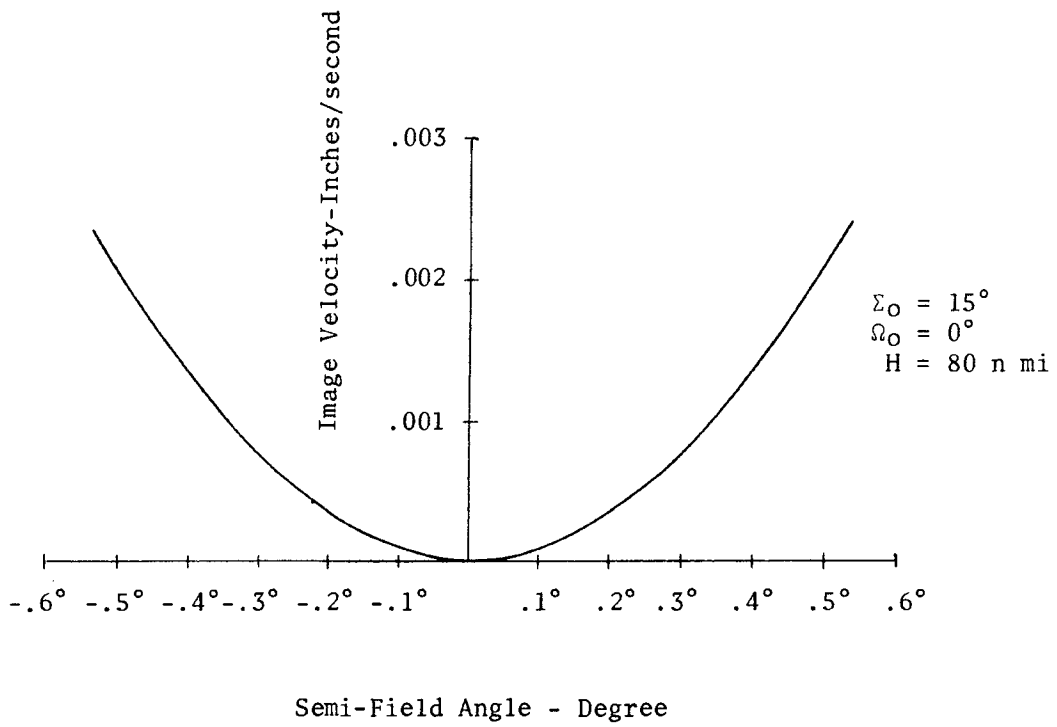


Figure A.3-9. Image Velocity vs Semi-Field Angle
Nonlinear Term

~~SECRET~~ D

~~SECRET~~ D

BIF-008- [REDACTED] -68
(Control Number)

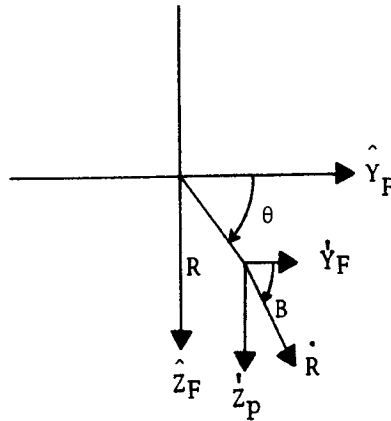


Figure A.4-1 Polar Transformation

now:

$$\dot{R}^2 = \dot{Y}_F^2 + \dot{Z}_F^2, \text{ and}$$

$$\tan B = \dot{Y}_F / \dot{Z}_F,$$

or

$$\dot{R}^2 = R^2(A_0 + B_1 \sin 2\theta + B_2 \cos 2\theta) \quad \text{Equation A.4-3}$$

$$\tan B = \frac{C_{11} \cos \theta + C_{12} \sin \theta}{C_{21} \cos \theta + C_{22} \sin \theta}, \quad \text{Equation A.4-4}$$

where:

$$A_0 = \frac{1}{2}(C_{11}^2 + C_{12}^2 + C_{21}^2 + C_{22}^2), \quad \text{Equation A.4-5}$$

~~SECRET~~ D

~~SECRET~~ D

BIF-008- [REDACTED] -68
(Control Number)

$$B_1 = C_{11}C_{12} + C_{21}C_{22}, \text{ and} \quad \text{Equation A.4-6}$$

$$B_2 = \frac{1}{2}(C_{11}^2 + C_{21}^2 - C_{12}^2 - C_{22}^2). \quad \text{Equation A.4-7}$$

Equation A.4-3 can be further simplified as follows;

$$B_1 = B_0 \sin \gamma, \text{ and}$$

$$B_2 = B_0 \cos \gamma,$$

where:

$$B_0 = +(B_1^2 + B_2^2)^{\frac{1}{2}} \quad \text{Equation A.4-8}$$

$$\tan \gamma = \frac{B_1}{B_2}. \quad \text{Equation A.4-9}$$

Substituting into equation A.4-3;

$$\dot{R}^2 = R^2 A_0 + B_0 \cos(2\theta - \gamma). \quad \text{Equation A.4-10}$$

Figure A.4-2 shows the graphical interpretation of equations A.4-10 and equation A.4-4.

As seen in Figure A.4-2, for a particular θ and $\theta + 180$ -degrees, the magnitude of the off-axis image rate varies as a linear function of distance from format center and the direction is independent of R except for a reversal in direction about the format center. For other θ , the pattern is the same except for a sinusoidal variation of magnitude.

~~SECRET~~ D

~~SECRET~~ D

BIF-008- [REDACTED] -68
(Control Number)

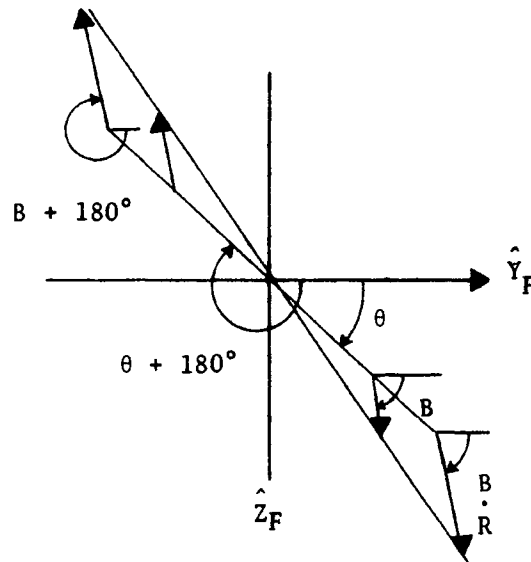


Figure A.4-2 Linear Image Rates

A.4.2 SLIT ANGLE - S

The slit angle is the value of θ when $\frac{\dot{R}^2}{R^2}$ is a maximum.

From equation A.4-10, the maximum value of $\frac{\dot{R}^2}{R^2}$ is;

$$\frac{\dot{R}^2}{R^2}_{\max} = A_0 + B_0,$$

and occurs when;

$$\cos(2\theta - \gamma) = 1,$$

~~SECRET~~ D

~~SECRET~~ D

BIF-008- [REDACTED] -68
(Control Number)

or

$$2\theta - \gamma = 2n\pi, \quad n = 0, \pm 1, \pm 2 \dots$$

Therefore,

$$S = n\pi + \frac{\gamma}{2}, \quad n = 0, \pm 1, \pm 2 \dots \quad \text{Equation A.4-11}$$

where: γ is given by equation A.4-9

A.4.2.1 Primary Slit Angles - S_p . Primary Slit Angles are defined as values of S such that;

$$-\pi/2 < S_p \leq \pi/2.$$

They are obtained from equation A.4-11 by setting $n=0$

$$S_p = \frac{\gamma}{2}, \quad \text{Equation A.4-12}$$

where:

$$\tan \gamma = \frac{B_1}{B_2} \quad -180^\circ < \gamma \leq 180^\circ. \quad \text{Equation A.4-13}$$

A.4.2.2 Alternate Slit Angles - S_A . Alternate slit angles are defined as values of S such that;

$$90^\circ < S_A \leq 111^\circ \\ \text{or} \\ -111^\circ \leq S_A < -90^\circ$$

~~SECRET~~ D

~~SECRET~~ D

BIF-008-██████████-68
(Control Number)

They are obtained from the primary slit angles by; (See Figure A.4-3)

$$S_A = S_p + 180^\circ, S_p - \text{negative, and}$$
$$S_A = S_p - 180^\circ, S_p - \text{positive.}$$

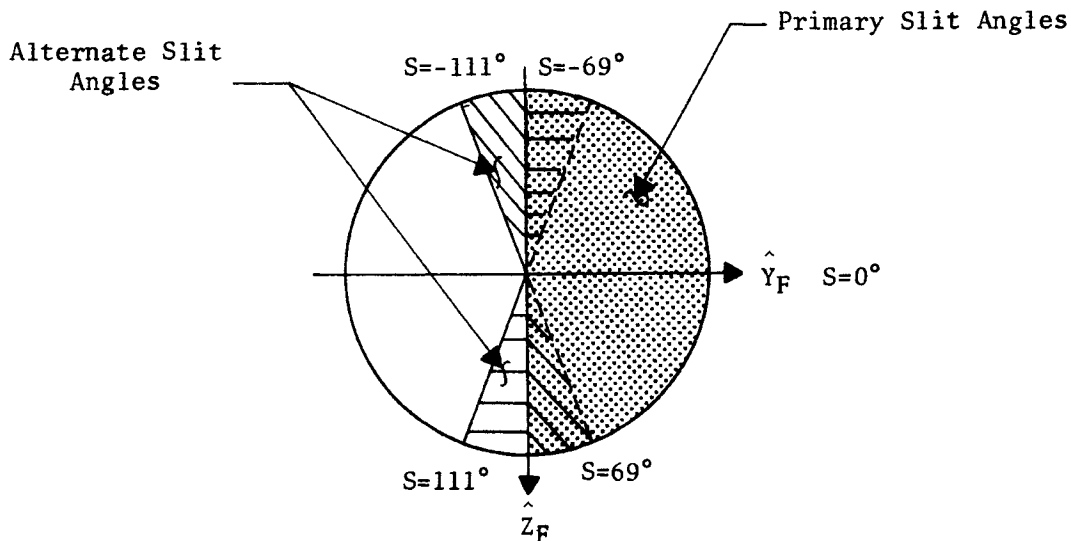


Figure A.4-3 Alternate Slit Angles

Figure A.4-3 shows the range of primary slit angles for which alternate slit angles exist. The alternate slit angles are used for those cases where they would give a smaller angular change in the slit angle between frames.

A.4.3 Platen Angle - J

The platen angle is the angle of the linear image rates for $\theta = S$ (See Figure A.4-4)

A-32
~~SECRET~~ D

Handle via BYEMAN
Control System Only

~~SECRET~~ D

BIF-008- [REDACTED] -68
(Control Number)

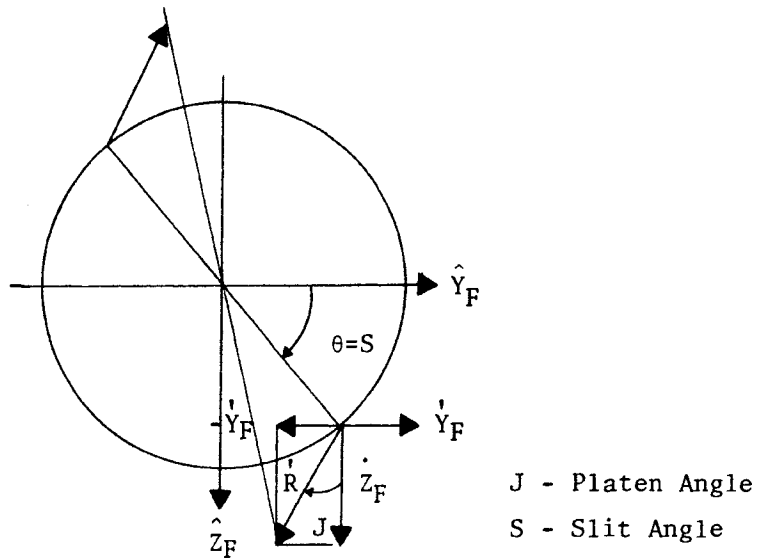


Figure A.4-4 Platen Angle

$$\tan(J) = A_3 = \frac{-\dot{Y}_F|_{\theta=S}}{Z_F|_{\theta=S}}, \quad \text{Equation A.4-14}$$

where:

$$A_3 = - \left(\frac{A_1}{A_2} \right), \quad \text{Equation A.4-15}$$

and

$$A_1 = C_{11}\cos(s) + C_{12}\sin(s), \text{ and} \quad \text{Equation A.4-16}$$

$$A_2 = C_{21}\cos(s) + C_{22}\sin(s). \quad \text{Equation A.4-17}$$

~~SECRET~~ D

A.4.4 Maximum Platen Velocity - V_{max}

A.4.4.1 Magnitude. The magnitude of V_{max} is the value of \dot{R} for $\theta = S$ and $R = 4.7$ inches. From Equation A.4-10,

$$|V_{max}| = 4.7(A_0+B_0)^{\frac{1}{2}} - \text{inches/second.} \quad \text{Equation A.4-18}$$

A.4.4.2 Sign of V_{max} . The slit is a bidirectional mechanism which can travel either left or right across the film plane. The sign of V_{max} in the software logic assumes the slit to be travelling in a positive direction as defined in paragraph A.2.4. The camera electronics reverses the sign of V_{max} when the slit travels in the opposite or negative direction.

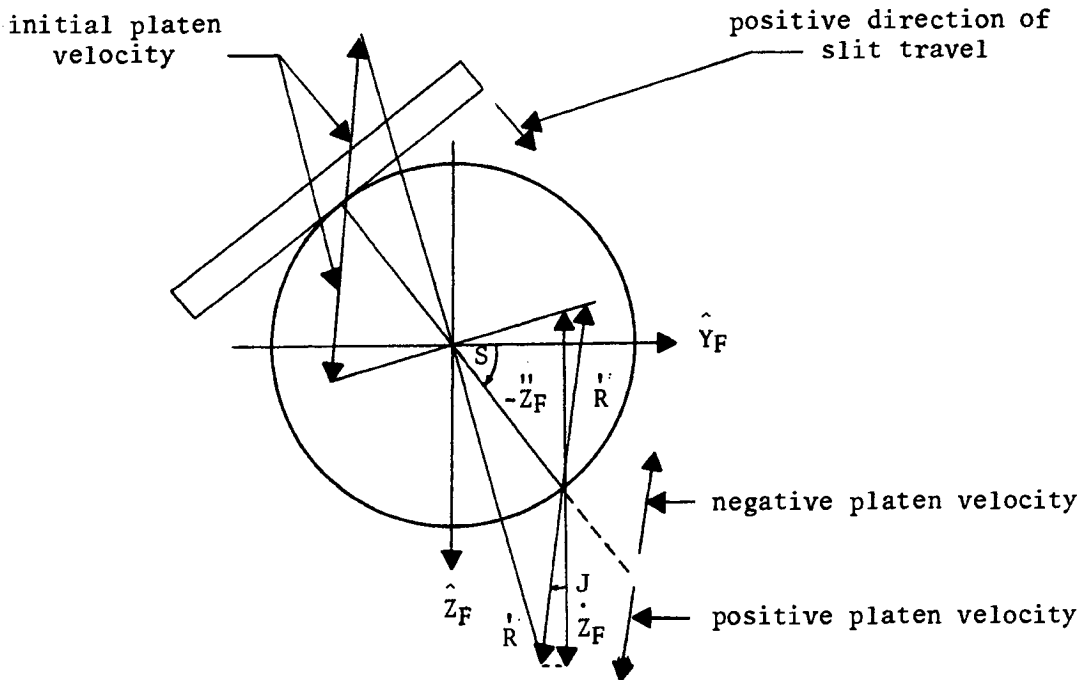


Figure A.4-5 Sign of V_{max}

~~SECRET~~ D

BIF-008- [REDACTED] -68
(Control Number)

As seen from Figure A.4-5, the Sign of V_{max} is given by;

$$\text{Sign of } V_{max} = \text{Sign of } [-\dot{Z}_F|_{\theta=S}],$$

or:

$$\text{Sign of } V_{max} \equiv \text{Sign of } [-C_{21} \cos(s) - C_{22} \sin(s)].$$

Equation A.4-19

A.4.5 Typical Values of S, J and V_{max}

Figures A.4-6, A.4-7, and A.4-8 give typical values for S, J and V_{max} .

~~SECRET~~ D

~~SECRET~~ D

BIF-008- [REDACTED] -68
(Control Number)

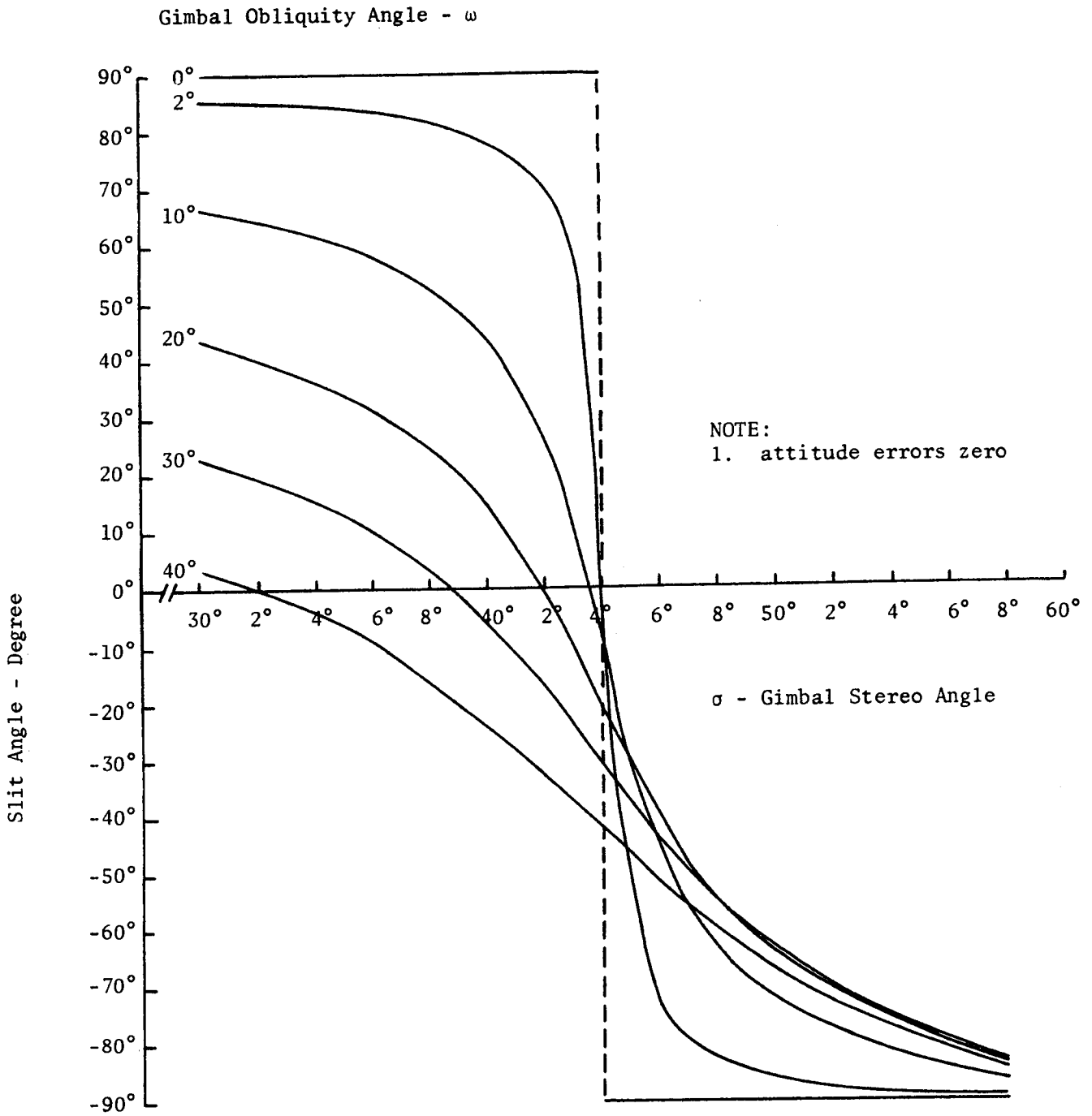


Figure A.4-6. Slit Angle(S) vs Gimbal Stereo Angle(σ) for Fixed Gimbal Obliquity Angles(ω)

A-36

~~SECRET~~ D

Handle via BYEMAN
Control System Only

~~SECRET~~ D

BIF-008- [REDACTED] -68
(Control Number)

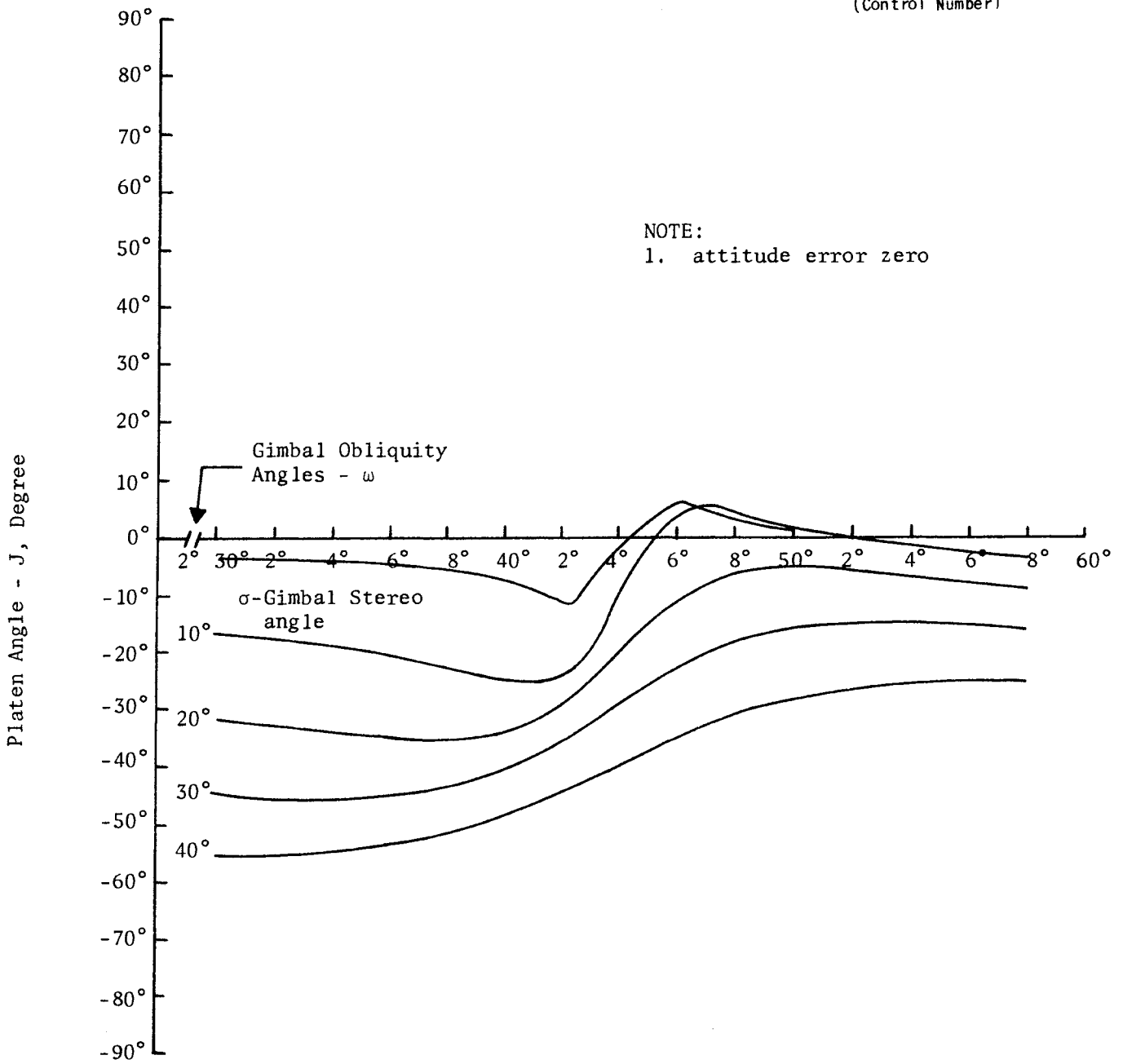


Figure A.4-7. Platen Angle(J) vs Gimbal Stereo Angle(σ)
for Fixed Gimbal Obliquity Angles(ω)

~~SECRET~~ D

~~SECRET~~ D

BIF-008- [REDACTED] -68
(Control Number)

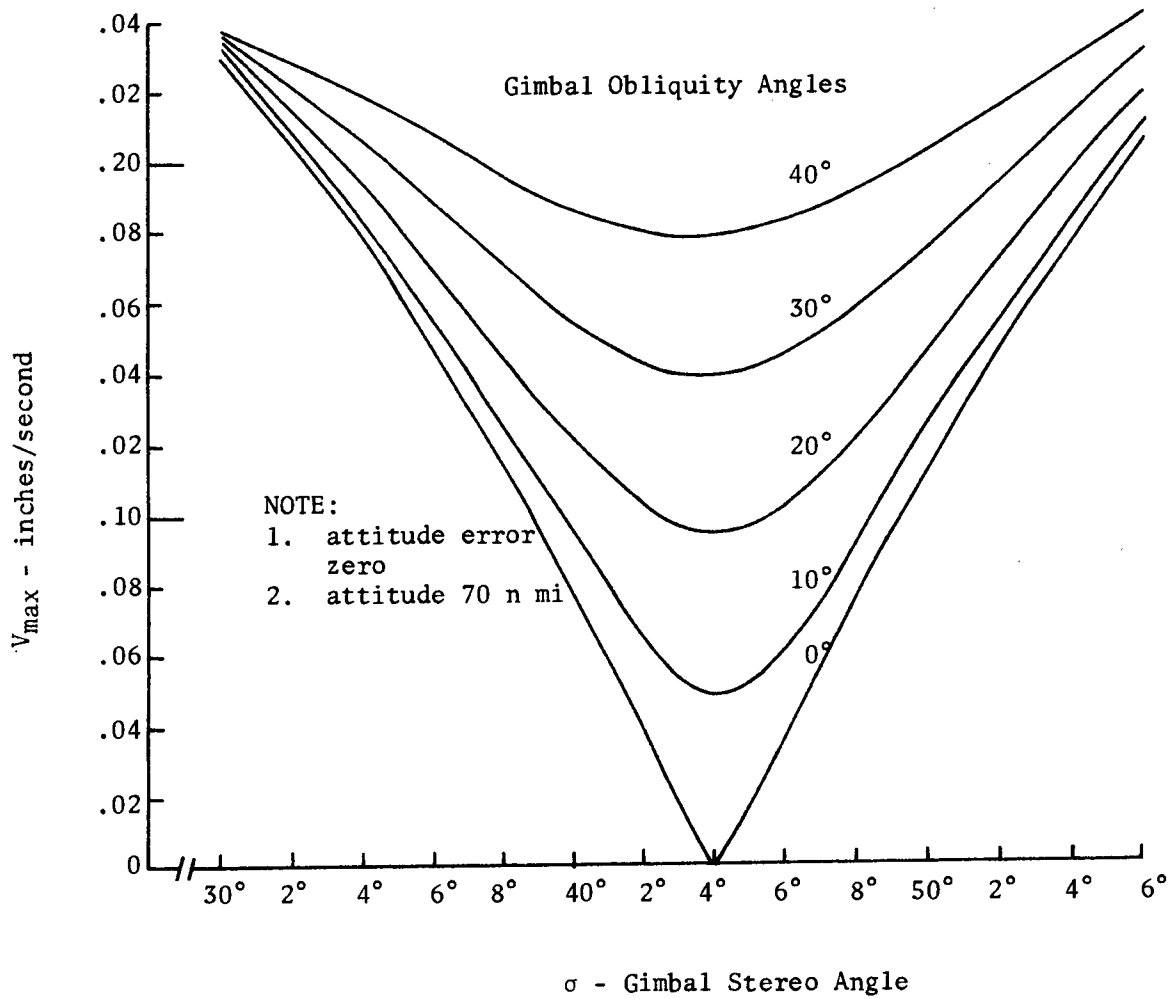


Figure A.4-8. Maximum Platen Velocity (V_{max}) vs Gimbal Stereo (σ) Angle for Fixed Gimbal Obliquity Angles (ω)

~~SECRET~~ D

~~SECRET~~ D

BIF-008- [REDACTED] -68
(Control Number)

APPENDIX B
TIME-DEPENDENT IMAGE STRUCTURE

B.1 INTRODUCTION

There are two time-dependent effects which modify the structure of a photographic exposure image. The first of these is image motion. The second is the time-varying shape of the exit pupil produced by the action of the shutter. These two effects are interdependent but they can be evaluated independently if both contribute only slightly to the degradation of the exposure image.

By treating the time-dependent degrading factors in this manner, the modulation transfer function (MTF) of the exposure image can be determined by cascading the MTF of the lens with the transfer function for image motion and exit-pupil shuttering:

$$G_E(\nu) = G_L(\nu) \cdot G_I(\nu) \cdot G_S(\nu),$$

where $G_E(\nu)$ is the transfer function for the exposure image, $G_L(\nu)$ for the lens, $G_I(\nu)$ for image motion, and $G_S(\nu)$ for the shutter; ν is the spatial frequency at which the MTF is evaluated.

The transfer function for the time-dependent effects are developed in the following sections. The transfer function for image motion, $G_I(\nu)$ is evaluated by assuming the lens to have a time-dependent MTF; that is, $G_S(\nu) = 1$ (perfect lens shuttering). The exit-pupil shuttering transfer function is developed under the assumption that there is no image motion; that is, $G_I(\nu)$ is assumed to equal one.

B-1

~~SECRET~~ D

Handle via BYEMAN
Control System Only

~~SECRET~~ D

BIF-008-XXXXXXXXXX-68
(Control Number)

B.2 IMAGE MOTION

The magnitude of the image-motion-compensation (IMC) error, or smear, in the film plane can generally be determined from camera tolerances. For performance studies, it is necessary to convert the image spread caused by smear to an MTF. The following discussion indicates the method of converting the calculated values of smear to an MTF.

Figure B.2-1 is the line spread function which appears on the film of a point object if the slit (shutter) is 100 percent efficient. The point is smeared to a distance τ_o , and no other degradations are present.

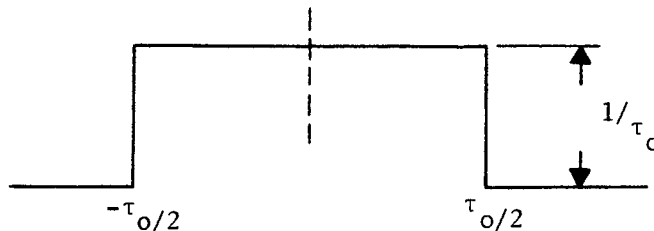


Figure B.2-1. Line-Spread Function-100-percent Efficient Slit

If the slit is not 100-percent efficient, then two things happen:

- a. the total smear is slightly greater, and
- b. the edges are no longer as sharp.

B-2

~~SECRET~~ D

Handle via **BYEMAN**
Control System Only

~~SECRET~~ D

BIF-008- [REDACTED] -68
(Control Number)

This is depicted in Figure B.2-2.

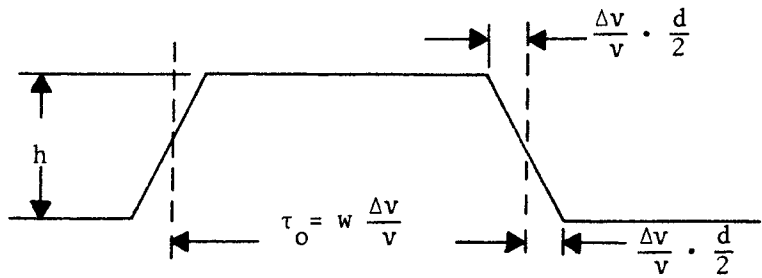


Figure B.2-2. Line Spread Function with a less than 100-percent Efficient Slit

where: d = diameter of the cone of light rays at the slit aperture plate,
 w = slit width, and
 $\frac{\Delta v}{v}$ = uncompensated image motion.

Note in particular that the definition of τ_0 is the smear which would occur if the slit were 100-percent efficient.

With reference to Figure B.2-2 the total illumination which would have produced the image if all points had received the same amount is proportional to:

$$h(w + d) \frac{\Delta v}{v} .$$

The total illumination which produces the image is proportional to:

$$\frac{h[(w + d) + (w - d)]}{2} \frac{\Delta v}{v} = hw \frac{\Delta v}{v} .$$

~~SECRET~~ D

The ratio of these two quantities is used as a measure of slit efficiency and is denoted by E. Therefore:

$$E = \frac{w}{w + d}, \text{ and } d = \frac{w - wE}{E}.$$

In terms of the E notation, the length of the base of Figure B.2-2 is:

$$(w + d) \frac{\Delta v}{v} = \frac{\Delta v}{v} \frac{w}{E} = \frac{\tau_o}{E}.$$

The length of the top is:

$$(w - d) \frac{\Delta v}{v} = \frac{\Delta v}{v} w - \frac{w - wE}{E} = \frac{\tau_o(2E - 1)}{E}.$$

By theory of linear systems then, if the area of Figure B.2-2 is normalized to 1, the MTF is the Fourier Transform of the resulting function. This function is shown in Figure B.2-3.

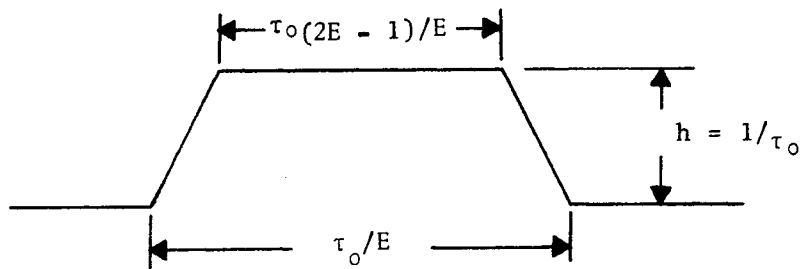


Figure B.2-3. Normalized Line-Spread Function

There are several methods for obtaining the transform of Figure B.2-3. The method used was to appeal to the linearity property of the Fourier Transform and recognize that Figure B.2-3 is the difference between the two triangles given in Figure B.2-4.

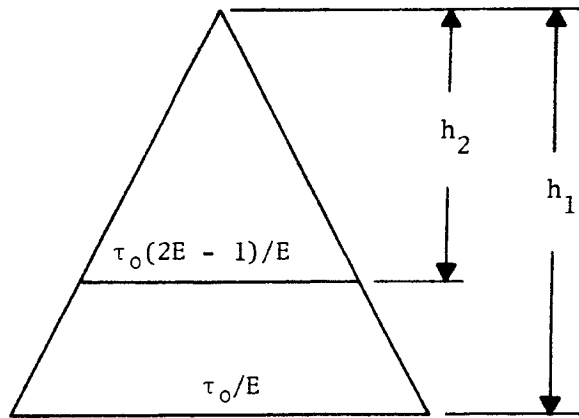


Figure B.2-4. Normalized Line-Spread Function Expressed as a Difference of Two Triangles

The values of h_1 and h_2 satisfy the relations:

$$h_1 - h_2 = \frac{1}{\tau_0},$$

and

$$\frac{h_1}{h_2} = \frac{\tau_0/E}{\tau_0(2E - 1)/E} = \frac{1}{2E - 1}.$$

~~SECRET~~ D

BIF-008- [REDACTED] -68
(Control Number)

If these equations are solved, the result is:

$$h_1 = \frac{1}{2\tau_0 (1 - E)}, \text{ and}$$

$$h_2 = \frac{(2E - 1)}{2\tau_0 (1 - E)}.$$

Now the transform of the triangle in Figure B.2-5 is:

$$G(v) = B \left(\frac{\sin \alpha}{\alpha} \right)^2,$$

where: $B = A\tau_1$, $\alpha = \pi\tau_1 v$, and $v = \text{Spatial Frequency}$.

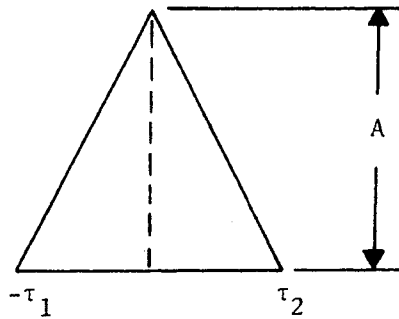


Figure B.2-5. Triangle used in Transformation

B-6
~~SECRET~~ D

Handle via BYEMAN
Control System Only

~~SECRET~~ D

BIF-008- [REDACTED] -68
(Control Number)

Therefore the Fourier Transform of Figure B.2-3 is:

$$G_I(\nu) = \frac{1}{2\tau_o(1-E)} \left(\frac{\tau_o}{2E} \right) \left[\frac{\sin(\pi\nu\tau_o/2E)^2}{\pi\nu\tau_o/2E} \right]$$

$$\left(- \frac{2E-1}{2\tau_o(1-E)} \right) \left(\frac{\tau_o(2E-1)}{2E} \right) \left[\frac{\sin(\pi\nu\tau_o(2E-1)/2E)^2}{\pi\nu\tau_o(2E-1)/2E} \right]$$

$$G_I(\nu) = \left(\frac{E}{\pi^2\nu^2\tau_o^2(1-E)} \right) \left[\sin^2(\pi\nu\tau_o/2E) - \sin^2(\pi\nu\tau_o(2E-1)/2E) \right]$$

$$\text{or } G_I(\nu) = \left(\frac{\sin(\pi\nu\tau_o)}{\pi\nu\tau_o} \right) \left(\frac{\sin[\pi\nu\tau_o(\frac{1}{E}-1)]}{\pi\nu\tau_o(\frac{1}{E}-1)} \right)$$

Before the structural dynamics of the system are understood, it is not possible to say how much, if any, of the smear will be linear. For this reason, the smear tolerance is specified in terms of equivalent linear smear (in the sense of the MTF loss) and is treated in the same manner as other linear contributors.

Once structural analyses have been performed which reveal the probable path of the image motion as a result of vibrations, the validity of the linear assumption can be ascertained. If it turns out that a significant degree of nonlinear or reversible motion occurs, it will be necessary to evaluate $G_I(\nu)$ from the general equation*:

$$G_I(\nu) = t_e^{-1} \int_{-t_e/2}^{t_e/2} [S(t) \exp -2\pi i \nu u(t)] dt,$$

* This expression is derived in Reference 13.

B-7
~~SECRET~~ D

Handle via BYEMAN
Control System Only

~~SECRET~~ D

BIF-008- [REDACTED] -68
(Control Number)

where:

- t_e - exposure time,
- $S(t)$ - shutter function,
- v - spatial frequency, and
- $\mu(t)$ - path of the image motion during exposure.

B.3 FOCAL PLANE SHUTTER

The shutter on a camera modifies the structure of the exposure image by vignetting the exit pupil of the camera's optical system in a time-dependent manner. The following discussion develops the transfer function for a focal plane shutter.

The focal plane shutter being considered is comprised of a slit placed some distance in front of the focal plane. The mathematics developed below apply to any focal plane-shuttered system where either the slit or the film or both are translated with uniform velocity to produce the desired shuttering effect.

It is assumed for the purposes of this discussion that the focal plane shutter is far enough in front of the focal plane so that the shutter can be projected to the plane of the exit pupil of the optical system.

Consider a shutter which has projected width, W , at the exit pupil and is parallel to the y coordinate axis in the plane. (See Figure B.3-1.) Assume that the shutter is moving with uniform velocity along the x coordinate axis.

B-8

~~SECRET~~ D

Handle via BYEMAN
Control System Only

~~SECRET~~ D

BIF-008-[REDACTED]-68
(Control Number)

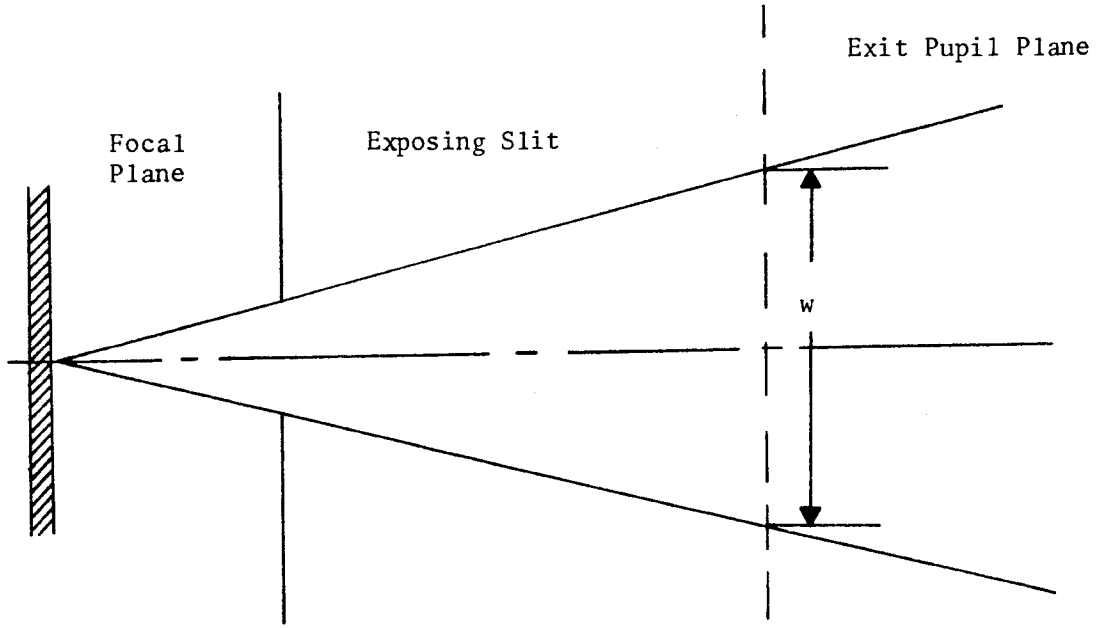


Figure B.3-1. Focal Plane Shutter Geometry

B-9
~~SECRET~~ D

Handle via BYEMAN
Control System Only

~~SECRET~~ D

BIF-008-[REDACTED]-68
(Control Number)

With this geometry, each point on the exit pupil will illuminate the image plane for an amount of time proportional to the slit width.

The shuttering function for the slit can be expressed in the following manner. The leading edge of the shutter passing across a given point on the exit pupil is given by:

$$\begin{aligned} r(x, t) &= 1, & \text{if } x - xt \leq 0, \text{ and} \\ r(x, t) &= 0, & \text{if } x - xt > 0, \end{aligned}$$

where $r(x, t) = 1.0$ has the meaning that the leading edge of the slit has passed a point with coordinates (x, y) on the exit pupil. The term x is the slit velocity and t is time.

The trailing edge of the slit can be similarly defined:

$$\begin{aligned} q(x, t) &= 1, & \text{if } x + W - xt \geq 0, \text{ and} \\ q(x, t) &= 0, & \text{if } x + W - xt < 0, \end{aligned}$$

where $q(x, t) = 0$ has the meaning that the trailing edge of the slit has passed the exit pupil point (x, y) .

The shutter function for the slit shutter is given by:

$$S(x, t) = r(x, t) q(x, t),$$

and has the desired property that the shutter be open, for each point on the exit pupil, a time proportional to the slit width; that is,

~~SECRET~~ D

BIF-008- [REDACTED] -68
(Control Number)

$$W = K \int_{-\infty}^{\infty} s(x, t) dt.$$

The optical transfer function of an optical system can be obtained by evaluating the autocorrelation integral over the exit pupil of the lens system. Since the pupil function is assumed to be time-dependent, the autocorrelation integral must be modified by the shutter function:

$$G(\nu, \eta) = \frac{\int_{-\infty}^{\infty} \int_{-\infty}^{\infty} \int_{-\infty}^{\infty} [S(x, t) \cdot F(x, y)] \cdot [S^*(x-\nu, t) \cdot F^*(x-\nu, y-\eta)] dx dy dt}{\int_{-\infty}^{\infty} \int_{-\infty}^{\infty} \int_{-\infty}^{\infty} [S(x, t) \cdot F(x, y)] \cdot [S^*(x, t) \cdot F^*(x, y)] dx dy dt}.$$

where $F(x, y)$ is the pupil function of the lens, $F^*(x, y)$ is the complex conjugate pupil function. The spatial frequencies, ν and η , are normalized to the diameter of the exit pupil. The complex conjugate of the shutter function $S^*(x, t)$ is given by:

$$S^*(s, t) = S(x, t),$$

since $S(x, t)$ is always real.

The time dependent autocorrelation integral given above can be reduced to a simple form by taking advantage of the properties of the shutter function. This function as set up is dependent only on the slit width, the slit velocity and time; that is, every point on the exit pupil is shuttered-on for the same amount of time. Because the shuttering function is independent of the exit pupil coordinate system, the autocorrelation integral can be rewritten:

$$G(\nu, \eta) = \frac{[\int_{-\infty}^{\infty} S(x, t) \cdot S(x-\nu, t) dt] \cdot [\int_{-\infty}^{\infty} \int_{-\infty}^{\infty} F(x, y) \cdot F^*(x-\nu, y-\eta) dx dy]}{[\int_{-\infty}^{\infty} S(x, t) \cdot S(x, t) dt] \cdot [\int_{-\infty}^{\infty} \int_{-\infty}^{\infty} F(x, y) \cdot F^*(x, y) dx dy]}$$

B-11

~~SECRET~~ D

Handle via BYEMAN
Control System Only

~~SECRET~~ D

BIF-008- [REDACTED] -68
(Control Number)

which reduces to:

$$G(v, \eta) = \frac{\int_{-\infty}^{\infty} S(x, t) \cdot S(x-v, t) dt}{\int_{-\infty}^{\infty} [S(x, t)]^2 dt} (G_L)(v, \eta),$$

where:

$G_L(v, \eta)$ is the transfer function of the unshuttered optical system.

The above result leads immediately to the transfer function for the slit shutter namely:

$$G_s(v, \eta) = \frac{\int_{-\infty}^{\infty} S(x, t) \cdot S(x-v, t) dt}{\int_{-\infty}^{\infty} [S(x, t)]^2 dt} .$$

The shutter function is binary in form; therefore, the normalizing integral in the denominator of the above expression can be reduced to:

$$\int_{-\infty}^{\infty} [S(x, t)]^2 dt = \int_{-\infty}^{\infty} S(x, t) dt = \frac{W}{K} .$$

The numerator of the shutter transfer-function integral can be evaluated by looking at the relationship between the shutter function at the point (x, y) and the point $(x-v, y-\eta)$ on the exit pupil. This relationship is shown by Figure B.3-2.

~~SECRET~~ D

~~SECRET~~ D

BIF-008- [REDACTED] -68
(Control Number)

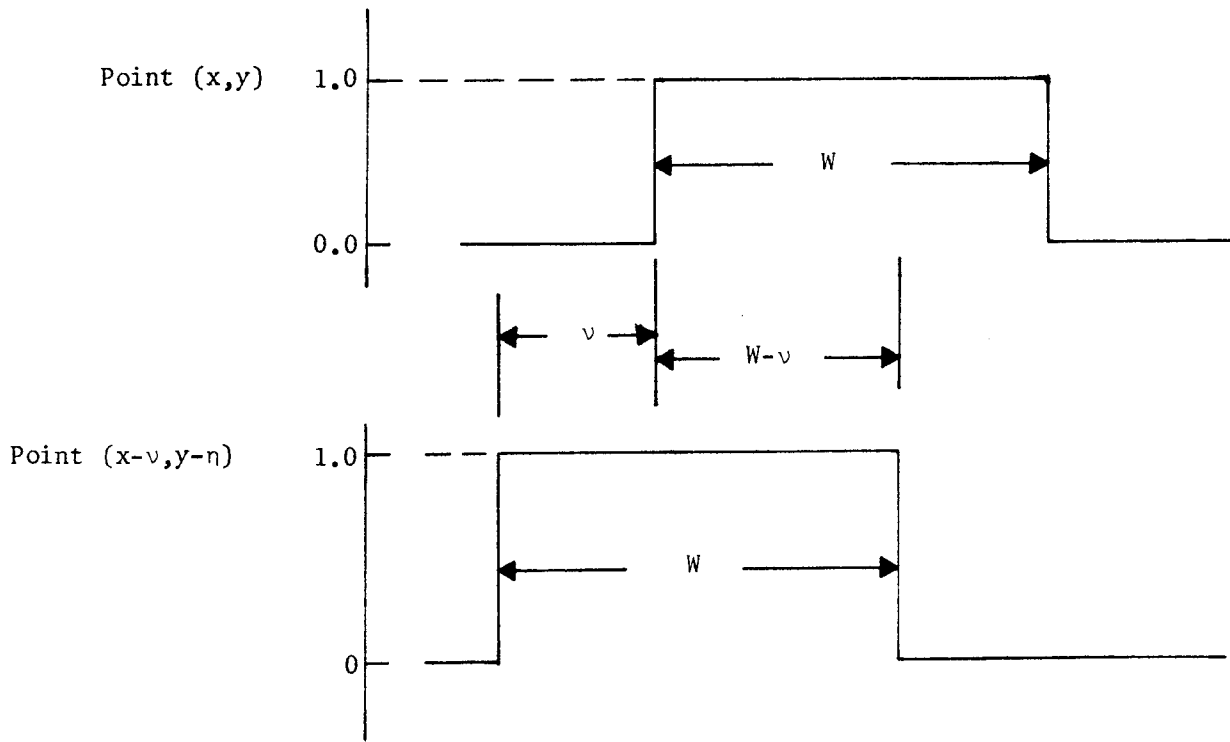


Figure B.3-2. Shutter Function Relationship

B-13

~~SECRET~~ D

Handle via BYEMAN
Control System Only

~~SECRET~~ D

BIF-008- [REDACTED] -68
(Control Number)

Figure B.3-2 shows that the shutter is at each point (x,y) for a time proportional to the slit width, W , but that the point $(x-v,y-\eta)$ starts exposing the image plane before the point (x,y) by an amount of time proportional to the separation between points, v . Therefore, the denominator of the transfer-function integral exists for a time proportional to $W-v$ and so:

$$W-v = K \int_{-\infty}^{\infty} S(x,t) \cdot S(x-v,t) dt, \text{ and}$$

the slit transfer function is

$$G_s(v,0) = \frac{W-v}{W} \text{ or } 1 - \frac{v}{W} = 0 \text{ if } v > W, \text{ and}$$

$$G_s(0,\eta) = 1 \text{ for all values of } \eta.$$

~~SECRET~~ D

~~SECRET~~ D

BIF-008- [REDACTED] -68
(Control Number)

References

1. R. V. Shack, "Characteristics of an Image-Forming System," J. Research National Bureau of Standards, 56: 245-260 (1956).
2. R. L. Lamberts, G. C. Higgins, and R. N. Wolfe, "Measurement and Analysis of the Distribution of Energy in Optical Images," J. Opt. Soc. Am., 48: 487-490 (1958).
3. R. L. Lamberts, "Relationship between the Sine-Wave Response and the Distribution of Energy in the Optical Image of a Line," J. Opt. Soc. Am., 48: 490-495 (1958).
4. O.H. Schade, "A New System of Measuring and Specifying Image Definition", in Optical Image Evaluation, National Bureau of Standards Circular 526, Government Printing Office, Washington, D.C. 1954, Chap. 17.
5. O. H. Schade, "A Method of Measuring the Optical Sine-Wave Spatial Spectrum of Television Image Display Devices", Jour. SMPTE, 67: 561-566 (1958).
6. G. C. Higgins and F. H. Perrin, "Evaluation of Optical Images", Photo. Sci. and Tech., 66-76 (1958).
7. E. Inglestam, E. Djurle, and B. Sjogren, "Contrast-Transmission Functions Determined Experimentally for Asymmetrical Images and for the Combination of Lens and Photographic Emulsion", J. Opt. Soc. Am. 46: 707-714 (1956).
8. P. Lindberg, "Measurement of Contrast Transmission Characteristics in Optical Image Formation", Optica Acta, 1: 80-89 (1954).
9. D. R. Herriott, "Recording Electronics Lens Bench", J. Opt. Soc. Am., 48: 968-971 (1958).
10. R. L. Lamberts, "Measurement of Sine-Wave Response of a Photographic Emulsion", J. Opt. Soc. Am., 49: 425-428 (1949).
11. J. A. Eyer, "Spatial Frequency Response of Certain Photographic Emulsions", J. Opt. Soc. Am., 938-944 (1958).
12. J. L. Bower and P. M. Schultheiss, "Introduction to the Design of Servomechanisms", John Wiley and Sons Inc., New York, Chapter 1 (1958).
13. R. V. Shack, "The Influence of Image Motion and Shutter Operation on the Photographic Transfer Function", Applied Optics, Vol 3, No. 10, Oct. 1964.

B-15

~~SECRET~~ D

Handle via **BYEMAN**
Control System Only

~~SECRET~~ D

BIF-008- [REDACTED] -68
(Control Number)

APPENDIX C
COMMAND AND INSTRUMENTATION LISTS

This appendix contains the commands and instrumentation points assigned to photographic payload (PP) equipment for the manned/automatic (M/A) mode of operation. These commands and instrumentation points were established according to the philosophy described in paragraphs 4.8.2 and 4.8.3. The commands and instrumentation reflect the requirements as of 1 September 1968 and can be expected to change somewhat as design progresses.

C.1 COMMANDS

Tables C.1-1, C.1-2, and C.1-3 list the command requirements for the PP set-up subphase, the photographic operations subphase, and power control respectively. The tables identify the commands and their associated information according to the following key:

MODULE	L - Laboratory Module
	M - Mission Module
SOURCE	U - Uplink (ground to satellite)
	A - Crewman
	C - Computer
REDUNDANCY CATEGORY	1 - Mission critical (functions which, if lost, would cause virtual elimination of primary photographic capability.)
	2 - Mission semi-critical (Functions which, if lost, would seriously degrade the performance of the primary photographic mission.)
	3 - Mission non-critical (Functions which, if lost, would cause little or no degradation of the primary photographic mission.)

C-1
~~SECRET~~ D

Handle via **BYEMAN**
Control System Only

~~SECRET~~ D

BIF-008- [REDACTED] -68
(Control Number)

TABLE C.1-1
PHOTOGRAPHIC PAYLOAD SET-UP SUBPHASE

<u>Command</u>	<u>States</u>	<u>Module</u>	<u>Source</u>	<u>Redundancy Category</u>	<u>Relay Configuration</u>
PRIMARY MIRROR (PM) LAUNCH LOCK SET A PRIME	UNLOCK	M	U	3	C
PM LAUNCH LOCK SET A BACKUP	UNLOCK	M	U	3	C
PM LAUNCH LOCK SET B PRIME	UNLOCK	M	U	3	C
PM LAUNCH LOCK SET B BACKUP	UNLOCK	M	U	3	C
TRACKING MIRROR (TM) LAUNCH LOCK SET A PRIME	UNLOCK	M	U	3	C
TM LAUNCH LOCK SET A BACKUP	UNLOCK	M	U	3	C
TM LAUNCH LOCK SET B PRIME	UNLOCK	M	U	3	C
TM LAUNCH LOCK SET B BACKUP	UNLOCK	M	U	3	C
REMOTE ALIGNMENT ON	ON	M	U	3	A
REMOTE ALIGNMENT OFF	OFF	M	U	3	A
AUTOMATIC ALIGNMENT ON	ON	M	U/A	3	A
AUTOMATIC ALIGNMENT OFF	OFF	M	U/A	3	A
MIRROR AND SERVO SELECT	16	M	U/A	2	A
MIRROR POSITION CHANGE	64	M	U/A	2	A
SUPPLY CONTROL ENABLE	ENABLE	L	U	3	A
SUPPLY CONTROL INHIBIT	INHIBIT	L	U	3	A

~~SECRET~~ D

~~SECRET~~ D

BIF-008- [REDACTED] -68
(Control Number)

TABLE C.1-1 (Continued)

<u>Command</u>	<u>States</u>	<u>Module</u>	<u>Source</u>	<u>Redundancy Category</u>	<u>Relay Configuration</u>
SUPPLY REEL BRAKE	BRAKE ENGAGED	L	U	3	A
SUPPLY REEL CLUTCH	BRAKE DISENGAGED	L	U	3	A
FILM HANDLING SYSTEM PROTECTION ENABLE	ENABLE	L	U	3	A
FILM HANDLING SYSTEM PROTECTION INHIBIT	INHIBIT	L	U	3	A
FILM HANDLING SYSTEM RESET No. 1	RESET No. 1	L	U	3	A
FILM HANDLING SYSTEM RESET No. 2	RESET No. 2	L	U	3	A
TAKE-UP CONTROL PRIMARY	PRIMARY IN	L	U	3	A
TAKE-UP CONTROL BACK-UP	BACK-UP IN	L	U	3	A
FOCUS DETECTOR PRIME IN	IN	L	U	2	E
FOCUS DETECTOR PRIME OUT	OUT	L	U	3	E
FOCUS DETECTOR BACK-UP OUT	OUT	L	U	3	A
FOCUS DETECTOR BACK-UP OUT REJECT	OUT- RESET	L	U	3	A

~~SECRET~~ D

~~SECRET~~ - D

BIF-008- [REDACTED] -68
(Control Number)

TABLE C.1-2
PHOTOGRAPHIC OPERATIONS SUBPHASE

<u>Command</u>	<u>States</u>	<u>Module</u>	<u>Source</u>	<u>Redundancy Category</u>	<u>Relay Configuration</u>
SLIT WIDTH (Part of 23v)*	8	L	U/A	2	E
INITIATE PHOTOGRAPHIC CYCLE SET	SET	L	C/A	1	D
INITIATE PHOTOGRAPHIC CYCLE RESET	RESET	L	C/A	1	D
INITIATE PHOTOGRAPHIC CYCLE REJECT OVERRIDE	ENABLE	L	U	3	A
INITIATE PHOTOGRAPHIC CYCLE REJECT OVERRIDE	INHIBIT	L	U	3	A
PLATEN (Part of 6v)*	PRIMARY SECONDARY	L L	U/A U/A	2 3	A A
PLATEN POSITION (Part of 23v)*	167	L	C/A	2	E
SLIT ANGLE (Part of 23v)*	75	L	C	3	A
INITIAL JOG VELOCITY (Part of 6v)*	31	L	C	3	A
JOG ANGLE (Part of 23v)*	31	L	C	3	A
FILM RUNOUT ONE FRAME EXECUTE	EXECUTE	L	U/A	3	A
FILM RUNOUT ONE FRAME RESET	RESET	L	U/A	3	A
PRIMARY FILM RUNOUT ENABLE	ENABLE	L	U/A	3	A
PRIMARY FILM RUNOUT INHIBIT	INHIBIT	L	U/A	3	A

* 6v and 23v are command word designations.

C-4

~~SECRET~~ - D

Handle via BYEMAN
Control System Only

~~SECRET~~ D

BIF-008- [REDACTED] -68
(Control Number)

TABLE C.1-2 (Continued)

<u>Command</u>	<u>States</u>	<u>Module</u>	<u>Source</u>	<u>Redundancy Category</u>	<u>Relay Configuration</u>
SECONDARY FILM RUNOUT ENABLE	ENABLE	L	U/A	3	A
SECONDARY FILM RUNOUT INHIBIT	INHIBIT	L	U/A	3	A
VISUAL OPTICS (VO) MAGNIFICATION (Part of 6v)*	4	L	U/A	3	A
IMAGE DEROTATION	16	L	C	3	A
VO SLANT RANGE COMPENSATION (SRC) (Derived from Bits 9-12 of PLATEN POSITION COMMAND)	12	L	C	3	A
VO EYEPIECE BAY 8	BAY 8 IN	L	C/A	3	A
VO EYEPIECE BAY 2	BAY 2 IN	L	C/A	3	A
VO SRC ENABLE	ENABLE	L	C/A	3	A
VO SRC INHIBIT	INHIBIT	L	C/A	3	A

* 6v and 23v are command word designations.

C-5
~~SECRET~~ D

Handle via BYEMAN
Control System Only

~~SECRET~~ D

BIF-008- [REDACTED] -68
(Control Number)

TABLE C.1-3
POWER CONTROL

<u>Command</u>	<u>States</u>	<u>Module</u>	<u>Source</u>	<u>Redundancy Category</u>	<u>Relay Configuration</u>
ALIGNMENT POWER PRIME ON	ON	M	U/A	3	A
ALIGNMENT POWER PRIME OFF	OFF	M	U/A	3	A
ALIGNMENT POWER BACKUP ON	ON	M	U	3	A
ALIGNMENT POWER BACKUP OFF	OFF	M	U	3	A
LAUNCH LOCK UNLOCK POWER PRIME ON	ON	M	U	3	A
LAUNCH LOCK UNLOCK POWER PRIME OFF	OFF	M	U	3	A
LAUNCH LOCK UNLOCK POWER BACKUP ON	ON	M	U	3	A
LAUNCH LOCK UNLOCK POWER BACKUP OFF	OFF	M	U	3	A
CAMERA POWER PRIME ON	ON	L	U/A	3	A
CAMERA POWER PRIME OFF	OFF	L	U/A	3	A
CAMERA POWER BACKUP ON	ON	L	U	3	A
CAMERA POWER BACKUP OFF	OFF	L	U	3	A
FILM HANDLING POWER PRIME ON	ON	L	U/A	3	A
FILM HANDLING POWER PRIME OFF	OFF	L	U/A	3	A
FILM HANDLING POWER BACKUP ON	ON	L	U	3	A
FILM HANDLING POWER BACKUP OFF	OFF	L	U	3	A
X-IMC POWER ON	ON	L	U/A	3	A
X-IMC POWER OFF	OFF	L	U/A	3	A

C-6
~~SECRET~~ D

Handle via BYEMAN
Control System Only

~~SECRET~~ D

BIF-008- [REDACTED] -68
(Control Number)

TABLE C.1-3 (Continued)

<u>Command</u>	<u>States</u>	<u>Module</u>	<u>Source</u>	<u>Redundancy Category</u>	<u>Relay Configuration</u>
FOCUS POWER PRIME ON	ON	L	U	3	A
FOCUS POWER PRIME OFF	OFF	L	U	3	A
FOCUS POWER BACKUP ON	ON	L	U	3	A
FOCUS POWER BACKUP OFF	OFF	L	U	3	A
LABORATORY MODULE (LM) ASCENT POWER ON	VIB. AMPS. ON	L	U	3	A
LM ASCENT POWER OFF	VIB. AMPS. OFF	L	U	3	A
MISSION MODULE (MM) ASCENT POWER ON	VIB. AMPS. ON	M	U	3	A
MM ASCENT POWER OFF	VIB. AMPS. OFF	M	U	3	A
ENVIRONMENTAL POWER ON	ALL EKC HEATERS ON	M	U	1	D
ENVIRONMENTAL POWER OFF	ALL EKC HEATERS OFF	M	U	1	D

C-7

~~SECRET~~ D

Handle via BYEMAN
Control System Only

~~SECRET~~ D

BIF-008- [REDACTED] -68
(Control Number)

COMMAND	A	
RELAY		
CONFIGURATION	C	(as shown in Figure 4.8-2)
	D	
	E	

C.2 INSTRUMENTATION

The current PP instrumentation points for the M/A mode are listed in Tables C.2-1 through C.2-8. These tables give the instrumentation points in accordance with their criticalness to the mission. The definitions of these eight categories are as follows:

Table C.2-1 - Category 1 - Mission Critical Points. Those points which monitor functions in which a failure is catastrophic to the continuation of the photographic mission or to completion of the mission. All category 1 points will have completely redundant instrumentation to provide confirmation that a malfunction in a critical area has occurred.

Table C.2-2 - Category 2 - Mission Semi-Critical Points. Those points which either monitor events which indicate degree of mission completion or detect any malfunction which will significantly degrade the quality of the photography, but will not by themselves completely prevent additional photography. Category 2 points will have sufficient redundant instrumentation to provide capability to diagnose the malfunction.

~~SECRET~~ D

Handle via BYEMAN
Control System Only

~~SECRET~~ D

BIF-008- [REDACTED] -68
(Control Number)

Table C.2-3 - Category 3 - Optimization Points. Those points which monitor the operation of equipment used to optimize performance, but of which failure to perform will not by itself jeopardize the mission or greatly degrade photographic quality.

Table C.2-4 - Category 4 - Launch and Ascent Points. Those points which monitor such factors as shock, vibration, and pressure during launch and ascent phases.

Table C.2-5 - Category 5 - Post-Flight and Engineering Data Points. Those points which are not essential to commanding of the mission, but which provide data for examination during test or post-flight diagnosis.

Table C.2-6 - Category 6 - Flight-Crew Safety Points. Those points which monitor functions or events affecting flight-crew safety. Points in category 6 are mutually exclusive with points in categories 1 through 5, except absolute temperature points.

Table C.2-7 - Category 7 - Prelaunch and Test Points. Those points which monitor such factors as ground conditioning during prelaunch phase, and those test points used for acceptance or prelaunch checkout, but which are not required for orbital or post-flight data. Redundancy is not required.

Table C.2-8 - Category 8 - Launch-Abort Points. Those test points which are brought out through umbilical lines at the launch pad and which are monitored pre-launch to establish whether or not the countdown should proceed.

C-9

~~SECRET~~ D

Handle via **BYEMAN**
Control System Only

~~SECRET~~ D

BIF-008- [REDACTED] -68
(Control Number)

The lists identify the type of sensor, mode of operation, sampling rates, redundancy requirements, and monitor and alarm subsystem assignments according to the following key:

Symbols

Sensor Type A - Analog
D - Digital
L - Level
H - Hybrid (combination analog and level)

Sample Rate C - Continuous channel
N/A - Not applicable

Mode (This table is concerned with the manned/automatic mode)
M/A - Manned/Automatic
A - Automatic
M/A
ξ - Both Modes
A

Monitor and Alarm (MAS)
W - Warning
C - Caution

Sample Rate
C - Continuous channel

C-10

~~SECRET~~ D

Handle via **BYEMAN**
Control System Only

~~SECRET~~ D

BIF-008- [REDACTED] -68
(Control Number)

Symbols

Unit for Mission Module (MM)

- Unit 1 Mission Module Control Unit (MMCU)
- Unit 2 Instrumentation Processor (IP)
- Unit 3 Alignment Sensor Electronics
- Unit 4 Signal Indicator
- Unit 5 Primary Mirror and Alignment Servos
- Unit 6 Diagonal Mirror and Alignment Servos
- Unit 7 Flight Heater System
- Unit 8 Ground Heater System
- Unit 9 Alignment Sensor
- Unit 10 Primary Mirror and Lock Set
- Unit 11 Tracking Mirror Lock Set
- Unit 12 Vibration Amplifiers
- Unit 13 Vibration Sensors
- Unit 14 Temperature Sensor Set
- Unit 15 Mission Module Power Unit (MMPU)
- Unit 17 MM Temporarily Unassigned

Unit for Laboratory Module (LM)

- Unit 19 LM Temporarily Unassigned
- Unit 21 LM Control Unit (LMCU)
- Unit 22 Camera
- Unit 23 Camera Auxiliary Electronics
- Unit 24 Focus Control Electronics
- Unit 25 Data Conversion Unit (DCU)
- Unit 26 Controls and Displays

C-11
~~SECRET~~ D

Handle via BYEMAN
Control System Only

~~SECRET~~ D

BIF-008- [REDACTED] -68
(Control Number)

Unit for Laboratory Module (LM) (Continued)

- Unit 27 Processor Control Electronics
- Unit 28 Take-Up Sequence Electronics
- Unit 29 RV Automatic Film Handling
- Unit 31 Film Handling Electronics
- Unit 32 LM Power Unit (LMPU)
- Unit 33 Vibration Amplifiers
- Unit 34 Vibration Sensors
- Unit 35 Visual Optics (VO)
- Unit 36 Film Holder
- Unit 37 Film Chute

C-12
~~SECRET~~ D

Handle via BYEMAN
Control System Only

TABLE C.2-1
MISSION CRITICAL POINTS

FUNCTION DESCRIPTOR	MODE	PANEL IC	MAS	SENSOR SAMPLES /SEC.	RANGE	ACCURACY	UNIT	POWER BUS	IMP
CAMERA									
SHUTTER SLIT POSITION	M/A			64		0.2 INCHES	23		1145
SHUTTER SLIT PULSES	M/A			64		N/A	25		993 B
LEAST SIGNIFICANT BIT	M/A			64			25		994 B
PLATEN BACK POSITION PC	M/A			2		N/A	23		1100
LEAST SIGNIFICANT BIT	M/A			2			23		1099
PLATEN BACK POSITION PC COARSE	M/A			8		4.5 DEG	23		1096
PLATEN BACK POSITION PC FINE	M/A			16		0.25 DEG	23		1097
PLATEN BACK POSITION SC	M/A			8		0.10 INCHES	23		1138
VACUUM PULLDOWN PC	M/A			8		N/A	23		876
VACUUM PULLDOWN PC REDT	M/A			8		N/A	23		889
PLATEN FILM PINCH-SUPPLY	M/A			8		N/A	23		890
PLATEN FILM PINCH-TAKEUP	M/A			8		N/A	23		795
PLATEN FILM PINCH-SUPPLY/TAKEUP	M/A			8		N/A	23		894
LEAST SIGNIFICANT BIT	M/A			8			23		895
LOOPER POSITION PC	M/A			2		N/A	23		1148
LEAST SIGNIFICANT BIT	M/A			2			23		1143
LOOPER POSITION PC REDT	M/A			8		0.5 INCHES	23		1190
METERING DRIVE PC (FRAME COUNT)	M/A			1	10.64 INCHES	N/A	23		1149
2ND MOST SIGNIFICANT BIT	M/A			1			23		1150
3RD MOST SIGNIFICANT BIT	M/A			1			23		1151
4TH MOST SIGNIFICANT BIT	M/A			1			23		1152
5TH MOST SIGNIFICANT BIT	M/A			1			23		1153
6TH MOST SIGNIFICANT BIT	M/A			1			23		1154
7TH MOST SIGNIFICANT BIT	M/A			1			23		1155
8TH MOST SIGNIFICANT BIT	M/A			2			23		1156
LEAST SIGNIFICANT BIT	M/A			2			23		1157
METERING DRIVE PC REDT	M/A			2		N/A	23		1187
IPC REJECT	M/A			64		N/A	23		821 A
IPC REJECT REDT	M/A			64		N/A	23		820 A

* - TO BE SUPPLIED BY A LATER REVISION

Handle via BYEMAN
Control System Only

~~SECRET~~ D

BIF-008-

(Control Number)

-68

TABLE C.2-1 (Continued)

FUNCTION DESCRIPTOR	MODE	PANEL IC	SENSOR MAS TYPE	SAMPLES /SEC.	RANGE	ACCURACY	UNIT	POWER BUS	IMP
FILM HANDLING									
SUPPLY REEL BRAKE	M/A		DISCRETE	1	2 LEVEL	N/A	19	5	950 A
SUPPLY REEL BRAKE REDT	M/A		ANALOG	1		N/A	19	12,-6	952 A
SUPPLY REEL CLUTCH	M/A		DISCRETE	1	2 LEVEL	N/A	19	5	957 A
SUPPLY REEL CLUTCH REDT	M/A		ANALOG	1		N/A	19	12,-6	959 A
FILM TENSION									
(ACCURACY FROM 2 TO 4 POUNDS)	M/A		ANALOG	1	0-6 POUNDS	0.2 POUNDS	37	5	962 B
FILM TENSION REDT									
(ACCURACY FROM 2 TO 4 POUNDS)	M/A		ANALOG	1	0-6 POUNDS	0.2 POUNDS	37	12,-6	963 B
OPERATIONAL POWER									
CAMERA BUS VOLTAGE	M/A		ANALOG	1	19.5-33.5 VOLT		1 VOLT	32	975
CAMERA BUS CURRENT	M/A		ANALOG	32	0-25 AMPERE	0.75 AMPERE	1 VOLT	32	976
FILM HANDLING BUS VOLTAGE	M/A		ANALOG	1	19.5-33.5 VOLT		1 VOLT	32	12,-6 989 B
FILM HANDLING BUS CURRENT	M/A		ANALOG	1	0-15 AMPERE	0.45 AMPERE	32	12,-6	990 B
FILM HANDLING BACKUP VOLTAGE	M/A		ANALOG	1	19.5-33.5 VOLT		1 VOLT	32	12,-6 991 B
CAMERA BACKUP BUS VOLTAGE	M/A		ANALOG	1	19.5-33.5 VOLT		1 VOLT	32	12,-6 974 B
CAMERA BACKUP BUS CURRENT	M/A		ANALOG	1	19.5-33.5 VOLT		1 VOLT	15	12,-6 51 B
ALIGNMENT BACKUP VOLTAGE	M/A		ANALOG	1	19.5-33.5 VOLT		1 VOLT	15	12,-6 986 B
DCU BUS VOLTAGE	M/A		ANALOG	1	19.5-33.5 VOLT		1 VOLT	15	12,-6 89 B
LL BACKUP BUS VOLTAGE	M/A		ANALOG	1	19.5-33.5 VOLT		1 VOLT	1	80
MM LAUNCH LOCK BUS VOLTAGE	M/A		ANALOG	1	0-4 AMPERE	0.12 AMPERE	1	1	81
MM LAUNCH LOCK BUS CURRENT	M/A		ANALOG	32					800
VISUAL OPTICS BUS VOLTAGE	M/A		ANALOG	1	19.5-33.5 VOLT		1 VOLT	32	801
VISUAL OPTICS BUS CURRENT	M/A		ANALOG	32	0-20 AMPERE	0.6 AMPERE	32		802
FOCUS BUS VOLTAGE	M/A		ANALOG	1	19.5-33.5 VOLT		1 VOLT	32	980
FOCUS BUS CURRENT	M/A		ANALOG	16	0-5 AMPERE	0.15 AMPERE	32		981
ALIGNMENT BUS VOLTAGE	M/A		ANALOG	1	19.5-33.5 VOLT		1 VOLT	15	82
ALIGNMENT BUS CURRENT	M/A		ANALOG	32	0-33 AMPERE	1.0 AMPERE	15		83
LH LAUNCH & BOOST BUS VOLTAGE	M/A		ANALOG	1	19.5-33.5 VOLT		1 VOLT	15	982
LH LAUNCH & BOOST BUS CURRENT	M/A		ANALOG	1	19.5-33.5 VOLT		1 VOLT	15	984

* - TO BE SUPPLIED BY A LATER REVISION

Handle via BYEMAN
Control System Only

~~SECRET~~ D

TABLE C.2-1 (Continued)

FUNCTION DESCRIPTOR	MODE	PANEL IC	SENSOR TYPE	SAMPLES /SEC.	RANGE	ACCURACY	UNIT	POWER BUS	IMP
LAUNCH LOCKS									
PM LOCK STATUS	M/A		DIGITAL	1/4	2 BITS	N/A	1		43 B
LEAST SIGNIFICANT BIT	M/A		1/4				1		48 B
PM LAUNCH LOCK 1	M/A		HYBRID	2	-5/105 PCT TV	5 PCT TV	1		52
PM LAUNCH LOCK 2	M/A		HYBRID	2	-5/105 PCT TV	5 PCT TV	1		53
PM LAUNCH LOCK 3	M/A		HYBRID	2	-5/105 PCT TV	5 PCT TV	1		54
PM LAUNCH LOCK 4	M/A		HYBRID	2	-5/105 PCT TV	5 PCT TV	1		55
PM LAUNCH LOCK 5	M/A		HYBRID	2	-5/105 PCT TV	5 PCT TV	1		56
PM LAUNCH LOCK 6	M/A		HYBRID	2	-5/105 PCT TV	5 PCT TV	1		57
TM LOCK STATUS	M/A		DIGITAL	1/4	2 BITS	N/A	1		65
LEAST SIGNIFICANT BIT	M/A		1/4				1		64 B
TM LAUNCH LOCK 1	M/A		HYBRID	2	-5/105 PCT TV	5 PCT TV	1		67
TM LAUNCH LOCK 2	M/A		HYBRID	2	-5/105 PCT TV	5 PCT TV	1		68
TM LAUNCH LOCK 3	M/A		HYBRID	2	-5/105 PCT TV	5 PCT TV	1		69
TM LAUNCH LOCK 4	M/A		HYBRID	2	-5/105 PCT TV	5 PCT TV	1		70
TM LAUNCH LOCK 5	M/A		HYBRID	2	-5/105 PCT TV	5 PCT TV	1		71
TM LAUNCH LOCK 6	M/A		HYBRID	2	-5/105 PCT TV	5 PCT TV	1		72

* - TO BE SUPPLIED BY A LATER REVISION

Handle via BYEMAN
Control System Only

~~SECRET~~ D

BIF-008- [REDACTED] -68
(Control Number)

TABLE C.2-2
MISSION SEMI-CRITICAL POINTS

FUNCTION DESCRIPTOR	MODE	PANEL IC	SENSOR TYPE	SAMPLES /SEC.	RANGE	ACCURACY	UNIT	POMER BUS	IMP
CAMERA									
FOCUS MIRROR UNIT POSITION	M/A		HYBRID	8	* 2 BITS	0.10 INCHES	23		1161
FOCUS MIRROR UNIT POSITION REDY	M/A		DIGITAL	1		N/A	23		1180 B
LEAST SIGNIFICANT BIT	M/A			1			23		1191 B
EXPOSURE SLIT WIDTH	M/A		ANALOG	8	0-5 INCHES	*	23		1162
EXPOSURE SLIT WIDTH REDY	M/A		DIGITAL	8	8 BITS	*	23		1058
2ND MOST SIGNIFICANT BIT	M/A			8			23		1059
3RD MOST SIGNIFICANT BIT	M/A			8			23		1060
4TH MOST SIGNIFICANT BIT	M/A			8			23		1061
5TH MOST SIGNIFICANT BIT	M/A			8			23		1062
6TH MOST SIGNIFICANT BIT	M/A			8			23		1063
7TH MOST SIGNIFICANT BIT	M/A			8			23		1064
LEAST SIGNIFICANT BIT	M/A			8			23		1065
PLATEN POSITION COARSE	M/A		ANALOG	2	0.1 INCHES	0.005 INCHES	23		1163
PLATEN POSITION FINE	M/A		ANALOG	16	0.008 INCHES	0.0002 INCHES	23		1165 A
PLATEN POSITION	M/A		DIGITAL	1	10 BITS		23		1206 B
2ND MOST SIGNIFICANT BIT	M/A			1			23		1205
3RD MOST SIGNIFICANT BIT	M/A			1			23		1204
4TH MOST SIGNIFICANT BIT	M/A			1			23		1203
5TH MOST SIGNIFICANT BIT	M/A			1			23		1202
6TH MOST SIGNIFICANT BIT	M/A			1			23		1201
7TH MOST SIGNIFICANT BIT	M/A			1			23		1200
8TH MOST SIGNIFICANT BIT	M/A			8			23		1199
9TH MOST SIGNIFICANT BIT	M/A		DIGITAL	8			23		1198 B
LEAST SIGNIFICANT BIT	M/A		DIGITAL	32			23		1197 B
FRAME COUNT (SHUTTER ACTUATIONS)									
PC EXPOSURES ONLY	M/A		DIGITAL	1/4	9 BITS	N/A	23		1169
2ND MOST SIGNIFICANT BIT	M/A			1/4			23		1170
3RD MOST SIGNIFICANT BIT	M/A			1/4			23		1171
4TH MOST SIGNIFICANT BIT	M/A			1/4			23		1172
5TH MOST SIGNIFICANT BIT	M/A			1/4			23		1173
6TH MOST SIGNIFICANT BIT	M/A			1			23		1174
7TH MOST SIGNIFICANT BIT	M/A			1			23		1175
8TH MOST SIGNIFICANT BIT	M/A			2			23		1176
LEAST SIGNIFICANT BIT	M/A			2			23		1177
FRAME COUNT (SHUTTER ACTUATIONS)									
SC EXPOSURES ONLY	M/A		DIGITAL	1/4	7 BITS	N/A	23		1102
2ND MOST SIGNIFICANT BIT	M/A			1/4			23		1103

* - TO BE SUPPLIED BY A LATER REVISION

Handle via BYEMAN
Control System Only

~~SECRET~~ D

TABLE C.2-2 (Continued)

FUNCTION DESCRIPTOR	MODE	PANEL IC	MAS	SENSOR TYPE	SAMPLES /SEC.	RANGE	ACCURACY	UNIT	POWER BUS	IMP
3RD MOST SIGNIFICANT BIT	M/A				1/4			23		1104
4TH MOST SIGNIFICANT BIT	M/A				1/4			23		1105
5TH MOST SIGNIFICANT BIT	M/A				1			23		1106
6TH MOST SIGNIFICANT BIT	M/A				2			23		1107
LEAST SIGNIFICANT BIT	M/A				2			23		1108
SECONDARY CASSETTE IDENT.	M/A			DIGITAL	1	3. BITS	N/A	23		1140
2ND MOST SIGNIFICANT BIT	M/A				1			23		1141
LEAST SIGNIFICANT BIT	M/A				1			23		1142
PRIMARY FILM QUANTITY										
FILM SUPPLY										
2ND MOST SIGNIFICANT BIT	M/A			DIGITAL	1/4	15 BITS	*	19		1257
3RD MOST SIGNIFICANT BIT	M/A				1/4			19		1258
4TH MOST SIGNIFICANT BIT	M/A				1/4			19		1259
5TH MOST SIGNIFICANT BIT	M/A				1/4			19		1260
6TH MOST SIGNIFICANT BIT	M/A				1/4			19		1261
7TH MOST SIGNIFICANT BIT	M/A				1/4			19		1262
8TH MOST SIGNIFICANT BIT	M/A				1/4			19		1263
9TH MOST SIGNIFICANT BIT	M/A				1/4			19		1264
10TH MOST SIGNIFICANT BIT	M/A				1/4			19		1265
11TH MOST SIGNIFICANT BIT	M/A				1/4			19		1266
12TH MOST SIGNIFICANT BIT	M/A				1			19		1267
13TH MOST SIGNIFICANT BIT	M/A				1			19		1268
14TH MOST SIGNIFICANT BIT	M/A				2			19		1269
LEAST SIGNIFICANT BIT	M/A				2			19		1270
FILM TAKEUP										
2ND MOST SIGNIFICANT BIT	M/A			DIGITAL	1/4	15 BITS	*	19		1287
3RD MOST SIGNIFICANT BIT	M/A				1/4			19		1288
4TH MOST SIGNIFICANT BIT	M/A				1/4			19		1289
5TH MOST SIGNIFICANT BIT	M/A				1/4			19		1290
6TH MOST SIGNIFICANT BIT	M/A				1/4			19		1291
7TH MOST SIGNIFICANT BIT	M/A				1/4			19		1292
8TH MOST SIGNIFICANT BIT	M/A				1/4			19		1293
9TH MOST SIGNIFICANT BIT	M/A				1/4			19		1294
10TH MOST SIGNIFICANT BIT	M/A				1/4			19		1295
11TH MOST SIGNIFICANT BIT	M/A				1/4			19		1296
12TH MOST SIGNIFICANT BIT	M/A				1/4			19		1297
13TH MOST SIGNIFICANT BIT	M/A				1			19		1298
14TH MOST SIGNIFICANT BIT	M/A				1			19		1299
LEAST SIGNIFICANT BIT	M/A				2			19		1300

* - TO BE SUPPLIED BY A LATER REVISION

Handle via BYEMAN
Control System Only

~~SECRET~~ D

BIF-008-

-68

(Control Number)

TABLE C.2-2 (Continued)

FUNCTION DESCRIPTOR	MODE	PANEL IC	MAS	SENSOR TYPE	SAMPLES /SEC.	RANGE	ACCURACY	UNIT	POWER BUS	IMP
LEAST SIGNIFICANT BIT	M/A				2			19		1301
FILM TAKEUP REDT	M/A			DIGITAL	1/4	15 BITS		37	12-6	1317 B
2ND MOST SIGNIFICANT BIT	M/A			DIGITAL	1/4			37	12-6	1329 B
3RD MOST SIGNIFICANT BIT	M/A			DIGITAL	1/4			37	12-6	1328 B
4TH MOST SIGNIFICANT BIT	M/A			DIGITAL	1/4			37	12-6	1327 B
5TH MOST SIGNIFICANT BIT	M/A			DIGITAL	1/4			37	12-6	1326 B
6TH MOST SIGNIFICANT BIT	M/A			DIGITAL	1/4			37	12-6	1325 B
7TH MOST SIGNIFICANT BIT	M/A			DIGITAL	1/4			37	12-6	1324 B
8TH MOST SIGNIFICANT BIT	M/A			DIGITAL	1/4			37	12-6	1323 B
9TH MOST SIGNIFICANT BIT	M/A			DIGITAL	1/4			37	12-6	1322 B
10TH MOST SIGNIFICANT BIT	M/A			DIGITAL	1/4			37	12-6	1321 B
11TH MOST SIGNIFICANT BIT	M/A			DIGITAL	1/4			37	12-6	1320 B
12TH MOST SIGNIFICANT BIT	M/A			DIGITAL	1			37	12-6	1319 B
13TH MOST SIGNIFICANT BIT	M/A			DIGITAL	1			37	12-6	1318 B
14TH MOST SIGNIFICANT BIT	M/A			DIGITAL	2			37	12-6	1330 B
LEAST SIGNIFICANT BIT	M/A			DIGITAL	2			37	12-6	1331 B
SECONDARY FILM QUANTITY										
FILM SUPPLY QUANTITY SC	M/A			ANALOG	1/4	575 FEET		50 FEET	23	12-6 1110 B
FILM TAKEUP QUANTITY SC	M/A			ANALOG	1/4	575 FEET		50 FEET	23	12-6 1118 B
OPERATIONAL POWER										
ECS BUS A VOLTAGE	M/A			ANALOG	1	19.5-33.5 VOLT		1 VOLT	15	12-6 91 B
ECS BUS B VOLTAGE	M/A			ANALOG	1	19.5-33.5 VOLT		1 VOLT	15	12-6 92 B
ECS BUS C VOLTAGE	M/A			ANALOG	1	19.5-33.5 VOLT		1 VOLT	15	12-6 88 B
ECS BUS A CURRENT	M/A			ANALOG	1	0-12 AMPERE		0.36 AMPERE	15	12-6 85 B
ECS BUS B CURRENT	M/A			ANALOG	1	0-12 AMPERE		0.36 AMPERE	15	12-6 86 B
ECS BUS C CURRENT	M/A			ANALOG	1	0-12 AMPERE		0.36 AMPERE	15	12-6 87 B

* - TO BE SUPPLIED BY A LATER REVISION

Handle via BYEMAN
Control System Only

~~SECRET~~ D

TABLE C.2-2 (Continued)

FUNCTION DESCRIPTOR	MODE	PANEL IC	SENSOR TYPE	SAMPLES /SEC.	RANGE	ACCURACY	UNIT	POWER RUS	IMP
FOCUS SENSOR									
ERROR SIGNAL COARSE	M/A		ANALOG	1	+/- 0.02 INCHES	30 PCT	24		910
ERROR SIGNAL FINE	M/A		ANALOG	8	+/- 0.005 INCHES	0.001 INCHES	24		911
ERROR SIGNAL FINE REDT	M/A		ANALOG	2	+/- 0.005 INCHES	0.001 INCHES	24		912
SIGNAL-TO-NOISE	M/A		ANALOG	8	0.5-25 INCHES	30 PCT	24		913
SAMPLING FREQUENCY	M/A		ANALOG	1	20-60 HERTZ	1-5 HERTZ	24		914
GAIN SIGNAL LEVEL	M/A		ANALOG	8	5-250 MVOLT	5 PCT	24		915
DC LEVEL	M/A		ANALOG	1	3-150 UVOLT	10 PCT	24		916
DIAGNOSTIC SIGNAL (ELECTRONICS)	M/A		ANALOG	1	*	*	24		917
DIAGNOSTIC SIGNAL (ELECTRONICS)	M/A		ANALOG	1	*	*	24		918
ALIGNMENT									
FUNCTIONING SIGNAL	M/A		DIGITAL	1	2 LEVEL	N/A	3		346 R
NO ALIGNMENT LIGHT SOURCE(TILT)	M/A		DISCRETE	1/4	2 LEVEL	N/A	3		445 R
NO ALIGNMENT LIGHT SOURCE(DEC)	M/A		DISCRETE	1/4	2 LEVEL	N/A	3		391 R
NO ALIGNMENT ERROR SIGNAL X	M/A		DIGITAL	1	10 BITS	*	3		311
2ND MOST SIGNIFICANT BIT	M/A			1			3		312
3RD MOST SIGNIFICANT BIT	M/A			1			3		313
4TH MOST SIGNIFICANT BIT	M/A			1			3		314
5TH MOST SIGNIFICANT BIT	M/A			1			3		315
6TH MOST SIGNIFICANT BIT	M/A			1			3		316
7TH MOST SIGNIFICANT BIT	M/A			1			3		317
8TH MOST SIGNIFICANT BIT	M/A			1			3		318
9TH MOST SIGNIFICANT BIT	M/A			1			3		319
LEAST SIGNIFICANT BIT	M/A			2			3		320
NO ALIGNMENT ERROR SIGNAL X-COARSE	M/A		ANALOG	1	+/-18 ARCMIN	+/-0.5 ARCMIN	3		337 R
NO ALIGNMENT ERROR SIGNAL Y-FINE	M/A		ANALOG	8	+/-120 ARCSEC	+/-5 ARCSEC	3		339 B
NO ALIGNMENT ERROR SIGNAL Y	M/A		DIGITAL	1	10 BITS	*	3		321
2ND MOST SIGNIFICANT BIT	M/A			1			3		322
3RD MOST SIGNIFICANT BIT	M/A			1			3		323
4TH MOST SIGNIFICANT BIT	M/A			1			3		324
5TH MOST SIGNIFICANT BIT	M/A			1			3		325
6TH MOST SIGNIFICANT BIT	M/A			1			3		326
7TH MOST SIGNIFICANT BIT	M/A			1			3		327
8TH MOST SIGNIFICANT BIT	M/A			1			3		328
9TH MOST SIGNIFICANT BIT	M/A			1			3		329
LEAST SIGNIFICANT BIT	M/A			2			3		330

* - TO BE SUPPLIED BY A LATER REVISION

Handle via BYEMAN
Control System Only

TABLE C.2-2 (Continued)

FUNCTION DESCRIPTOR	MODE	PANEL IC	SENSOR MAS TYPE	SAMPLES /SEC.	RANGE	ACCURACY	UNIT	PWR BUS	IMP
NO ERROR SIGNAL Y-COARSE	M/A		ANALOG	1	+/- 18 ARCMIN	+/- .51	3		343 B
COARSE	M/A		ANALOG	8	+/-120 ARCSEC	+/-5	3		345 B
NO ALIGNMENT ERROR SIGNAL Y-FINE	M/A		DIGITAL	1	10 BITS	*	3		355
PM POSITION A	M/A			1			3		356
2ND MOST SIGNIFICANT BIT	M/A			1			3		357
3RD MOST SIGNIFICANT BIT	M/A			1			3		358
4TH MOST SIGNIFICANT BIT	M/A			1			3		359
5TH MOST SIGNIFICANT BIT	M/A			1			3		360
6TH MOST SIGNIFICANT BIT	M/A			1			3		361
7TH MOST SIGNIFICANT BIT	M/A			1			3		362
8TH MOST SIGNIFICANT BIT	M/A			1			3		363
9TH MOST SIGNIFICANT BIT	M/A			2			3		364
LEAST SIGNIFICANT BIT	M/A			8			3		365
PM POSITION A COARSE	M/A		ANALOG	1	0.3 INCHES	*	3		365
PM POSITION A FINE	M/A		ANALOG	8	*	*	3		366
PM POSITION B	M/A		DIGITAL	1	10 BITS	*	3		367
2ND MOST SIGNIFICANT BIT	M/A			1			3		368
3RD MOST SIGNIFICANT BIT	M/A			1			3		369
4TH MOST SIGNIFICANT BIT	M/A			1			3		370
5TH MOST SIGNIFICANT BIT	M/A			1			3		371
6TH MOST SIGNIFICANT BIT	M/A			1			3		372
7TH MOST SIGNIFICANT BIT	M/A			1			3		373
8TH MOST SIGNIFICANT BIT	M/A			1			3		374
9TH MOST SIGNIFICANT BIT	M/A			2			3		375
LEAST SIGNIFICANT BIT	M/A			8			3		376
PM POSITION B COARSE	M/A		ANALOG	1	0.3 INCHES	*	3		377
PM POSITION B FINE	M/A		ANALOG	8	*	*	3		378
PM POSITION C	M/A		DIGITAL	1	10 BITS	*	3		379
2ND MOST SIGNIFICANT BIT	M/A			1			3		380
3RD MOST SIGNIFICANT BIT	M/A			1			3		381
4TH MOST SIGNIFICANT BIT	M/A			1			3		382
5TH MOST SIGNIFICANT BIT	M/A			1			3		383
6TH MOST SIGNIFICANT BIT	M/A			1			3		384
7TH MOST SIGNIFICANT BIT	M/A			1			3		385
8TH MOST SIGNIFICANT BIT	M/A			1			3		386
9TH MOST SIGNIFICANT BIT	M/A			2			3		387
LEAST SIGNIFICANT BIT	M/A			8			3		388
PM POSITION C COARSE	M/A		ANALOG	1	0.3 INCHES	*	3		388
PM POSITION C FINE	M/A		ANALOG	8	*	*	3		389
PM POSITION A	M/A		DIGITAL	1	10 BITS	*	3		390
2ND MOST SIGNIFICANT BIT	M/A			1			3		400
									401

* - TO BE SUPPLIED BY A LATER REVISION

Handle via BYEMAN
Control System Only

TABLE C.2-2 (Continued)

FUNCTION DESCRIPTOR	MODE	PANEL IC	MAS	SENSOR TYPE	SAMPLES /SEC.	RANGE	ACCURACY	UNIT	POWER BUS	IMP
3RD MOST SIGNIFICANT BIT	M/A				1			3		402
4TH MOST SIGNIFICANT BIT	M/A				1			3		403
5TH MOST SIGNIFICANT BIT	M/A				1			3		404
6TH MOST SIGNIFICANT BIT	M/A				1			3		405
7TH MOST SIGNIFICANT BIT	M/A				1			3		406
8TH MOST SIGNIFICANT BIT	M/A				1			3		407
9TH MOST SIGNIFICANT BIT	M/A				2			3		408
LEAST SIGNIFICANT BIT	M/A				8			3		409
RM POSITION A COARSE	M/A			ANALOG	1	0.1 INCHES	*	3		410
RM POSITION A FINE	M/A			ANALOG	8	*	*	3		411
RM POSITION B	M/A			DIGITAL	1	10 BITS	*	3		412
2ND MOST SIGNIFICANT BIT	M/A				1			3		413
3RD MOST SIGNIFICANT BIT	M/A				1			3		414
4TH MOST SIGNIFICANT BIT	M/A				1			3		415
5TH MOST SIGNIFICANT BIT	M/A				1			3		416
6TH MOST SIGNIFICANT BIT	M/A				1			3		417
7TH MOST SIGNIFICANT BIT	M/A				1			3		418
8TH MOST SIGNIFICANT BIT	M/A				1			3		419
9TH MOST SIGNIFICANT BIT	M/A				2			3		420
LEAST SIGNIFICANT BIT	M/A				8			3		421
RM POSITION B COARSE	M/A			ANALOG	1	0.1 INCHES	*	3		422
RM POSITION B FINE	M/A			ANALOG	8	*	*	3		423
RM POSITION C	M/A			DIGITAL	1	10 BITS	*	3		424
2ND MOST SIGNIFICANT BIT	M/A				1			3		425
3RD MOST SIGNIFICANT BIT	M/A				1			3		426
4TH MOST SIGNIFICANT BIT	M/A				1			3		427
5TH MOST SIGNIFICANT BIT	M/A				1			3		428
6TH MOST SIGNIFICANT BIT	M/A				1			3		429
7TH MOST SIGNIFICANT BIT	M/A				1			3		430
8TH MOST SIGNIFICANT BIT	M/A				1			3		431
9TH MOST SIGNIFICANT BIT	M/A				2			3		432
LEAST SIGNIFICANT BIT	M/A				8			3		433
RM POSITION C COARSE	M/A			ANALOG	1	0.1 INCHES	*	3		434
RM POSITION C FINE	M/A			ANALOG	8	*	*	3		435
PM SERVO A DRIVE SIGNAL	M/A			DISCRETE	2	2 LEVEL	N/A	3		331
PM SERVO B DRIVE SIGNAL	M/A			DISCRETE	2	2 LEVEL	N/A	3		332
PM SERVO C DRIVE SIGNAL	M/A			DISCRETE	2	2 LEVEL	N/A	3		333
RM SERVO A DRIVE SIGNAL	M/A			DISCRETE	2	2 LEVEL	N/A	3		334
RM SERVO B DRIVE SIGNAL	M/A			DISCRETE	2	2 LEVEL	N/A	3		335
RM SERVO C DRIVE SIGNAL	M/A			DISCRETE	2	2 LEVEL	N/A	3		336

* - TO BE SUPPLIED BY A LATER REVISION

~~SECRET~~ D

BIF-008-

-68

(Control Number)

TABLE C.2-2 (Continued)

FUNCTION DESCRIPTOR	MODE	PANEL IC	SENSOR SAMPLES /SEC.	RANGE	ACCURACY	UNIT	POWER BUS	IMP
VISUAL OPTICS								
VO RETICLE/FOCUS	M/A		2	0.1 INCHES	0.005 INCHES	35		781
VO RETICLE DRIVE SIGNAL	M/A		1	2 BITS	N/A	35		780
VO LEAST SIGNIFICANT BIT	M/A		8	*	*	35		782
VO FLIP MIRROR POSITION	M/A		1	2 BITS	N/A	35		779
VO FLIP MIRROR DRIVE SIGNAL	M/A		1	2 BITS	N/A	35		778
VO LEAST SIGNIFICANT BIT	M/A		1	2 BITS	N/A	35		783
VO MAGNIFICATION DRIVE SIG 1	M/A		1	2 BITS	N/A	35		772
VO LEAST SIGNIFICANT BIT	M/A		1	2 BITS	N/A	35		785
VO MAGNIFICATION DRIVE SIG 2	M/A		1	2 BITS	N/A	35		774
VO LEAST SIGNIFICANT BIT	M/A		1	2 BITS	N/A	35		784
VO MAG POSITION 2ND LENS	M/A		1	60 DEG	6 DEG	35		770
VO MAG POSITION 1ST LENS	M/A		8	60 DEG	6 DEG	35		769
VO DEROTATION-COARSE PRI STA	M/A		8	40 DEG	2.5 DEG	35		767
VO DEROTATION-FINE PRI STA	M/A		8	20 DEG	1 DEG	35		768
VO DEROTATION-COARSE SEC STA	M/A		8	40 DEG	2.5 DEG	35		765
VO DEROTATION-FINE SEC STA	M/A		8	20 DEG	1 DEG	35		766
DEROT PRI DRIVE SIGNAL	M/A		2	2 BITS	N/A	35		771
DEROT SEC DRIVE SIGNAL	M/A		2	2 BITS	N/A	35		786
DEROT LEAST SIGNIFICANT BIT	M/A		2	2 BITS	N/A	35		773
DEROT LEAST SIGNIFICANT BIT	M/A		2	2 BITS	N/A	35		787

PROCESSOR/DRYER

BIMAT SUPPLY QUANTITY (400-1500 FT ACCURACY 100 FT)	M/A		1/4	70-1500 FEET	20 FEET	27		1210 B
--	-----	--	-----	--------------	---------	----	--	--------

* - TO BE SUPPLIED BY A LATER REVISION

Handle via BYEMAN
Control System Only

~~SECRET~~ D

TABLE C.2-2 (Continued)

FUNCTION DESCRIPTOR	MODE	PANEL IC	SENSOR TYPE	SAMPLES /SEC.	RANGE	ACCURACY	UNIT	POWER BUS	IMP
ENVIRONMENTAL									
TEMP-TM REAR SURFACE	-S450/		ANALOG	1/4	60/80 DEG F	0.5 DEG F	2		295
TEMP-TM REAR SURFACE	-S450/		ANALOG	1/4	60/80 DEG F	0.5 DEG F	2		281
S TEMP-TM REAR SURFACE	-S450/		ANALOG	1/4	60/80 DEG F	0.5 DEG F	2		282
S TEMP-TM REAR SURFACE	-S450/		ANALOG	1/4	60/80 DEG F	0.5 DEG F	2		283
TM-DTEMP EFFECTIVE AVERAGE (FOCUS)			ANALOG	1/4	60/80 DEG F	0.5 DEG F	2		284
O TEMP-TM FRONT-TO-BACK	-S450/		ANALOG	1/4	-1/+3(70) DEG F	0.2 DEG F	2		90
O TEMP-TM FRONT-TO-BACK	-S450/		ANALOG	1/4	-1/+3(70) DEG F	0.2 DEG F	2		98
S OTEMP-TM FRONT-TO-BACK	-S450/		ANALOG	1/4	-1/+3(70) DEG F	0.2 DEG F	2		99
O TEMP-TM FRONT-TO-BACK	-S450/		ANALOG	1/4	-1/+3(70) DEG F	0.2 DEG F	2		100
O TEMP-TM FRONT-TO-BACK	-S450/		ANALOG	1/4	-1/+3(70) DEG F	0.2 DEG F	2		101
O TEMP-PRIMARY MIRROR-5090			ANALOG	1/4	-1/+3(70) DEG F	0.2 DEG F	2		102
O TEMP-PM FRONT-TO-BACK	-S090/		ANALOG	1/4	-1/3(70) DEG F	0.2 DEG F	2	12,-6	103 B
O TEMP-RF FRONT-TO-BACK	-S395/		ANALOG	1/4	-1/+3(70) DEG F	0.2 DEG F	2		104
O TEMP-NF FRONT-TO-BACK	-S398/		ANALOG	1/4	-1/+3(70) DEG F	0.2 DEG F	2		106
O TEMP-TM FRONT-TO-BACK	-S450/		ANALOG	1/4	-1/+3(70) DEG F	0.2 DEG F	2		107
O TEMP-TM FRONT-TO-BACK	-S450/		ANALOG	1/4	-1/+3(70) DEG F	0.2 DEG F	2		108
S OTEMP-TM FRONT-TO-BACK	-S450/		ANALOG	1/4	-1/+3(70) DEG F	0.2 DEG F	2		109
S OTEMP-TM FRONT-TO-BACK	-S450/		ANALOG	1/4	-1/+3(70) DEG F	0.2 DEG F	2		110
S OTEMP-TM FRONT-TO-BACK	-S450/		ANALOG	1/4	-1/+3(70) DEG F	0.2 DEG F	2		111
TEMP-PRI FILM SUPPLY-INSIDE HUB			ANALOG	1/4	-1/+3(70) DEG F	0.2 DEG F	2		112
TEMP-PRIMARY TAKE-UP			ANALOG	1/4	40/150 DEG F	2 DEG F	21		948
					40/150 DEG F	2 DEG F	21		1139 B
PP CREW CONTROLS									
VO RETICLE MODE (AUTO/MANUAL)	M/A		DIGITAL	1	1 BITS		26		1332 B
VO RETICLE CONTROL	M/A		DIGITAL	8	2 BITS		26		1333 B
LEAST SIGNIFICANT BIT	M/A		DIGITAL	1	1 BITS		26		1334 B
VO POWER CONTROL (ON/OFF)	M/A		DIGITAL	1	1 BITS		26	5	1335 B
VO OEROTATION CONTROL PRIMARY EYEPIECE (AUTO/INHIBIT)	M/A		DIGITAL	1	1 BITS		26	5	1336 B
VO OEROTATION CONTROL SECONDARY EYEPIECE (AUTO/INHIBIT)	M/A		DIGITAL	1	1 BITS		26	5	1337 B
ALIGNMENT POWER CONTROL (UN/OFF)	M/A		DIGITAL	1	1 BITS		26	5	1338 B
ALIGNMENT MODE CONTROL	M/A		DIGITAL	1	2 BITS		26	5	1339 B
LEAST SIGNIFICANT BIT	M/A		DIGITAL	1	2 BITS		26	5	1340 B
ALIGNMENT ERROR SELECT CONTROL	M/A		DIGITAL	1	2 BITS		26	5	1341 B

* - TO BE SUPPLIED BY A LATER REVISION

Handle via BYEMAN
Control System Only

TABLE C.2-2 (Continued)

FUNCTION DESCRIPTOR	MODE	PANEL IC	MAS	SENSOR TYPE	SAMPLES /SEC.	RANGE	ACCURACY	UNIT	POWER BUS	IMP
LEAST SIGNIFICANT BIT	M/A			DIGITAL	1	2 BITS		26	5	1342 B
ALIGNMENT ERROR CORRECT CONTROL	M/A			DIGITAL	8			26	5	1343 B
LEAST SIGNIFICANT BIT	M/A				8			26	5	1344 B
CAMERA AND FILM HANDLING POWER CONTROL (ON/OFF) AT F/T	M/A			DIGITAL	1	1 BITS		26	5	1346 B
PRIMARY FILM SELECT (ON/OFF) AT F/T	M/A			DIGITAL	1	2 BITS		26	5	1350 B
SECONDARY FILM SELECT (ON/OFF) AT 1-C	M/A			DIGITAL	1	2 BITS		26	5	1349 B
FRAME ADVANCE CONTROL AT IC	M/A			DIGITAL	8	1 BITS		26	5	1347 B
CAMERA POWER CONTROL (ON/OFF) AT IC	M/A			DIGITAL	1	1 BITS		26	5	1345 B
PROCESSOR STANDBY	M/A			DIGITAL	1	1 BITS	N/A	27		1208 B
PROCESSOR OPERATE	M/A			DIGITAL	1	1 BITS	N/A	27		1207 B
FRAME ADVANCE CONTROL AT F/T	M/A			DIGITAL	8	1 BITS		26	5	1348 B

* - TO BE SUPPLIED BY A LATER REVISION

Handle via BYEMAN
Control System Only

TABLE C.2-3
OPTIMIZATION POINTS

FUNCTION DESCRIPTOR	MODE	PANEL IC	MAS	SENSOR SAMPLES /SEC.	RANGE	ACCURACY	UNIT	POWER BUS	IMP
CAMERA									
PLATEN JOG VELOCITY	M/A			64	+/-0.25 IN/SEC	0.004	IN/SEC	23	1181
SHUTTER SLIT ORIENTATION COARSE	M/A			8	+/-111 DEG	8	DEG	23	1182
SHUTTER SLIT ORIENTATION FINE	M/A			8	24 DEG	1	DEG	23	1183
PLATEN JOG ORIENTATION COARSE	M/A			8	+/- 60 DEG	6	DEG	23	1184
PLATEN JOG ORIENTATION FINE	M/A			8	20 DEG	1	DEG	23	1185
VACUUM PULLDOWN SC	M/A			8	2 LEVEL	N/A		23	1127
METERING DRIVE SC (FRAME COUNT)	M/A			1/4	7 BITS	N/A		23	1128
2ND MOST SIGNIFICANT BIT	M/A			1/4				23	1129
3RD MOST SIGNIFICANT BIT	M/A			1/4				23	1130
4TH MOST SIGNIFICANT BIT	M/A			1				23	1131
5TH MOST SIGNIFICANT BIT	M/A			1				23	1132
6TH MOST SIGNIFICANT BIT	M/A			2				23	1133
LEAST SIGNIFICANT BIT	M/A			2				23	1134
SUPPLY REEL BRAKE SC	M/A			1	2 LEVEL	N/A		23	1136
TAKEUP REEL BRAKE SC	M/A			1	2 LEVEL	N/A		23	1126
FILM TENSION SC	M/A			1	0-6 POUNDS	N/A		23	1137 A
DATA HEAD IN/OUT PC	M/A			8	2 LEVEL	N/A		23	891
DATA HEAD IN/OUT SC	M/A			8	2 LEVEL	N/A		23	896
PLATEN CLAMP +Y	M/A			8	2 LEVEL	N/A		23	1121 R
PLATEN CLAMP -Y	M/A			8	2 LEVEL	N/A		23	1122 R
FILM HANDLING									
FILM VELOCITY PROFILE GENERATOR	M/A			16	0-10 IN/SEC	3 PCT		31	12*-6 877 A
PRIMARY TAKE-UP MOTOR CURRENT	M/A			16	0-3 AMPERE	3 PCT		31	12*-6 794 A
SECONDARY TAKE-UP MOTOR CURRENT	M/A			16	*	3 PCT		23	793
SUPPLY MOTOR CURRENT	M/A			16	0-3 AMPERE	5 PCT		31	12*-6 802 A
PRIMARY FILM VELOCITY	M/A			16	0-10 IN/SEC	5 PCT		31	12*-6 803 A

* - TO BE SUPPLIED BY A LATER REVISION

TABLE C.2-3 (Continued)

FUNCTION DESCRIPTION	MODE	PANEL IC	SENSOR TYPE	SAMPLES /SEC.	RANGE	ACCURACY	UNIT	POWER BUS	IMP
OPERATIONAL POWER									
PROCESSOR BUS VOLTAGE	M/A		ANALOG	1	19.5-33.5 VOLT *	1 VOLT	27		1226
PROCESSOR BUS CURRENT	M/A		ANALOG	16		3 PCT	27		1227
REFERENCE									
LM 12V SUPPLY	M/A		ANALOG	1	10-14 VOLT	1.0 PCT	21		866 A
LM 5V SUPPLY	M/A		ANALOG	1	4-6 VOLT	1.0 PCT	21		867 A
LM -6V SUPPLY	M/A		ANALOG	1	-8-(-4) VOLT	1.0 PCT	21		868 A
MH 12V SUPPLY	M/A		ANALOG	1	10-14 VOLT	1.0 PCT	1		26 A
MH 5V SUPPLY	M/A		ANALOG	1	4-6 VOLT	1.0 PCT	1		27 A
MH -6V SUPPLY	M/A		ANALOG	1	-8-(-4) VOLT	1.0 PCT	1		28 A
IP 40/90 DEG F REFERENCE PT 1	M/A		ANALOG	1	*	1.0 PCT	2		269 A
IP 40/90 DEG F REFERENCE PT 2	M/A		ANALOG	1	*	1.0 PCT	2		268 A
IP 60/80 DEG F REFERENCE PT 3	M/A		ANALOG	1	*	1.0 PCT	2		267 A
PROCESSOR/DRYER									
BIMAT MOTION	M/A		DISCRETE	1	2 LEVEL	N/A	27		1213
FILM DELAMINATION	M/A		DISCRETE	1	2 LEVEL	N/A	27		1215
ENVIRONMENTAL									
PROCESSOR/LM OIFF PRESSURE	M/A		ANALOG	1	-5/+5 PSI	0.25 PSI	27		1219
PROCESS ZONE TEMPERATURE	M/A		ANALOG	1/4	50/100 DEG F	1.5 DEG F	27		1223
DRYER GAS TEMPERATURE	M/A		ANALOG	1/4	50/100 DEG F	1.5 DEG F	27		1221
BIMAT SUPPLY TEMPERATURE	M/A		ANALOG	1/4	30/80 DEG F	1.5 DEG F	27		1225
PROC DRYER GAS OIFF TEMP	M/A		ANALOG	1/4	0-15 DEG F	0.5 DEG F	27		1218
DRYER RELATIVE HUMIDITY	M/A		ANALOG	1/4	40/60 PCT RH	5 PCT RH	27		1216
TEMP 7 PROCESSOR WATER 1	M/A		ANALOG	1/4	30/80 DEG F	1.5 DEG F	27		1232 B
TEMP 8 PROCESSOR WATER 2	M/A		ANALOG	1/4	50/100 DEG F	1.5 DEG F	27		1231 B
PROC WATER OIFF TEMP 1	M/A		ANALOG	1/4	0-15 DEG F	0.5 DEG F	27		1236
PROC WATER OIFF TEMP 2	M/A		ANALOG	1/4	0-15 DEG F	0.5 DEG F	27		1235
TEMP-LM CONTROL UNIT	M/A		ANALOG	1/4	40/90 DEG F	1 DEG F	21		939
TEMP-CAMERA AUX. ELECTRONICS 1	M/A		ANALOG	1/4	40/90 DEG F	1 DEG F	21		1168
TEMP-CAMERA AUX. ELECTRONICS 2	M/A		ANALOG	1/4	40/90 DEG F	1 DEG F	21		1178
TEMP-FOCUS CONTROL ELECTRONICS	M/A		ANALOG	1/4	40/150 DEG F	2 DEG F	21		892

* - TO BE SUPPLIED BY A LATER REVISION

Handle via BYEMAN
Control System Only

TABLE C.2-3 (Continued)

FUNCTION DESCRIPTOR	MODE	PANEL IC	SENSOR TYPE	SAMPLES /SEC.	RANGE	ACCURACY	UNIT	POWER BUS	IMP
TEMP-DATA CONVERSION UNIT	M/A		ANALOG	1/4	40/90 DEG F	1 DEG F	21		893
TEMP-FILM HANDLING ELECTRONICS	M/A		ANALOG	1/4	40/150 DEG F	2 DEG F	21		947
TEMP-LM POWER UNIT	M/A		ANALOG	1/4	40/90 DEG F	1 DEG F	21		983
TEMP-IP ELECTRONICS -5340/	M/A		ANALOG	1/4	40/90 DEG F	1 DEG F	2		179
TEMP-CAMERA DRIVE MOTOR	M/A		ANALOG	1/4	40/150 DEG F	2 DEG F	21		1135
TEMP-FILM ENVIRONMENT 1 (CHUTE)	M/A		ANALOG	1/4	40/150 DEG F	2 DEG F	21		944
TEMP-FILM ENVIRONMENT 2 (CHUTE)	M/A		ANALOG	1/4	40/150 DEG F	2 DEG F	21		945
MISCELLANEOUS									
DCU OUTPUT CURRENT	M/A		ANALOG	64	*	*	21		933
DCU INITIATE OUTPUT SIGNAL	M/A		DIGITAL	64	1 BITS		25	5	919 B
DCU DATA REQUEST/START	M/A		DIGITAL	16	2 BITS		25	5	920 B
LEAST SIGNIFICANT BIT	M/A		DIGITAL	16	2 BITS		25	5	921 B
COMMAND VERIFICATION									
SUPPLY REEL LOCK/UNLOCK	M/A		DIGITAL	2	2 BITS	N/A	21		864 A
LEAST SIGNIFICANT BIT	M/A		DIGITAL	2	1 BITS	N/A	21		865 A
FOCUS DETECTOR PRIME IN/OUT	M/A		DIGITAL	2	1 BITS	N/A	21		862 A
FOCUS DETECTOR BACKUP IN/OUT	M/A		DIGITAL	2	1 BITS	N/A	21		888 A
AUTOMATIC ALIGNMENT ON/OFF	M/A		DIGITAL	8	1 BITS	N/A	1		5
REMOTE ALIGNMENT ON/OFF	M/A		DIGITAL	8	1 BITS	N/A	1		6
MIRROR POSITION CHANGE	M/A		DIGITAL	8	6 BITS	N/A	1		35
2ND MOST SIGNIFICANT BIT	M/A		DIGITAL	8	1 BITS	N/A	1		36
3RD MOST SIGNIFICANT BIT	M/A		DIGITAL	8	1 BITS	N/A	1		37
4TH MOST SIGNIFICANT BIT	M/A		DIGITAL	8	1 BITS	N/A	1		38
5TH MOST SIGNIFICANT BIT	M/A		DIGITAL	8	1 BITS	N/A	1		39
LEAST SIGNIFICANT BIT	M/A		DIGITAL	8	1 BITS	N/A	1		40
MIRROR POSITION CHANGE DIRECTION	M/A		DIGITAL	8	1 BITS	N/A	1		15
NEGATIVE/POSITIVE	M/A		DIGITAL	8	3 BITS	N/A	1		59
MIRROR AND SERVO SELECT	M/A		DIGITAL	8	1 BITS	N/A	1		60
2ND MOST SIGNIFICANT BIT	M/A		DIGITAL	8	1 BITS	N/A	1		61
LEAST SIGNIFICANT BIT	M/A		DIGITAL	8	1 BITS	N/A	1		16 A
PM LL SET A PRIME UNLOCK/UNLOCK	M/A		DIGITAL	8	1 BITS	N/A	1		17 A
STOP	M/A		DIGITAL	8	1 BITS	N/A	1		
PM LL SET B PRIME UNLOCK/UNLOCK	M/A		DIGITAL	8	1 BITS	N/A	1		
STOP	M/A		DIGITAL	8	1 BITS	N/A	1		

* - TO BE SUPPLIED BY A LATER REVISION

Handle via BYEMAN
Control System Only

TABLE C.2-3 (Continued)

FUNCTION DESCRIPTOR	MODE	PANEL IC	SENSDR TYPE	SAMPLES /SEC.	RANGE	ACCURACY	UNIT	POWER BUS	IMP
PM LL SET A BACKUP UNLCK/UNLCK STDP	N/A		DIGITAL	8	1 BITS	N/A	1	3 B	
PM LL SET B BACKUP UNLCK/UNLCK STDP	N/A		DIGITAL	8	1 BITS	N/A	1	4 B	
TM LL SET A PRIME UNLCK/UNLCK STDP	N/A		DIGITAL	8	1 BITS	N/A	1	7 B	
TM LL SET B PRIME UNLCK/UNLCK STDP	N/A		DIGITAL	8	1 BITS	N/A	1	8 B	
TM LL SET A BACKUP UNLCK/UNLCK STDP	N/A		DIGITAL	8	1 BITS	N/A	1	10 B	
TM LL SET B BACKUP UNLCK/UNLCK STDP	N/A		DIGITAL	8	1 BITS	N/A	1	11 B	
PLATEN POSITION	N/A		DIGITAL	8	8 BITS	N/A	21	851	
2ND MOST SIGNIFICANT BIT	N/A		DIGITAL	8	8 BITS	N/A	21	852	
3RD MOST SIGNIFICANT BIT	N/A		DIGITAL	8	8 BITS	N/A	21	853	
4TH MOST SIGNIFICANT BIT	N/A		DIGITAL	8	8 BITS	N/A	21	854	
5TH MOST SIGNIFICANT BIT	N/A		DIGITAL	8	8 BITS	N/A	21	855	
6TH MOST SIGNIFICANT BIT	N/A		DIGITAL	8	8 BITS	N/A	21	856	
7TH MOST SIGNIFICANT BIT	N/A		DIGITAL	8	8 BITS	N/A	21	857	
LEAST SIGNIFICANT BIT	N/A		DIGITAL	8	8 BITS	N/A	21	858	
SLIT ANGLE	N/A		DIGITAL	8	7 BITS	N/A	21	823 A	
2ND MOST SIGNIFICANT BIT	N/A		DIGITAL	8	7 BITS	N/A	21	824	
3RD MOST SIGNIFICANT BIT	N/A		DIGITAL	8	7 BITS	N/A	21	825	
4TH MOST SIGNIFICANT BIT	N/A		DIGITAL	8	7 BITS	N/A	21	826	
5TH MOST SIGNIFICANT BIT	N/A		DIGITAL	8	7 BITS	N/A	21	827	
6TH MOST SIGNIFICANT BIT	N/A		DIGITAL	8	7 BITS	N/A	21	828	
LEAST SIGNIFICANT BIT	N/A		DIGITAL	8	7 BITS	N/A	21	829	
SLIT WIDTH	N/A		DIGITAL	8	3 BITS	N/A	21	830 A	
2ND MOST SIGNIFICANT BIT	N/A		DIGITAL	8	3 BITS	N/A	21	831	
LEAST SIGNIFICANT BIT	N/A		DIGITAL	8	3 BITS	N/A	21	832	
JOG ANGLE	N/A		DIGITAL	8	5 BITS	N/A	21	833 A	
2ND MOST SIGNIFICANT BIT	N/A		DIGITAL	8	5 BITS	N/A	21	834	
3RD MOST SIGNIFICANT BIT	N/A		DIGITAL	8	5 BITS	N/A	21	835	
4TH MOST SIGNIFICANT BIT	N/A		DIGITAL	8	5 BITS	N/A	21	836	
LEAST SIGNIFICANT BIT	N/A		DIGITAL	8	5 BITS	N/A	21	837	
INITIAL JOG VELOCITY	N/A		DIGITAL	8	5 BITS	N/A	21	805 A	
2ND MOST SIGNIFICANT BIT	N/A		DIGITAL	8	5 BITS	N/A	21	806	
3RD MOST SIGNIFICANT BIT	N/A		DIGITAL	8	5 BITS	N/A	21	807	
4TH MOST SIGNIFICANT BIT	N/A		DIGITAL	8	5 BITS	N/A	21	808	
LEAST SIGNIFICANT BIT	N/A		DIGITAL	8	5 BITS	N/A	21	809	
PLATEN PRIMARY/SECONDARY	N/A		DIGITAL	8	1 BITS	N/A	21	756 A	

* - TO BE SUPPLIED BY A LATER REVISION

Handle via BYEMAN
Control System Only

TABLE C.2-3 (Continued)

FUNCTION DESCRIPTOR	MODE	PANEL IC	MAS	SENSOR TYPE	SAMPLES /SEC.	RANGE	ACCURACY	UNIT	POWER BUS	IMP
IPC SET/RESET	M/A			DIGITAL	8	2 BITS	N/A	21		796 A
LEAST SIGNIFICANT BIT	M/A			DIGITAL	8	1 BITS	N/A	21		797 A
IMC ENABLE/INHIBIT	M/A			DIGITAL	8	4 BITS	N/A	21		863
IMAGE DEROTATION	M/A			DIGITAL	8			21		760
2ND MOST SIGNIFICANT BIT	M/A			DIGITAL	8			21		761
3RD MOST SIGNIFICANT BIT	M/A			DIGITAL	8			21		762
LEAST SIGNIFICANT BIT	M/A			DIGITAL	8			21		763
VO MAGNIFICATION	M/A			DIGITAL	2	2 BITS	N/A	21		753 A
LEAST SIGNIFICANT BIT	M/A			DIGITAL	2	1 BITS	N/A	21		754 A
VO EYEPIECE BAY 2/8AY 8	M/A			DIGITAL	2	1 BITS	N/A	21		759 A
VO SRC ENABLE/INHIBIT	M/A			DIGITAL	2	1 BITS	N/A	21		764 B
CAMERA POWER PRIME ON/OFF	M/A			DIGITAL	1	1 BITS	N/A	21		810 A
CAMERA POWER BACKUP ON/OFF	M/A			DIGITAL	1	1 BITS	N/A	21		879 A
FH POWER PRIME ON/OFF	M/A			DIGITAL	1	1 BITS	N/A	21		998 B
FH POWER BACKUP ON/OFF	M/A			DIGITAL	1	1 BITS	N/A	21		999 B
FOCUS POWER PRIME ON/OFF	M/A			DIGITAL	1	1 BITS	N/A	21		812 A
FOCUS POWER BACKUP ON/OFF	M/A			DIGITAL	1	1 BITS	N/A	21		881 A
LM ASCENT POWER ON/OFF	M/A			DIGITAL	1	1 BITS	N/A	21		818 A
ALIGNMENT POWER PRIME ON/OFF	M/A			DIGITAL	1	1 BITS	N/A	21		29 A
ALIGNMENT POWER BACKUP ON/OFF	M/A			DIGITAL	1	1 BITS	N/A	21		19 A
LL UNLOCK POWER PRIME ON/OFF	M/A			DIGITAL	1	1 BITS	N/A	21		31 A
LL UNLOCK POWER BACKUP ON/OFF	M/A			DIGITAL	1	1 BITS	N/A	21		20 A
MH ASCENT POWER ON/OFF	M/A			DIGITAL	1	1 BITS	N/A	21		30 A
ENVIRONMENTAL POWER ON/OFF	M/A			DIGITAL	1	1 BITS	N/A	21		32 A
LEAST SIGNIFICANT BIT	M/A			DIGITAL	1	2 BITS	N/A	21		33 A
FILM RUNOUT ONE FRAME	M/A			DIGITAL	1			21		
EXECUTE/RESET	M/A			DIGITAL	8	1 BITS	N/A	21		859 A
FILM RUNOUT PRIMARY/SECONDARY	M/A			DIGITAL	8	1 BITS	N/A	21		860 A
SUPPLY REEL MODE	M/A			DIGITAL	8	2 BITS	N/A	21		838 A
LEAST SIGNIFICANT BIT	M/A			DIGITAL	8			21		839 A

* - TO BE SUPPLIED BY A LATER REVISION

Handle via BYEMAN
Control System Only

(Control Number)

TABLE C.2-4
LAUNCH AND ASCENT POINTS

FUNCTION DESCRIPTION	MODE	PANEL IC	MAS	SENSOR TYPE	SAMPLES /SEC.	RANGE	ACCURACY	UNIT	POWER BUS	IMP
LM CIRC VIB 10-500HZ	M/A			ANALOG	C	.2-10 G		33		1248 B
MM PRI MIR VIB 10-500HZ	M/A			ANALOG	C	.2-10 G		12		450 B
MM CDA AMT VIB 10-500HZ	M/A			ANALOG	C	.2-10 G		12		451 B
MM RC MIR VIB 10-500HZ	M/A			ANALOG	C	.2-10 G		12		452 B

DYNAMICS

* - TO BE SUPPLIED BY A LATER REVISION

TABLE C.2-5
POST FLIGHT AND ENGINEERING DATA POINTS

FUNCTION DESCRIPTOR	MODE	PANEL IC	SENSOR TYPE	SAMPLES /SEC.	RANGE	ACCURACY	UNIT	POWER BUS	IMP
ENVIRONMENTAL									
TEMP-LM CONTROL UNIT	M/A		ANALOG	1/4	40/150 DEG F	2 DEG F	21		922
TEMP-CAMERA AUX. ELECTRONICS 1	M/A		ANALOG	1/4	40/150 DEG F	2 DEG F	21		924
TEMP-CAMERA AUX. ELECTRONICS 2	M/A		ANALOG	1/4	40/150 DEG F	2 DEG F	21		929
TEMP-FILM HANDLING ELECTRONICS	M/A		ANALOG	1/4	40/150 DEG F	2 DEG F	21		927
TEMP-LM POWER UNIT	M/A		ANALOG	1/4	40/150 DEG F	2 DEG F	21		928
TEMP-MM OUTER SKIN/INSIDE OUTER	M/A		ANALOG	1/4	40/150 DEG F	2 DEG F	21		
HALES-S265/C000	M/A		ANALOG	1/4	-150/250 DEG F	15 DEG F	2		117 B
TEMP-MM OUTER SKIN/INSIDE OUTER	M/A		ANALOG	1/4	-150/250 DEG F	15 DEG F	2		118 B
HALES-S265/C030	M/A		ANALOG	1/4	-150/250 DEG F	15 DEG F	2		119 B
TEMP-MM OUTER SKIN/INSIDE OUTER	M/A		ANALOG	1/4	-150/250 DEG F	15 DEG F	2		120 B
HALES-S265/C060	M/A		ANALOG	1/4	-150/250 DEG F	15 DEG F	2		121 B
TEMP-MM OUTER SKIN/INSIDE OUTER	M/A		ANALOG	1/4	-150/250 DEG F	15 DEG F	2		122 B
HALES-S265/C100	M/A		ANALOG	1/4	-150/250 DEG F	15 DEG F	2		123 B
TEMP-MM OUTER SKIN/INSIDE OUTER	M/A		ANALOG	1/4	-150/250 DEG F	15 DEG F	2		124 B
HALES-S265/C140	M/A		ANALOG	1/4	-150/250 DEG F	15 DEG F	2		125 B
TEMP-MM OUTER SKIN/INSIDE OUTER	M/A		ANALOG	1/4	-150/250 DEG F	15 DEG F	2		126 B
HALES-S265/C180	M/A		ANALOG	1/4	-150/250 DEG F	15 DEG F	2		127
TEMP-MM OUTER SKIN/INSIDE OUTER	M/A		ANALOG	1/4	-150/250 DEG F	15 DEG F	2		128
HALES-S265/C220	M/A		ANALOG	1/4	-150/250 DEG F	15 DEG F	2		129
TEMP-MM OUTER SKIN/INSIDE OUTER	M/A		ANALOG	1/4	-150/250 DEG F	15 DEG F	2		130
HALES-S265/C260	M/A		ANALOG	1/4	-150/250 DEG F	15 DEG F	2		131
TEMP-MM OUTER SKIN/INSIDE OUTER	M/A		ANALOG	1/4	-150/250 DEG F	15 DEG F	2		132
HALES-S265/C300	M/A		ANALOG	1/4	-150/250 DEG F	15 DEG F	2		
TEMP-MM OUTER SKIN/INSIDE OUTER	M/A		ANALOG	1/4	-150/250 DEG F	15 DEG F	2		
HALES-S265/C330	M/A		ANALOG	1/4	-150/250 DEG F	15 DEG F	2		
TEMP-MM OUTER SKIN	M/A		ANALOG	1/4	-150/250 DEG F	15 DEG F	2		
S100/C000	M/A		ANALOG	1/4	-150/250 DEG F	15 DEG F	2		
TEMP-MM OUTER SKIN	M/A		ANALOG	1/4	-150/250 DEG F	15 DEG F	2		
S100/C030	M/A		ANALOG	1/4	-150/250 DEG F	15 DEG F	2		
TEMP-MM OUTER SKIN	M/A		ANALOG	1/4	-150/250 DEG F	15 DEG F	2		
S100/C060	M/A		ANALOG	1/4	-150/250 DEG F	15 DEG F	2		
TEMP-MM OUTER SKIN	M/A		ANALOG	1/4	-150/250 DEG F	15 DEG F	2		
S100/C090	M/A		ANALOG	1/4	-150/250 DEG F	15 DEG F	2		
TEMP-MM OUTER SKIN	M/A		ANALOG	1/4	-150/250 DEG F	15 DEG F	2		
S100/C135	M/A		ANALOG	1/4	-150/250 DEG F	15 DEG F	2		
TEMP-MM OUTER SKIN	M/A		ANALOG	1/4	-150/250 DEG F	15 DEG F	2		
S100/C180	M/A		ANALOG	1/4	-150/250 DEG F	15 DEG F	2		

* - TO BE SUPPLIED BY A LATER REVISION

TABLE C.2-5 (Continued)

FUNCTION DESCRIPTOR	MODE	PANEL IC	MAS	SENSOR TYPE	SAMPLES /SEC.	RANGE	ACCURACY	UNIT	POWER BUS	IMP
TEMP-NM OUTER SKIN	M/A			ANALOG	1/4	-150/250 DEG F	15 DEG F	2		133
S100/C210										
TEMP-NM OUTER SKIN	M/A			ANALOG	1/4	-150/250 DEG F	15 DEG F	2		134
S100/C 21										
TEMP-NM OUTER SKIN	M/A			ANALOG	1/4	-150/250 DEG F	15 DEG F	2		135
S100/C270										
TEMP-NM OUTER SKIN	M/A			ANALOG	1/4	-150/250 DEG F	15 DEG F	2		136
S100/C315										
TEMP-NM OUTER SKIN/AFT BULKHEAD	M/A			ANALOG	1/4	-150/250 DEG F	15 DEG F	2		137
S075/C060										
S TEMP-NM OUTER SKIN/AFT BULKHEAD	M/A			ANALOG	1/4	-150/250 DEG F	15 DEG F	2		138
S075/C180										
S TEMP-NM OUTER SKIN/AFT BULKHEAD	M/A			ANALOG	1/4	-150/250 DEG F	15 DEG F	2		139
S075/C300										
TEMP-FORWARD COA.OVERHEAD	M/A			ANALOG	1/4	60/80 DEG F	0.5 DEG F	2		263
S380/C003										
TEMP-FORWARD COA,UNDERSIDE	M/A			ANALOG	1/4	60/80 DEG F	0.5 DEG F	2		263 B
S459/C020										
S TEMP-FORWARD COA,UNDERSIDE	M/A			ANALOG	1/4	60/80 DEG F	0.5 DEG F	2		250 B
S459/C340										
S TEMP-FORWARD COA, SIDE PANEL	M/A			ANALOG	1/4	60/80 DEG F	0.5 DEG F	2		252
S380/C030										
S TEMP-FORWARD COA, SIDE PANEL	M/A			ANALOG	1/4	60/80 DEG F	0.5 DEG F	2		253
S380/C330										
S TEMP-FORWARD COA, OVER ROSS	M/A			ANALOG	1/4	60/80 DEG F	0.5 DEG F	2		254
CORRECTOR-S425/C000										
S TEMP-RINGD STRUCTURE	M/A			ANALOG	1/4	60/80 DEG F	0.5 DEG F	2		255
S370/C										
S TEMP-RINGD STRUCTURE	M/A			ANALOG	1/4	60/80 DEG F	0.5 DEG F	2		256
S370/C										
TEMP-RINGD STRUCTURE	M/A			ANALOG	1/4	60/80 DEG F	0.5 DEG F	2		257
S385/C										
TEMP-RINGD STRUCTURE	M/A			ANALOG	1/4	60/80 DEG F	0.5 DEG F	2		258
S385/C										
TEMP-RINGD STRUCTURE	M/A			ANALOG	1/4	60/80 DEG F	0.5 DEG F	2		259
S340/C										
TEMP-RINGD STRUCTURE	M/A			ANALOG	1/4	60/80 DEG F	0.5 DEG F	2		264
S340/C										
S TEMP-INVAR REFERENCE ROD	M/A			ANALOG	1/4	60/80 DEG F	0.5 DEG F	2		95
S120/C060										

* - TO BE SUPPLIED BY A LATER REVISION

Handle via BYEMAN
Control System Only

TABLE C.2-5 (Continued)

FUNCTION DESCRIPTOR	MODE	PANEL IC	MAS	SENSOR TYPE	SAMPLES /SEC.	RANGE	ACCURACY	UNIT	POWER BUS	IMP
S TEMP-INVAR REFERENCE ROD S120/C180	M/A			ANALOG	1/4	60/80 DEG F	0.5 DEG F	2		96
S TEMP-INVAR REFERENCE ROD S120/C300	M/A			ANALOG	1/4	60/80 DEG F	0.5 DEG F	2		97
S TEMP-INVAR REFERENCE ROD S343/C060	M/A			ANALOG	1/4	60/80 DEG F	0.5 DEG F	2		94
S TEMP-INVAR REFERENCE ROD S343/C180	M/A			ANALOG	1/4	60/80 DEG F	0.5 DEG F	2		113
S TEMP-INVAR REFERENCE ROD S343/C300	M/A			ANALOG	1/4	60/80 DEG F	0.5 DEG F	2		114
TEMP-INSULATION SUPPORT STRUCTURE-S340/C003	M/A			ANALOG	1/4	40/90 DEG F	1 DEG F	2		170 B
TEMP-COA REAR BULKHEAD S085/C000/R18	M/A			ANALOG	1/4	60/80 DEG F	0.5 DEG F	2		260
S TEMP-COA REAR BULKHEAD S085/C180/R18	M/A			ANALOG	1/4	60/80 DEG F	0.5 DEG F	2		261
TEMP-COA FORWARD SUPPORT POINT S459/C000	M/A			ANALOG	1/4	60/80 DEG F	0.5 DEG F	2		262
TEMP-COA SUPPORT STRUT, INNER END S459/C000	M/A			ANALOG	1/4	40/90 DEG F	1 DEG F	2		171
TEMP-COA SUPPORT STRUT, INNER END S200/C070	M/A			ANALOG	1/4	40/90 DEG F	1 DEG F	2		172
S TEMP-COA SUPPORT STRUT, INNER END S200/C070	M/A			ANALOG	1/4	40/90 DEG F	1 DEG F	2		173
TEMP-COA SUPPORT STRUT, INNER END S200/C290	M/A			ANALOG	1/4	40/90 DEG F	1 DEG F	2		174
S TEMP-COA SUPPORT STRUT, INNER END S200/C290	M/A			ANALOG	1/4	40/90 DEG F	1 DEG F	2		175
TEMP-COA SUPPORT STRUT, OUTER END S183/C285	M/A			ANALOG	1/4	-100/200 DEG F	5 DEG F	2		155
S TEMP-COA SUPPORT STRUT, OUTER END S183/C285	M/A			ANALOG	1/4	-100/200 DEG F	5 DEG F	2		156
TEMP-COA SUPPORT STRUT, OUTER END S183/C075	M/A			ANALOG	1/4	-100/200 DEG F	5 DEG F	2		157
S TEMP-COA SUPPORT STRUT, OUTER END S183/C090	M/A			ANALOG	1/4	-100/200 DEG F	5 DEG F	2		158
TEMP-COA SUPPORT STRUT, OUTER END S459/C005	M/A			ANALOG	1/4	-100/200 DEG F	5 DEG F	2		159 B
S TEMP-COA SUPPORT STRUT, OUTER END TEMP-LENS TUBE, FORWARD END S340/C110	M/A			ANALOG	1/4	60/80 DEG F	0.5 DEG F	2		225

* - TO BE SUPPLIED BY A LATER REVISION

Handle via BYEMAN
Control System Only

TABLE C.2-5 (Continued)

FUNCTION DESCRIPTOR	MODE	PANEL IC	SENSOR TYPE	SAMPLES /SEC.	RANGE	ACCURACY	UNIT	POWER BUS	IMP
TEMP-LENS TUBE, FORWARD END	M/A		ANALDG	1/4	60/80 DEG F	0.5 DEG F	2		226
TEMP-LENS TUBE, FORWARD END	M/A		ANALOG	1/4	60/80 DEG F	0.5 DEG F	2		227
S TEMP-LENS TUBE, FORWARD END	M/A		ANALOG	1/4	60/80 DEG F	0.5 DEG F	2		229
S TEMP-LENS TUBE, AFT SUPPORT	M/A		ANALDG	1/4	60/80 DEG F	0.5 DEG F	2		230
TEMP-LENS TUBE, AFT SUPPORT	M/A		ANALDG	1/4	60/80 DEG F	0.5 DEG F	2		231
TEMP-LENS TUBE, OUTER SKIN	M/A		ANALDG	1/4	60/80 DEG F	0.5 DEG F	2		232 B
TEMP-LENS TUBE, OUTER SKIN	M/A		ANALOG	1/4	60/80 DEG F	0.5 DEG F	2		233 B
TEMP-LENS TUBE, OUTER SKIN	M/A		ANALOG	1/4	60/80 DEG F	0.5 DEG F	2		234 B
TEMP-LENS TUBE, OUTER SKIN	M/A		ANALDG	1/4	60/80 DEG F	0.5 DEG F	2		235 B
TEMP-LENS TUBE, OUTER SKIN	M/A		ANALDG	1/4	60/80 DEG F	0.5 DEG F	2		299 B
TEMP-LENS TUBE, OUTER SKIN	M/A		ANALDG	1/4	60/80 DEG F	0.5 DEG F	2		300
TEMP-LENS TUBE, OUTER SKIN	M/A		ANALDG	1/4	60/80 DEG F	0.5 DEG F	2		301
TEMP-LENS TUBE, OUTER SKIN	M/A		ANALDG	1/4	60/80 DEG F	0.5 DEG F	2		302
TEMP-LENS TUBE, OUTER SKIN	M/A		ANALDG	1/4	60/80 DEG F	0.5 DEG F	2		303
TEMP-LENS TUBE, OUTER SKIN	M/A		ANALDG	1/4	60/80 DEG F	0.5 DEG F	2		304
TEMP-RC BARREL, TOP OUTSIDE SURFACE -S416/C000	M/A		ANALDG	1/4	60/80 DEG F	0.5 DEG F	2		211
S TEMP-RC BARREL, BOTTOM OUTSIDE SURFACE -S416/C000	M/A		ANALDG	1/4	60/80 DEG F	0.5 DEG F	2		212
TEMP-RF REAR SURFACE -S395/	M/A		ANALDG	1/4	60/80 DEG F	0.5 DEG F	2		214
TEMP-NF REAR SURFACE -S395/	M/A		ANALDG	1/4	60/80 DEG F	0.5 DEG F	2		222
TEMP-PH REAR SURFACE -S090/	M/A		ANALDG	1/4	60/80 DEG F	0.5 DEG F	2		223
TEMP-NF SUPPORT BEAM-RT -S395/	M/A		ANALDG	1/4	60/80 DEG F	0.5 DEG F	2		215
TEMP-NF SUPPORT BEAM-CTR -S395/	M/A		ANALDG	1/4	60/80 DEG F	0.5 DEG F	2		216
TEMP-NF SUPPORT BEAM-LT -S395/	M/A		ANALDG	1/4	60/80 DEG F	0.5 DEG F	2		217
TEMP-NF VERTICAL SUPPORT -S340/	M/A		ANALDG	1/4	60/80 DEG F	0.5 DEG F	2		218

* - TD 8E SUPPLIED BY A LATER REVISION

Handle via BYEMAN
Control System Only

TABLE C.2-5 (Continued)

FUNCTION DESCRIPTOR	MODE	PANEL IC	MAS	SENSOR TYPE	SAMPLES /SEC.	RANGE	ACCURACY	UNIT	POWER BUS	IMP
S TEMP-NF VERTICAL SUPPORT -S375/ TEMP-LENS TUBE, ENCLOSURE FLUX S395/C	M/A			ANALOG	1/4	60/80 DEG F	0.5 DEG F	2		219
TEMP-LENS TUBE, ENCLOSURE FLUX S395/C	M/A			ANALOG	1/4	60/80 DEG F	0.5 DEG F	2		210
S TEMP-LENS TUBE, ENCLOSURE FLUX S395/C	M/A			ANALOG	1/4	60/80 DEG F	0.5 DEG F	2		213
S TEMP-LENS TUBE, ENCLOSURE FLUX S395/C	M/A			ANALOG	1/4	60/80 DEG F	0.5 DEG F	2		220
TEMP-PRIMARY FILM STORAGE TEMP-SECONDARY FILM STORAGE	M/A			ANALOG	1/4	60/80 DEG F	0.5 DEG F	2		221
	M/A			ANALOG	1/4	40/150 DEG F	2 DEG F	21		965
	M/A			ANALOG	1/4	40/150 DEG F	2 DEG F	21		966

* - TO BE SUPPLIED BY A LATER REVISION

Handle via BYEMAN
Control System Only

TABLE C.2-7
PRELAUNCH AND TEST POINTS

FUNCTION DESCRIPTOR	MODE	PANEL IC	MAS TYPE	SENSOR SAMPLES /SEC.	RANGE	ACCURACY	UNIT	POWER BUS	IMP
ENVIRONMENTAL									
TEMP-LENS TUBE AIR EXIT	M/A		ANALOG	C	60/80 DEG F	0.5 DEG F	17		3
S095/000									
TEMP-LENS TUBE AIR EXIT	M/A		ANALOG	C	60/80 DEG F	0.5 DEG F	17		3
S095/140									
TEMP-LENS TUBE AIR EXIT	M/A		ANALOG	C	60/80 DEG F	0.5 DEG F	17		3
S095/220									
LENS TUBE, EXIT AIR MASS FLOW	M/A		ANALOG	C	0/150 LB/MIN	1 LB/MIN	17		3
S095/000									
LENS TUBE, EXIT AIR MASS FLOW	M/A		ANALOG	C	0/150 LB/MIN	1 LB/MIN	17		3
S095/140									
LENS TUBE, EXIT AIR MASS FLOW	M/A		ANALOG	C	0/150 LB/MIN	1 LB/MIN	17		3
S095/220									
TEMP-LENS TUBE PROFILE	M/A		ANALOG	C	60/80 DEG F	0.5 DEG F	17		3
S275/003									
TEMP-LENS TUBE PROFILE	M/A		ANALOG	C	60/80 DEG F	0.5 DEG F	17		3
S275/140									
TEMP-LENS TUBE PROFILE	M/A		ANALOG	C	60/80 DEG F	0.5 DEG F	17		3
S275/220									
PROCESSOR/LM DIFF PRESSURE	M/A		ANALOG	C	60/80 DEG F	0.5 DEG F	17		3
TEMP-CDA REAR WALL-STATION 85	M/A		ANALOG	C	-5/+5 PSI	0.25 PSI	27		3
TEMP-TH REAR SURFACE	M/A		ANALOG	C	60/80 DEG F	0.5 DEG F	17		3
TEMP-TM FRONT-TO-BACK	M/A		ANALOG	C	60/80 DEG F	0.5 DEG F	17		3
TEMP-PM REAR SURFACE	M/A		ANALOG	C	-1/+3(170) DEG F	0.2 DEG F	17		3
TEMP-NF REAR SURFACE	M/A		ANALOG	C	60/80 DEG F	0.5 DEG F	17		3
TEMP-RF REAR SURFACE	M/A		ANALOG	C	60/80 DEG F	0.5 DEG F	17		3
TEMP-RC REAR SURFACE	M/A		ANALOG	C	60/80 DEG F	0.5 DEG F	17		3
TEMP-RC FORWARD ELEMENT	M/A		ANALOG	C	60/80 DEG F	0.5 DEG F	17		3
TEMP-RC BARREL AT FLEX CONNECTOR	M/A		ANALOG	C	60/80 DEG F	0.5 DEG F	17		3
RC REL. HUMIDITY AT VENT-STA 420	M/A		ANALOG	C	40/60 PCT RH	5 PCT RH	17		3
RC REL. HUMIDITY AT VENT-STA 420	M/A		ANALOG	C	40/60 PCT RH	5 PCT RH	17		3
FILM ENVIRONMENT REL. HUMIDITY	M/A		ANALOG	C	40/60 PCT RH	5 PCT RH	19		3

* - TO BE SUPPLIED BY A LATER REVISION

Handle via BYEMAN
Control System Only

TABLE C.2-7 (Continued)

FUNCTION DESCRIPTOR	MODE	PANEL IC	MAS	SENSOR TYPE	SAMPLES /SEC.	RANGE	ACCURACY	UNIT	POWER BUS	IMP
DYNAMICS										
PH STRAIN GAUGE 1,R,H,F	M/A			ANALOG	C	D-100 POUNDS	2.5 PCT FS	17		3 8
PH STRAIN GAUGE 2,R,H,F	M/A			ANALOG	C	0-100 POUNDS	2.5 PCT FS	17		3 8
PH STRAIN GAUGE 3,R,H,F	M/A			ANALOG	C	0-100 POUNDS	2.5 PCT FS	17		3 8
COMMAND VERIFICATION										
LAUNCH LOCKS RESET	M/A			DISCRETE	1/4	2 LEVEL	N/A	1		22

* - TO BE SUPPLIED BY A LATER REVISION

Handle via **BYEMAN**
Control System Only

TABLE C.2-8
LAUNCH - ABORT POINTS

Function Descriptor	Panel		MAS	Sensor		Range	Accuracy	Unit	Power	
	Mode	IC		Type	/Sec.				Bus	IMP
*	M/A			*	C			19		1499

* - To be supplied by a later revision

~~SECRET~~ D

BIF-008- [REDACTED] -68
(Control Number)

APPENDIX D
RELIABILITY BLOCK DIAGRAMS AND BASIS FOR TIMES USED IN MATH MODEL

D.1 RELIABILITY BLOCK DIAGRAMS

The diagrams represent the functional arrangement of the equipment necessary to perform the various operations. The failure rate times 10^6 or the reliability of each individual subcomponent or event is indicated on the diagrams. Reliability calculation is discussed in Section 7.

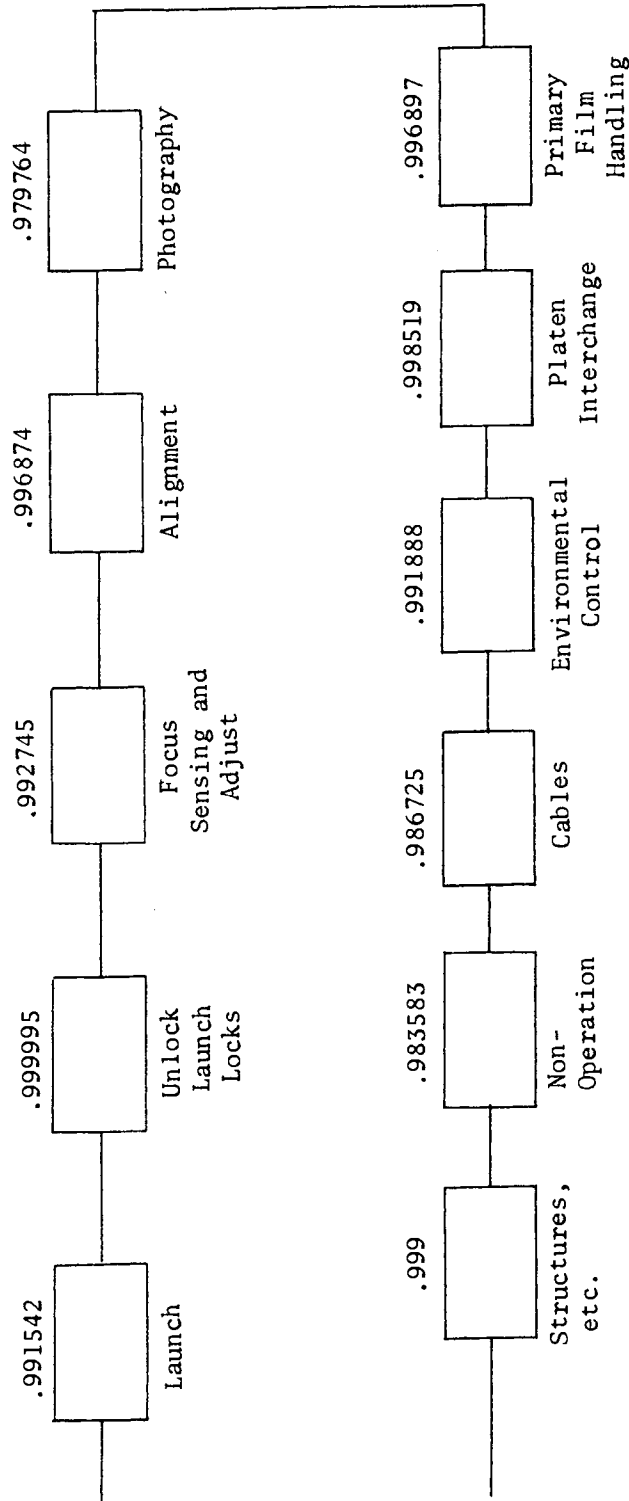
For most of the operations, standard reliability calculations were used. A brief description of the reliability techniques used is given in the text which follows.

Figure D.1 shows the relationship between each of the mission-essential operations and the overall success of the mission. Figures D.2 through D.8 give a more complete model for each of the operations represented in Figure D.1 except the launch, nonoperation, structures, and cables blocks. The launch and nonoperation are treated separately in Table D.4. The estimated reliability for the cables represents the laboratory module (LM) and mission module (MM) cable set with all connectors assumed to be in line and operating over the entire mission, therefore a diagram is not presented for this function. Structural items are covered in Section 7.

~~SECRET~~ D

~~SECRET~~ D

BIF-008-- [redacted] -68
(Control Number)

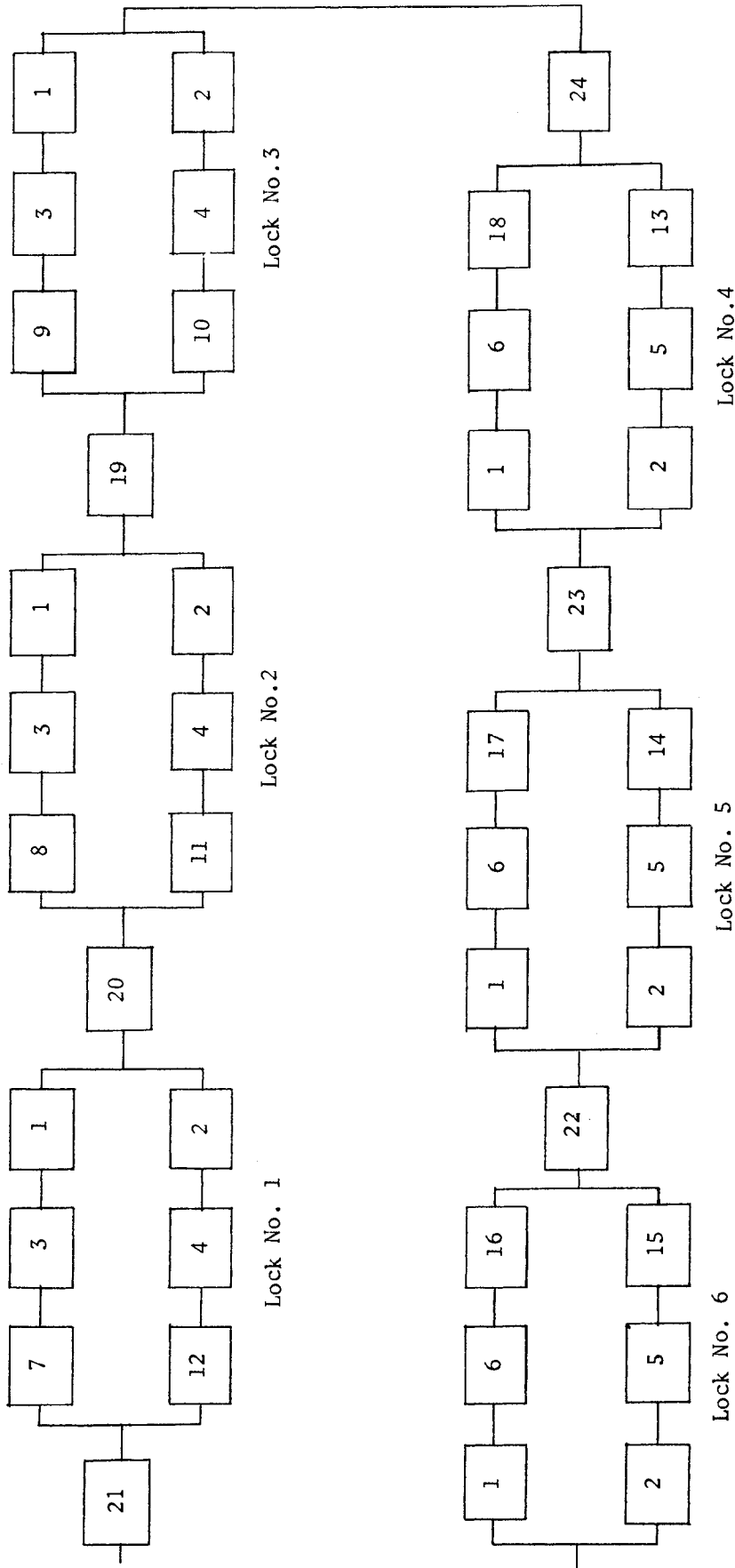


Note: 1. See Figures D-2 and D-8 for more complete models of individual operations.
 2. All numerical values are reliabilities.

Figure D-1. Mission-Essential Operations

Handle via **BYEMAN**
Control System Only

~~SECRET~~ D



Note: 1. See Lock Set Key for Hardware-Number Equivalents.

2. There is only one hardware unit associated with each distinct integer even though that integer may appear more than once in the diagram.

Handle via **BYEMAN**
Control System Only

Figure D-2. Lock Set (Primary or Tracking Mirror)

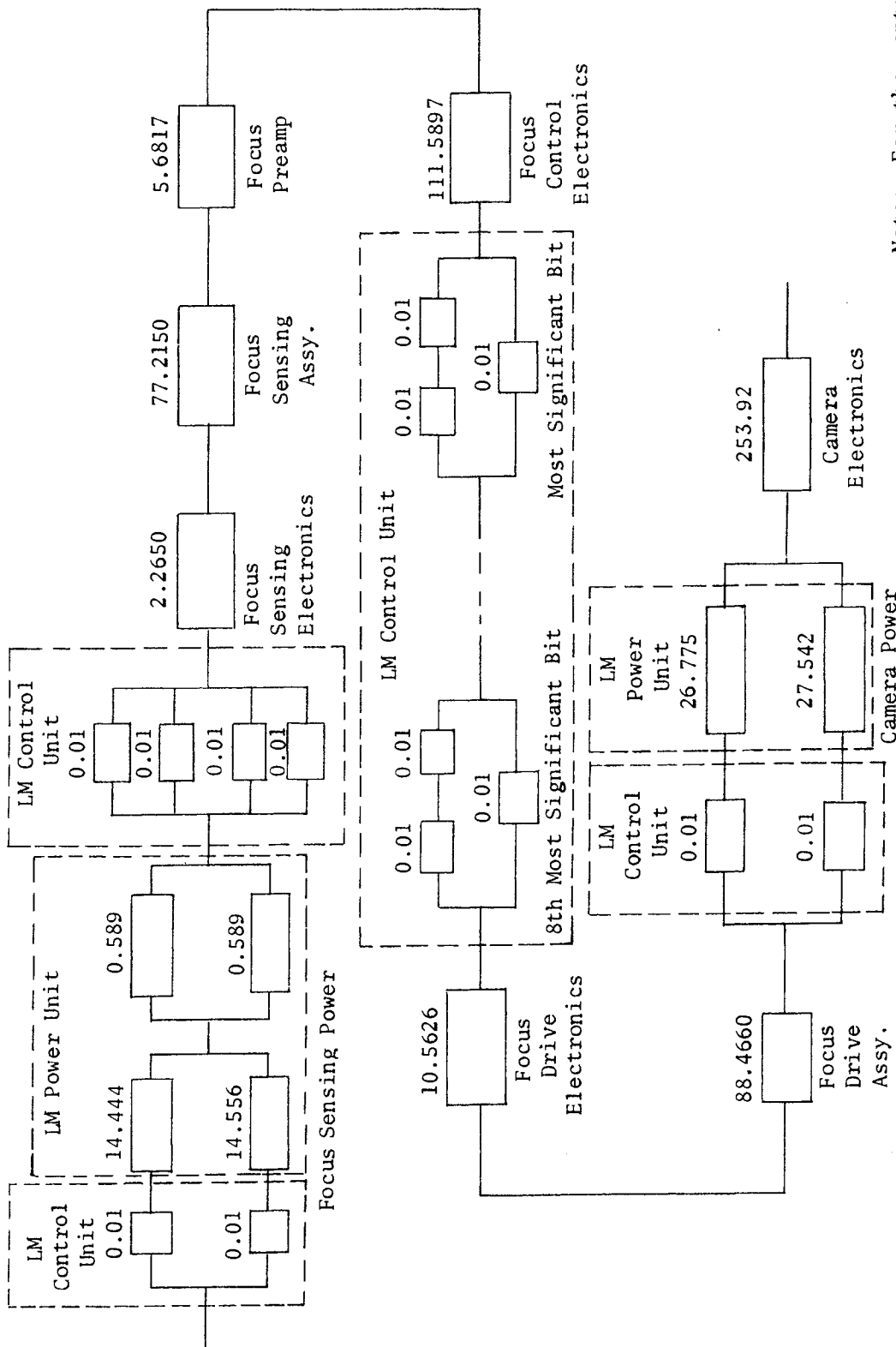
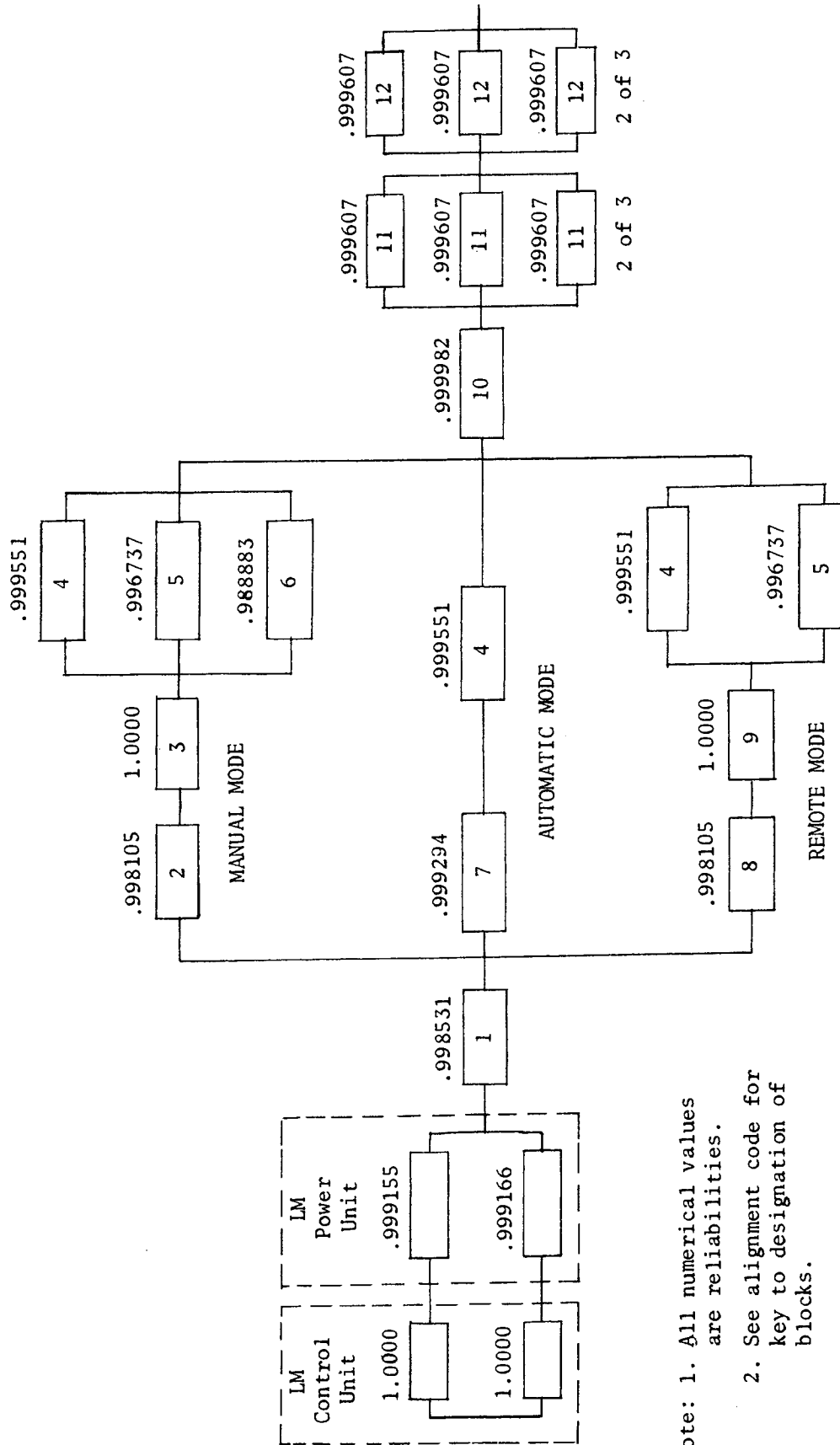


Figure D-3. Focus Sensing and Adjust

Note: For the control unit the numerical values represent the failures per million actuations. All other numerical values are failures per million hours.

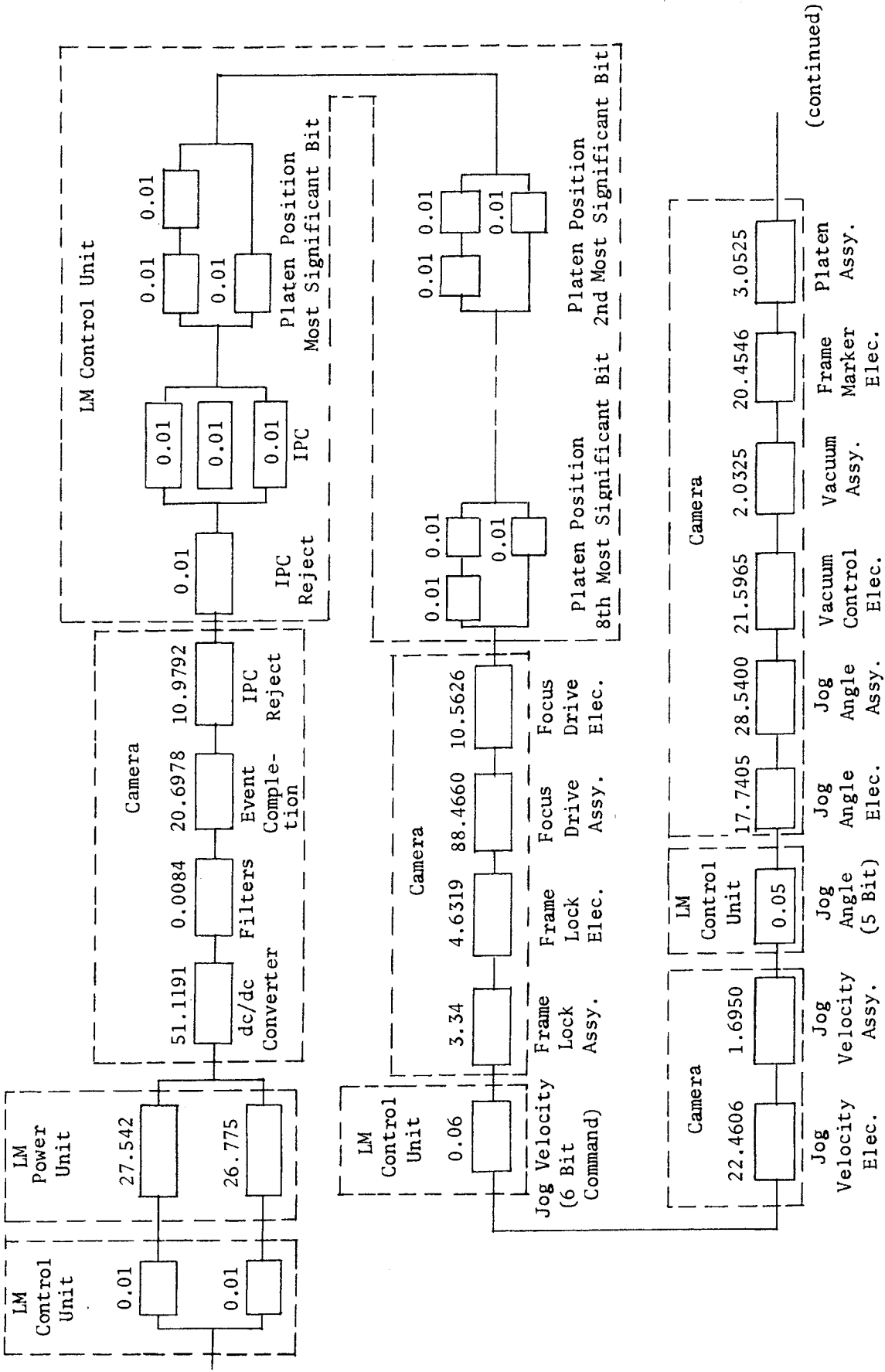


- Note: 1. All numerical values are reliabilities.
 2. See alignment code for key to designation of blocks.

Figure D-4. Alignment

~~SECRET~~ D

BIF-008 - [REDACTED] -68
(Control Number)

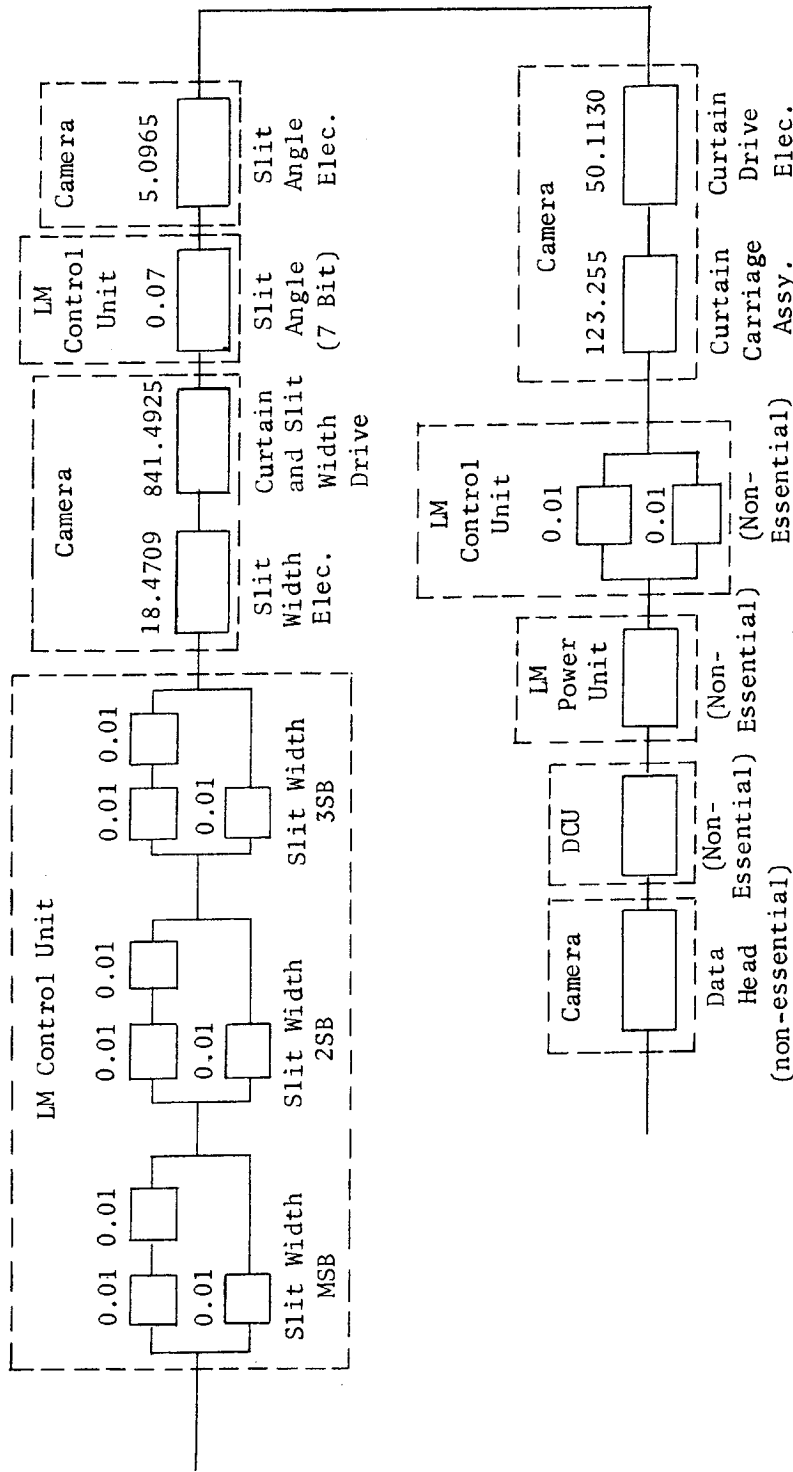


(continued)

Figure D-5. Photographic Cycle

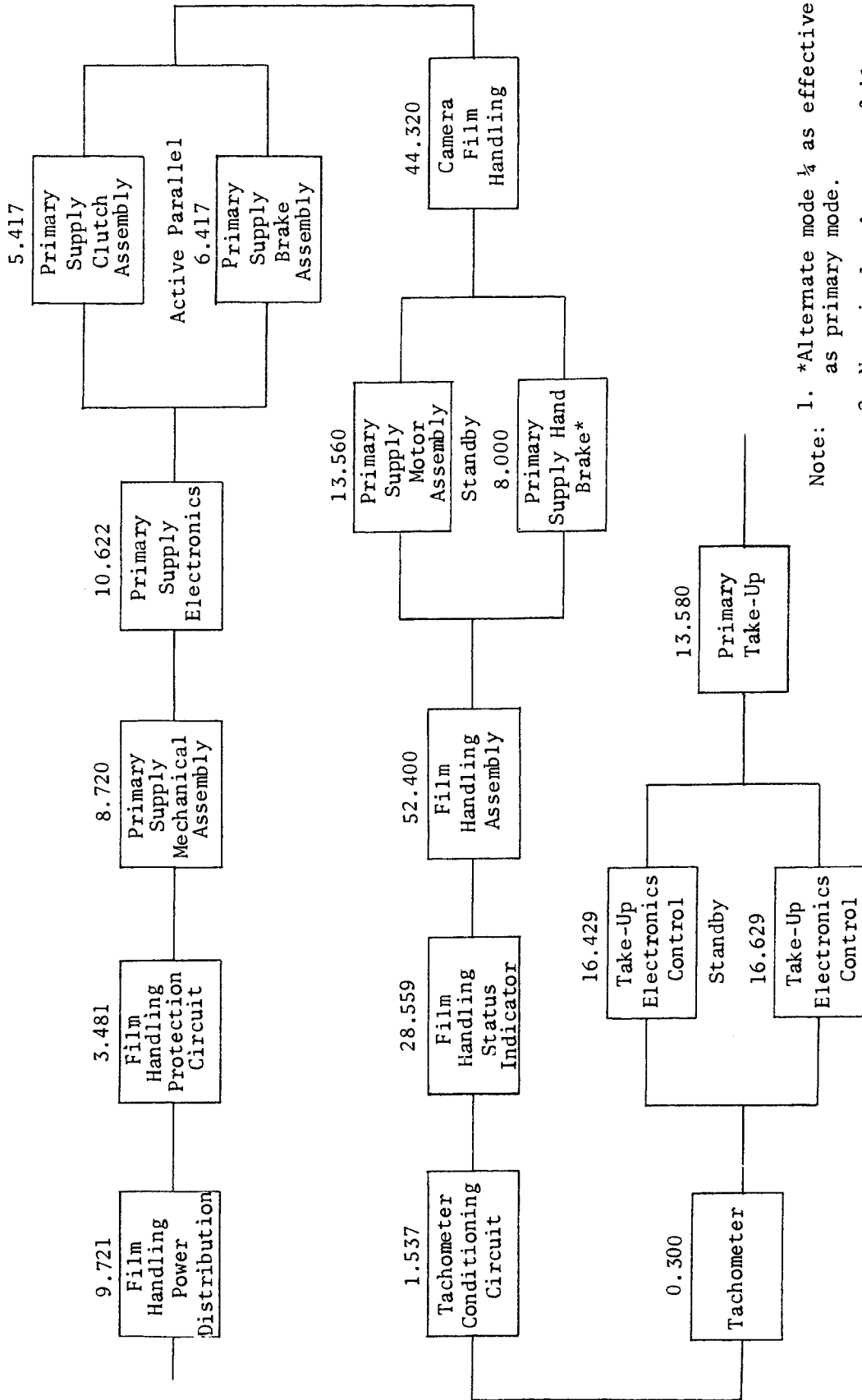
Handle via **BYEMAN**
Control System Only

~~SECRET~~ D



Note: For control unit, numerical values are failures per million actuations. All other numerical values are failures per million hours.

Figure D-5 (continued). Photographic Cycle (continued)

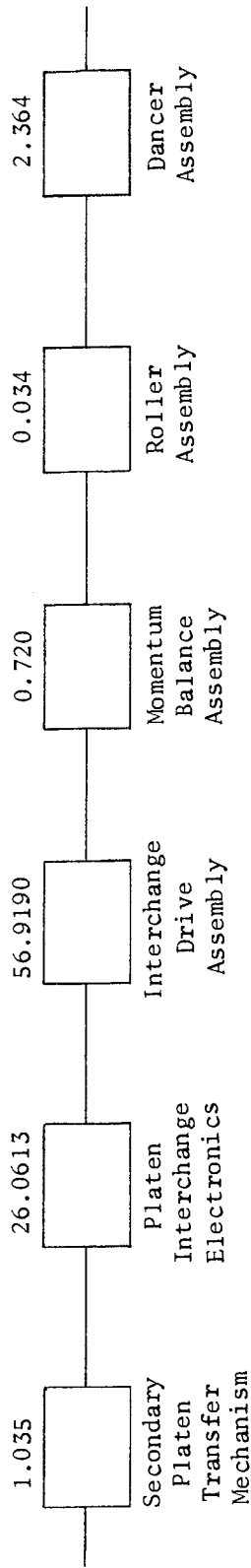


Note: 1. *Alternate mode $\frac{1}{4}$ as effective as primary mode.
2. Numerical values are failures per million hours.

Figure D-6. Film Handling

~~SECRET~~ D

BIF-008- [REDACTED] -68
(Control Number)



Note: Numerical values are failures per million hours.

Figure D-7. Platen Interchange

Handle via **BYEMAN**
Control System Only

~~SECRET~~ D

~~SECRET~~

D

BIF-008- [REDACTED] -68
(Control Number)

Note: All numerical values are reliabilities.

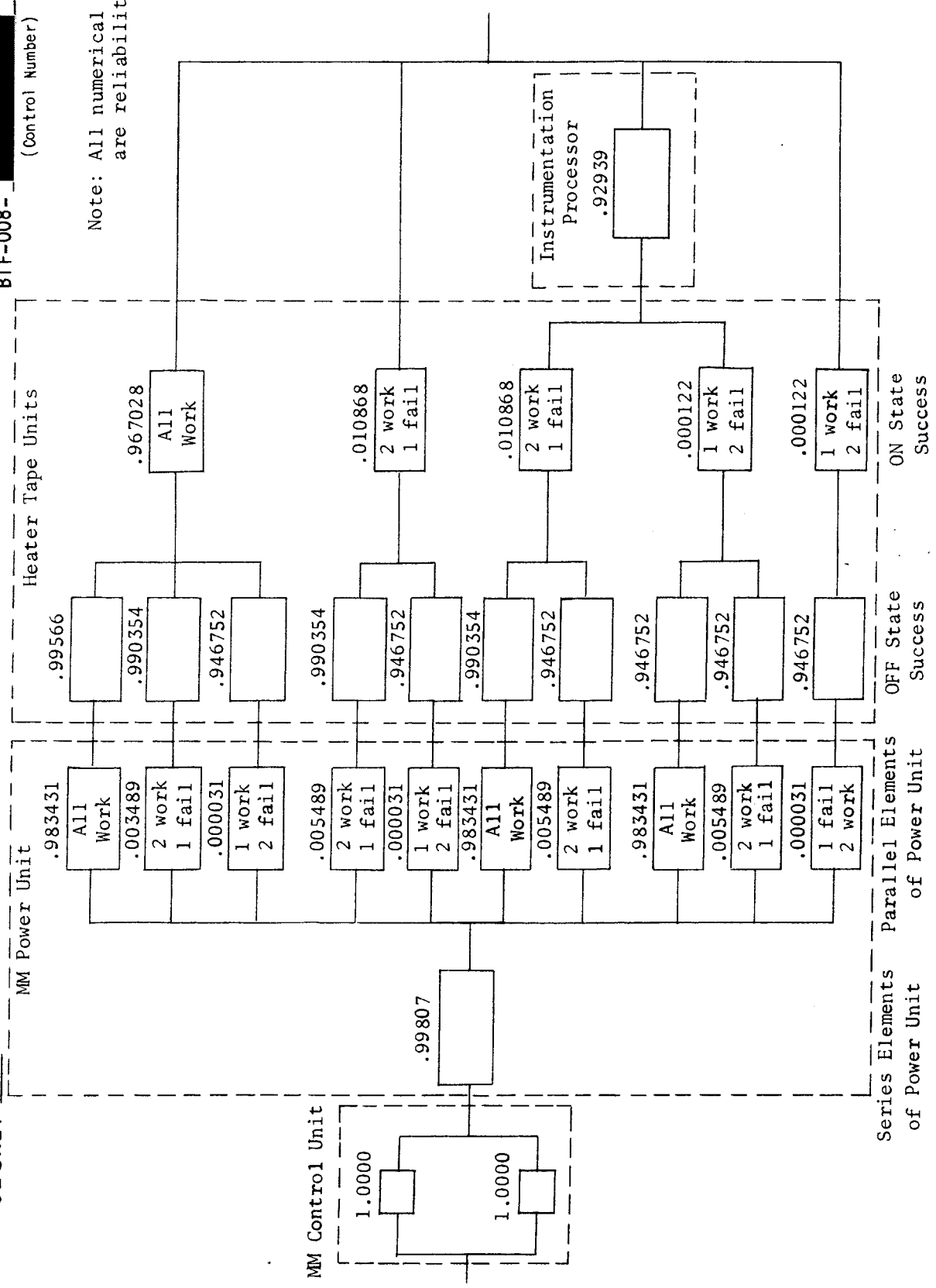


Figure D-8 (b). Environmental Control

Handle via **BYEMAN**
Control System Only

~~SECRET~~ D

~~SECRET~~ D

BIF-008- [REDACTED] -68
(Control Number)

Figure D.2 is a schematic representation of all possible success paths for the unlocking of the launch locks. The diagram uses integer representation for hardware units; the correspondence between hardware unit and integer along with individual failure rates is shown in Table D.1. The reliability estimate was calculated assuming an exponential distribution of part failures and using a multiple application of the standby redundancy formula.

The reliability associated with Figure D.3, focus sensing and adjust, was evaluated by the standard techniques of MIL-HDBK-217A.

Figure D.4 represents the possible paths to successful alignment. Equipment which is used in more than one mode of operation appears in all paths in which it is used. The numerical evaluation of this operation has accounted for the fact that a failure of one of those pieces of equipment which is in more than one path eliminates all paths which include this equipment. In order to evaluate the resultant reliability of the three servos on each mirror, it was assumed that one half the time all three servos would be required for correct alignment and that half the time any two of the three would be adequate for making the correct adjustments. Equipment descriptions are given in Table D.2.

The reliability associated with Figure D.5 and Figure D.6 was evaluated by the standard techniques of MIL-HDBK-217A.

Figure D.7 represents the platen interchange operation. This operation is considered to be mission-essential because certain failure modes could result in the inability to relocate the primary platen in the correct position after having inserted the secondary platen.

~~SECRET~~ D

~~SECRET~~ D

BIF-008- [REDACTED] -68
(Control Number)

TABLE D.1
LOCK SET KEY

<u>Block Number</u>	<u>Hardware</u>	<u>Failure Rate (FPMH) *</u>
1.	Primary Power Relay and Power Buss	12.833
2.	Redundant Power Relay and Power Buss	13.042
3.	Primary Control Relay and Steering Circuit (for three of the six locks)	2.666
4.	Redundant Control Relay and Steering Circuit (for three of six locks)	2.666
5.	Redundant Control Relay and Steering Circuit (for three of six locks)	2.666
6.	Primary Control Relay and Steering Circuit (for three of six locks)	2.666
7.	Primary Motor Drive Circuit and Motor No. 1	50.032
8.	Primary Motor Drive Circuit and Motor No. 2	50.032
9.	Primary Motor Drive Circuit and Motor No. 3	50.032
10.	Redundant Motor Drive Circuit and Motor No. 3	45.358
11.	Redundant Motor Drive Circuit and Motor No. 2	45.358
12.	Redundant Motor Drive Circuit and Motor No. 1	45.358
13.	Redundant Motor Drive Circuit and Motor No. 4	45.358
14.	Redundant Motor Drive Circuit and Motor No. 5	45.358
15.	Redundant Motor Drive Circuit and Motor No. 6	45.358
16.	Primary Motor Drive Circuit and Motor No. 6	50.032
17.	Primary Motor Drive Circuit and Motor No. 5	50.032
18.	Primary Motor Drive Circuit and Motor No. 4	50.032

* Failures per million hours.

D-13
~~SECRET~~ D

Handle via BYEMAN
Control System Only

~~SECRET~~ D

BIF-008- [REDACTED] -68
(Control Number)

TABLE D.1 (Continued)

<u>Block Number</u>	<u>Hardware</u>	<u>Failure Rate (FPMH) *</u>
19.	Speed Reducer, Gearing, and Differential No. 3	17.260
20.	Speed Reducer, Gearing, and Differential No. 2	17.260
21.	Speed Reducer, Gearing and Differential No. 1	17.260
22.	Speed Reducer, Gearing and Differential No. 6	17.260
23.	Speed Reducer, Gearing and Differential No. 5	17.260
24.	Speed Reducer, Gearing and Differential No. 4	17.260

* Failures per million hours.

D-14
~~SECRET~~ D

Handle via **BYEMAN**
Control System Only

~~SECRET~~ D

BIF-008- [REDACTED] -68
(Control Number)

TABLE D.2
ALIGNMENT CODE

1. Circuitry common to all modes, power supply electromagnetic interference (EMI) filters, micrometer loops.
2. Manual mode circuitry, control unit and control panel associated circuitry, manual read, and step logic circuitry.
3. Flight crew
4. Instrumentation digital
AC to digital converter multiplexing, preamps, micrometer, detectors, and sample hold circuitry.
5. Instrumentation analog
Analog resolver circuitry, preamps, micrometer, detectors, and sample hold circuitry.
6. Parfocal motor, associated circuitry, and visual optics.
7. Automatic mode circuitry, control unit associated circuitry, automatic read, and step logic circuitry.
8. Remote mode circuitry, control unit associated circuitry, remote read, and step logic circuitry.
9. Instrumentation circuitry associated with automatic mode.
10. Internal and external light source and their power supplies.
11. Servo drive logic and amplifier, linear actuating device, motor, buffers for primary mirror.
12. Servo drive logic and amplifier, linear actuating device, motor, buffers, for Ross corrector diagonal mirror.

D-15

~~SECRET~~ D

Handle via BYEMAN
Control System Only

~~SECRET~~ D

BIF-008- [REDACTED] -68
(Control Number)

Figure D.8-a represents the hardware configuration of the heater-tape units in the MM. Each heater-tape unit consists of a heater controller, a heater tape, and a thermistor probe. The units are arranged in three banks, each controlled by a separate portion of the power buss (see Figure D.8-a) which permits separate control of the three banks of tapes. If a failure of a heater tape unit results in an overheating condition, the power can be removed from the bank of heater tape units containing the failed tape without affecting the operation of the other two banks. It is assumed that this configuration can correctly maintain thermal control as long as: (1) there are no failures which result in a tape remaining ON, and (2) there are never three consecutive tapes permanently OFF.

Figure D.8-b represents the permissible combinations of individual parts operating or not operating which will result in successfully maintaining correct thermal control. The reliabilities associated with the events represented by the various blocks on the diagram were calculated using combinational analysis and assuming an exponential distribution of individual part failures. The column labeled Parallel Elements of Power Unit represents the various ways in which the parallel portions of the power unit (Figure D.8-a) can operate or not operate. The column labeled On State Success represents the events in which the three banks of heater tape units (Figure D.8-a) either do or do not experience a failure which results in a tape remaining ON. Each block in the column labeled OFF State Success represents, for a given state of the parallel elements of the power unit, all possible combinations of the individual heater-tape units operating or failing OFF

D-16
~~SECRET~~ D

Handle via BYEMAN
Control System Only

~~SECRET~~ D

BIF-008- [REDACTED] -68
(Control Number)

which will result in successfully maintaining the thermal control. The instrumentation processor was included only in those paths which require a decision to be made based on its output. The probability of any one success path occurring is the product of the probabilities associated with the events represented by the individual blocks along the path. The reliability, which is the total probability of success, is the sum of the probabilities for each path.

D.2 COMPUTATION HYPOTHESES AND DATA

Table D.3 lists assumptions used in the evaluation of the model relating to the operational capability of the equipment.

Table D.4 is a partial summary of the numerical data used in the calculation of the reliability estimate for the photographic payload (PP). This table contains failure rates shown on the block diagrams. Also included is an estimate of the operating time for each component or subcomponent listed. With these failure rates and operating times and the applicable application factors, the reliability of the launch and nonoperational phases of the mission were calculated. Table D.4 also includes the estimated reliability for each of the listed subcomponents during launch and nonoperation. These calculations complete the reliability estimates for all mission-essential operations.

~~SECRET~~ D

~~SECRET~~ D

BIF-008- [REDACTED] -68
(Control Number)

TABLE D.3
EVALUATION ASSUMPTIONS OF EQUIPMENT OPERATIONAL CAPABILITY

1. Shutter travel time per photo	0.2 sec
2. Frame rate (primary film)	1 frame/sec (max.)
3. Primary frames per target	10 (max.)
4. Time from exposure start of secondary frame to exposure start of primary frame	2 sec
5. Secondary frame rate	1 frame/3 sec (max.)
6. Secondary frames per target	2 (max.)
7. Time over area of interest	100 min./day
8. Average frames per day	450
9. Average frames per target	6
10. Average targets per day	75
11. Film handling	100 min./day
12. Primary frames	12,425
13. Secondary frames	2,575
14. Recycle time between sequences	5 sec (minimum)
15. Focus sensing	
a. minimum Good Data Sample	3 min.
b. warm-up time	10 sec
c. retract mirror	10 sec
16. Optical align check	Once per active revolution
17. Alignment operation	Once per active revolution
18. Alignment	
a. Servo decentering correction	2 min. for initialization 1 min./correction thereafter

~~SECRET~~ D

~~SECRET~~ D

BIF-008- [REDACTED] -68
(Control Number)

TABLE D.3 (Continued)

18. Alignment (Continued)	
b. Servo tilt correction	3 min. for initialization 1 min./correction thereafter
c. Remote mode of alignment	11 min. for initialization 8 min./correction thereafter
d. Automatic mode of alignment	4 min./correction
19. Time during which launch factor is applicable	15 min.
20. Operating time for each heater tape	Approximately 1/3 of mission

~~SECRET~~ D

~~SECRET~~ D

BIF-008- [REDACTED] -68
(Control Number)

TABLE D.4
RELIABILITY NUMERICAL SUMMARY

	<u>Failure Rate (FPMH) (1)</u>	<u>Operating Time t (hr.)</u>	<u>Launch Reliability</u>	<u>Non-Operation Reliability</u>
CAMERA				
Electronics	305.334	65	.999924	.998000
Mechanical				
1) Focus Drive	88.466	18.33	.999978	.999379
2) Frame Lock Assy.	3.34	3.33	.999999	.999976
3) Jog Velocity Assy.	1.695	.690	1.000000	.999988
4) Jog Angle Assy.	28.54	.690	.999993	.999795
5) Vacuum Assy.	2.0325	.833	.999995	.999985
6) Platen Assy.	3.0525	5.623	.999999	.999978
7) Slit-Width Drive	841.4925	3.33	.999790	.993969
8) Curtain Assy.	123.255	4.163	.999969	.999118
9) Platen Interchange	61.038	2.92	.999985	.999562
10) Film Handling	(2)	(2)	(2)	(2)
FOCUS SENSING ELECTRONICS	119.536	16.66	.999970	.999159
FOCUS SENSING ASSEMBLY	77.215	1.66	.999981	.999445
ALIGNMENT				
Remote Mode	171.064	40.36	.999958	.998837
Automatic Mode	35.312	20.0	.999991	.999753
Lamps & Power Supply	7.239	2.5	.999998	.999986
Servos	67.039(3)	10.00	.999793(3)	.998512(3)
LM CABLE SET	10.061	720	.999748	
MM CABLE SET	8.384	720	.999790	
LM POWER UNIT				
Buss				
23 Camera	(4)	65	1.000	1.000
24 Focus	(4)	16.66	1.000	1.000
25 DCU			Non-Essential	
31 Film Handling	(4)	6.87	1.000	1.000
33 Vibration Amplifiers			Non-Essential	
35 Visual Optics			Non-Essential	

~~SECRET~~ D

~~SECRET~~ D

BIF-008- [REDACTED] -68
(Control Number)

TABLE D.4 (Continued)

	<u>Failure Rate (FDMH) (1)</u>	<u>Operating Time t (hr.)</u>	<u>Launch Reliability</u>	<u>Non-Operation Reliability</u>
MM POWER UNIT				
3 Alignment	(4)	40.36	1.000	1.000
7 Heaters	(4)	720	.999062	
10,11 Launch Locks		Included in Launch Lock Operation		
12 Vibration Amplifiers			Non-Essential	
LM CONTROL UNIT	54.35	(5)	.999986	.999609
MM CONTROL UNIT	15.53	(5)	.999996	.999888
FILM HANDLING	(4)	6.87	.999128	.998548
LAUNCH LOCKS				
PRIMARY MIRROR LOCK SET	(4)	30 sec	.999880	.999999
TRACKING MIRROR LOCK SET	(4)	30 sec	.999880	.999999
THERMAL CONTROL SYSTEM				
1. INSTRU. PROCESSOR	101.7	720	.999975	
2. HEATER TAPE UNITS				
a. HEATER CONTROLLER				
1/3 ON	3.67	223	.997431	
2/3 OFF	3.67	497	.999949	
b. HEATER TAPES				
1/3 ON	0.1	223	.999930	
2/3 OFF	0.1	497	.999999	
c. TEMP. SENSOR				
ALL ON	1.2	720	.997450	

~~SECRET~~ D

~~SECRET~~ D

BIF-008- [REDACTED] -68
(Control Number)

FOOTNOTES:

- (1) Failures per million hours.
- (2) All film handling portions of the camera are included in the film handling operation.
- (3) Failure rate is for one servo, reliabilities are for all servos.
- (4) The failure rates for this subcomponent are not listed because the unit contains internal redundancy. The redundancy configuration and individual failure rates can be obtained from block diagrams.
- (5) The failure rate supplied in the table is appropriate for the calculations of the nonoperational and launch reliabilities. It was assumed that all individual parts of the control units are in series during these operations. Note that the operational reliability of the control units was calculated as a function of the number of actuations; the failure rate appropriate for such calculations is shown in the reliability block diagrams of the mission-essential operations.

~~SECRET~~ D

~~SECRET~~ D

BIF-008- [REDACTED] -68
(Control Number)

APPENDIX E
ANALYSIS AND DESIGN OF TEST TOWERS

The minimization of relative motion between various optical elements in a test tower can be accomplished in three ways; (1) elimination of the sources of vibration, (2) isolation of the test tower from the vibrations, and (3) designing the tower so that it does not respond to the vibrations. All three of these approaches were used in designing the test towers and are discussed in the following paragraphs.

E.1 SOURCES OF VIBRATION

Vibrations detrimental to correct tower function result from four basic sources; (1) ground-transmitted vibrations, (2) acoustically coupled vibrations, (3) vibrations caused by air temperature and pressure variations, and (4) vibrations caused by dynamic equipment installed on the test tower.

Ground vibrations are either controllable (elevators, pumps, fans, motors, etc.) or uncontrollable (tides, wind loading on trees and buildings, micro-seisms, railroads, etc.).

Vibrations caused by local machinery movement are reduced by (1) balancing rotating parts, (2) isolating residual forces, and (3) building acoustic enclosures to absorb noise transmission. The isolation principle is one of impedance mismatch to prevent a transmission of force from the machine to the foundation. Its effectiveness can best be described by example:

E-1

~~SECRET~~ D

Handle via **BYEMAN**
Control System Only

~~SECRET~~ D

BIF-008- [REDACTED] -68
(Control Number)

Consider a rotary pump turning at 3600 rpm with a mass unbalance of 3.86 lb at 10 inches. Because of the centrifugal principle a radial force is produced.

$$F_R = mr\omega^2, \quad (1)$$

where: F_R = centrifugal force,

m = mass unbalance,

r = eccentricity,

ω = $2\pi \times \text{rpm}/60$ - radian/second, and

$$F_R = \frac{3.86}{386} (10) (2\pi)^2 (60)^2 = 14,400 \text{ lb acting radially.}$$

As the machine rotates, a vertical component of force equal to $14,400 \sin 2\pi 60t$ and a horizontal component of force equal to $14,400 \cos 2\pi 60t$ is "seen" by the foundation.

If, however, the same pump is mounted on a spring mass having a natural frequency of 2 Hz.

$$f_n = \frac{1}{2\pi} \sqrt{\frac{K}{m}}, \quad (2)$$

where: f_n = natural frequency in Hz ,

K = spring constant of the suspension - lb/inch, and

m = total spring mass (pad plus pump) - lb second²/inch.

~~SECRET~~ D

Handle via BYEMAN
Control System Only

~~SECRET~~ D

BIF-008- [REDACTED] -68
(Control Number)

The following equation for the force transmitted to the foundation is valid:

$$F = F_v \sqrt{\frac{1 + \left(2 \zeta \frac{\omega}{\beta}\right)^2}{\left[1 - \frac{\omega}{\beta}\right]^2 + \left(2 \zeta \frac{\omega}{\beta}\right)^2}}, \quad (3)$$

where: F = force transmitted to the foundation - lb

F_v = the vertical component of the centrifugal force - lb
(An identical equation can be written for the horizontal component),

$\beta = \frac{K}{m} = 2 \pi f_n$ radian/second, and

ζ = critical damping ratio (assumed 0.1).

Evaluating the above equation for the given parameters yields

$F = 96$ lb (a reduction of 150:1).

This is the objective and result of correct isolation.

The residual ground vibrations, which are not controllable, were measured at the test tower sites prior to the start of construction and averaged 10^{-6} g in the frequency range of 2 Hz to 250 Hz. It was estimated that when the entire test complex was completed this level would rise to 10^{-4} g.

~~SECRET~~ D

~~SECRET~~ D

BIF-008- [REDACTED] -68
(Control Number)

Where feasible, to minimize acoustic coupling to the test towers, all pumps and motors were located in separate enclosures, separated from the high bay by heavy sound-absorbing walls. In addition, because many optical tests are to be performed in vacuum, acoustic and temperature/pressure effects are greatly reduced.

E.2 VIBRATION ISOLATION

After eliminating as many sources of vibration as possible, calculations still indicated a problem in achieving $\lambda/40$ accuracies in the optical tests. The need for isolating the test towers was therefore established.

Four basic types of isolation were investigated.

- a. Inertia pads
- b. Metal-spring isolators
- c. Pendulous isolation
- d. Pneumatic isolators

E.2.1 Inertia Pads

Inertia pads not only do not attenuate vibrations but actually increase it. This fact has been confirmed by experiences of EKC and others.

E.2.2 Metal-Spring Isolators

Metal springs exhibit two serious disadvantages. As before, the natural frequency is given by equation (2). The static deflection, δ_{st} , is given by

~~SECRET~~ D

~~SECRET~~ D

BIF-008-[REDACTED]-68
(Control Number)

$$\delta_{st} = \frac{mg}{K} = \frac{g}{(2\pi f_n)^2} \quad (4)$$

$$g = 386 \text{ inches/second}^2.$$

For a 1.5 Hz isolation system δ_{st} must equal 4.85 inches. This means that the spring must deflect almost 5 inches under static loads, implying that this spring must be almost 3-feet long (from stress considerations). A spring of this length would be very unstable laterally and would be highly sensitive to spring surges or localized resonances. Because of this instability and also because steel springs transmit high-frequency noise (in violation of classical theory), this method for isolation was deemed unacceptable.

E.2.3 Pendulous Isolators

A pendulous system has three degrees-of-freedom or three natural frequencies. The pendulous mode is well known and

$$f_n = \frac{1}{2\pi} \sqrt{\frac{g}{l}} \text{ Hz.} \quad (5)$$

l = length of the pendulum - inches.

A vertical natural frequency can also be determined and is given by

$$f_n = \frac{1}{2\pi} \sqrt{\frac{NAE}{W}} \cdot \sqrt{\frac{g}{l}} \text{ Hz,} \quad (6)$$

E-5

~~SECRET~~ D

Handle via **BYEMAN**
Control System Only

~~SECRET~~ D

BIF-008- [REDACTED] -68
(Control Number)

where: N = number of suspension cables,
A = cross sectional area of the cable in inches²,
E = modulus of elasticity of the cable in lb/inch², and
W = suspended load in lb.

A torsional mode is also possible and its natural frequency is given by

$$f_n = \frac{1}{2\pi} \frac{R}{K} \sqrt{\frac{g}{l}} \text{ Hz,} \quad (7)$$

where: R = radius of the suspended load to the support point in inches, and
K = radius of gyration of the load about a vertical axis in inches.

Typically l equals 540 inches. Natural frequencies of less than 3 Hz are feasible.

$$f_n = 0.135 \text{ Hz pendulous,}$$
$$f_n = 2.7 \text{ Hz vertically, and}$$
$$f_n = 0.162 \text{ Hz torsional.}$$

The relatively high vertical natural frequency can be reduced by introducing a series spring without any great difficulty as the spring is now in tension and lateral stability is no longer a criterion.

~~SECRET~~ D

~~SECRET~~ D

BIF-008- [REDACTED] -68
(Control Number)

This combined approach was found satisfactory and was used in Chamber IIIa, IIIb, and A. However, it does entail the design and construction of a high and complex support structure from which the pendulum is to be hung.

E.2.4 Pneumatic Isolators

Investigations were continued to find an optimum isolation method for the remaining test towers. It was determined that pneumatic isolators came the closest to achieving this result.

Figure E.2-1 is a schematic diagram of a pneumatic isolator. The natural frequency equation for a pneumatic isolator can be derived using the following four basic equations:

$$PV^n = \text{constant}, \quad (8)$$

$$W = P \frac{A}{g}, \quad (9)$$

$$V = h_{\text{eff}} A, \text{ and} \quad (10)$$

$$K = \frac{dW}{dh}. \quad (11)$$

Combining equations (8), (9), (10), and (11) gives

$$K = \frac{nAP}{V/A} = \frac{nW}{h_{\text{eff}}} \frac{(P/g)}{(P)}, \quad (12)$$

and from equation (2):

$$f_n = \frac{1}{2\pi} \sqrt{\frac{ng}{h_{\text{eff}}} \frac{(P/g)}{(P)}}, \quad (13)$$

~~SECRET~~ D

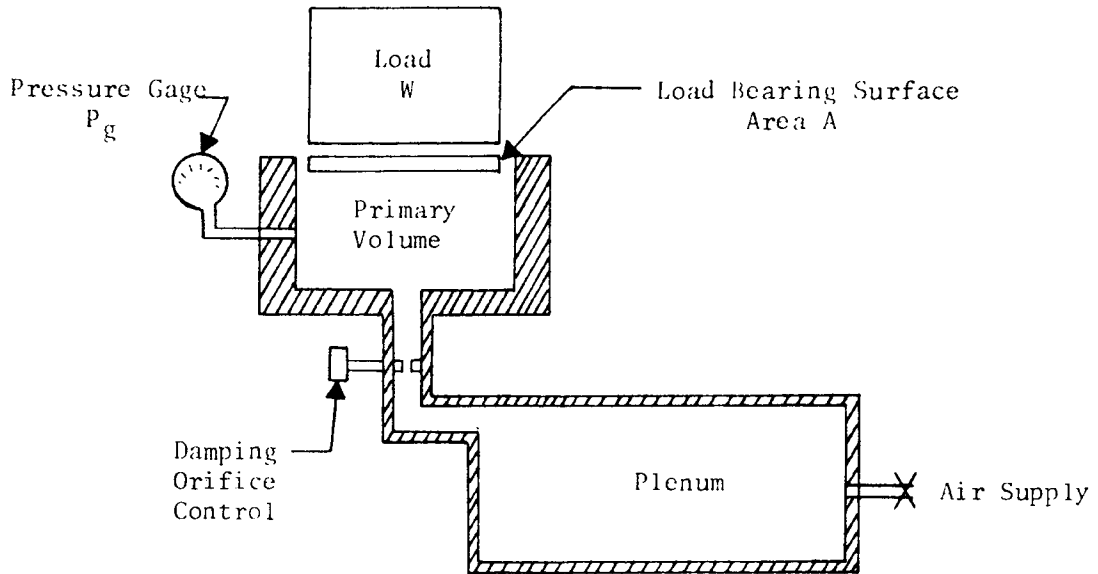


Figure E.2-1. Pneumatic Isolator

~~SECRET~~ D

BIF-008-[REDACTED]-68
(Control Number)

where: A = cross sectional area of the isolator in inch^2 ,

 h = vertical distance in inches,

 h_{eff} = effective height of the isolator in inches,

 n = gas constant,

 P = absolute pressure in lb/inch^2 ,

 P_g = gage pressure in $\text{lb}/\text{inches}^2$,

 V = volume of the isolator in inches^3 , and

 W = isolated weight in lb.

It is seen that the natural frequency is independent of the supported load and can be varied readily by changing the effective height. For sufficiently high pressure, P_g/P is near unity. Because the effective height is defined by equation (10), it can be made as large as desired by just adding volume (plenum chambers) thus lowering the natural frequency.

An additional advantage of pneumatic isolators is that they inherently exhibit a 12 db/octave transmissibility roll-off regardless of the critical damping ratio.

Looking again at the pump example, after isolation the pump put a force of $96 \sin(2\pi 60t)$ into the ground. Also assume that as a result of this force an acceleration of $10^{-2}g$ is imparted to the ground. This acceleration corresponds to a ground motion of $386 \times 10^{-2}/(2\pi f)^2 \approx 3 \times 10^{-6}$ inches ($\lambda/7$). The effect of spring isolation is given by equation (3) with F replaced by X ,

E-9

~~SECRET~~ D

Handle via BYEMAN
Control System Only

~~SECRET~~ D

BIF-008-[REDACTED]-68
(Control Number)

the motion of the test tower, and F replaced by X_g , the motion of the ground. The reduction factor of 150:1 still applies as before. The tower experiences an acceleration at 60 Hz of $7 \times 10^{-5}g$ and a displacement of 2×10^{-8} inches. Although this appears excellent, it must be remembered that in this analysis the test tower was assumed to be perfectly rigid at least to 60 Hz, and no allowance has been made for local tower resonances. An input force of 14,400 lb which would have accelerated a 60,000 lb structure (typical for the test towers) at 0.24g was so modified by isolation that an acceleration of only $7 \times 10^{-5}g$ results.

The performance of pneumatic isolators was validated empirically on test towers I_{EM} and II_{EM}. The isolation natural frequencies were shown to be less than 2 Hz with no stability problems. This test was performed by mounting a shaker on the floor and exciting it. The two curves shown in Figure E.2-2 are the acceleration on the floor adjacent to the shaker and on the isolated tower. Vibration attenuation is considerable as depicted in Figure E.2-2.

E.3 TOWER DESIGN

Design and performance prediction for the test towers requires a knowledge of their natural frequencies and normal modes of vibrations. A number of computer programs have been developed to achieve these results.

For analysis, the structure was idealized (modeled) as a combination of discrete masses and simple prismatic members.

~~SECRET~~ D

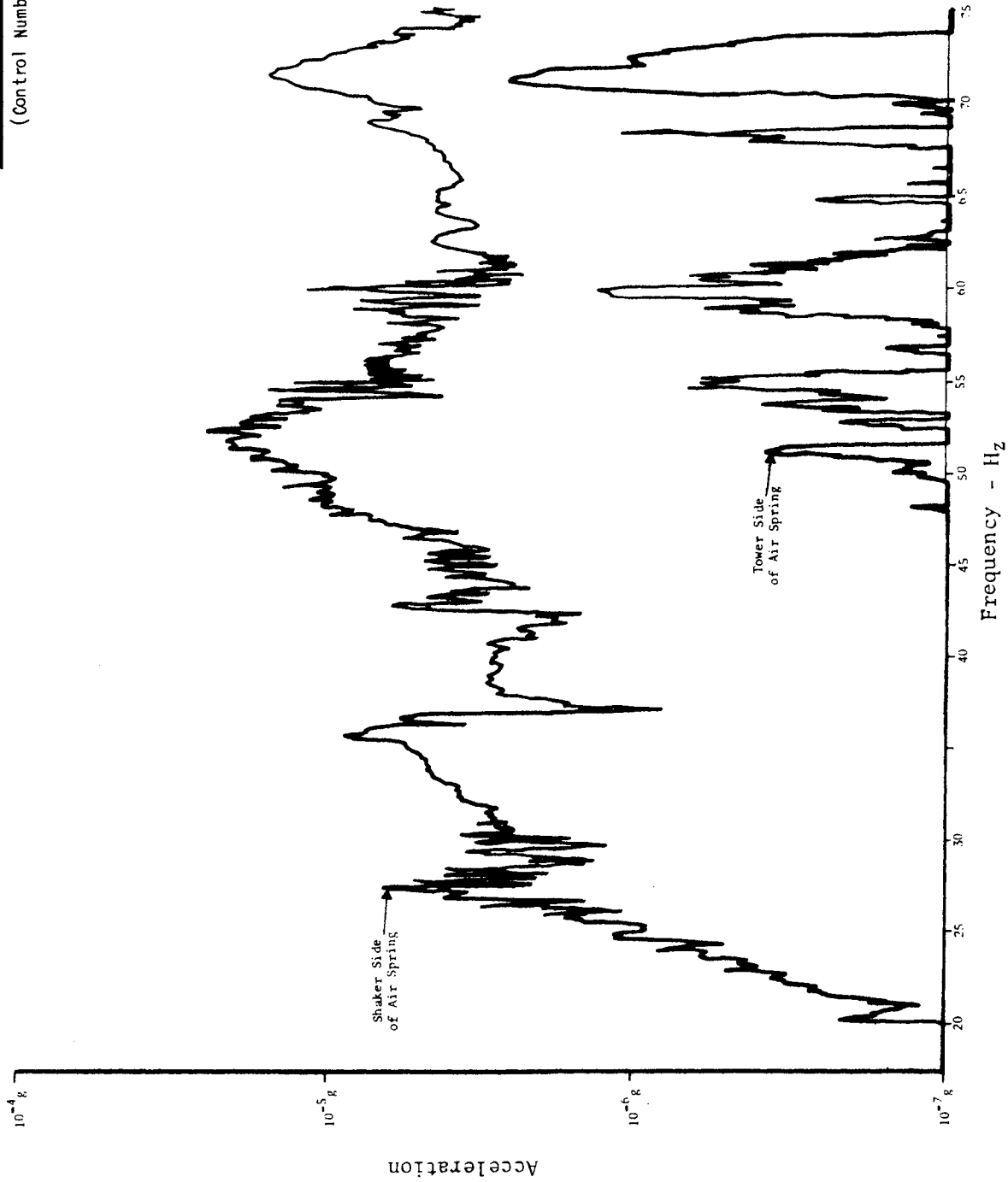


Figure E.2-2. Chamber I_{em} Tower Attenuation Across Air Spring Isolators

Handle via BYEMAN
Control System Only

~~SECRET~~ D

BIF-008-

(Control Number)

-68

Because of the symmetric characteristics of the Chamber II structure, a two-dimensional simplification as shown in Figure E.3-1a was chosen for analysis. Structural and optical characteristics involving the direction and sensitivity of the optical beam were considered.

A total stiffness matrix [K] and an inertia matrix [M] were then generated. The [K] matrix was inverted to give an influence matrix, $[A] = [K]^{-1}$, and a static deflection and stress analysis was performed.

The [A] and [M] matrices were then used to set up an eigenvalue solution by iteration:

$$[A] [M] \{\phi\} = \lambda^2 \{\phi\} \quad (14)$$

$\{\phi\}$ = column matrix - eigenvector

λ^2 = eigenvalue.

The natural frequency is related to the eigenvalue by:

$$f_n = \frac{1}{2\pi\lambda} \quad (15)$$

The eigenvector represents a generalized coordinate and defines the vibration mode shape at that frequency. Figure E.3-1 depicts the mode shapes found for the Chamber II test tower (a) before excitation and (b) exaggerated first (fundamental) free-free mode of vibration.

E-12

~~SECRET~~ D

Handle via BYEMAN
Control System Only

~~SECRET~~ D

BIF-008- [REDACTED] -68
(Control Number)

Table E.3-1 lists the predicted first mode natural frequencies for the various towers, comparing those values to the first mode natural frequencies which were empirically evaluated.

TABLE E.3-1
FIRST MODE NATURAL FREQUENCIES FOR TOWERS

Tower	Fundamental Mode Natural Frequency	
	Calculated	Verified
I _{EM}	38.6	35.0
II _{EM}	37.6	37.1
I	28.4	27
I _G	28.9	31
II	37.6	36.2
C	31.2	*
IIG	22	20

* Not verified as of 1 September.

Once the characteristics of the test tower are known, optimizations are undertaken. Attempts are made to locate critical optics at nodes (quiescent points) and to eliminate vibration sources at critical frequencies.

~~SECRET~~ D

